

Dissertation

submitted to the

Combined Faculties for the Natural Sciences and for Mathematics

of the Ruperto-Carola University of Heidelberg, Germany

for the degree of

Doctor of Natural Sciences

Presented by

Diplom-Biologist Katharina Elisabeth Pelka née Schneider

born in Mannheim, Germany

Day of oral examination:.....

**The applicability of the Fish Embryo Toxicity Test
(FET) for the testing of chemical substances with
particular reference to a possible barrier function of
the chorion**

Referees

Prof. Dr. Thomas Braunbeck,
COS, University of Heidelberg

Prof. Dr. Stephan Frings
COS, University of Heidelberg

Hiermit erkläre ich, dass ich die vorliegende Dissertation selbst verfasst und mich dabei keiner anderen als der von mir ausdrücklich bezeichneten Quellen und Hilfen bedient habe.

Kapitel 1 dieser Arbeit, welches ich eigenständig verfasst habe, wurde im Lauf der Dissertation als eigenständiger Artikel wie folgt veröffentlicht:

- Katharina E. Pelka, Kirsten Henn, Andreas Keck, Benjamin Sapel, Thomas Braunbeck “Size does matter – determination of the critical molecular size for the uptake of chemicals across the chorion of zebrafish (*Danio rerio*) embryos.” *Aquatic Toxicology*. Received 17 July 2016, Revised 19 November 2016, Accepted 16 December 2016, Available online 21 December 2016. <http://dx.doi.org/10.1016/j.aquatox.2016.12.015>.

Die Ergebnisse aus den folgenden Bachelorarbeiten sind in diese Dissertation integriert. Die Arbeiten beruhen auf meinen Ideen und die durchgeführten Versuche wurden von mir konzipiert und betreut. Alle entnommenen Daten wurden von mir gemeinsam mit den Bachelorstudenten erhoben, ausgewertet und dargestellt.

- Andreas Keck (2014) „Effekte von Polyethylenglycolen auf das Chorion des Zebrabärblings *Danio rerio* und der Dickkopfelnitze *Pimephales promelas*.“ Integriert in Kapitel 1 und Kapitel 4.3
- Benjamin Sapel (2015) “Time- and Size-dependent Uptake of Polyethylene Glycols across the Chorion of Zebrafish (*Danio rerio*).” Integriert in Kapitel 1.

Des Weiteren erkläre ich, dass ich an keiner Stelle ein Prüfungsverfahren beantragt oder die Dissertation in dieser oder einer anderen Form bereits anderweitig als Prüfungsarbeit verwendet oder einer anderen Fakultät als Dissertation vorgelegt habe.

Heidelberg, den _____

Katharina Pelka

Danksagung

Mein herzlicher Dank gilt:

Herrn Prof. Dr. Braunbeck für die Möglichkeit meine Doktorarbeit in seiner Arbeitsgruppe anzufertigen - mit all den Freiheiten und Verpflichtungen durch die man stetig wächst und sich selbst verbessert. Danke!

Herrn Prof. Dr. Frings für die Übernahme des Koreferats und sein jahrelanges Interesse an der Ökotoxikologie. Danke für das gute Arbeitsgruppen-Miteinander in 504.

Scott Belanger, for the interesting project, his expertise and the support to understand the mechanisms of oxidative hair dye precursors. Thanks for the financial support by the Procter & Gamble Company!

Herrn Dr. Möhrle für seinen Rat und Tat bei allen Gerätschaften, neuen Methoden (PCR - was??) und für die sehr entspannte Arbeitsatmosphäre und Einblicke in die Uni-Politik.

Ralf Petto, Melanie Böttcher und Christoph Deller für die gute Zusammenarbeit und die finanzielle Unterstützung im letzten Projekt-Jahr.

Danke an die Menschen, die den Uni-Alltag durch ihre nette und hilfsbereite Art so viel besser machen: Herr Greulich, Herr Böttger, Denis Drebert, Herr Schade, Gisela Adam, Gabi Günther und Christina Godel. Besonders Erik Leist, für seinen Rat zu Fischzucht und -haltung. Ohne ihn und Pluto wäre der Fischkeller nur ein öder Keller.

Daniel Jay Stengel, für all die Stunden im Labor und Fischkeller, im Büro, vor Mikroskopen, über Fotoarbeiten, für all die Diskussionen und Ratschläge seit der Diplomarbeit. Wir haben es tatsächlich mehr oder weniger unbeschadet überlebt ;-)

Ein riesen Dankeschön an den Beistand und die Motivation der zeitweise weitverstreuten Uni-Crew Lisa Baumann, Raoul Wolf und Philipp Janz sowie an die Heidelberger-Erweiterung Annika Batel, Svenja Böhler und Franziska Neureither.

Den Arbeitsgruppen Braunbeck & Frings, für die netten Jahre mit Grillfeiern und Containerparties: Franziska Förster, Britta Kais, Patrick Heinrich, Christopher Faßbender, Ruben Strecker, Leon Kreuter, Suse Knörr, Philipp Daiber, Semir Jeridi, Kristin Dauner, Kerstin Vocke, Fede Genovese, Anne Hahn und Weiping Zhang. Danke an all die Bachelor- und Masterstudenten die im Lauf der Zeit einen Zwischenstopp bei uns eingelegt haben und uns oft bereichert haben. Vielen Dank für die tatkräftige Unterstützung an Julian Blumenröder, Andreas Keck und Benjamin Sapel!

Ein riesen Dankeschön an meine Familie für die jahrelange Unterstützung, den Rückhalt und das Aushalten der seltsamen und abwesenden Phasen! Danke, dass ihr mich immer wieder von der Uni-Wolke auf den Boden der Tatsachen runtergeholt habt!

Sebastian, ich bin von tiefstem Herzen dankbar, dich an meiner Seite zu haben! Danke für das Durchleben von Diplom- und nun auch Doktorarbeit und dass du mich immer so sehr unterstützt und aufgebaut hast. Dein Vorstandsposten des „*Danio rerio*“-Selbsthilfevereins steht nun ab sofort zur Verfügung!

Figure Index

- Figure 1: Overview of the different testing scenarios for various chemicals and the target systems and endpoints in the zebrafish embryo tests. 8
- Figure 2: Adult *Danio rerio*. Upper individual: female can be recognized by its swollen body, lower individual: male with reddish tint in the silvery bands. Picture: E. Leist..... 9
- Figure 3: Procedure of the FET according to OECD TG 236 (OECD, 2013a). After spawning, the eggs are distributed into the respective test concentration in crystallization dishes, checked for fertilization success under the binocular and then distributed separately into the wells of pre-saturated 24-well plates. Last 4 wells are for internal negative control (white wells). Observation of embryo development is performed daily until 96 hpf. Graph according to Lammer et al. (2009) and Sessa et al. (2008)..... 12
- Figure 4: Ultrastructure images of the zebrafish chorion. (A) TEM image of a cross section through the chorion of an unfertilized egg shows the organization into an outer, electron-dense (Z1), a middle, electron-lucid (Z2) and an inner, electron-dense (Z3) layers. The pore canal (P) does not pierce the outer layer (Z1), which is covered by a loose film (x17775; Hart and Donovan (1983)). (B and C) FE-SEM images showing the view on the inner surface of the chorion and reveal the cone-shaped form of the chorion pore canals (CPC; scale bars: 1 μm in panel B and 0.5 μm in panel C; Rawson et al. (2000)). SEM image of the outer surface of the chorion (D) reveals a dense polypeptide layer, recessing into the pore canals, with distinct projections and microorganisms adhere to it (x8 000, scale bar: 2 μm ; Lillicrap (2010)) 15
- Figure 5: Acute (LC_{50}) and sublethal (EC_{50}) effects of differently sized polyethylene glycols (PEGs) in zebrafish (*Danio rerio*) after exposure for 96 h. Data were computed with ToxRat[®] and are given as mean \pm standard deviation; n= 3 runs (taken from Pelka et al.)..... 27
- Figure 6: Sublethal effects in zebrafish (*Danio rerio*) embryos after 96 h exposure to (A & B) 12.5 g/L, (C) 25 g/L and (D) 50 g/L PEG 6,000. Note the absence (A) or deformation of the eyes (B - C), sharply bent tails, formation of edemata as well as yolk deformations of PEG-exposed embryos (taken from Pelka et al.). 27
- Figure 7: Subsequently to transfer into PEG test solutes, the chorion of zebrafish (*Danio rerio*) embryos showed concentration-dependent shrinkage due to effects by (A-C) PEG 3,000 and (D-F) PEG 6,000. Only very small depressions of the chorion were found at 3.125 g/L PEG 3,000 (A) and PEG 6,000 (D), while at 25 g/L (B, E) and 100 g/L (C, F) stronger depressions of the chorion were evident, finally leading to a tightly wrapped chorion around the yolk and cell pole (C and F) (taken from Pelka et al.). .. 28
- Figure 8 Exposure of zebrafish eggs for 24 hours to different polyethylene glycols reveals chorion deformation (grey column) in almost all concentrations of the differently sized PEGs. Likewise, for all tested PEGs, there was a concentration-dependent increase of acute mortality (black line) and sublethal effects (blue line) (taken from Pelka et al.). 29
- Figure 9: Change in chorion area of PEG-exposed zebrafish (*Danio rerio*) eggs. Data are given for three independent runs (n = 3) as % of the area measured from micrographs of eggs in corresponding negative controls. In addition, the time until no further shrinkage of the chorion area was observed is listed (taken from Pelka et al.)..... 30
- Figure 10: Chronological sequence of deformation of the zebrafish (*Danio rerio*) chorion following exposure to differently sized polyethylene glycols (PEGs). Each column

shows the same egg exposed to dilution water (ctrl) or 9.67 mM of the different PEGs at start of exposure (approx. 1 hpf) as well as at 24 and 48 hpf. Whereas the chorions of embryos exposed to PEG 2,000 and 3,000 regained a round shape, the chorions of PEG $\geq 4,000$ Da remain deformed. Note coagulation of embryos exposed to PEG $\geq 8,000$ Da (taken from Pelka et al.). 32

Figure 11: Changes in the area of micrographs of the chorion of zebrafish (*Danio rerio*) embryos exposed to polyethylene glycols (PEGs) of different sizes (molecular weight) in relation to the areas at the start of exposure. The exposure covers the time period from the onset of exposure (approx. 5 min) to the time point of no further shrinkage of the chorion (approx. 24 h). For PEG 3,000, additional measurements were made after 36 and 48 h. Note that maximum shrinkage is already reached after approx. 7 h for most PEGs. Data are given as percent change over negative controls at the beginning of the exposure for three independent runs with 20 embryos (n = 3). Coagulate eggs at PEGs 8,000 and 12,000 were excluded from evaluation (taken from Pelka et al.)...... 33

Figure 12: Orientation of the pictures presented in this chapter. Zebrafish embryos were exposed within their chorion to 0.1 μm sized microspheres. Pictures were taken at 48 hpf; HV: 10; TD: 58. Scale bars: 150 μm , 10x magnification. 47

Figure 13: Fluorescence signal detected on the surface of the chorion of 24 hpf embryos (A-C) and of 48 hpf embryos (D-F). The 0.2 μm sized fluorescent microspheres are evenly distributed over the chorion surface, however, feces and other distinct projection on the chorion surface are strongly fluorescent (see asterisk). Settings: HV12, TD 50; all panels; 4x magnification; scale bars in A, B, D, E: 200 μm 48

Figure 14: Fluorescence signal detected on the surface of the chorion of 24 hpf embryos (A-C) and of 48 hpf embryos (D-F). The 0.1 μm sized fluorescent microspheres are evenly distributed over the chorion surface, however, feces and some distinct projection on the chorion surface are strongly fluorescent (see asterisk at 24 hpf). Settings: HV12, TD 50; all panels: 4x magnification; scale bars in A, B, D, E: 200 μm 49

Figure 15: Fluorescence signal detected on the surface of the chorion of 24 hpf embryos (A-C) and of 48 hpf embryos (D-F). The 0.048 μm sized fluorescent microspheres are evenly distributed over the chorion surface. However, dents on the chorion surface seem to be less fluorescent than the normally shaped surface (see asterisks). Settings: HV 12, TD 50. Panel A: 4x magnification; scale bar: 200 μm . Panel B-F: 10x magnification; scale bars in B, D, E: 300 μm 50

Figure 16: Embryos exposed for 48 hours within the chorion to 0.2 μm microspheres (first row), 0.1 μm microspheres (second row) and 0.048 μm microspheres (third row). For the detection of microspheres on the surface, embryos were dechorionated at 48 hpf. No signal on or within the embryos were detected after exposure to 0.2, 0.1 and 0.048 μm microspheres. One embryo exposed to 0.2 μm microspheres showed single fluorescent signal at the head area, however, signal is negligible and cannot be detected in the micrographs (first row). Settings: HV12, TD 50; scale bars: 200 μm , 4x magnification. 51

Figure 17: Close-up on zebrafish eggs at 48 hpf exposed to 0.1 μm (A) and 0.048 μm (B) microspheres. The merged images of TD and laser reveal the pores (black arrow) piercing the chorion and the fluorescent microspheres (red arrowhead) adhering onto the chorion surface. Settings: HV 10; TD 58; scale bars: 150 μm ; 10x magnification. 52

- Figure 18: Distribution of 0.2 μm carboxylate-modified microspheres on the chorion surface (18 μm sections) of zebrafish eggs at 24 hpf (A & B) and 48 hpf (C & D). Panel A and C show an overview of the chorion section while panel B and respectively D is a detailed view on the selected area marked in panel A and C. The chorion pores are either dark or light, depending on the optical refraction. Laser power: 100%, HV: 30; TD: 72. Magnification: 60x (A, C) with scale bars: 50 μm ; 60x3.145 (B, D) with scale bars: 10 μm 53
- Figure 19: Distribution of 6 μm microspheres on the chorion of zebrafish embryos at 24 hpf (A-C) and 48 hpf (D-F). Merged (A, D), calcium green (B, E) and transmitted light (C, F) images illustrate the attached microspheres to the chorion surface but not within the egg or embryo. At 48 hpf, the chorion is strongly shrunken due to handling and embedding. HV: 15 (A-C); 12 (D-F); TD: 37; 4x magnification; scale bar: 200 μm . . 67
- Figure 20: Distribution of 1 μm microspheres on the chorion of zebrafish embryos at 24 hpf (A-C) and 48 hpf (D-F). Merged TD and calcium green (A, D), calcium green (B, E) and z-stack (C, F) images illustrate the attached microspheres to the chorion surface but not within the egg or embryo. HV: 15 (A-C); 12 (D-F); TD: 37; 4x magnification; scale bar: 200 μm 68
- Figure 21: Distribution of 0.2 μm microspheres on the chorion of zebrafish embryos at 24 hpf (A-C) and 48 hpf (D-F). Merged (A, D), calcium green (B, E) and z-stacks (C, F) illustrate the attached microspheres to the chorion surface and very low signals in the yolk (see arrowheads in D). Arrow indicates aggregates of microspheres on fungal hyphae. A-E: HV: 5; F: HV: 1; TD 35; 10x magnification; scale bar: 150 μm 69
- Figure 22: Embryos exposed within the chorion to 0.2 μm microspheres and dechorionated before analyzing. At 24 hpf (A,B), z-stacks of the embryo were taken at HV: 12 (A) and HV 22 (B) illustrating fluorescent signal within the yolk (y), the yolk extension (ye) and no signal in head (h) and tail (t). At 48 hpf (C) signal was detected within the yolk (optical section) at HV 5. 10x magnification. 69
- Figure 23: Distribution of 0.1 μm microspheres on the chorion of embryos at 24 hpf (A-C) and 48 hpf (D-F). Merged TD and calcium green (A, D), calcium green (B, E) and z-stack(C, F) images illustrate the attached microspheres to the chorion surface but not within the egg or embryo. A – E: HV: 25; TD: 45; F: HV: 20; 10x magnification; scale bar: 300 μm 70
- Figure 24: Zebrafish embryos exposed within the chorion to 0.1 μm microspheres and dechorionated before analyzing. At 24 hpf (A), the fluorescent signal can be found in the yolk sack, however, signal is very light although the image was taken with HV 22. At 48 hpf (B, B1-2, C), differences in intensity between the embryos were found. Z-stacks of the images taken with HV 30 (B and C) reveal different signal intensity. A single optical section image taken from the middle of the embryo shown in B, revealed a low signal at the yolk (B1 merged image, B2 calcium green only).B1-2: HV: 30; TD: 45; 10x magnification..... 71
- Figure 25: Distribution of 0.05 μm microspheres on the chorion of embryos at 24 hpf (A-C) and 48 hpf (D-F). Merged TD and calcium green (A, D), calcium green (B, E) and additionally z-stacks (C, F) images illustrate the attached microspheres to the chorion surface and within the embryo. At 48 hpf, the chorion is strongly shrunken due to handling and embedding and fungal infection can be found (asterisk). A-C: HV: 5; TD: 35; D-F: HV: 1; TD: 35; 10x magnification; scale bar: 300 μm 72
- Figure 26: Zebrafish embryos exposed within the chorion to 0.05 μm microspheres and dechorionated before analyzing. At 24 hpf a signal is detected in the yolk (A). The

- signal increases at 48 hpf (B) and expands to the somites and the head. HV: 1; TD: 35; 10x magnification..... 73
- Figure 27: An overview of the fathead minnow chorion. SEM images of the outside (A and B) taken by Lillicrap (2010) show a very smooth and lustrous surface of the chorion (A; 80x magnification) in which the outer pore openings can be discovered (B; magnification: 8000x). TEM images of the chorion (C and D) taken by Böhler (2012) show the outer surface of the chorion to be electron-dense, while the thickest part of the chorion is made of different orientated layer, through which the pore canals (arrowheads D; 16000x magnification) meander and form little lacunae (arrowheads in C; 6200x magnification)..... 85
- Figure 28: Sublethal effects in fathead minnow embryos at 120 hpf exposed to 20 g/L PEG 3,000 (A), PEG 6,000 (B) and PEG 12,000 (C, D). Note the effects on eye development (arrow), blood accumulation (arrowhead) and the edema above the yolk (asterisk) and deformation of the yolk itself. Also very prominent are the deformations of the head (A-D) and the formation of pericardial edema (A, B and D) and the bent tails (A, C, D). Pictures taken by A. Keck. 92
- Figure 29: Effects in fathead minnow embryos exposed from 0 hpf to 120 hpf to differently sized PEGs at 20 g/L. A size-dependent increase in affected embryos could be found for PEGs \geq 6,000 Da. ANOVA with comparison to control group (Dunnett's method; * P < 0.1, ** P < 0.01, *** P < 0.001). n= 3 runs à 10 embryos. Data produced jointly with A. Keck..... 93
- Figure 30: Effects in fathead minnow embryos exposed from 24 hpf to 120 hpf to differently sized PEGs at 20 g/L. A size-dependent increase in affected embryos could be found for PEGs \geq 6,000 Da, however only PEG 8,000 and 12,000 revealed statistically significances in affected embryos compared to control (ANOVA with comparison to control group (Dunnett's method; * P < 0.1, ** P < 0.01, *** P < 0.001). n= 3 runs à 10 embryos. Data produced jointly with A. Keck. 94
- Figure 31: Effects in fathead minnow embryos exposed from 48 hpf to 120 hpf to differently sized PEGs at 20 g/L. Overall response of embryos to the different PEG did not exceed 60% threshold. Only PEG 12,000 revealed statistically significances in affected embryos after 48 and 72 hours of exposure (at 96 hpf and 120 hpf) compared to control (ANOVA with comparison to control group (Dunnett's method; * P < 0.1, ** P < 0.01, *** P < 0.001). n= 3 runs à 10 embryos. Data produced jointly with A. Keck..... 95
- Figure 32: Percentage of fathead minnow eggs showing chorion deformations exposed from 0 hpf onwards to PEG 4,000 – 12,000. Deformation of the chorions was rated according to a scale from 0 (no deformation) to 3 (very strong deformation) and are given as the mean. n=3 runs à 10 eggs, except for PEG 12,000 at 120 hpf: 2 runs à 10 eggs, 1 run à 9 eggs. Data produced jointly with A. Keck. 97
- Figure 33: Percentage of fathead minnow eggs showing chorion deformations exposed from 24 hpf onwards to PEG 4,000 – 12,000. Deformation of the chorions was rated according to a scale from 0 (no deformation) to 3 (very strong deformation) and are given as the mean. n=3 runs à 10 eggs, except for PEG 6,000: 1 run à 8 eggs; PEG 8,000: 1 run à 9 eggs; PEG 12,000: 1 run à 7 eggs. Data produced jointly with A. Keck..... 98
- Figure 34: Percentage of fathead minnow eggs showing chorion deformations exposed from 48 hpf onwards to PEG 4,000 – 12,000. Deformation of the chorions was rated

according to a scale from 0 (no deformation) to 3 (very strong deformation) and are given as the mean. n=3 runs à 10 eggs. Data produced jointly with A. Keck..... 99

Figure 35: The distribution pattern of 0.048 µm carboxylate-modified microspheres across the chorion of fathead minnow eggs at 24 hpf (A, B), 48 hpf (C, D) and 72 hpf (E, F). The left pictures (A, C, E) show one plane cross section of the egg and the right pictures (B, D, F) illustrate the 3D picture of the same eggs (all z-stacks). The main fluorescent signal can be found in the adherends of the eggs (arrows) and some fluorescent signal can be found across the chorion. However, no fluorescent signal is found within the egg and the embryos. Scale bars in A, C and E are 300 µm. 106

Figure 36: Optical cross section of the surface of the chorion of a 24 hpf egg exposed to 0.048 µm microspheres showing the adherend. The adherend is not smooth, each distinct fluorescent signal is supposed to represent one microsphere. Scale bar: 150 µm..... 107

Figure 37: Structure of the human hair. The outer cell layer is formed by overlapping cuticle cells, which are composed by the epicuticle, the A-layer, exo- and endocuticle. The cuticle cells surround the cortex. Corticle cells contain pigment granula and nuclear remnants. Their substructures are: macrofibrils composed of intermediate filaments (IF) and the matrix. The further substructures of the IF are coiled coil proteins formed by α-keratin. Scheme taken from Morel and Christie (2011)..... 115

Figure 38: Reaction scheme of the oxidation of *para*-phenylenediamine (PPD) by hydrogen peroxide (H₂O₂) and possible coupling processes. Pathway A: In a first oxidation of PPD, quinonediimine (QDI) is formed which further reacts with a present coupler (here: resorcinol) to form a colorless dimer (leuco-dye). In further oxidative coupling reactions, trinuclear (here indoaniline dye) or polynuclear compounds are formed, resulting in the desired color range. Pathway B: in the absence of couplers, PPD is able to form Bandrowski's base as a result of self-coupling, oxidized by hydrogen peroxide. Scheme taken from Nohynek et al. (2004), adopted from Spengler and Bracher (1990)..... 118

Figure 39: Structural formula of *para*-phenylenediamine (PPD), toluene-2,5-diamine sulfate (PTD) and 2-methoxymethyl-*p*-phenylenediamine (MBB) to illustrate the structural relationship of the three precursor molecules. PTD differs from PPD by an additional methyl group, while MBB is substituted by an additional methoxy-methyl group. Formulas illustrated using PerkinElmer, ChemDraw Professional 15.0 (1998-2015 PerkinElmer Informatics, Inc.). 119

Figure 40: Cumulative mortality (%) of zebrafish embryos exposed for 96 hours to differently aged PPD solutions. PPD solutions aged for 16 hours (blue line) showed the highest toxicity. Insert illustrates LC₅₀ (filled dot) and EC₅₀ (empty dot) values determined for PPD solutions aged between 1 and 24 h. Graphs based on ToxRat[®] calculations and illustrated with SigmaPlot 12.0. 127

Figure 41: Phenotypes of 48 hpf embryos inside the chorion and hatched larvae at 96 hpf exposed to PPD. Column 1 shows the control embryos; column 2 represents 2 mg/L of 4 hours aged PPD stock solution; 3 column shows embryos exposed to 2 mg/L of the 8 hours aged PPD stock solution. Differences in whole body but especially in eye pigmentation can be seen in the PPD treated embryos. A brownish accumulation, indicated by asterisks, in a well-defined area above the gut and the yolk sac is seen. 128

Figure 42: Cumulative mortality (%) of zebrafish embryos exposed for 96 hours to differently aged PTD solutions. Stock solution aged for 8 hours showed the highest toxicity (red

line), while stock solutions aged for more than 24 hours resulted in lower toxicity (blue-green, green and bright green functions). The insert illustrates the concentration at which 50% of the introduced embryos were lethally affected (LC_{50} values) as determined via ToxRat[®] probit analysis. A clear reduction of toxicity with LC_{50} values above 1 mg/L could be shown for PTD solutions aged ≥ 24 h. Graphs based on ToxRat[®] calculations and illustrated with SigmaPlot 12.0. 129

Figure 43: Cumulative mortality (%) of zebrafish embryos exposed for 96 hours to differently aged MBB solutions. All stock solutions showed similar responses in zebrafish embryos. Stock solution aged for 16 hours showed the highest toxicity (blue line). Insert illustrates LC_{50} (filled dot) and EC_{50} (empty dot) values determined for MBB solutions aged between 1 and 48 h. Graphs based on ToxRat[®] calculations and illustrated with SigmaPlot 12.0. 130

Figure 44: Dose-dependent increase of brownish accumulation in 96 hpf zebrafish embryos exposed to MBB solutions aged for 4 hours. The accumulation is found in a distinct area between yolk/intestine tract and swim bladder/notochord (see asterisks). Embryos were exposed to 2 mg/L (A), 4 mg/L (B), 8 mg/L (C), 32 mg/L (D) and 64 mg/L (E) MBB for 96 hours. The accumulation increases between 2 and 8 mg/L, all embryos exposed to higher concentrations showed similar intensity of the accumulation. With rising exposure concentration, also a reduction of body pigmentation can be found. 131

Figure 45: Course of the Neckar River through the German Federal Land of Baden-Württemberg (www.Fahrrad-Tour.de, 2013) 144

Figure 46: Particulate matters of the river water during a flood event settles from the water column onto the well bottoms. Without siphoning most of the precipitations were found at the bottoms of the wells (A), at 24 hpf when the precipitations were pushed aside using a pipette tip for a better identification of effects in embryos (B) and at 96 hpf, when the hatched larva was observed at different places within the well (C). ... 155

Figure 47: Zebrafish embryos exposed for 96 hours to PTD stock solutions in Neckar River flood water: Whereas no effects were seen in embryos exposed to Neckar River flood water alone (A, negative control), embryos exposed to 1 mg/L PTD aged for 8 hours (B), 2 mg/L (C) and 4 mg/L (D) PTD aged for 16 hours showed a yellow-brownish, dose-dependent accumulation in tissue between the swim bladder and the intestine tract (see asterisks). For the pictures, embryos were anesthetized in MS-222 and the precipitations were washed away as much as possible. 156

Table Index

Table 1: Summary of the lethal and sublethal endpoints of the FET determined according to OECD TG 236 (OECD, 2013a), Schulte and Nagel (1994) and Bachmann (2002)... 13	13
Table 2: Changes in chorion area over time on micrographs of zebrafish (<i>Danio rerio</i>) eggs after exposure to PEGs of various molecular weight. Data are given for three independent runs (n = 3) as % of the area measured for micrographs of eggs in corresponding negative controls. In addition, the time until no further shrinkage of the chorion area was observed is listed (taken from Pelka et al.). 31	31
Table 3: General information and technical data for the unstained polystyrene microspheres taken from the certificated of analysis (COA) obtained by Invitrogen, Life Technologies™..... 43	43
Table 4: Laser and microscope settings for evaluation of fluorescent signal within the chorion. 46	46
Table 5: Physical and chemical information of the differently sized microspheres. 64	64
Table 6: Laser and microscope settings for evaluation of fluorescent signal within the chorion 66	66
Table 7: The most important facts about spawning and the chorion of the two common OECD fish species for chemical testing, the zebrafish and the fathead minnow..... 86	86
Table 8: Summary of the lethal and sublethal endpoints of the FET determined according to OECD TG 236 adjusted to the development of the fathead minnow according to Devlin et al. (1996) and Böhler (2012) 90	90
Table 9: Rating system for the different chorion deformations as a result of PEG-induced osmotic effects. Effects were rated from 0 = no deformation with glue-patches visible to 3 = very strong deformations of the chorion with no or only little room for the embryo. Pictures taken by A. Keck. 91	91
Table 10: Laser and microscope settings for evaluation of fluorescent signal within the chorion..... 104	104
Table 11: Chemical names, structures and properties of the tested hair dye precursors PPD, PTD sulfate and MBB. Structural formula illustrated using PerkinElmer, ChemDraw Professional 15.0 (1998-2015 PerkinElmer Informatics, Inc.)..... 122	122
Table 12: All concentrations of the tested PPD, PTD and MBB solutions, their aging process, the amendments with ascorbic acid (AA), the stock solutions and the final concentrations tested in the FET with zebrafish embryos. All concentrations are nominal concentrations..... 125	125
Table 13: Toxicity of the tested hair dye precursors to zebrafish embryos at 96 hpf in the standard fish embryo toxicity (FET) test and with the addition of 0.04% ascorbic acid (AA). A strong reduction of toxicity is found with AA, hence only one LC ₅₀ value could be determined. All listed LC ₅₀ and EC ₅₀ values determined via ToxRat [®] probit analysis. 133	133
Table 14: The concentrations used in the FETs to investigate the influences of 0, 2 or 8 mg/L humic acids (HA) on the toxicity of PTD in zebrafish embryos. Stock solutions and the final test concentrations are listed as nominal concentrations..... 149	149
Table 15: Test design and nominal concentrations of PTD tested in zebrafish FET under supplementation by Neckar River water. 150	150

Table 16: Overview of LC ₅₀ and EC ₅₀ values determined in zebrafish embryos at 96 hpf exposed to PTD with the amendment of humic acid. All listed LC ₅₀ and EC ₅₀ values determined <i>via</i> ToxRat [®] probit analysis.....	152
Table 17: Characterization of the Neckar River water used for the assessment of PTD toxicity under environmentally relevant conditions	154
Table 18: Overview of LC ₅₀ and EC ₅₀ values determined in FET with zebrafish embryos at 96 hpf exposed to PTD in Neckar River water. All listed LC ₅₀ and EC ₅₀ values were determined <i>via</i> ToxRat [®] probit analysis.....	157

Index

Summary	1
Zusammenfassung	3
Introduction	5
Fish embryos as alternatives to animal testing	5
Zebrafish as a model species for ecotoxicological testing of chemicals	9
The Fish Embryo Acute Toxicity Test (FET)	11
Is the chorion a barrier?	14
Aims of the thesis	16
1. Size does matter – Determination of the critical molecular size for the uptake of chemicals across the chorion of zebrafish (<i>Danio rerio</i>) embryos	21
1.1 Abstract	21
1.2 Introduction	21
1.3 Materials and methods	24
1.3.1 Chemicals and materials	24
1.3.2 Fish maintenance	24
1.3.3 Zebrafish embryo acute toxicity test (FET)	25
1.3.4 Osmosis-related effects by PEG solutions	25
1.4 Results	26
1.4.1 Acute and sublethal effects of polyethylene glycols in the FET	26
1.4.2 Osmosis-dependent effects on chorion shape of zebrafish eggs: initial efflux from eggs	30
1.4.3 Osmosis-dependent effects on chorion shape of zebrafish eggs: gradual reflux leading to (partial) equilibrium	31
1.5 Discussion	33
1.6 Conclusions	38
2. Is the chorion an obstacle for nanoscale particles?	41
2.1 Abstract	41
2.2 Introduction	41
2.3 Materials and methods	43
2.3.1 Chemicals	43
2.3.2 Fish maintenance and egg production	44
2.3.3 Exposure	44
2.3.4 Preparation for microscopic evaluation	44
2.3.5 Preparation of cryosections of the chorion	45

2.3.6	Analysis of the microsphere uptake and distribution	45
2.4	Results	46
2.4.1	Distribution of microspheres on and across the chorions	47
2.4.2	Dechorionated embryos - exposure within the chorions	50
2.4.3	Details of the chorion	52
2.5	Discussion.....	54
2.6	Conclusions	57
3.	Influence of functional groups displayed on the surface of nanoscale polystyrene particles on the uptake across the chorion.....	61
3.1	Abstract.....	61
3.2	Introduction	61
3.3	Materials and methods.....	63
3.3.1	Chemicals	63
3.3.2	Fish maintenance and egg production	64
3.3.3	Exposure.....	64
3.3.4	Preparation for microscopic evaluation.....	65
3.3.5	Analysis of the microsphere uptake and distribution	65
3.4	Results	66
3.5	Discussion.....	73
3.6	Conclusions	78
4.	Permeability of the chorion of the fathead minnow, <i>Pimephales promelas</i>	81
4.1	Abstract.....	81
4.2	Introduction	81
4.3	The critical molecular size of polymers to cross the chorion of fathead minnow.....	88
4.3.1	Materials and methods	88
4.3.1.1	Chemicals.....	88
4.3.1.2	Fish maintenance and egg production.....	88
4.3.1.3	Egg exposure.....	89
4.3.1.4	Endpoints and evaluation.....	89
4.3.2	Results	92
4.3.2.1	Effects of differently sized PEG on embryonic development	92
4.3.2.2	Effects on chorion shape of fathead minnow embryos	96
4.3.3	Discussion	100

4.4	The permeability of the fathead minnow chorion to fluorescent microspheres	103
4.4.1	Materials and methods	103
4.4.1.1	Chemicals.....	103
4.4.1.2	Exposure and microscopically evaluation	103
4.4.2	Results	104
4.4.3	Discussion	107
4.5	Conclusions	109
5.	Potential of the fish embryo toxicity test (FET) to detect the varying toxicities of highly reactive substances	113
5.1	Abstract.....	113
5.2	Introduction	114
5.3	Material and methods	121
5.3.1	Chemicals	121
5.3.2	Zebrafish maintenance and egg production	122
5.3.3	Acute toxicity in the zebrafish embryo test (FET).....	123
5.3.4	Preparation of test solutions	123
5.3.5	Supplementation of the test solutions by ascorbic acid.....	124
5.3.6	Statistical analysis	124
5.4	Results	126
5.4.1	Age-dependent toxicity of PPD, PTD and MBB in zebrafish embryos at 96 hpf 126	
5.4.2	Influence of ascorbic acid on toxicity of PPD, PTD and MBB as determined in zebrafish embryos	132
5.5	Discussion.....	134
5.6	Conclusions	138
5.7	Acknowledgement.....	139
6.	Influences of humic acids and native river water on the toxicity of toluene-2,5-diamine sulfate (PTD).....	143
6.1	Abstract.....	143
6.2	Introduction	143
6.3	Material and methods	148
6.3.1	Chemicals	148
6.3.2	Zebrafish maintenance and egg production	148
6.3.3	Fish embryo toxicity test (FET)	148
6.3.4	Modulation of PTD toxicity by addition of humic acids	149

6.3.5	FET in native river water	150
6.3.6	Characterization of the river water	150
6.3.7	Statistical analysis	151
6.4	Results	151
6.4.1	Modulation of PTD toxicity by humic acids	151
6.4.2	Sampling conditions and river water characterization	152
6.4.3	Toxicity of <i>p</i> -toluenediamine sulfate (PTD) in Neckar River water	155
6.5	Discussion.....	157
6.6	Conclusions	159
6.7	Acknowledgements	160
7.	Final Conclusions.....	161
	References	165
	Annex	187

Summary

The Fish Embryo Toxicity Test (FET) has been proposed and adopted by the OECD as a suitable alternative method for the acute toxicity testing of chemicals in adult fish. The present study was conducted to evaluate boundary parameters of the standard test design and how different modules can be changed to fill in the need for more sophisticated endpoints. The key aspects of this thesis were (1) the definition of impacts of the chemical and physical properties of a substance to cross the chorion, the acellular envelope by which the developing embryo is surrounded during the first days of its development; (2) the possibility to assess the toxicity and behavior of highly reactive compounds in fish embryos; and (3) the transferability of the test design to study the behavior of substances in the environment under controlled conditions.

The chorion permeability was studied with differently sized polyethylene glycols (PEGs) which were applied to generate an osmotic gradient strong enough to result in deformed chorions, if no uptake across the chorion is feasible. The extent of chorion shrinkage depended on PEG molecular weight, thus size, and the duration of exposure. The barrier function of the zebrafish chorion for molecules larger than 3,000 at 24 hpf and 4,000 Da at 48 hpf was defined. For fathead minnow, the critical size to cross the chorion was narrowed down to 4,000 Da. Imaging with nano-sized fluorescent microspheres revealed that besides the size of a molecule the surface properties, e.g. residue groups, are a key factor for uptake. Carboxylate-modified microspheres (0.05 to 0.2 μm) of a size small enough to be able to cross the chorion *via* the pores were completely blocked by the chorion of zebrafish and fathead minnows. In further testing series with similarly sized microspheres bearing no additional functional groups on the surface were shown to be taken up into zebrafish embryos and thus across the chorion. In order to expand the FET beyond the standard test design, as a further variation of the protocol, tests were initiated with differently aged test solutions of highly reactive substances with the ability of self-coupling. To clarify if the mode of action is triggered by the formation of reactive oxygen species or other free radicals, ascorbic acid as a scavenger was shown to be effective. The transferability of the standard laboratory protocol to a more environmentally relevant approach was documented by tests both in modified test medium and natural waters. Whereas the complexity of aggregation, disaggregation and the formation of complexes with naturally occurring organic matters could not be imitated by the amendment of humic acids, the use of natural water samples could be shown to yield results comparable to those expected in the environment.

Zusammenfassung

Als Alternative zum akuten Fischtoxizitätstest mit adulten Fischen wurde von der OECD der Fisch Embryo Toxizitätstest mit dem Zebraärbling (*Danio rerio*) verabschiedet. Die vorliegende Studie sollte diverse Randparameter des Standardtestdesigns und die Veränderbarkeit von einzelnen Komponenten für eine anspruchsvollere Test-Auswertung ermitteln. Die Schwerpunkte lagen auf (1) der Klärung welche Rolle die chemischen und physikalischen Eigenschaften von Testsubstanzen bei der Überwindung des Chorions, das während der ersten Tage den Embryo umgibt, spielen; (2) der Möglichkeit, Toxizität und Verhalten von hochgradig reaktiven Substanzen in Fischembryonen zu testen; und (3) der Übertragbarkeit des Testprotokolls auf natürliche Umweltbedingungen, um das Verhalten von Substanzen in der Natur möglichst realistisch unter kontrollierten Bedingungen darzustellen.

Die Durchgängigkeit des Chorions wurde mit verschiedenen großen Polyethylenglykolen (PEGs) getestet. Diese wurden hoch-konzentriert eingesetzt um einen osmotischen Gradient zu erzeugen, der in der Lage ist das Chorion zu deformieren sofern keine Aufnahme über das Chorion stattfinden kann. Das Ausmaß des Schrumpfens war eindeutig abhängig von dem PEG-Molekulargewicht und der Belastungsdauer. Der Rückfluss von Wasser und PEG-Molekülen in das Zebraärblings-Ei wurde für Moleküle größer als 3.000 Da (24 h nach der Befruchtung), bzw. größer als 4.000 Da (48 h nach der Befruchtung) deutlich verringert. Die kritische Größe um das Chorion der Dickkopfritze (*Pimephales promelas*) zu überwinden, konnte auf 4,000 Da bestimmt werden. Mit Hilfe von fluoreszierenden Nano-Partikeln konnte gezeigt werden, dass neben der Substanzgröße die Oberflächenbeschaffenheit eines Moleküls von großer Bedeutung bei der Aufnahme durch das Chorion ist. Mit Carboxylgruppen modifizierte Partikel wurden, trotz ihrer Größe von 0.05 – 0.1 µm, die eine Passage durch die Chorionporen erlauben sollten, von der Eihülle von Zebraärbling und Dickkopfritze abgeblockt. Weitere Versuche mit nicht weiter modifizierten Partikeln zeigte eine Aufnahme in den Embryo und somit auch durch das Chorion des Zebraärblings.

Um die Anwendbarkeit des FETs weiter auszubauen, wurden weitere Änderungen des Testprotokolls vorgenommen. Durch das Altern von reaktiven Testsubstanzen wurde das toxische Potenzial von der Grundsubstanz und den jeweils geformten Produkten ermittelt. Um festzustellen, ob die Toxizität durch die Bildung von reaktiven Sauerstoffmolekülen oder anderen freien Radikalen getriggert wird, wurde Ascorbinsäure erfolgreich als Radikalfänger eingesetzt. Eine Übertragung des Testprotokolls auf umweltrelevantere Szenarien konnte sowohl durch die Durchführung mit modifiziertem Testwasser als auch mit natürlichem Wasser ge-

zeigt werden. Während die Zugabe von Huminsäuren die Komplexität von Aggregation, Disaggregation und die Komplexbildung mit natürlich vorkommendem organischem Material nicht ausreichend darstellen konnte, konnte bei Nutzung von natürlichen Gewässerproben als Matrix dem Verhalten in der Umwelt vergleichbare Resultate erzielt werden.

Introduction

Fish embryos as alternatives to animal testing

Acute toxicity tests with vertebrates are an integral part of the risk assessment and hazard identification of industrial chemicals, plant protection products, biocides, pharmaceuticals, feed additives and effluents (Scholz et al., 2013). The enormous amounts of chemicals produced and traded within the European Union lead to an increase in safety assessments and thus an increase in test animals (Basketter et al., 2012). Ethical concerns and animal welfare restrictions demand the development of non-animal testing strategies to ensure chemical safety for man and the environment. As early mentors for developing new alternative methods, Russel and Burch (1959) claimed to “*refine, reduce or replace*” animal testing. Thus, alternative methods should be developed to completely *replace* an animal test, to *reduce* the number of animals needed or to at least *refine* an existing test method to reduce pain and suffering of the test animals. This statement is also known as the 3R-principles and has been incorporated into current legislations and regulations. One of the biggest obstacles for the acceptance of alternative methods is that they should achieve similar results as obtained in animal testing, of which the bigger part had not been validated and whose reproducibility is partly scarce.

When in 2003 the 7th amendment (Directive 2003/15/EC) of the EU Directive 76/768/EEC on cosmetics (EU, 1976) came into force, the ban of animal testing was mandatory as soon as valid alternative methods were available. The pressure on development and validation of non-animal testing has been increased since 2009, when animal testing was completely banned for cosmetic products and their ingredients in the EU (Adler et al., 2011; Basketter et al., 2012; EU, 2009), supported by a marketing ban by Directive 1223/2009 (EU, 2009). In the field of human hazard identification the results from several non-animal *in vitro* methods are accepted by the OECD, especially in the area of skin sensitization (i.e., DPRA, ARE-Nrf2 Luciferase Test Method and KeratinoSens™), skin irritation/skin corrosion (i.e., RhE, TER, EpiSkin™, EpiDerm™) and eye damage/eye irritation (i.e., HET-CAM, BCOP, ICE, FL, EpiOcular™ EIT and STE; see status report by ECVAM (2015)).

In 2007, the EU Regulation on chemicals and their safe use – REACH (Registration, Evaluation, Authorization and Restriction of Chemical substances (EC, 2007)) came into force and the incorporation of the 3R-principles also became of major significance. The requirement of (eco)toxicological data is now strongly dependent on the tonnage of the produced or imported chemicals, and the extend of the tests batteries is exactly defined by the REACH Regulation (Annex VII – X, EC (2007)). According to the EU Regulation 1107/2009 (EC, 2009) all used

active substances and their formulated plant protection products need to be shown to pose an acceptable risk to humans, animals and plants before a successful registration in Europe. Since fish and amphibians play a major role in the aquatic food web, they are commonly used in higher tier studies for environmental hazard classification and risk assessment of chemicals. Traditionally, the acute toxicity is determined with fish after 96 hours of exposure (OECD, 1992), however, ethical concerns have arisen, since fish are also considered capable of the nociception and pain perception (Sneddon, 2009). Moreover, *in vitro* alternative methods often offer a differentiated testing approach and promise a more economic, low-cost procedure. The development, validation and approval of relevant ecotoxicological alternative methods became mandatory to implement the demand of the REACH Regulation (Lilienblum et al., 2008) and thus, enormous effort was taken to fulfill these demands. The OECD formed a working group and published a Fish Toxicity Framework document, discussing all test guidelines (TG) and strategies adopted until 2011, reviews animal welfare and suggests possibilities to minimize fish toxicity testing (Hutchinson et al., 2016; OECD, 2012). To replace the acute toxicity tests with fish, e.g. OECD TG 203 (OECD, 1992), different approaches have been suggested: (1) the use of non-testing strategies for predicting the toxicity, such as grouping of chemical substances, quantitative structure-activity relationships (QSAR), read-across and waiving (Burden et al., 2016; Scholz et al., 2013), (2) the use of cell cultures (Fent, 2001; Schirmer et al., 2008; Segner, 1998, 2004) and (3) the use of fish embryos, especially zebrafish, *Danio rerio*, embryos (Lange et al., 1995; Nagel, 2002).

Various studies found good correlations of toxicity in adults and that in zebrafish embryos (Belanger et al., 2013; Knobel et al., 2012; Lammer et al., 2009; Nagel, 2002; Ratte and Hammers-Wirtz, 2003b; Roex et al., 2002), making the use of fish embryos the most promising approach as an alternative for acute fish toxicity tests. Moreover, embryonic fish are suggested to be suitable for the screening of large numbers of toxic substances (McKim, 1977; Van Leeuwen et al., 1985). In Germany, the 48 hours wastewater test with zebrafish embryos (DIN, 2001; ISO, 2007) has replaced in 2003 the traditional toxicity test using adult fish in the sewage water assessment. Consequentially, in 2006 the German Federal Environmental Agency (UBA) submitted an extended version of the zebrafish embryo acute toxicity test (zFET) as an alternative method to the acute toxicity test with fish to the Working Group of the National Coordinators of the OECD Test Program (Braunbeck et al., 2014). After several years of planning, a two-phase validation of inter- and intra-laboratory reproducibility and two rounds of commenting and revisions, the validation team submitted the final draft in April 2013 (Braunbeck et al., 2014; Busquet et al., 2014; Halder et al., 2012). In July 2013,

the OECD has finally assembled the new guideline 236 “*Fish Embryo Acute Toxicity Test (FET)*” for the testing of chemicals (OECD, 2013a), which has been officially recommended by the EURL ECVAM (European Union Reference Laboratory for Alternatives to Animal Testing) in 2014 (ECVAM, 2014). One of the recommended fish species for testing is the zebrafish, *Danio rerio*, as the use of its embryos before 120 hours post fertilization (hpf) are declared as non-protected stages (Belanger et al., 2010; EU, 2010; Strähle et al., 2012), because they do not feed externally (EU, 2010).

In the last decades, the zebrafish embryo has emerged as an intensively used model organism in developmental biology, pharmacology and (eco)toxicology (Aleström et al., 2006; Braunbeck et al., 2014; Chakraborty et al., 2009; Dooley and Zon, 2000; Hill et al., 2005; Lele and Krone, 1996; McGrath and Li, 2008; Nagel, 2002; Parng et al., 2002; Peterson and MacRae, 2012; Rubinstein, 2006; Schulte and Nagel, 1994; Selderslaghs et al., 2009; Sipes et al., 2011; Yang et al., 2009). In (eco)toxicological studies, chemicals are tested with zebrafish embryos and have been shown to provide reliable endpoints for safety and risk assessment (Belanger et al., 2010; Braunbeck et al., 2005; Eaton et al., 1978; Hill et al., 2005; Lammer et al., 2009; McKim, 1977; Nagel, 2002; Scholz et al., 2008; Schulte and Nagel, 1994). Besides acute toxicity evaluating only mortality, other endpoints can be implemented to differentiate the mode of actions of the tested chemicals (summarized in Figure 1).

The fish embryos can be exposed in various scenarios under controlled conditions in the laboratory. Traditionally, test substances are dissolved in the medium, however, some substance classes' demand for more elaborated exposure scenarios. Highly lipophilic substances can be applied *via* passive dosing or *via* injection into the perivitelline space inside the egg envelope or the embryo. In a modified FET, embryos can be exposed to native sediment to gain information about environmental conditions of lakes and rivers. After exposure in the FET, the embryos can be used to identify genotoxicity of single substances or complex environmental samples such as sediments or sediment extracts (Braunbeck et al., 2014; Garcia-Käufer et al., 2015; Häfeli et al., 2011; Kosmehl et al., 2006; Osterauer et al., 2011). Also endocrine disrupting potential of environmental relevant substances have been detected and their modes of action have been investigated in zebrafish embryos (Brion et al., 2004; Brion et al., 2012; Cohen et al., 2008; Cohen et al., 2014; Schiller et al., 2013). Moreover, single target organs in the endocrine system like the thyroid can be addressed easily in zebrafish embryos and eleutheroembryos (Baumann et al., 2016; Elsalini and Rohr, 2003; Huang et al., 2016; Power et al., 2001; Thienpont et al., 2011). There has been an increasing focus on establishing zebrafish embryos for the screening of non-animal developmental toxicity and chemical mode

of action within vertebrates (Augustine-Rauch et al., 2010; Brannen et al., 2010; Panzica-Kelly et al., 2010; Paskova et al., 2011; Selderslaghs et al., 2009; Volz et al., 2015). Since early life stages were shown to be capable of metabolic transformation (Ito et al., 2010; Otte et al., 2010; Weigt et al., 2011; Weigt et al., 2012), the zebrafish embryo is the most promising model organism for detecting teratogenicity of chemicals and pharmaceuticals. However, harmonization of the testing systems and the endpoints for the identification of potential teratogens are crucial for prioritizing the chemicals for testing in higher vertebrates (Beekhuijzen et al., 2015; Ducharme et al., 2015; Gustafson et al., 2012; Nishimura et al., 2016). Expanding the FET towards more sophisticated endpoints like behavior, histology or enzyme activities, zebrafish embryos and hatched larvae have received increasing attention in the evaluation of neurotoxicity (de Esch et al., 2012; Klüver et al., 2015; Küster, 2005; Legradi et al., 2015; Linney et al., 2004; Nishimura et al., 2015; Padilla et al., 2011; Parng et al., 2007; Peterson et al., 2008; Tierney, 2011; Ton et al., 2006). Additionally, the lateral line system of the larvae with hair-cell bearing neuromasts can detect specifically ototoxic compounds (Chiu et al., 2008; Froehlicher et al., 2009; Ton and Parng, 2005). The broad applicability and the advantages of non-animal testing with zebrafish embryos makes the FET a versatile tool for the detection of various general or highly specialized endpoints. An overview of the different testing scenarios and endpoints as described above is found in Figure 1.

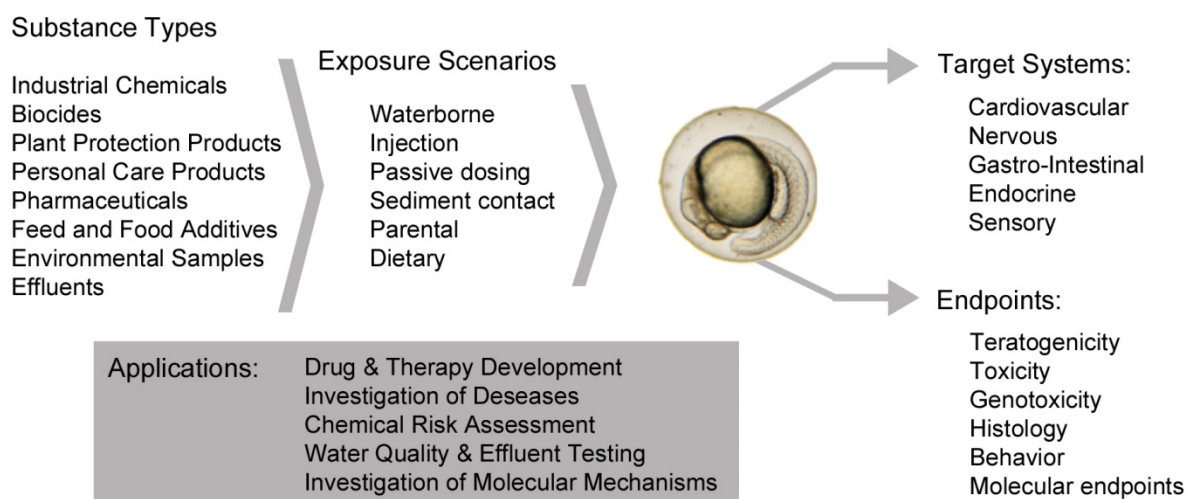


Figure 1: Overview of the different testing scenarios for various chemicals and the target systems and endpoints in the zebrafish embryo tests.

Zebrafish as a model species for ecotoxicological testing of chemicals

The zebrafish, *Danio rerio* (Figure 2), was first described by Hamilton-Buchanan in 1822 (Hamilton-Buchanan, 1822). It is a small benthopelagic freshwater representative of the family Cyprinidae and originates from the Ganges River system, Burma and Sumatra (Eaton and Farley, 1974). As adults, they measure 3 to 5 cm with a fusiform and laterally compressed body. The mouth is directed upwards with two pairs of barbels.

Male and female fish are both brownish-green colored with a white-yellow belly and five to seven dark blue horizontal lateral stripes extending from behind the operculum onto the end of the caudal fin. Only under spawning conditions, males can be easily distinguished from females by their more slender body and an orange to reddish tint in the silvery stripes along the body, while females can be recognized by their swollen bellies.



Figure 2: Adult *Danio rerio*. Upper individual: female can be recognized by its swollen body, lower individual: male with reddish tint in the silvery bands. Picture: E. Leist

The zebrafish is an excellent laboratory model species for toxicology, neurobiology and genetics, as well as in general molecular and developmental biology (Hill et al., 2005; Kimmel et al., 1995; Laale, 1977; Lele and Krone, 1996; Spitsbergen and Kent, 2003; Westerfield, 2000; Yang et al., 2009). It is comparably small, inexpensive, readily maintainable, easy to care for in the laboratory and will provide a large number of eggs (Laale, 1977). Maturity is reached within three months, so this short generation time is a striking feature for genetic and reproduction research. Egg production is possible throughout the year and one female produces 50-200 transparent eggs per day (Braunbeck et al., 2005; Eaton and Farley, 1974). Due to the transparency of the egg envelope, the chorion, the development of the embryos and its organs can be observed under a microscope. The embryos fully develop within 96 hours at 26 °C and the embryonic development was described in detail in numerous studies (Hisaoka and Battle, 1958; Kimmel et al., 1995; Laale, 1977). Therefore not only normal development can be studied, but also teratogenic and embryotoxic effects produced by chemicals.

A detailed description of embryonic development is a fundamental prerequisite for estimating aberrations due to chemical exposure and the investigation of the modes of action. This para-

graph summarizes the important stages of embryonic ontogenesis under optimal conditions as described by Kimmel et al. (1995), Westerfield (2000) and (Strähle et al., 2012).

The eggs of *Danio rerio* are telolecithal and measure 0.7 – 1 mm in diameter. The first discoidal partial cleavage occurs after about 45 minutes and thereafter cleavage continues every 15 minutes until entering the blastula period. In this stage, several important developments take place: the embryo enters midblastula transition, the yolk syncytial layer forms, and epiboly begins. The gastrula period starts 5.25 hours post-fertilization. At this point, 50% of the yolk is covered by the yolk syncytial layer and the blastodisc, defining the 50% epiboly stage. 10 hours post fertilization (hpf), epiboly is finished and the embryo enters the segmentation period, in which the somites develop, the primary organs become visible, the tail bud becomes more prominent and the embryo elongates. During the next hours, the developing tail begins to detach from the yolk and the embryo grows in size. By now, the trunk myotomes produce weak muscular contractions, the lens placode appears and the otic placode has hollowed out into the otic vesicle. Furthermore, differentiation of the brain and the neuronal system takes place. At the beginning of the pharyngeal period (24 - 48 hpf), the embryo is about 1.9 mm long and characterized by a well-developed notochord and a completed set of 30 somites. The nervous system is expanded, and the brain is sculptured into five lobes. The final body shape of the larva can be recognized by now, since the head begins to straighten, the tail has detached completely from the yolk and fins begin to form. Moreover, spontaneous movement becomes visible. The anlage of the eye is clearly visible. The heart begins to beat irregularly and blood cells begin to circulate. At an age of 30 hours, the embryo is about 2.5 mm long and tail morphogenesis comes to an end. Pigmentation of the eyes and the body become visible. The heart beat is becoming more prominent, and blood circulation is stronger. Shallow pectoral fin buds become visible and more prominent at 42 hpf. During the hatching period between 48 and 72 hpf, the embryo grows in size. Pigmentation in form of star-shaped melanophores spreads out over the body. The mouths repositions from a midventral position between the eyes to an anterior position, protruding beyond the eyes. The majority of embryos have hatched by 72 hpf, and the larvae have already completed most of its early morphogenesis and now grow very rapidly. The mouth slits open and digestive organs are developed, but the anus open 24 h later, at 96 hpf. Although some swimming movements of the larvae become visible shortly after hatch, the free swimming stage of embryos can be found only after 120 hpf. The swim bladder has to be fully filled with air, which takes the embryo 3 - 4 days, startling at 72 hpf. At 28.5 °C, feeding starts at about 120 hpf, however, this is strongly dependent on rearing temperature.

The Fish Embryo Acute Toxicity Test (FET)

Fish maintenance and egg production have repeatedly been described in detail (Kimmel et al., 1995; Nagel, 2002; Spence et al., 2008) and have been updated for the purpose of the zebrafish embryo acute toxicity test (Lammer et al., 2009). The day before a test starts, breeding groups of non-treated, mature zebrafish at a ratio of 2 males and 1 female are transferred into special spawning tanks. These tanks hold one smaller tank with a grid instead of a bottom, under which a spawning tray is placed. The smaller tank is inserted onto a small platform to achieve a water depth gradient (modification according to Sessa et al. (2008)). At the shallower end, an artificial plant made of green plastic is placed to stimulate mating (see Figure 3). Since zebrafish are photoperiod-dependent in their breeding, mating, spawning and fertilization of the eggs take place within 30 to 60 minutes after onset of the light-period in the morning. Subsequently, the trays are removed and the eggs are transferred into big crystallization dishes with clean water.

After checking the quality of the spawned eggs, the pre-exposure is started as quickly as possible (< 1.5 hpf). Fertilized eggs are transferred into small glass dishes bearing about 5 - 10 ml of the respective test concentration. Only viable, fertilized and well divided eggs are transferred each separately into one well containing 2 ml of freshly prepared test concentration. The test is conducted with 20 embryos per concentration and 24 embryos per negative control. The four wells in the last column of each plate are internal negative controls. To verify sensitivity of the used batch, an additional positive control (4 mg/L 3,4-dichloroaniline) is performed. To prevent any loss of the chemical due to binding to the plastic wells, the plates are pre-saturated for 24 hours with the respective test concentration. The plates are covered with self-adhesive tape and the lid and placed in an incubator at 26 ± 1 °C with a light regime of 14 h light and 10 h dark. Figure 3 shows an overview of the FET procedure. The quality controls of the test are: fertility rate $\geq 70\%$, survival of the negative control embryos $\geq 90\%$ and in the positive control a mortality rate of $\geq 30\%$.

Embryos are examined every 24 hours until 96 hours post fertilization (see Figure 1), and lethal and sublethal endpoints (compare Table 1) are determined according to OECD TG 236 (2013a), Schulte and Nagel (1994) and Bachmann (2002).

Lethal effects: Coagulated embryos are determined at each observation time point. Besides, every 24 hours the detachment of the tail from the yolk and the lack of somites are recorded. The heartbeat in normal developed embryos is visible after 48 hours; thus, absence of the heartbeat is recorded from this time point onwards.

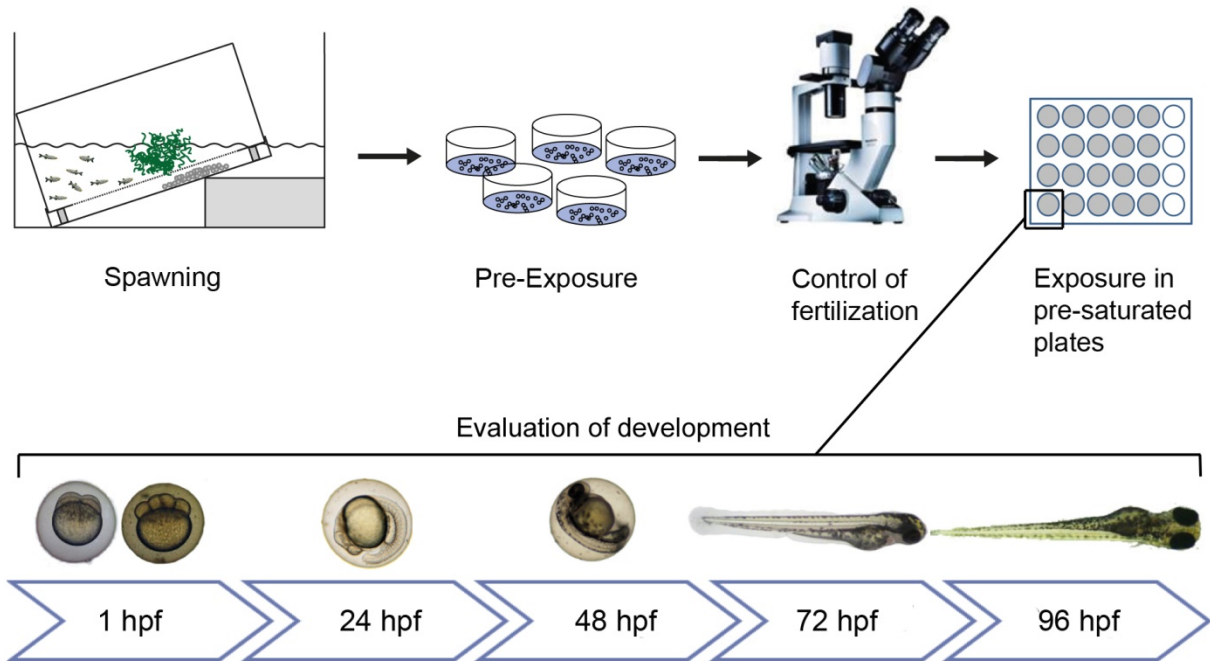


Figure 3: Procedure of the FET according to OECD TG 236 (OECD, 2013a). After spawning, the eggs are distributed into the respective test concentration in crystallization dishes, checked for fertilization success under the binocular and then distributed separately into the wells of pre-saturated 24-well plates. Last 4 wells are for internal negative control (white wells). Observation of embryo development is performed daily until 96 hpf. Graph according to Lammer et al. (2009) and Sessa et al. (2008).

Sublethal effects: Embryos are examined for their development and, if retarded, recorded as underdeveloped. After 24 hours, the lack of spontaneous movement is considered as sublethal, if no movement occurred within 30 seconds. This is terminated to 24 hpf since at this point the embryo has reached a length which confined the ability to move inside the chorion. Lack or reduction of blood circulation is recorded, as well as a reduced heartbeat. From 48 hpf onwards, the pigmentation of the eyes and the body are checked and edemata of the yolk sac or the pericardium are recorded. Embryos showing malformations of the eye anlage, the whole head, the spine, the tail or the somites are recorded separately. In general, all aberrations from the normal development and the negative control are noted in detail at each time point.

Table 1: Summary of the lethal and sublethal endpoints of the FET determined according to OECD TG 236 (OECD, 2013a), Schulte and Nagel (1994) and Bachmann (2002).

Toxicological endpoints	Exposure time (hpf)				
	24	48	72	96	120
Lethal endpoints					
Coagulation	*	*	*	*	*
Non-detachment of the tail	*	*	*	*	*
Lack of somites	*	*	*	*	*
Lack of heartbeat		*	*	*	*
Sublethal endpoints					
Lack of spontaneous movement	*				
Reduced heartbeat rate		*	*	*	*
Reduced or lack of blood circulation		*	*	*	*
Reduced or lack of pigmentation		*	*	*	*
Affected eye development	*	*	*	*	*
Edema formation (yolk sack or pericardium)		*	*	*	*
Tail deformation ^a	*	*	*	*	*
Spine deformation ^a	*	*	*	*	*
Somite deformation	*	*	*	*	*
Head deformation	*	*	*	*	*
Retardation in development	*	*	*	*	*

^a might be difficult to see within the chorion at 24 and 48 hpf

Is the FET protocol transferable to assess difficult substances?

To expand the full potential and advantages of the FET for testing and screening of a variety of chemical substance classes further modifications of the standard testing procedure are needed. An alternative method using non-protected stages is especially attractive for the high throughput testing of industrial chemicals, pharmaceuticals or ingredients of cosmetic products. Challenging chemicals, such as quickly degrading substances are hard to assess properly and need special considerations.

Hair dye molecules for example, are a class of highly reactive molecules able to react with air- and waterborne oxygen to form a variety of oxidized products and metabolites. Only previously, Belanger et al. (2013) have well established the relationship between FET and classical acute fish toxicity *in vivo* including some oxidative dyes.

The assessment of the toxicity of the parent compound and the formed metabolites and by-products in the FET might be challenging in the standard approach. If only diluted in water, a mixture of parent molecules and age-dependent amounts and classes of metabolites and/or

products will be assessed. To cover the ability of auto-oxidation and self-coupling of these reactive molecules, the process of aging of the stock solution before introducing the test organisms, freshly fertilized fish eggs, might be a small but powerful modification to cover the transformation of the molecules to various products. A possible option for assessing only the parent compound toxicity might be the prevention of oxidation by the amendment of scavengers.

Is the chorion a barrier?

Although an excellent correlation between acute toxicity data determined with adult fish and fish embryos (Lammer et al., 2009; Nagel, 2002; Ratte and Hammers-Wirtz, 2003a; Roex et al., 2002), the egg envelope, the chorion, has repeatedly been discussed as a potential barrier for the uptake of chemical substances.

For the first 2-3 days, the developing zebrafish embryo is surrounded by this acellular chorion known to be about 1.5 – 2.5 μm thick, consisting of three layers (Bonsignorio et al., 1996; Hisaoka, 1958; Laale, 1977; Rawson et al., 2000). The chorion is pierced by pore canals (see Figure 4) which are supposed to be important for the exchange of gas and excretion products (Hisaoka, 1958). The pores are distributed all over the chorion, with an estimated amount of 7.2×10^5 (Hart and Donovan, 1983). Taking a closer look at the pores, they pierce only the innermost and middle layers. The outer diameter of the chorion pores have been measured to be 0.2 μm in an unfertilized egg (Hart and Donovan, 1983) and 0.5 - 0.7 μm in a fertilized egg in gastrula stage (Rawson et al., 2000). Rawson et al. (2000) determined the center-to-center distance to 1.5 – 2.0 μm , which Lee et al. (2007) verified in the chorion of living embryos using optical microscopy. The pore canals are cone-shaped, displaying a corkscrew ridged wall with a larger diameter at the inner surface (Rawson et al., 2000). However, on the outside of the chorion, several studies applying electron microscopy have found an electron-dense layer, which at some points appear to plug the pores completely (Hart and Donovan, 1983; Lillicrap, 2010; Rawson et al., 2000). Scanning electron microscopic (SEM) images taken by Lillicrap (2010) at 8000-fold magnification showed this layer to consist of individual polypeptides covering the outside of the chorion recessing into the pores (Figure 4 D).

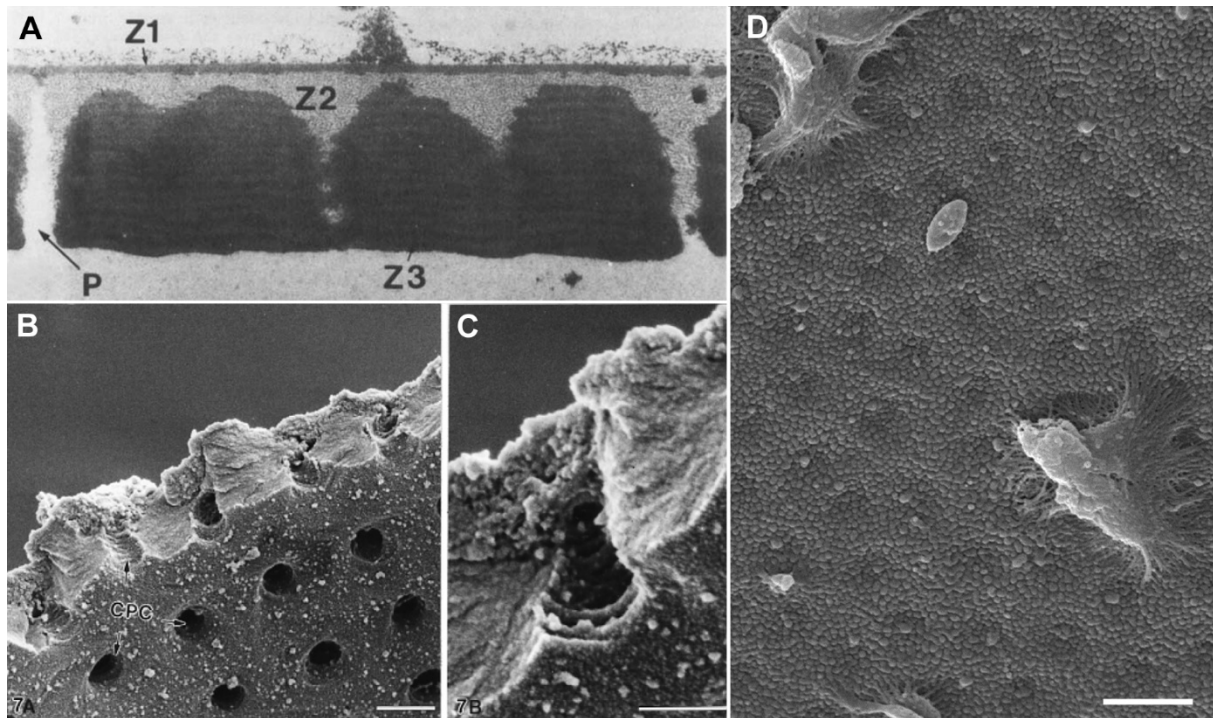


Figure 4: Ultrastructure images of the zebrafish chorion. (A) TEM image of a cross section through the chorion of an unfertilized egg shows the organization into an outer, electron-dense (Z1), a middle, electron-lucent (Z2) and an inner, electron-dense (Z3) layers. The pore canal (P) does not pierce the outer layer (Z1), which is covered by a loose film (x17775; Hart and Donovan (1983)). (B and C) FE-SEM images showing the view on the inner surface of the chorion and reveal the cone-shaped form of the chorion pore canals (CPC; scale bars: 1 μm in panel B and 0.5 μm in panel C; Rawson et al. (2000)). SEM image of the outer surface of the chorion (D) reveals a dense polypeptide layer, recessing into the pore canals, with distinct projections and microorganisms adhere to it (x8 000, scale bar: 2 μm ; Lillicrap (2010))

Under the influence of estrogens, the female produces in its liver vitellogenin which accumulates in the maturing oocyte as the yolk. However, the proteins to form the egg envelope derive only from the ovary (Del Giacco et al., 2000; Guraya, 1986; Wang and Gong, 1999). These chorion forming proteins, also called *zona radiata* (*zr-*) or *zona pellucida* (*zp-*) proteins, are found to be homologous to mammalian *zona pellucida* proteins (Del Giacco et al., 2000; Murata, 2003; Wang and Gong, 1999) and are clearly conserved among teleostean fish (Arukwe and Goksoyr, 2003). cDNA analysis revealed two major genes encoding for the chorion (*zona pellucida*) proteins, Zp2 and Zp3 (Mold et al., 2001; Mold et al., 2009; Sano et al., 2008; Wang and Gong, 1999), while Bonsignorio et al. (1996) found four major polypeptides (116, 97, 50 and 43 kDa). The 116 and 50 kDa proteins were stained by lectins, suggesting being N-linked glycoproteins. Amino acid analysis revealed more serine but less proline content compared to other species and Pullela et al. (2006) detected thiol-rich proteins in the chorion of zebrafish *via* DSSA probes. Shortly after fertilization *via* the micropyle, the chorion proteins are cross-linked by a transglutaminase, leading to chorion hardening. This process is assumed to prevent polyspermy and to ensure an effective protection of the embryo (Hart and Donovan, 1983; Kim et al., 2004; Murata, 2003; Sano et al., 2008).

During development, the chorion structure and its permeability change dramatically. Within the first hours post fertilization (hpf), the chorion hardens and thus prevents polyspermy, protects the developing embryo and leads to a reduced permeability. This hardening process has been demonstrated with effluent to which embryos exposed from 0 - 1 hpf were more sensitive compared to embryos exposed from 4 hpf onwards (Gellert and Heinrichsdorff, 2001). The stability of the chorion also decreases with age, as Kim et al. (2004) showed with an increased penetration force needed for punctuating the chorions of blastula and gastrula staged embryos than for the ones of pre-hatching staged embryos. Additionally, Kais et al. (2013) illustrated a time-dependent increase in permeability of the chorion at 48 hpf compared to 24 hpf by an increased uptake of 2,7-dichlorofluorescein.

Whether a molecule is able to pass the chorion or not, seems to be dependent on its chemical and physical properties or its size. A restriction in uptake across the chorion was postulated for some small molecules, heavy metals, highly lipophilic substances and nanomaterials (Böhme et al., 2015b; Braunbeck et al., 2005; Fent et al., 2010; Meinelt et al., 2006; Osborne et al., 2013; Ozoh, 1980). Big and bulky substances, like polymers might also be restricted. These polymers and some high molecular weight surfactants (40,000 – 100,000 g/mol) were less toxic to embryos than to eleutheroembryos (Léonard et al., 2005) and dechorionated embryos (Bodewein et al., 2016; Henn and Braunbeck, 2011). Furthermore, Creton (2004) showed the passage of 3 kDa fluorescent-labeled dextran across the chorion, but a restriction of 10 kDa fluorescent dextran. Besides molecular weight, also the structure of the molecule itself and different steric residue groups influence the uptake across the chorion, which was demonstrated with different substituted fluorescent molecules by Kais et al. (2013). This has led to the recommendation by the OECD, to switch to other, more appropriate toxicity tests for substances causing a delayed hatch, exceeding the molecular weight of 3 kDa or with a bulky molecular structure (OECD, 2013a).

Aims of the thesis

The need for reliable, quick and low-cost non-vertebrate-studies is increasing, thus as a potential alternative method, the zebrafish embryo toxicity test (FET) has been developed. With the FET, various general but also highly specific endpoints can be assessed to gain more information on the toxicity of a chemical, but also on its mode of action. The test has been developed for zebrafish, but can be easily transferred to other cyprinids, such as the fathead minnow. Zebrafish embryos are exposed for 96 hpf and thus a 48-hours period after hatch is covered. However, the uptake of chemicals across the chorion of teleost fish has been the key

point of criticism on this alternative method. Especially in regards with potentially upcoming issues with nanoscale particles, the concerns of false-negative classifications have risen. Therefore, the first four chapters of this thesis intend to clarify the question, whether the chorion acts as an effective barrier for molecules and nano-sized particles: In Chapter I, differently sized polymer molecules are tested in the FET. High concentrations of these polymers are used to evoke effects on the chorion of zebrafish, which then serves as endpoints to determine the critical molecular size for an uptake. In Chapter II and III, different nano-sized polystyrene beads, capsuling a fluorescent dye, are applied to determine the influences of size and surface properties on the uptake across the chorion of zebrafish. In Chapter IV, the chorion of another OECD-recommended fish species, the fathead minnow, is further evaluated with the materials and methods described in Chapter I and II. The results are shown in context to the results derived from tests with the zebrafish.

To expand the FET beyond the standard test design according to OECD TG 236, further small but effective variations of the protocol have been evaluated. Highly reactive hair dye molecules, and thus hard to assess in the standard FET, have been chosen to develop further adaptations in the FET test. The main emphasis of Chapter V was the observation of auto-oxidation of the parent molecules, the formation of self-coupling products and the evaluation of the toxic potential of this mixture of molecules. To prevent auto-oxidation and thus to illustrate mainly the toxicity caused by the parent substance, the amendment of scavengers was tested. As part of an ecotoxicological test battery, the results derived in FET studies must be transferable to realistic scenarios, i.e. natural waters and their communities. The assessment of the FET in real aquatic environment, such as lakes, rivers and ponds is not feasible. However, the transferability of realistic natural scenarios such as elevated dissolved organic matter levels, non-standardized test water and interactions with other, anthropogenically introduced substances in natural waters into the laboratory, has been evaluated in Chapter VI.

Each chapter provides some additional background information relevant for the subject of the respective section. At the end of the thesis, all findings and conclusions are briefly summarized.

Chapter I.

Size does matter - Determination of the critical molecular size for the uptake of chemicals across the chorion of zebrafish (*Danio rerio*) embryos¹

¹ This chapter has been written by myself and has been accepted for publication by the Journal Aquatic Toxicology as: Katharina E. Pelka, Kirsten Henn, Andreas Keck, Benjamin Sapel, Thomas Braunbeck “Size does matter – determination of the critical molecular size for the uptake of chemicals across the chorion of zebrafish (*Danio rerio*) embryos.” Received 17 July 2016, Revised 19 November 2016, Accepted 16 December 2016, Available online 21 December 2016. <http://dx.doi.org/10.1016/j.aquatox.2016.12.015>

1. Size does matter – Determination of the critical molecular size for the uptake of chemicals across the chorion of zebrafish (*Danio rerio*) embryos

1.1 Abstract

In order to identify the upper limits of the molecular size of chemicals to cross the chorion of zebrafish, *Danio rerio*, differently sized, non-toxic and chemically inert polyethylene glycols (PEGs; 2,000 – 12,000 Da) were applied at concentrations (9.76 mM) high enough to provoke osmotic pressure. Whereas small PEGs were expected to be able to cross the chorion, restricted uptake of large PEGs was hypothesized to result in shrinkage of the chorion. Due to a slow but gradual uptake of PEGs over time, molecular size-dependent equilibration in conjunction with a regain of the spherical chorion shape was observed. Thus, the size of molecules able to cross the chorion could be narrowed down precisely to $\leq 4,000$ Da and the time-dependency of the movement across the chorion could be described. To account for associated alterations in embryonic development, fish embryo toxicity tests (FETs) according to OECD test guideline 236 (OECD, 2013a) were performed with special emphasis to changes in chorion shape.

FETs revealed clear-cut size-effects: the higher the actual molecular weight (= size) of the PEG, the more effects (both acutely toxic and sublethal) were found. No effects were seen with PEGs of 2,000 and 3,000 Da. In contrast, PEG 8,000 and PEG 12,000 were found to be most toxic with LC₅₀ values of 16.05 and 16.40 g/L, respectively. Likewise, the extent of chorion shrinkage due to increased osmotic pressure strictly depended on PEG molecular weight and duration of exposure. A reflux of water and PEG molecules into the chorion and a resulting re-shaping of the chorion could only be observed for eggs exposed to PEGs $\leq 4,000$ Da. Results clearly indicate a barrier function of the zebrafish chorion for molecules larger than 3,000 to 4,000 Da.

1.2 Introduction

Since the principles of Russel and Burch (1959) to “refine, reduce or replace” animal testing were incorporated into the 2007 EU Regulation on Chemicals and their Safe use, the Registration, Evaluation, Authorization and Restriction of Chemical substances (REACH; EC, 2007), considerable efforts were taken to standardize, validate and approve an alternative to the acute fish toxicity test. In July 2013, the OECD has assembled the new guideline 236 “Fish Embryo Acute Toxicity Test (FET)” for the testing of chemicals. The test guideline has primarily been

developed for zebrafish, *Danio rerio*, but can also be applied to other small laboratory fishes such as medaka, *Oryzias latipes*, and fathead minnow, *Pimephales promelas* (Braunbeck et al., 2005; Braunbeck et al., 2014). With regard to animal welfare, zebrafish embryos younger than 120 hours post fertilization (hpf) are regarded as non-protected stages (Belanger et al., 2010; EU, 2010; Strähle et al., 2012). For this and numerous other reasons, the zebrafish embryo has emerged as an intensively used model organism in developmental biology, pharmacology and (eco-)toxicology (Aleström et al., 2006; Braunbeck et al., 2014; Chakraborty et al., 2009; Dooley and Zon, 2000; Hill et al., 2005; Lele and Krone, 1996; McGrath and Li, 2008; Nagel, 2002; Parnig et al., 2002; Peterson and MacRae, 2012; Rubinstein, 2006; Schulte and Nagel, 1994; Selderslaghs et al., 2009; Sipes et al., 2011; Yang et al., 2009). In ecotoxicological studies, chemical safety is frequently tested for risk assessment purpose with zebrafish embryos (Belanger et al., 2010; Braunbeck et al., 2005; Eaton et al., 1978; Hill et al., 2005; Lammer et al., 2009; McKim, 1977; Nagel, 2002; Scholz et al., 2008; Schulte and Nagel, 1994). Besides acute toxicity, multiple additional endpoints such as teratogenicity (Brannen et al., 2010; Dooley and Zon, 2000; Panzica-Kelly et al., 2010; Paskova et al., 2011; Selderslaghs et al., 2009; Weigt et al., 2011), neurotoxicity (de Esch et al., 2012; Linney et al., 2004; Padilla et al., 2011; Parnig et al., 2007; Ton et al., 2006), genotoxicity (Braunbeck et al., 2014; Garcia-Käufer et al., 2015; Häfeli et al., 2011) and endocrine disruption (Brion et al., 2004; Brion et al., 2012; Cohen et al., 2008; Cohen et al., 2014; Schiller et al., 2013) can be implemented.

Although an excellent correlation has been determined for acute toxicity data with adult fish (Lammer et al., 2009; Nagel, 2002; Ratte and Hammers-Wirtz, 2003a; Roex et al., 2002), the egg envelope, the chorion, has repeatedly been discussed as a potential barrier for the uptake of chemical substances: For approximately 72 hours, the developing zebrafish embryos are surrounded by the acellular chorion, which is known to be about 1.5 - 2.5 μm thick and to consist of three layers pierced by pore canals (Bonsignorio et al., 1996; Hisaoka, 1958; Laale, 1977; Rawson et al., 2000). The pores are evenly distributed over the chorion with diameters varying between 0.2 μm in unfertilized eggs (Hart and Donovan, 1983) and 0.5 - 0.7 μm in fertilized eggs at the gastrula stage (Rawson et al., 2000). During development, both chorion structure and permeability change. Within the first hours post fertilization, the chorion hardens and thus prevents polyspermy, protects the developing embryo and leads to a reduced permeability. Changes in permeability during the first hours of development have been demonstrated with e.g. effluents: embryos exposed from 0 - 1 hpf were more sensitive than

embryos exposed from ≥ 4 hpf (Gellert and Heinrichsdorff, 2001). In contrast, the stability of the chorion decreases with age, shown by Kim et al. (2004), who demonstrated that higher penetration force was needed to puncture the chorion of blastula and gastrula staged embryos than that of pre-hatching staged embryos. Additionally, Kais et al. (2013) illustrated a time-dependent increase in permeability of the chorion at 48 hpf compared to 24 hpf using the fluorescent dye marker 2,7-dichlorofluorescein.

Whether a molecule is able to pass the chorion or not, seems to depend on its chemical and physical properties as well as its size. A restriction in uptake across the chorion was postulated for some small molecules, heavy metals, highly lipophilic substances and nanomaterials (Böhme et al., 2015b; Braunbeck et al., 2005; Fent et al., 2010; Meinelt et al., 2006; Osborne et al., 2013; Ozoh, 1980). However, a restriction was also found for big and bulky substances, such as polymers. These polymers and some high molecular weight surfactants (40,000 – 100,000 g/mol) were less toxic to embryos than to eleutheroembryos (Léonard et al., 2005) and dechorionated embryos (Henn and Braunbeck, 2011). Furthermore, Creton (2004) showed the passage of 3 kDa fluorescently labeled dextrans across the chorion, but a restriction of 10 kDa fluorescent dextrans. Besides molecular weight, also the structure and related bulkiness of the molecule and different substitutes take influence on the uptake across the chorion, which was demonstrated with differently substituted fluorescent molecules by Kais et al. (2013).

Nevertheless, our understanding of whether a substance is able to pass the zebrafish chorion or not is still limited. For correct data interpretation and to avoid false-negative evaluations of acute toxicity data determined with the FET, more information on the mechanisms and the critical molecular size of a chemical substance for the uptake across the chorion is necessary. For this end, zebrafish embryos were exposed to high concentrations of differently sized non-toxic polymers, the hydrophilic polyethylene glycols (PEGs).

PEGs are macromolecules composed of repetitive identical structural units, typically connected by covalent bonds, i.e. single-chain hydrocarbons without any additional functional groups of the units confounding with the chorion and the pore canals. In plant physiology, PEGs are commonly used to study water relations (Hohl and Schopfer, 1991; Michel and Kaufmann, 1973) and cell wall porosity (Carpita et al., 1979; Money and Webster, 1988). This is exactly the mechanistic approach transferred to study the zebrafish chorion permeability: Freshly fertilized eggs exposed to solutions of a higher solute concentration than within the perivitelline space surrounding the embryo inside the chorion should result in water efflux from the eggs

into the external medium. As a consequence, the chorion shrinks immediately after transfer. If the molecules in the surrounding medium are too large to cross the chorion, osmotic equilibration due to medium reflux into the egg is impossible. As a result, the chorion remains shrunken and is not able to regain its spherical shape.

PEGs are synthesized in a variety of molecular weights, and these serve as a parameter for the respective size, e.g. PEGs 2,000 have an average molecular weight of 2,050 g/mol. In the present study, PEGs in a molecular weight range from 2,000 to 12,000 g/mol were applied to zebrafish embryos on the assumption that the molecular weight of the dissolved PEG, in which the normal shape of the chorion can just be regained during an exposure until 48 hpf, should be equivalent to the critical molecular size to cross the chorion.

1.3 Materials and methods

1.3.1 Chemicals and materials

All chemicals were of highest purity available and purchased from Sigma-Aldrich (Deisenhofen, Germany) unless noted otherwise. Tests were performed in 24-well polystyrene plates (TPP, Renner, Dannstadt, Germany) covered with self-adhesive foil (Nunc, Wiesbaden, Germany).

The PEGs (CAS 25322-68-3) used were: PEG 2,000 (average MW 2,050), PEG 3,000 (average MW 3,015 – 3,685), PEG 4,000 (average MW 3,500 – 4,500), PEG 6,000 (average MW 5,000 – 7,000), PEG 8,000 (average MW 8,000), and PEG 12,000 (average MW 11,000 – 15,000). All stock solutions and test concentrations were prepared in dilution water (294.0 mg/L $\text{CaC}_2 \times 2 \text{H}_2\text{O}$; 123.3 mg/L $\text{MgSO}_4 \times 7 \text{H}_2\text{O}$; 64.7 mg/L NaHCO_3 ; 5.7 mg/L KCl) according to OECD TG 236 (OECD, 2013a). Before use, the pH was adjusted to 7.7 ± 0.2 .

1.3.2 Fish maintenance

Wild-type zebrafish (*Danio rerio*, Westaquarium strain) derived from own stock facilities at the University of Heidelberg. Fish maintenance and egg production have repeatedly been described in detail (Kimmel et al., 1995; Nagel, 2002; Spence et al., 2008) and have been updated for the purpose of the zebrafish embryo acute toxicity test (Lammer et al., 2009). Egg production was performed *via* spawning groups as recommended by the OECD TG 236 (OECD, 2013a) with modifications according to Sessa et al. (2008).

1.3.3 Zebrafish embryo acute toxicity test (FET)

All fish embryo toxicity tests were performed according to OECD TG 236 (OECD, 2013a) in a semi-static exposure scenario. Dilution water was used as a negative control and 4 mg/L 3,4-dichloroaniline served as a positive control. All six PEGs were tested at 3.125; 6.25; 12.5; 25, 50 and 100 g/L; PEG 2,000 was tested at an additional concentration of 200 g/L. Stock solutions of 200 g/L were prepared in volumetric flasks. To correct the volume, the volume of the stirring bar was added after preparation of the solutions. For pre-saturation, 24-well plates had been pre-treated with the respective concentrations 24 h prior to the exposure of the embryos. The 24-well plates were covered with self-adhesive foil and incubated at 26.0 ± 1.0 °C. The embryos were examined every 24 hours until 96 hours post fertilization (hpf) for lethality according to OECD TG 236 (OECD, 2013a) and sublethal effects according to Bachmann (2002), Nagel (2002) and Schulte and Nagel (1994). Any additional effects on chorion integrity (shape) were recorded. Each PEG was tested in three independent runs with 20 eggs per concentration. Embryo tests were classified as valid, if mortality in the negative control was less than 10%, and mortality in the positive control was $\geq 30\%$. Determination of LC₅₀ values was performed using ToxRat[®] (3.0 beta version 2014, ToxRat[®] Solution, Alsdorf, Germany) probit analysis using linear maximum likelihood regression.

1.3.4 Osmosis-related effects by PEG solutions

For precise comparison of the shrinkage and the equilibration processes, the test concentration of all PEGs was set to 9.76 mM, equal to 20 g/L PEG 2,000. For the other PEGs the 9.76 mM were equal to 32.68 g/L PEG 3,000, 39.02 g/L PEG 4,000, 58.54 g/L PEG 6,000, 78.05 g/L PEG 8,000 and 126.83 g/L PEG 12,000.

In order to obtain information about the time-dependency of the movement across the chorion, two different steps of the process were investigated: (1) the time-course of water efflux out of the perivitelline space immediately subsequent to the transfer into the high PEG concentration; (2) the process of equilibrium or until the chorion reached its final shape. For this end, repetitive micrographs were taken with a Zeiss AxioCam ICc1 (Zeiss, Germany), and the area of each egg was determined with ImageJ 1.47v (Rasband, 1997-2014) using the “analyze particles” tool. The area of the negative control eggs of each replicate served as a reference to calculate the relative percentage of shrinkage. Coagulated eggs were not taken into evaluation due to potential post-mortem changes in chorion structure and possible fungal infestation.

For a graphical representation of the differences in chorion area of the exposed eggs in relation to the start of evaluation, the delta (Δ) values were calculated with the mean chorion area in relation to the negative control (ctrl):

Δ = chorion area at time point n [% of ctrl] - chorion area at start (~5 min.) of exposure [% of ctrl]

The water efflux was determined in three independent runs with individual eggs per PEG, while the equilibrium process was performed in three independent runs with 20 eggs per PEG each.

1.4 Results

1.4.1 Acute and sublethal effects of polyethylene glycols in the FET

Fish embryo acute toxicity tests (FETs) revealed a dose- and size-dependent increase of toxicity of the tested PEGs to zebrafish embryos (see Figure 5). At 96 hpf, PEG 2,000 was the least toxic PEG with a LC_{50} value of 129.90 ± 15.50 g/L. Toxicities of PEG 8,000 and PEG 12,000 were almost identical with LC_{50} values of 16.05 ± 0.76 and 16.40 ± 2.21 g/L, respectively. No increase in toxicity of all PEGs could be observed over the time course of exposure after 24 hpf (details not shown). The major lethal effect was coagulation, which in most cases occurred within the first 24 hours. Occasionally, a lack of heartbeat was found as an additional lethal endpoint from 48 hpf onwards.

The EC_{50} value for PEG 2,000 was determined at 104.4 ± 7.04 g/L (no significant difference to LC_{50} value), whereas EC_{50} values for PEGs 3,000 and 4,000 slightly differed from corresponding LC_{50} values ($p < 0.05$). Following exposure to PEGs 6,000, 8,000 and 12,000, zebrafish embryos showed a much stronger response, with EC_{50} values of 8.99 ± 0.90 , 7.99 ± 0.81 and 7.06 ± 1.51 g/L compared to the LC_{50} values ($p < 0.01$).

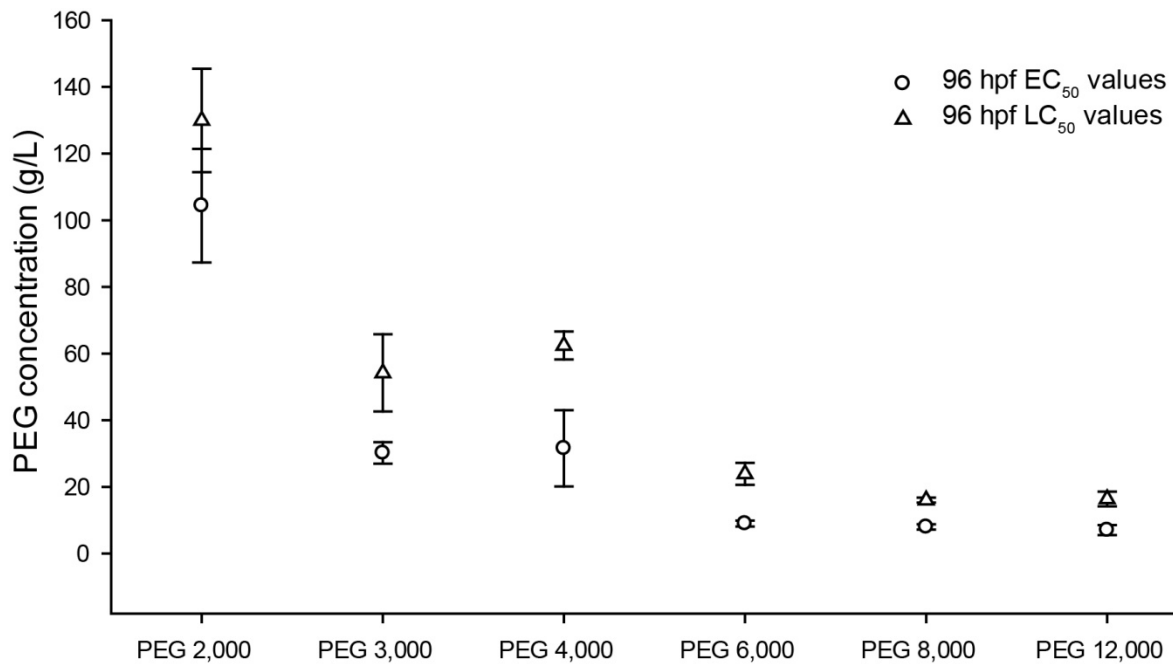


Figure 5: Acute (LC_{50}) and sublethal (EC_{50}) effects of differently sized polyethylene glycols (PEGs) in zebrafish (*Danio rerio*) after exposure for 96 h. Data were computed with ToxRat[®] and are given as mean \pm standard deviation; $n = 3$ runs (taken from Pelka et al.).

As sublethal effects following exposure to PEGs, deformations of the yolk and the head as well as sharply bent tails (Figure 6) were found. One prominent effect was the deformation of the eyes. Deformation of the head, the eyes, cyclopia and the lack of one or both eye cups were found in all treatments, especially among the surviving embryos at high concentrations (≥ 50 g/L in PEG 4,000 and ≥ 12.5 g/L in PEG 6,000 & 8,000).

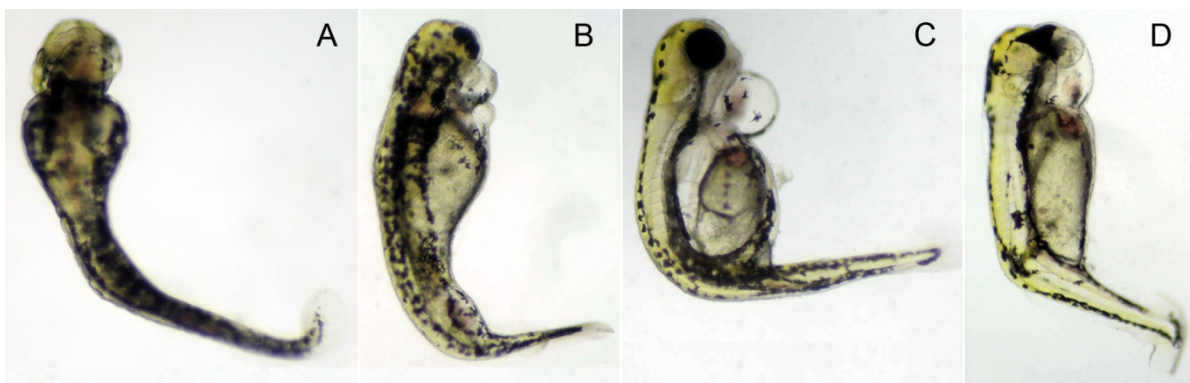


Figure 6: Sublethal effects in zebrafish (*Danio rerio*) embryos after 96 h exposure to (A & B) 12.5 g/L, (C) 25 g/L and (D) 50 g/L PEG 6,000. Note the absence (A) or deformation of the eyes (B - C), sharply bent tails, formation of edemata as well as yolk deformations of PEG-exposed embryos (taken from Pelka et al.).

PEG exposure during the FET produced conspicuous effects on the shape of the chorions of the exposed eggs (Figure 7). Subsequent to the transfer into the different PEG test solutions, the eggs rapidly developed depressions of the spherical chorion in a concentration-dependent fashion. Depressions were minor when exposed to lower concentrations (3.125 and 6.25 g/L);

in contrast at higher concentrations (≥ 12.5 g/L), strong to very strong depressions formed until the chorion was tightly wrapped around the yolk and the cell pole (see Figure 7). At the very beginning of exposure, there were no differences in the extent of this shrinking effect between the differently sized PEGs.

At 24 hpf, the minor depressions caused by the lower concentrations (3.125 and 6.25 g/L) had disappeared in chorions exposed to PEGs $\leq 4,000$ Da (Figure 8). In contrast, effects caused by high concentrations of the PEG solutions were persistent. For PEG 2,000 only eggs exposed to 100 and 200 g/L showed effects on chorion shape (65 and 100%, respectively). For PEG 3,000 and 4,000 at 12.5 g/L, respectively about 8% and 84% of the exposed eggs showed depressions of the chorion. For PEG $\geq 6,000$ all eggs exposed to concentrations ≥ 12.5 g/L showed persisting severe chorion deformations. Interestingly, the deformation of the chorion for PEG 12,000 increased stepwise with rising concentrations (15, 50 and 100% at 3.125, 6.25, 12.5 g/L), whereas a very steep increase was found for PEG 8,000 (40% and 95% at 3.125 and 6.25 g/L, respectively).

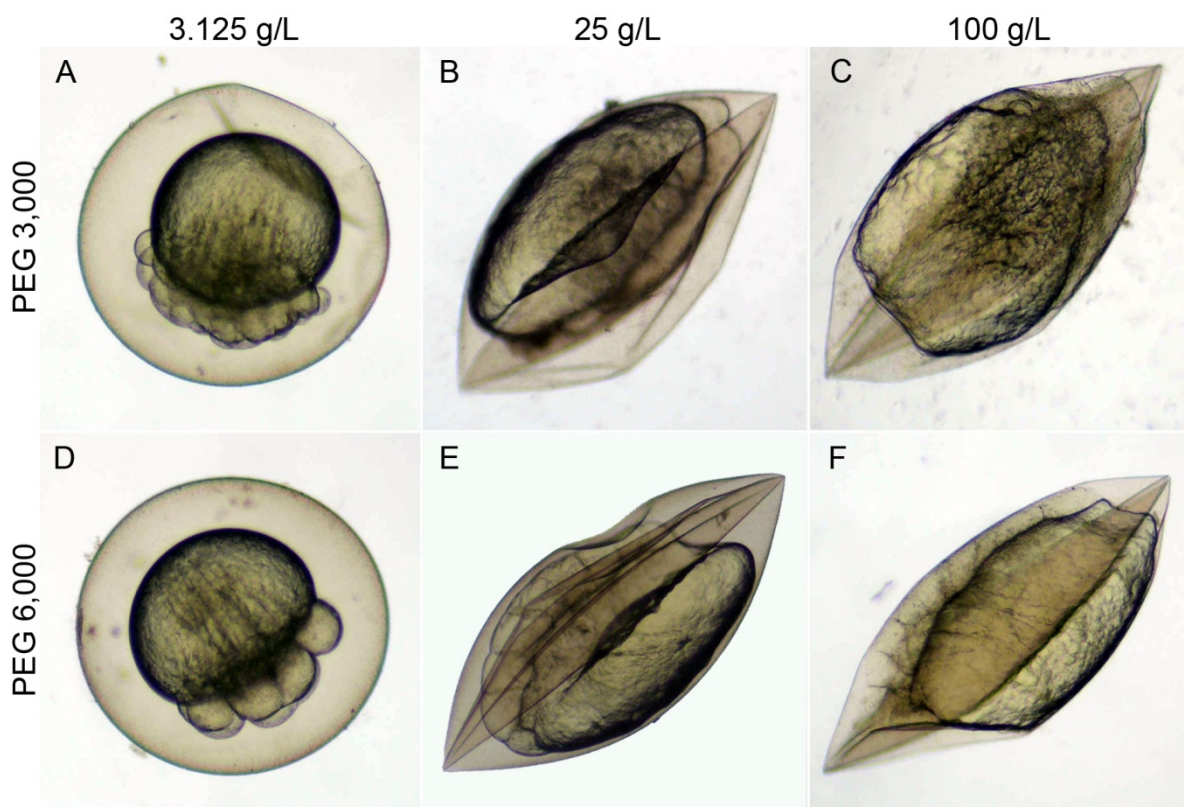


Figure 7: Subsequently to transfer into PEG test solutes, the chorion of zebrafish (*Danio rerio*) embryos showed concentration-dependent shrinkage due to effects by (A-C) PEG 3,000 and (D-F) PEG 6,000. Only very small depressions of the chorion were found at 3.125 g/L PEG 3,000 (A) and PEG 6,000 (D), while at 25 g/L (B, E) and 100 g/L (C, F) stronger depressions of the chorion were evident, finally leading to a tightly wrapped chorion around the yolk and cell pole (C and F) (taken from Pelka et al.).

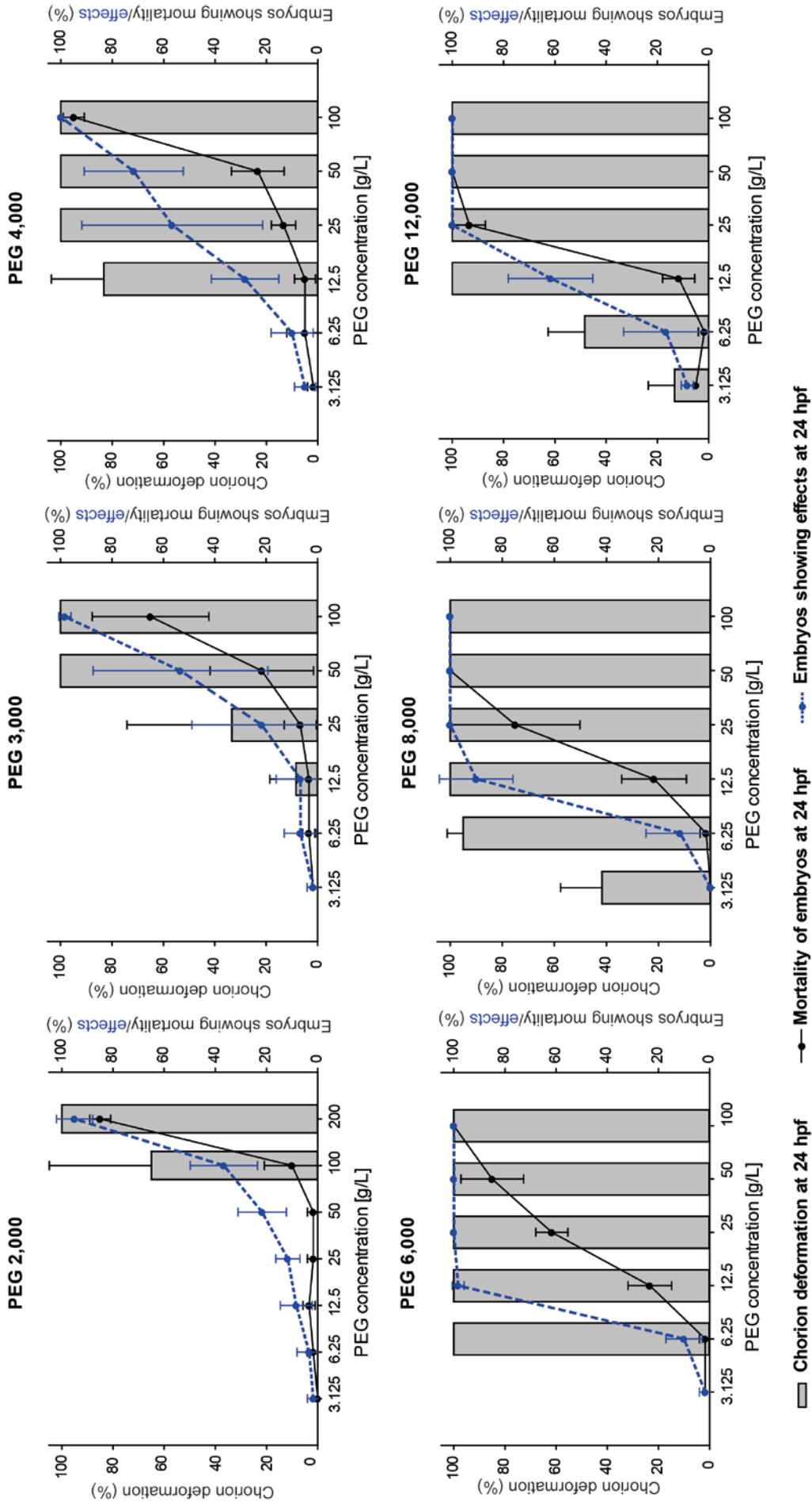


Figure 8 Exposure of zebrafish eggs for 24 hours to different polyethylene glycols reveals choron deformation (grey column) in almost all concentrations of the differently sized PEGs. Likewise, for all tested PEGs, there was a concentration-dependent increase of acute mortality (black line) and sublethal effects (blue line) (taken from Pelka et al.).

1.4.2 Osmosis-dependent effects on chorion shape of zebrafish eggs: initial efflux from eggs

In a second series of experiments, the PEG concentrations were exactly set to 9.76 mM in order to directly compare effects on the chorion shape by different PEGs. Thus, after transfer into 9.76 mM PEG solutions, the time until no further shrinkage of the chorions were identified, and the chorion areas were determined on the basis of micrographs.

Within the first minute of exposure, the chorion area of the eggs showed a PEG-size-dependent decrease (Table 2): after 1 minute of immersion, the areas of eggs exposed to PEG $\leq 8\,000$ Da were found in the range of 91.5% to 102.6% of the area of correspond negative controls. In contrast, following immersion in PEG 12 000 solution there was a shrinkage to 79.9% of the respective control after 1 minute (see Table 2).

Following 4 minutes of exposure, the decline in chorion area was almost linear for all treatments (Figure 9). However, comparing the PEG 3,000 line (red line, Figure 9) to those for other PEGs, the decline of chorion area is less steep, i.e. the chorion shrinks much slower. When comparing the chorion area at the different time points to the chorion area at the start point, significant changes for all PEGs can be found after 2 minutes ($p < 0.05$). Significance further increased after 2.5 minutes for all PEGs ($p < 0.001$), except PEG 3,000. After 3 minutes of exposure, significance also increased in the chorion area for PEG 3,000 ($p \leq 0.001$).

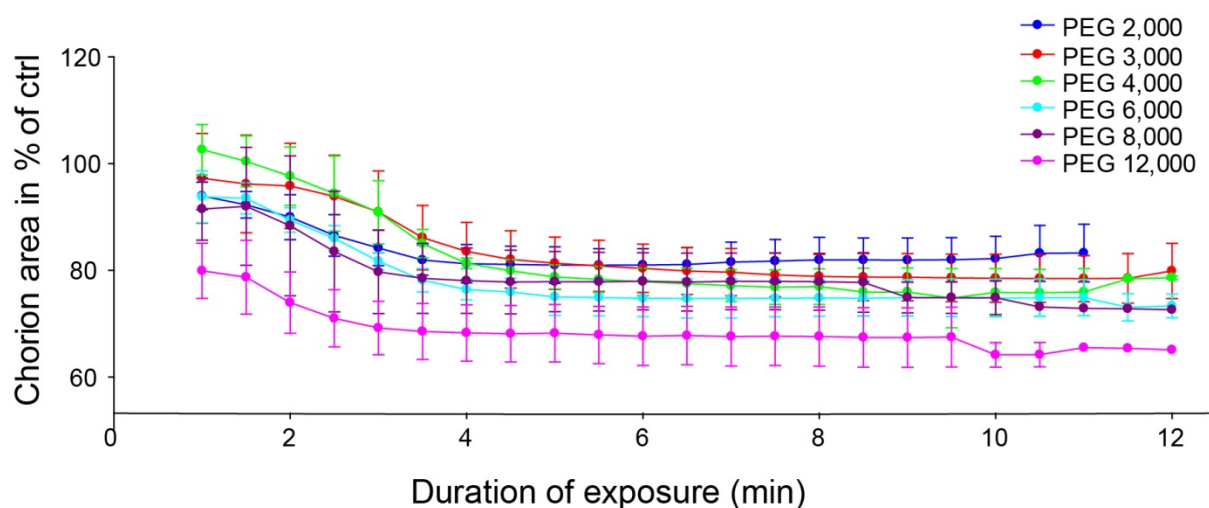


Figure 9: Change in chorion area of PEG-exposed zebrafish (*Danio rerio*) eggs. Data are given for three independent runs ($n = 3$) as % of the area measured from micrographs of eggs in corresponding negative controls. In addition, the time until no further shrinkage of the chorion area was observed is listed (taken from Pelka et al.).

Likewise, the time to reach maximum shrinkage showed a clear-cut correlation to PEG size (Table 2). Eggs exposed to PEG 2,000 shrank to approximately 81.0% of the control chorion area within 5.5 minutes, while eggs exposed to PEG 4,000 reached a maximum shrinkage to 75.8% of the control after 10.5 minutes. For all other PEGs, the first strong shrinkage of the chorion was completed after about 11 - 12 minutes. The strongest shrinkage (to 67.1% of the control chorion area) was found for PEG 12,000.

Table 2: Changes in chorion area over time on micrographs of zebrafish (*Danio rerio*) eggs after exposure to PEGs of various molecular weight. Data are given for three independent runs ($n = 3$) as % of the area measured for micrographs of eggs in corresponding negative controls. In addition, the time until no further shrinkage of the chorion area was observed is listed (taken from Pelka et al.).

	PEG 2,000	PEG 3,000	PEG 4,000	PEG 6,000	PEG 8,000	PEG 12,000
Area at start	93.9 ± 2.1	97.2 ± 6.9	102.6 ± 3.9	93.8 ± 4.0	91.5 ± 4.8	79.9 ± 4.2
Area at 4 min	81.2 ± 2.9	83.5 ± 4.5	81.3 ± 0.8	76.4 ± 1.6	78.0 ± 5.0	68.3 ± 4.3
Maximal shrinkage	81.0 ± 2.5	78.4 ± 3.5	75.8 ± 3.6	74.8 ± 2.9	77.7 ± 4.5	67.1 ± 4.7
Min. until maximal shrinkage	5:30	11:00	10:30	11:30	12:00	12:00

*at approximately 1 min

1.4.3 Osmosis-dependent effects on chorion shape of zebrafish eggs: gradual reflux leading to (partial) equilibrium

The minor (PEG 2,000 and PEG 3,000) to strong deformations of the chorions (PEGs $\geq 4,000$ Da) observed immediately after the onset of exposure gradually changed with progressing exposure. Whereas eggs exposed to PEG 2,000 quickly regained the spherical shape of their chorions (Figure 10), this recovery of chorion shape of embryos exposed to PEG 3,000 took 48 hours. For PEG 4,000, minor changes of chorion deformation could be observed. Since the space between the chorion and the embryo slightly increased within 48 hours, the embryos were able to resume their movements, even within the deformed chorions. For PEGs $\geq 6,000$ Da, however, the deformations of the chorion observed at the very start of exposure even seemed to increase after 24 and 48 hours, indicating a continuation of shrinkage process. Finally, embryos exposed to PEG 8,000 and 12,000 did not develop further and quickly coagulated (Figure 10).

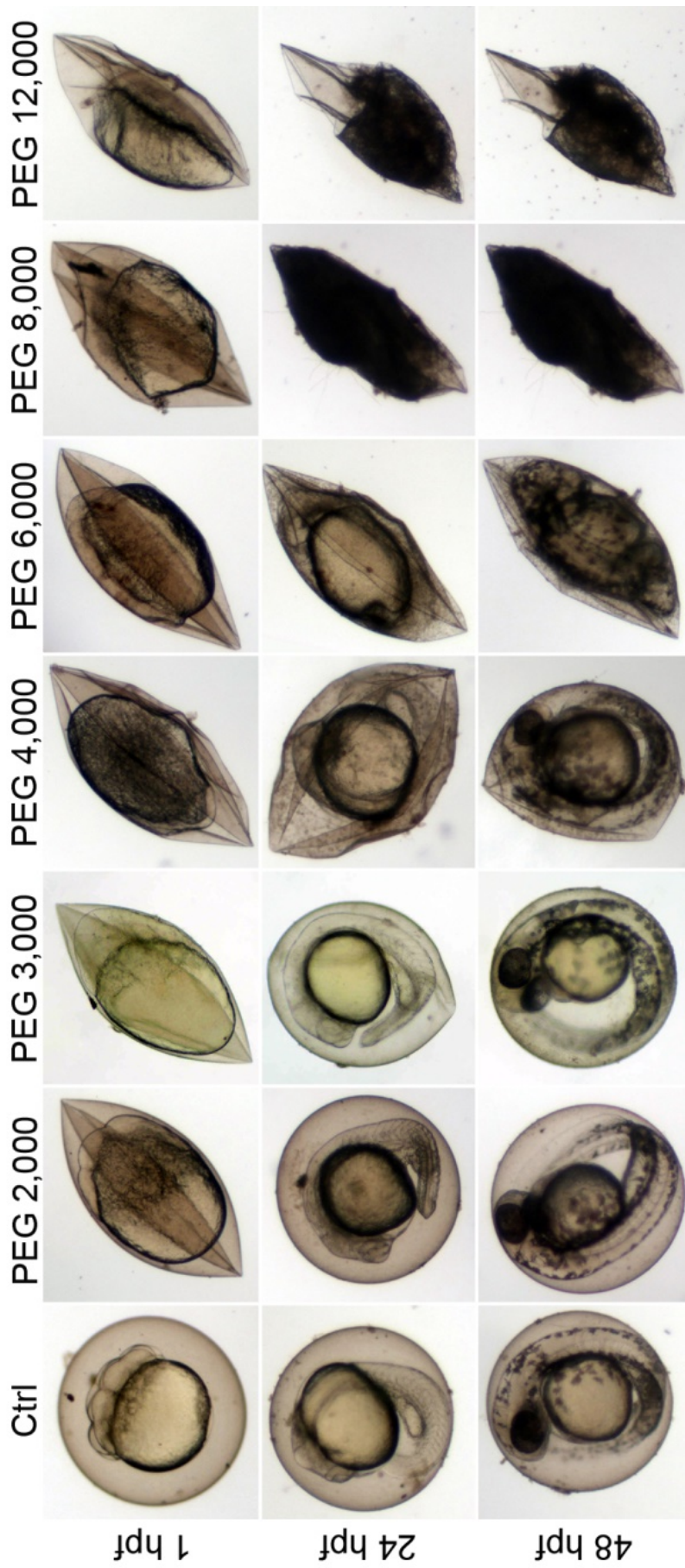


Figure 10: Chronological sequence of deformation of the zebrafish (*Danio rerio*) chorion following exposure to differently sized polyethylene glycols (PEGs). Each column shows the same egg exposed to dilution water (ctrl) or 9.67 mM of the different PEGs at start of exposure (approx. 1 hpf) as well as at 24 and 48 hpf. Whereas the chorions of embryos exposed to PEG 2,000 and 3,000 regained a round shape, the chorions of PEG \geq 4,000 Da remain deformed. Note coagulation of embryos exposed to PEG \geq 8,000 Da (taken from Pelka et al.).

In order to illustrate the PEG size- and time-dependence of the equilibrium process, the average difference of the chorion area at different time points in relation to the area at the start of exposure, was determined (Figure 11). Again, two groups of PEG size ranges could be distinguished: For PEGs $\leq 4,000$ an increase of the chorion area could be observed, indicating a recovery from the deformation due to gradual reflux of external medium. The biggest difference compared to the start of exposure was found for PEG 3,000 with a difference in chorion area of 13.16, 14.44 and 16.52% after 24, 36 and 48 hpf, respectively. In contrast, for PEG $\geq 6,000$ a decrease of chorion area was evident. For embryos exposed to PEG 8,000 and 12,000 the chorion area even decreased by 1.54 and 2.18, respectively. As already mentioned, embryos exposed to PEG 8,000 and 12,000 finally coagulated after 5 hours.

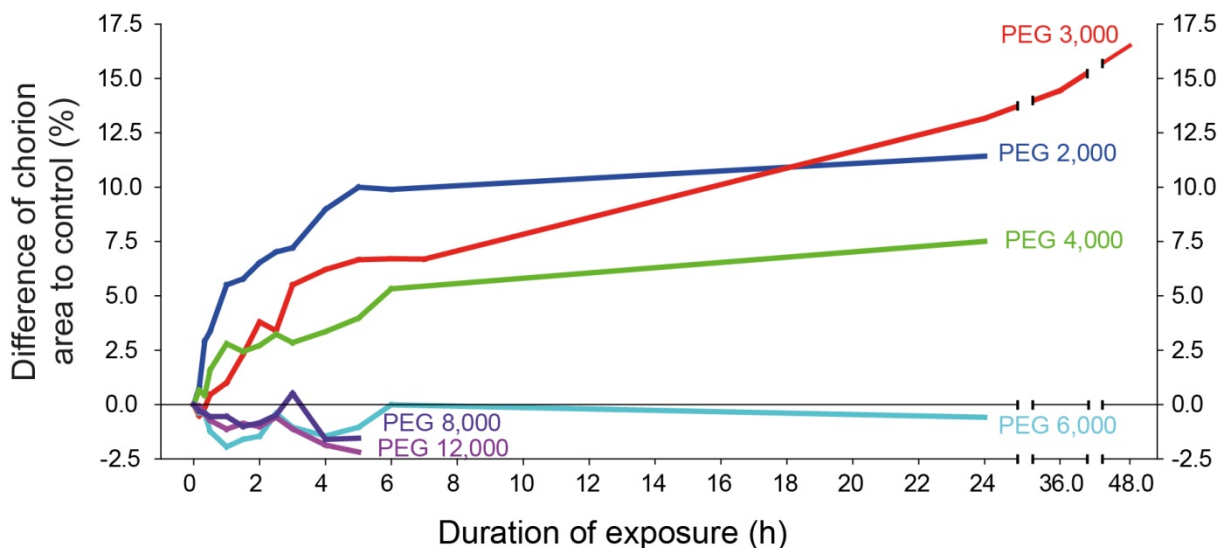


Figure 11: Changes in the area of micrographs of the chorion of zebrafish (*Danio rerio*) embryos exposed to polyethylene glycols (PEGs) of different sizes (molecular weight) in relation to the areas at the start of exposure. The exposure covers the time period from the onset of exposure (approx. 5 min) to the time point of no further shrinkage of the chorion (approx. 24 h). For PEG 3,000, additional measurements were made after 36 and 48 h. Note that maximum shrinkage is already reached after approx. 7 h for most PEGs. Data are given as percent change over negative controls at the beginning of the exposure for three independent runs with 20 embryos ($n = 3$). Coagulate eggs at PEGs 8,000 and 12,000 were excluded from evaluation (taken from Pelka et al.).

1.5 Discussion

PEGs have frequently been used in plant studies to induce osmotic stress (Hohl and Schopfer, 1991; Michel and Kaufmann, 1973) and to study the uptake across cell walls (Carpita et al., 1979; Money and Webster, 1988). Analogously, the present study makes use of the osmosis-provoking effect in order to study the permeability of the chorion of zebrafish embryos. The relatively low toxicity (Sheftel, 2000) makes PEGs suitable for testing the size-dependent uptake even at very high concentrations. In mammals, the oral LD_{50} of PEGs with molecular

weights $\leq 2,000$ ranges between 14 and 50 g/kg body weight, and PEGs are thus classified as non-toxic (Documentation, 2012). The use of PEGs has been declared safe for formulations for food supplements and PEG6,000 as a carrier for sweeteners (EFSA, 2006).

In zebrafish, PEG 400 is tolerated at concentrations up to 2.5% by different developmental stages (Maes et al., 2012). This observation was confirmed by the present study, since fish embryo acute toxicity tests (FETs) revealed LC_{50} values in the very high g/L range. The smaller the actual PEG molecular weight (= size), the less lethal and sublethal effects were found in embryos. Responses of embryos exposed to PEGs $\geq 6,000$ Da were very similar, resulting 96 h LC_{50} and EC_{50} values lower than those of PEGs $\leq 4,000$ Da. The differences between the effects of small sized PEGs and the ones found for large sized PEGs clearly indicate that the small PEG molecules are able to enter the chorion, supporting the assumption that osmotic is the driving force for the effects. In mammals, Rowe and Wolf (1982) found a decrease in toxicity of very high molecular weight PEGs due to decreasing bioavailability and thus low absorption rates. Given that most of the effects in fish eggs are supposed to derive due to osmotic effects, the difference between fish and mammals is easy to explain.

In the present study, the most frequent lethal effect was coagulation, which occurred within few hours of exposure. The concentration-dependent increase in the rate of deformations of the chorion found for all PEGs, makes osmotic pressure the most likely reason for the shrinkages and – at very high concentrations – for the toxicity of PEGs. For all six PEGs, there was a clear correlation between the extent of chorion deformations and the rate of embryo malformations. Most likely, the osmotic pressure of the external medium led to increasing osmotic pressure on both, the yolk and the cytoplasm of the cells, which eventually resulted in cellular damage and finally in coagulation of the entire embryo. Zebrafish embryos mechanically dechorionated at 24 hpf and subsequently exposed to PEG solutions at the same concentration ranges were found to be less sensitive to PEG exposure (Henn, 2011). A minor increase of lethal effects, mainly coagulation, at the end of the 120 h-exposure (at 144 hpf) was observed, however, it seems that the sensitive window for effects in embryonic development was skipped when exposure of dechorionated embryos started at 24 hpf. Since the chorion was absent in the trials, the resulting effects derived solely from the osmotic pressure of the surrounding medium. We conclude that the osmotic pressure is the main reason for an increased toxicity of zebrafish embryos.

A prominent specific sublethal effects occurring in PEG-exposed embryos, was the deformation of the eyes, including cyclopia and the absence of one or both eyes. In zebrafish de-

velopment at 28.5 °C, the early eye morphogenesis takes place from 12 to 24 hpf (Kimmel et al., 1995; Schmitt and Dowling, 1994). At bud stage (10 hpf), the neural plate thickens along the embryonic axis and at the animal pole this thickening becomes very prominent, forming a bulge. From this anterior region of the neural keel, the two optic primordia emerge at the 6-somite stage (12 hpf at 28.5 °C). By 24 hpf, the eye cups are formed and the lens has detached from the ectoderm. In parallel, the outgrowth of the optic axon to the brain starts (Schmitt and Dowling, 1994). As has been documented with the known teratogen ethanol, eye cup formation can easily be disrupted during the time period between 12 and 24 hpf (Arenzana et al., 2006; Blader and Strahle, 1998). Cyclopia or absence of eye(s) might result from alterations in developmental pathways *via* a reduction of midline tissue and a failure in separating the eye fields (Loucks et al., 2007). Such deformations of head and eyes might easily result from the tight wrapping of the chorion around the cell pole and the yolk, thus affecting early cell division and cell distribution patterns in the developing embryo. Especially ectodermal fate maps are located near the animal pole of the gastrula-staged embryo (Kimmel et al., 1995), which means that deformations of the nervous system including the eyes might be due to mechanic compression of the chorion in these areas. In fact, morphometry of the area encompassed by the chorion during the fish embryo tests revealed a significant reduction in the area and, thus, the volume of the chorion-surrounded space due to compression caused by osmotic pressure of the PEG solutions. The FETs revealed not only a low toxicity of the PEGs in zebrafish embryos, but also a concentration-dependent decrease of chorion area.

Osmotic pressure is the pressure needed to stop the flow of a solvent across a permeable membranes, it is proportional to the molar concentration of the solutions. Money (1989) discussed the relationship between molecular weight and osmotic pressure of aqueous PEGs and found that equivalent weight of differently sized PEGs in solution did not generate the same osmotic pressure. He showed PEG of a lower molecular weight to generate a higher osmotic pressure than the PEGs of a higher molecular weight. To account for that difference and achieve a better comparability of the effects deriving solely by PEG molecule size and given that the osmotic pressure of the PEG solutions is supposed to be not dependent on the size of the ions, but on the number of dissolved ions, the test concentrations for all PEG were standardized to 9.76 mM equaling approx. 1.175×10^{19} PEG molecules per test volume of 2 ml.

In order to graphically illustrate the shrinkage of the chorion, the chorion area was computed on the basis of micrographs taken at given intervals of PEG exposure. This indirect method

for volume assessment of the space encompassed by the chorion was used, since a direct determination of the volume seemed not possible without extreme investment. Potential disadvantages of the planimetric assessment are the facts (1) that micrographs were not taken at standardized angles, fixed focus and egg/embryo position and (2) that osmosis-related depressions of the chorion located in the photographic plane at the underside of the embryo may not have been picked by two-dimensional photography. However, the planimetry of serial micrographs of embryos allowed the analysis of a high number of individuals from each treatment and provided large datasets amenable to statistical analyses. Since all micrographs were treated identically and data were normalized to chorion areas of controls, the error could be minimized and the method should at least allow an approximation of the volume inside the chorion, if not a really powerful quantitative analysis.

The physical processes triggered by exposure to high strength PEG solutions could be separated into two phases: (1) a rapid response phase due to the osmotic gradients mainly characterized by solvent efflux, and (2) a slower phase of equilibration due to a more or less restricted flow of solutes (i.e. PEG molecules). During the initial rapid shrinkage phase, a very strong and quick decline in chorion area could be observed. The decline in chorion area was almost linear within the first 4 minutes of exposure; afterwards, decreasing slopes indicated slowing down of solvent flows. As shown by Adams et al. (2005) with D₂O, the zebrafish chorion is highly permeable to water. Consequentially, water can readily pass the chorion from the perivitelline space into the external medium to compensate for the osmotic pressure built up by the highly concentrated PEGs solutes in the external medium. Only very recently, a similar effect of “collapsed chorions” was published by Bodewein et al. (2016) in zebrafish embryos at 24 hpf exposed to 10 μ M PAMAM G5.0 dendrimers. They explained this effect by an interaction of the positively charged dendrimers with the negative charged chorion to form aggregations and subsequently clog the chorion pores, leading to an altered osmotic homeostasis between the perivitelline space and the outer surface of the chorion. Alternatively, they suggest the generation of an osmotic gradient between inside and outside the chorion due to accumulation of a larger amounts of molecules, leading to water efflux.

The structure of the zebrafish chorion, which consists of three layers, is quite flexible as has been shown by Kim et al. (2004), who measured the force needed to puncture the chorion at different developmental stages and also recorded the chorion deformation before puncturing. At the blastula stage, a chorion deformation of about 170 μ m was observed before rapture of the chorion. Hence, under osmotic pressure imposed by the PEG solutes, the chorion was

most likely able to cave in, leading to minor and finally strong depressions. During exposure over 24 and 48 hours, the small PEGs $\leq 4,000$ Da were apparently able to cross the chorion, which then functioned as a semipermeable membrane.

Since with PEG of a molecular weight of 2,000 Da equilibrium was reached after 24 h, a non-charged molecule of a size of 2,050 Da is able to readily cross the chorion and enter the perivitelline space. After 48 h of exposure, the same effect was observed for PEG 3,000, indicating that enough molecules were able to finally cross the chorion and leading to equilibrium. From these observations, a molecular weight of approximately 3,000 Da may be concluded as the threshold for non-charged, more or less linear molecules to pass the zebrafish chorion. 3,000 Da as the upper limit for free permeation of the zebrafish chorion was also concluded by Creton (2004), who parenthetical described the uptake of fluorescent labelled dextran of 3,000 Da. Alternatively or in addition, a reduction of the barrier function of the chorion from 24 to 48 hpf may be concluded. This assumption is supported by the findings by Kais et al. (2013) showing an increased in the uptake rate of fluorescein from 24 to 48 hpf.

Several authors also indicated the effect of “molecule folding” for PEGs, which consequently leads to smaller, condensed molecules. Lillicrap (2010) detected radiolabeled 4,000 and 40,000 Da PEGs inside the zebrafish embryo as early as 24 hpf. He speculated that larger PEG molecules might fold into smaller configurations, thus allowing the passage across the chorion pores. In fact, based on viscosity experiments, Michel and Kaufmann (1973) suggested that PEG molecules might change the configuration in correlation to the concentration: extended (linear) at low concentrations, but folding with increasing concentration. It should be noted, however, that Lillicrap (2010) did not differentiate between the chorion, the perivitelline fluid and the embryo itself, thus he included PEGs adsorbed to the outer surface of the chorion into his measurements.

For PEG 4,000 a slight increase of chorion area was found after 48 h of exposure, which, however, might have also been due to the growth and expansion of the embryo. From a molecular weight $\geq 6,000$ Da, a passage across the chorion is apparently completely blocked, since prolonged exposure did not result in a decompression of the chorion; rather the chorion showed a further shrinkage. As a consequence of the inability to compensate for the osmotic disequilibrium, embryos exposed to PEG $> 6,000$ Da soon died and coagulated due to efflux of fluids.

Standardization of the test media to 9.76 mM relied on the assumption, that osmotic pressure supposed to dependent solely on the number of dissolved ions, however, the behavior of PEG molecules in solution seems to be much more complex. For further experiments, the influences of the chain length of PEG molecules and the chemical interference of their ether oxygen atoms, which have been shown to attract water molecule by hydrogen bonding (Steuter et al., 1981) needs considerations.

1.6 Conclusions

The study clearly documented a strong size dependency of the uptake of substances across the chorion of zebrafish embryos. The rapid uptake of polyethylene glycols (PEGs) with a molecular weight $\leq 3,000$ Da indicates a more or less free passage of molecules up to these dimensions. Given apparent modifications of the chorion structure and permeability with time, a delayed uptake of PEGs of a molecular weight of 4,000 Da across the chorion also seems possible. As a conclusion, the size limit for the uptake of chemicals such as polyethylene glycols into the zebrafish egg is about 3,000 Da for embryos younger than 24 h and may at least partially reach 4,000 Da in 48 h embryos. However, as already indicated by observations by Kais et al. (2013) and Bodewein et al. (2016), other parameters such as lipophilicity, charge and specific molecular conformation may play an important role for the definition of the uptake of chemicals across the chorion of zebrafish embryo.

Chapter II.

Is the chorion an obstacle for nanoscale particles?

2. Is the chorion an obstacle for nanoscale particles?

2.1 Abstract

The zebrafish embryo has widely been applied in studies testing the *in vivo* toxicity, bioavailability and drug delivery potential of nanomaterials. Although the pore size (0.5 – 0.7 μm) is exceeding the size of nanomaterials (0.1 μm), there are still concerns and no clear statements about the potential barrier function of the chorion surrounding the embryo. To illustrate the uptake of nanomaterials of a well-defined size across the chorion, carboxylate-modified microspheres, 0.048, 0.1 and 0.2 μm in size, were applied to freshly fertilized zebrafish embryos within their chorion. The distribution pattern was analyzed *via* laser scanning confocal microscopy (LSCM) at 24 and 48 hpf *in vivo* but also in sections of the chorion. The fluorescent signal of the microspheres was easily detectable and single fluorescent spots were supposed to represent single microspheres. The different optical planes as well as the combined z-stacks of the images of the eggs showed that the fluorescent signal was only detected at the chorion surface and neither within the perivitelline space nor at or inside the embryo. Images of dechorionated embryos after exposure inside the chorion confirmed these findings. Cryosections of chorions and images at high magnifications revealed that the microspheres adhere to the chorion and are not directly associated with the pore canals.

2.2 Introduction

In recent years, nanotechnology has emerged as a fast growing sector, creating materials with wide applications in medicine, electronics, energy and consumer products such as cosmetics, textiles and biocides (Thomas et al., 2006). Nanomaterials are chemicals or particles 1 - 100 nm in size and among the most intensively studied nanomaterials are nanoparticles (NPs). Engineered nanoparticles can be made of metals, metal oxides, non-metals, carbon, lipids and polymers, and often differ significantly in their physicochemical properties from their bulk forms (Harper et al., 2015; Nel et al., 2015; Thomas et al., 2006). Several studies have already gathered information about behavior of NPs in the environment (see for example Baun et al., 2008; Bour et al., 2015; Dale et al., 2015; Grillo et al., 2015; Kahru and Dubourguier, 2010), however, little is known about toxicity, bioavailability, uptake and bioaccumulation as part of an extensive risk assessment (Nel et al., 2013; Nel et al., 2015; Savolainen et al., 2010; Syberg and Hansen, 2016; Thomas et al., 2006). Another emerging problem for aquatic ecology are the effects of nano-scaled plastic debris which may be emit-

ted or formed due to degradation processes in the aquatic environment (Koelmans et al., 2015; Mattsson et al., 2015; Wagner et al., 2014).

The zebrafish embryo has successfully been applied as an *in vivo* model organism in many studies on nanoparticles (Asharani et al., 2008; Clemente et al., 2014; Cunningham et al., 2013; Fako and Furgeson, 2009; Harper et al., 2015; Hua et al., 2014; Kovrižnych Jevgenij et al., 2013; Lin et al., 2013). Special considerations were taken on the uptake of NP in the embryo and across the chorion, which was visualized for silver NPs by Lee et al. (2007) and confirmed *via* transmission electron microscopy by Asharani et al. (2008). However, accumulation on or within the chorion of zebrafish suggest an effective barrier of differently sized nanoparticles (Böhme et al., 2015a; Böhme et al., 2015b; Fent et al., 2010; Osborne et al., 2013; Weil et al., 2015). Hence, no clear statement whether a nanoparticle is able to cross the chorion of zebrafish can be found in current publications.

A commonly used technique for *in vivo* imaging is the use of fluorescent dyes and fluorescence-labelled proteins. However, these fluorophores often suffer decomposition (photobleaching), making them unsuitable for handling in the light and long-term image acquisition *via* fluorescence microscopy. Novel fluorescent probes such as FluoSpheres[®] (Invitrogen) shield the fluorescent dye within a nano-scaled bead against environmental effects, decreasing photobleaching or quenching (Invitrogen, 2004). These microspheres are small manufactured ultraclean polystyrene beads, loaded with a fluorescent dye to create an intensive fluorescent signal, sufficient for the visualization and therefore localization of single particles. They have been used as markers for different biological applications such as neuronal tracing, cellular antigens and as standardization agents in flow cytometry (Invitrogen, 2005). Due to their broad availability, anionic microspheres have been applied frequently in biological methods. The surface of these microspheres is highly charged and relatively hydrophilic (Invitrogen, 2004). This makes them water-soluble, less likely to bind to negatively charged cell surfaces, but more likely to bind proteins and other biomolecules. However, binding is weaker than found for hydrophobic microspheres and coupling has to be supported by reagents (Invitrogen, 2004).

In this chapter, the uptake of 0.2, 0.1 and 0.048 μm sized fluorescent particles across the chorion of zebrafish is investigated. The carboxylate-modified microspheres (FluoSpheres[®], Invitrogen) were applied to freshly spawned zebrafish eggs at a concentration of 0.01% which has been shown sufficient for a stable and easily distinguishable fluorescent signal. Localization of microspheres at or within the chorion and the embryo was performed *via* laser scanning

confocal microscopy (LSCM). Distribution patterns of the fluorescent particles were evaluated at 24 and 48 hours post fertilization, representing the time before hatch of zebrafish embryos.

2.3 Materials and methods

2.3.1 Chemicals

All chemicals were of highest purity available and purchased from Sigma-Aldrich (Deisenhofen, Germany). Tests were performed in 24-well polystyrene plates (TPP, Renner, Dannstadt, Germany) covered with self-adhesive foil (Sealing tape SH, 236269, Thermo Fisher Scientific, Waltham, MA) and the lid. To avoid any agglomerations or disturbances, the ionic strength of the test medium (dilution water) was set to a minimum. Therefore, the FET dilution water according to TG 236 (OECD, 2013a), was prepared in a 1:5 dilution. Before usage, the pH was adjusted to 7.4 ± 0.2 .

The used microspheres are carboxylate-modified and have a size of 0.048 μm , 0.1 μm and 0.2 μm (FluoSpheres[®]; Invitrogen, Life Technologies[™] GmbH, Frankfurt, Germany). General information and technical data of the tested microspheres can be found in Table 3.

Table 3: General information and technical data for the unstained polystyrene microspheres taken from the certified of analysis (COA) obtained by Invitrogen, Life Technologies[™]

Microsphere	0.04 μm	0.1 μm	0.2 μm
Producer	Life Technologies, Molecular Probes [®] , Invitrogen		
Catalog number	F8793	F8801	F8810
Lot number	1301339	1421044	1008760
Concentration of particles/mL	$1,4 \times 10^{15}$	$3,6 \times 10^{13}$	$4,5 \times 10^{12}$
Fluorescent dye	red (580/605)		
Emission maximum	$605 \pm 0.5 \text{ nm}$		
Microscopy	few or no aggregates after sonication		
Technical Data ²			
Actual particle size [μm]	0.048 ± 0.006	0.10 ± 0.0072	0.201 ± 0.01
Charge [meq/g]	1.1078	0.3202	0.0895
Density of polystyrene	1.055 g/cm ³		
Specific surface area [cm ² /g]	1.2×10^6	5.7×10^5	2.8×10^5

² technical data for unstained microspheres

2.3.2 Fish maintenance and egg production

Wild-type zebrafish (Westaquarium strain) derived from own breeding facilities at the University of Heidelberg. Fish maintenance and egg production have repeatedly been described in detail (Kimmel et al., 1995; Nagel, 2002; Spence et al., 2008) and have been updated for the purpose of the zebrafish embryo acute toxicity test (Lammer et al., 2009). Egg production was performed *via* spawning groups as recommended by the OECD test guideline 236 (OECD, 2013a) with modifications according to Sessa et al. (2008).

2.3.3 Exposure

All solutions containing microspheres were wrapped in aluminum foil to prevent photo-bleaching. The steps, where light was inevitable (pipetting, transferring of eggs, evaluating of embryos), were kept at a minimum. The microspheres stock suspensions were sonicated for 5 minutes to gain homogenous suspensions before adding to the dilution water. The test concentrations were set to 0.01% and again sonicated for 5 minutes. Test design was basically according to OECD test guideline 236 (OECD, 2013a): plates were pre-saturated for 24 hours and the medium was renewed before insertion of the eggs and after 24 hours of exposure. The suitability of polystyrene plates was shown in pre-test by comparing fluorescent signal from embryos exposed in polystyrene plates and glass crystallization dishes. No differences were detected. Incubation of the eggs within the plates was performed in the dark at 26 ± 1 °C for 48 hours. A negative control without microspheres were run and evaluated in each test setup.

2.3.4 Preparation for microscopic evaluation

The distribution of microspheres at and within the zebrafish egg was evaluated at 24 and 48 hpf. Each egg was carefully washed three times with the modified dilution water (1:5). To immobilized the embryo within the egg, each egg was transferred into a well containing 1 mL of 0.016% tricaine solution (MS-222, ethyl 3-aminobenzoate methanesulfonate), prepared in 1:5 dilution water. At each time point, four exposed eggs were evaluated per microspheres. Care was taken to avoid light. Eggs were transferred within one small drop of tricaine solution into glass bottom culture dishes (MatTek Cooperation, Ashland, USA).

After semi-static exposure for 48 hours, four embryos were dechorionated after the washing steps with sharp forceps (DuMont™ No 5) as described by Henn and Braunbeck (2011). After dechoriation, the embryos were immobilized with 0.016% tricaine solution and transferred into glass bottom dishes.

To avoid any movement during laser scanning session, eggs were embedded in 1% low melting agarose (LMA; SeaPlaque[®] GTG[®] Agarose, FMC Bioproducts, Rockland, USA) prepared in 0.016% tricaine solution. Excess tricaine solution was removed from dechorionated embryos, which were orientated on their sides within the LMA. Before analyzing under the fluorescence microscope, the embedded embryos were covered by 1 mL tricaine solution to keep the embryo immobilized during scan sessions and to avoid drying-up.

2.3.5 Preparation of cryosections of the chorion

To get insight into the microsphere distribution at the chorion, cryosections were prepared. Eggs at 24 and 48 hpf were incubated for 1 hour in the microsphere solution and washed as described above. Chorions were removed from the embryos, embedded in tissue freezing medium (Ref. 14020108926, Leica Biosystems, Nussloch, Germany) and frozen at -80 °C. 18 µm thick cryosections were prepared at -15 °C using a cryotome (CM 3050, Leica Biosystems, Nussloch, Germany) and air-dried in the dark. Sections were cover-slipped with Gel Mount[™] (Aqueous Mounting Medium, Biomedica Corp., Sigma-Aldrich, Steinheim, Germany) and analyzed using a confocal microscope (Nikon 90i, Nikon Instruments, Netherlands). The pictures were taken with similar settings as for whole eggs (see Table 4), although higher magnifications were possible (used objective: Plan Apo VC 60x Oil DIC N2). The additional zoom is noted under the pictures. Texas Red Laser power was set to 100% with HV of 30, while the HV of the transmitted light channel (TD) was set to 72.

2.3.6 Analysis of the microsphere uptake and distribution

Analyzing was performed with Laser Scanning Confocal Microscopy (LSCM, Nikon 90i; Nikon Instruments, Netherlands) and micrographs were taken with Nikon C1 (Nikon Instruments, Netherlands). If not noted otherwise, laser power was set to 100%, high voltage to 12 and the HV of the transmitted light (TD) channel was set to 50. Fluorescent and TD images are shown either separately or merged. All microscope and laser settings are displayed in Table 4. Illustration of the microsphere distribution was performed using the Nikon imaging software NIS-Elements-Viewer (Vol. 4.20, Laboratory Imaging, 1991-2013).

Table 4: Laser and microscope settings for evaluation of fluorescent signal within the chorion.

Laser settings	Texas Red	
	Emission wavelength:	605.0 nm
	Excitation wavelength:	543.5 nm
	Pinhole radius:	30.00 μm
	Laser power	100%
	High voltage (HV)	12
	HV transmitted light (TD)	50
Microscope settings		
	Objectives:	Fluor 10x W DIC N1 Plan Fluor 4x
	First dichroic mirror:	408/488/543
	First filter cube:	450/35
	Second filter cube:	515/30 605/75

2.4 Results

All microspheres showed a well-defined fluorescent signal. No agglomerations could be detected in the tested solutions; however, the microspheres were strongly bounded to feces and food deposits from the spawning trays which might adhere to the freshly spawned eggs (see for example panel B in Figure 12).

At 48 hpf, the chorions were often very fragile and tended to rip or crumble during handling and embedding. Also, small protozoa which might bloom on the chorion surface might influence the bonding of the microspheres on the chorion and consequently the detection of fluorescent signal. Therefore, the pictures shown in this chapter were chosen to show the average rate of fluorescent found during the tests. Not only 3D illustrations of the z-stacks in $-z$ orientation (see panel D in Figure 12) are shown, but also optical sections at the widest diameter of the egg as well as some pictures taken with transmitted light modus (TD) to locate the embryos inside the eggs (see panel C in Figure 12). For an overall comparison of fluorescence, a high voltage (HV) setting of 12 was chosen, since at this setting the differently sized microspheres were detectable without any oversaturated signal. Any aberrations were recorded.

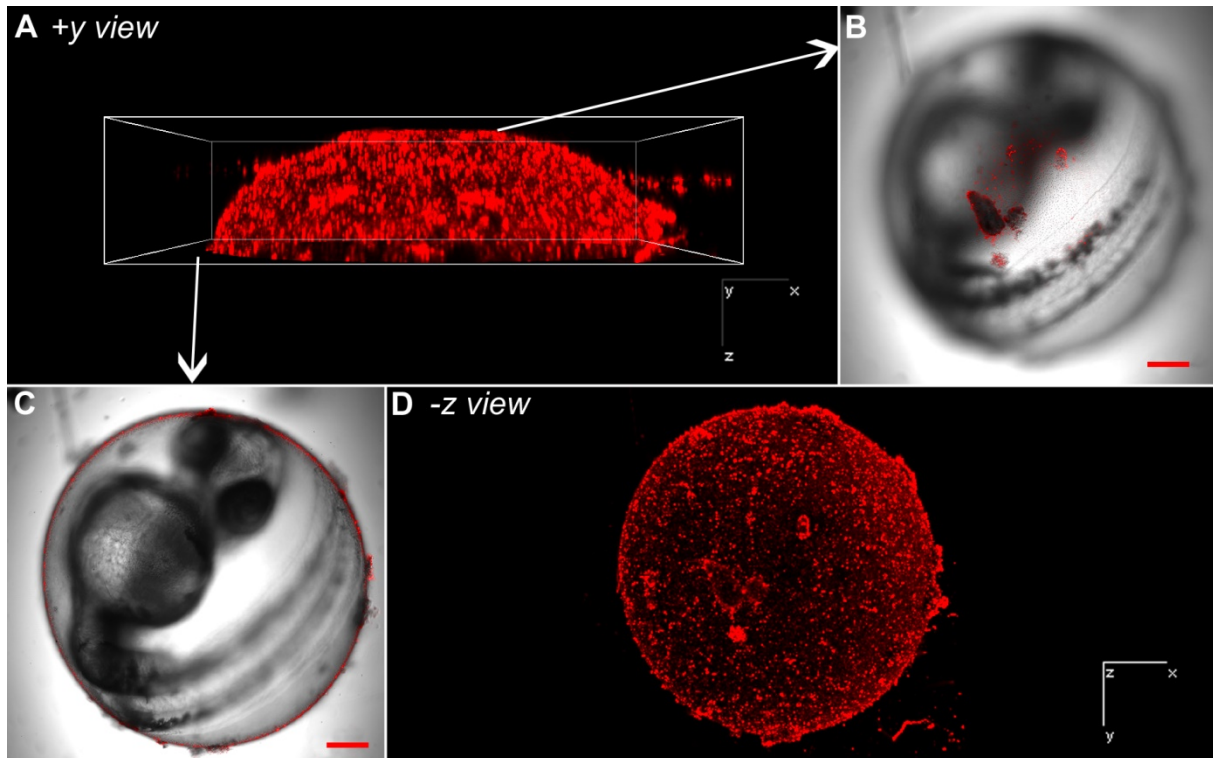


Figure 12: Orientation of the pictures presented in this chapter. Zebrafish embryos were exposed within their chorion to $0.1 \mu\text{m}$ sized microspheres. Pictures were taken at 48 hpf; HV: 10; TD: 58. Scale bars: $150 \mu\text{m}$, 10x magnification.

2.4.1 Distribution of microspheres on and across the chorions

0.2 μm sized microspheres

The microspheres were distributed all over the chorion of zebrafish after 24 hours (Figure 13 A-C) and 48 hours (Figure 13 D-F) of incubation. During exposure, the fluorescent signal of the chorion increased slightly. Depending whether the chorion surface showed deposits of the parents, such as feces or leftovers from the oviduct (Figure 13 D-F) in greater extent, the fluorescent signal increased equally.

On the optical planes, no signal of fluorescent microspheres was detected neither inside the chorions, nor in the embryos and on the surface of the embryos. At 48 hpf, the chorion showed distinct projections of feces and oviduct leftovers, enforcing the signal and leading to an fluorescent signal in the optical planes beneath the chorion surface (asterisk in Figure 13 D-F). This however, has to be counted as an *artefact*.

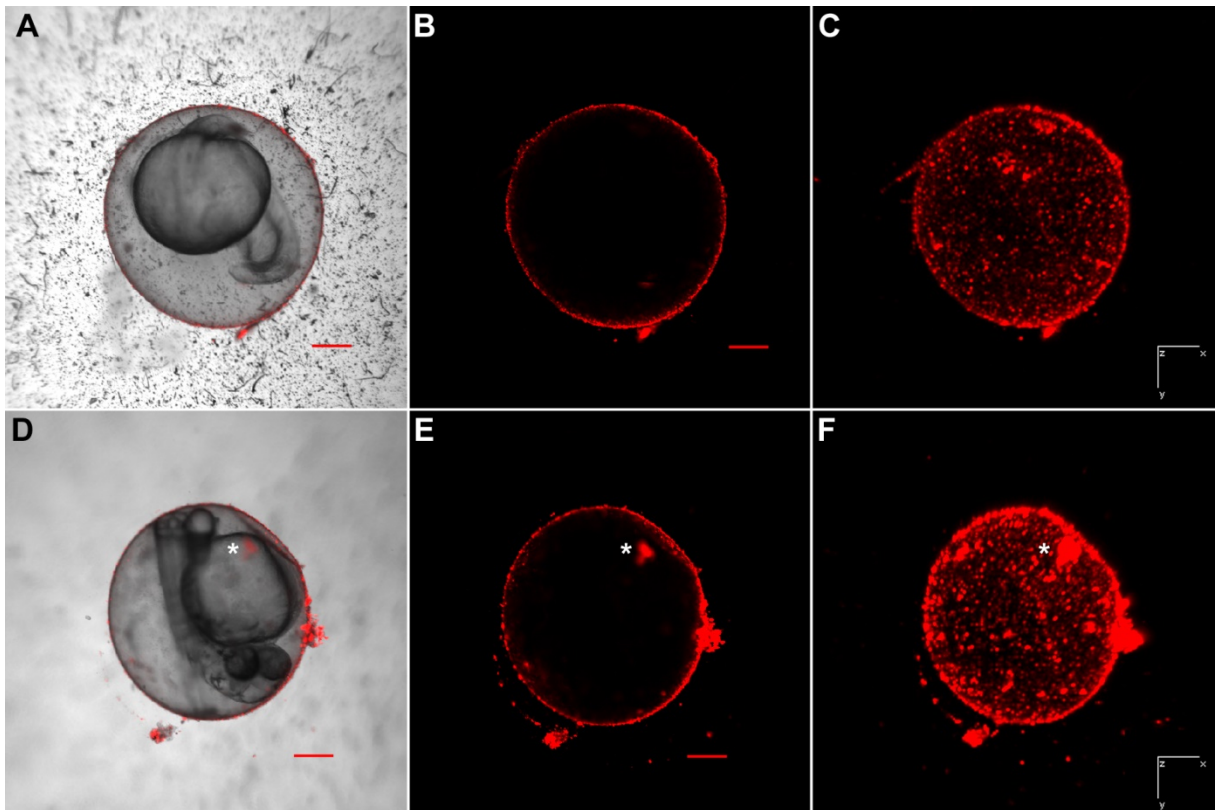


Figure 13: Fluorescence signal detected on the surface of the chorion of 24 hpf embryos (A-C) and of 48 hpf embryos (D-F). The $0.2\ \mu\text{m}$ sized fluorescent microspheres are evenly distributed over the chorion surface, however, feces and other distinct projection on the chorion surface are strongly fluorescent (see asterisk). Settings: HV12, TD 50; all panels; 4x magnification; scale bars in A, B, D, E: $200\ \mu\text{m}$.

0.1 μm sized microspheres

After 24 hours of exposure to $0.1\ \mu\text{m}$ microspheres, the chorion surface is again evenly covered by the small fluorescent beads, giving a bright signal. At 48 hpf, the signal is slightly uneven, with some distinct projections. At areas where strong signals were found, e.g. the widest diameter, the signals were also detected from higher and lower optical planes, overlying with each other and thus enforcing the signal. In addition, this leads to a shifted signal within the chorion (compare Figure 14 B and E).

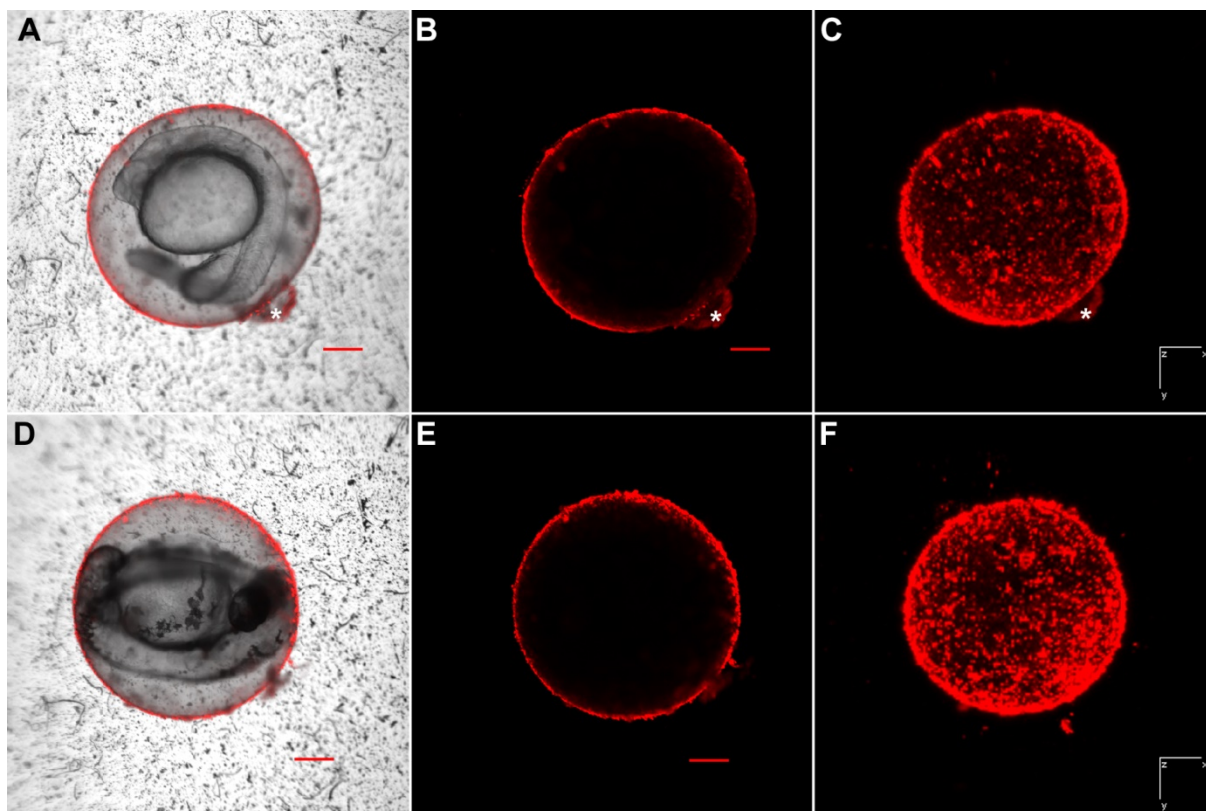


Figure 14: Fluorescence signal detected on the surface of the chorion of 24 hpf embryos (A-C) and of 48 hpf embryos (D-F). The $0.1 \mu\text{m}$ sized fluorescent microspheres are evenly distributed over the chorion surface, however, feces and some distinct projection on the chorion surface are strongly fluorescent (see asterisk at 24 hpf). Settings: HV12, TD 50; all panels: 4x magnification; scale bars in A, B, D, E: $200 \mu\text{m}$.

0.048 μm sized microspheres

Exposure to $0.048 \mu\text{m}$ sized microspheres revealed a time-dependent increase of the fluorescent signal on the chorion surface. The signal at 24 hpf was patchy and section of the widest diameter (Figure 15 B) shows areas with no fluorescent signal. After 48 hours of exposure, the signal was found to cover the chorion surface very evenly. Due to handling during embedding, the chorion was dented (see asterisks in Figure 15 C and F), giving the impression of no or only little fluorescent signal.

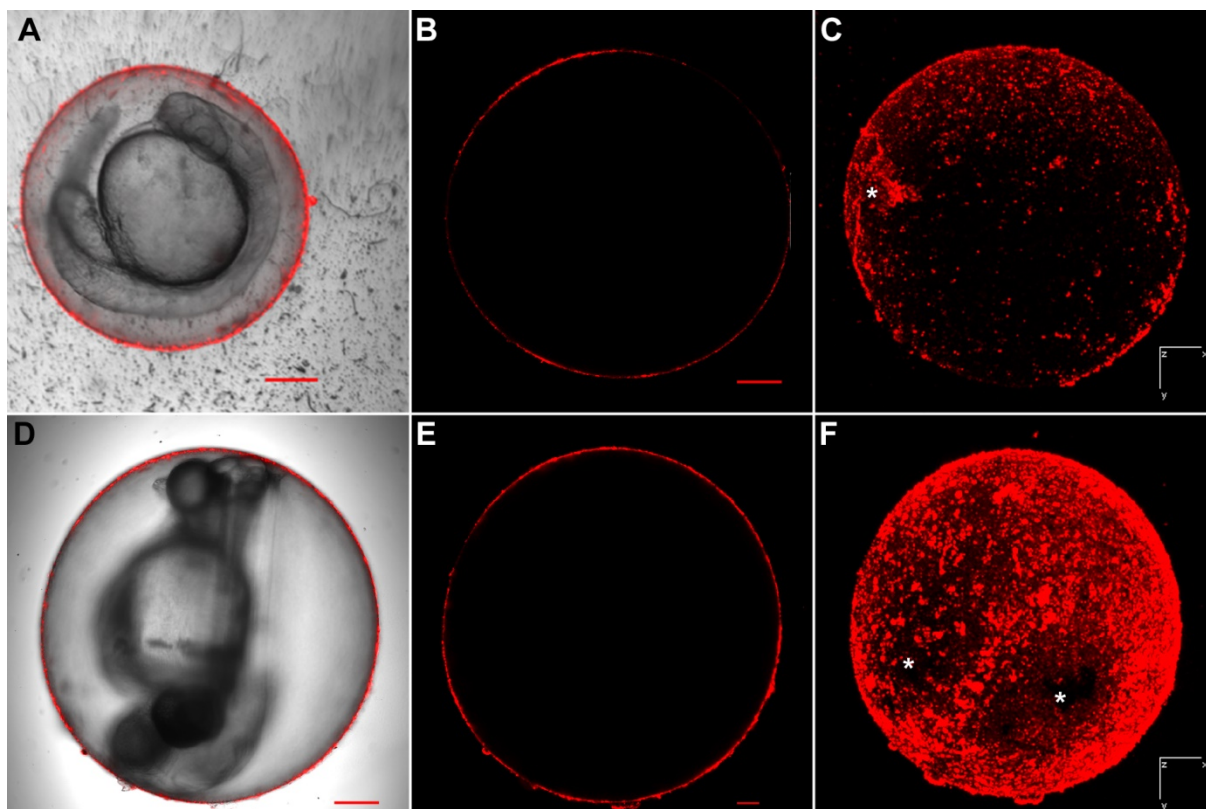


Figure 15: Fluorescence signal detected on the surface of the chorion of 24 hpf embryos (A-C) and of 48 hpf embryos (D-F). The $0.048\ \mu\text{m}$ sized fluorescent microspheres are evenly distributed over the chorion surface. However, dents on the chorion surface seem to be less fluorescent than the normally shaped surface (see asterisks). Settings: HV 12, TD 50. Panel A: 4x magnification; scale bar: $200\ \mu\text{m}$. Panel B-F: 10x magnification; scale bars in B, D, E: $300\ \mu\text{m}$.

2.4.2 Dechorionated embryos - exposure within the chorions

After 48 hpf, embryos exposed for 48 hours within the chorion were dechorionated mechanically. No signals at all were found within or attached to the embryos exposed to 0.2 , 0.1 and $0.048\ \mu\text{m}$ sized microspheres. Only one embryo exposed to $0.2\ \mu\text{m}$ sized microspheres showed some single, distinct signal in the head area. However, the signal was very low and thus it was not possible to illustrate properly in a micrograph. As this was found in only one exceptional embryo and the signal seem to be a result of only 3 to 5 microspheres adhered to the head (see arrowheads Figure 16). Therefore, a crossing of the microspheres across the chorion can be fairly excluded and the signal might derive by single microspheres displaced during handling.

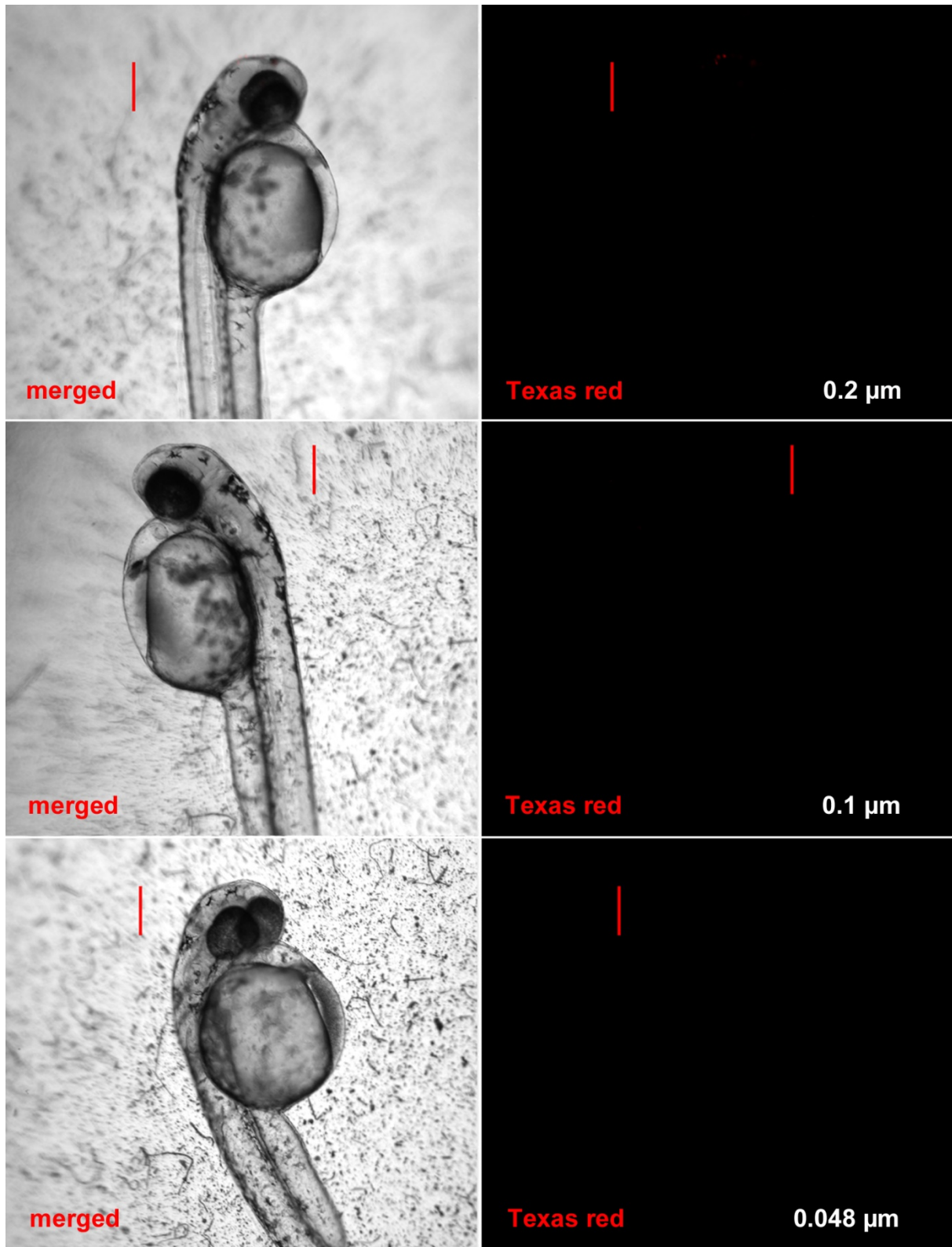


Figure 16: Embryos exposed for 48 hours within the chorion to 0.2 μm microspheres (first row), 0.1 μm microspheres (second row) and 0.048 μm microspheres (third row). For the detection of microspheres on the surface, embryos were dechorionated at 48 hpf. No signal on or within the embryos were detected after exposure to 0.2, 0.1 and 0.048 μm microspheres. One embryo exposed to 0.2 μm microspheres showed single fluorescent signal at the head area, however, signal is negligible and cannot be detected in the micrographs (first row). Settings: HV12, TD 50; scale bars: 200 μm, 4x magnification.

2.4.3 Details of the chorion

Taking a closer look on the chorion of the exposed eggs, small dark spots are seen in the transmitted light image (TD; black arrows in Figure 17). The merged images of the texas red channel and the TD channel illustrates that the fluorescent signal of the 0.1 μm sized microspheres does not arise directly from these spots. The fluorescent signal of 0.048 μm microspheres detected on the surface of the chorion is in some parts very distinct (red arrowhead in Figure 17) and might represent fluorescent beads stuck in the chorion pores. Nevertheless, some areas of the chorion surface emit a fluorescent signal distributed very even and in bigger clusters. This might be due to agglomeration and/or overlaying signal from optical sections beneath the one presented here.

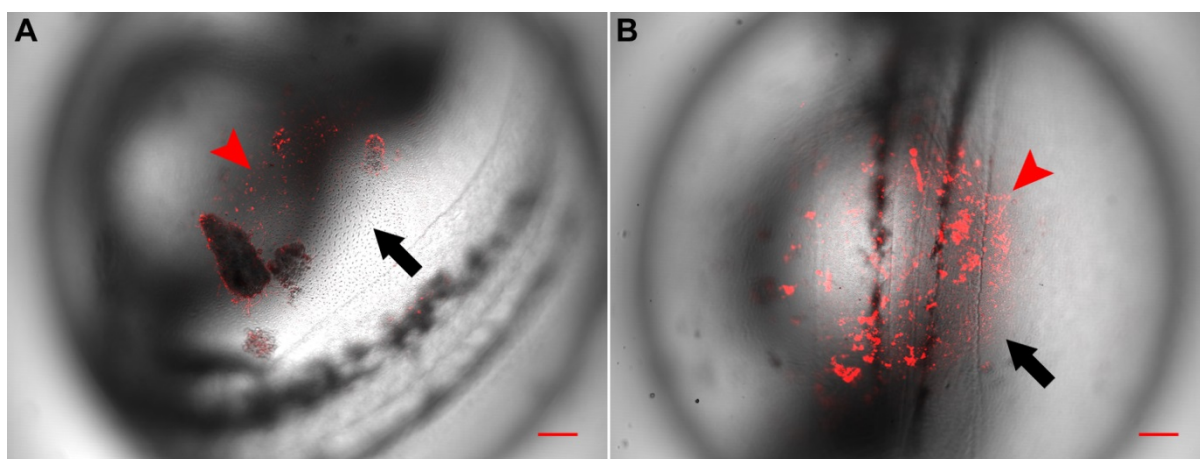


Figure 17: Close-up on zebrafish eggs at 48 hpf exposed to 0.1 μm (A) and 0.048 μm (B) microspheres. The merged images of TD and laser reveal the pores (black arrow) piercing the chorion and the fluorescent microspheres (red arrowhead) adhering onto the chorion surface. Settings: HV 10; TD 58; scale bars: 150 μm ; 10x magnification.

Higher magnification (60-fold and more) of sections of the chorion support the assumption of the dark spots seen in TD channel to represent the pores piercing the chorion of zebrafish (Figure 18 B and D). These pore canals seem to completely pierce the chorion and give the impression of a perforated membrane. The sections of the chorions were made after short term incubation of eggs to 0.2 μm microspheres at 24 and 48 hpf, Nevertheless, the cryosections show that the fluorescent signal of the 0.2 μm sized microspheres did not arising from the pores themselves. The microspheres adhere to one side of the chorion, which is assumed to be the outer surface of the egg envelope. Also, distinct projections on the surface are found on the surface.

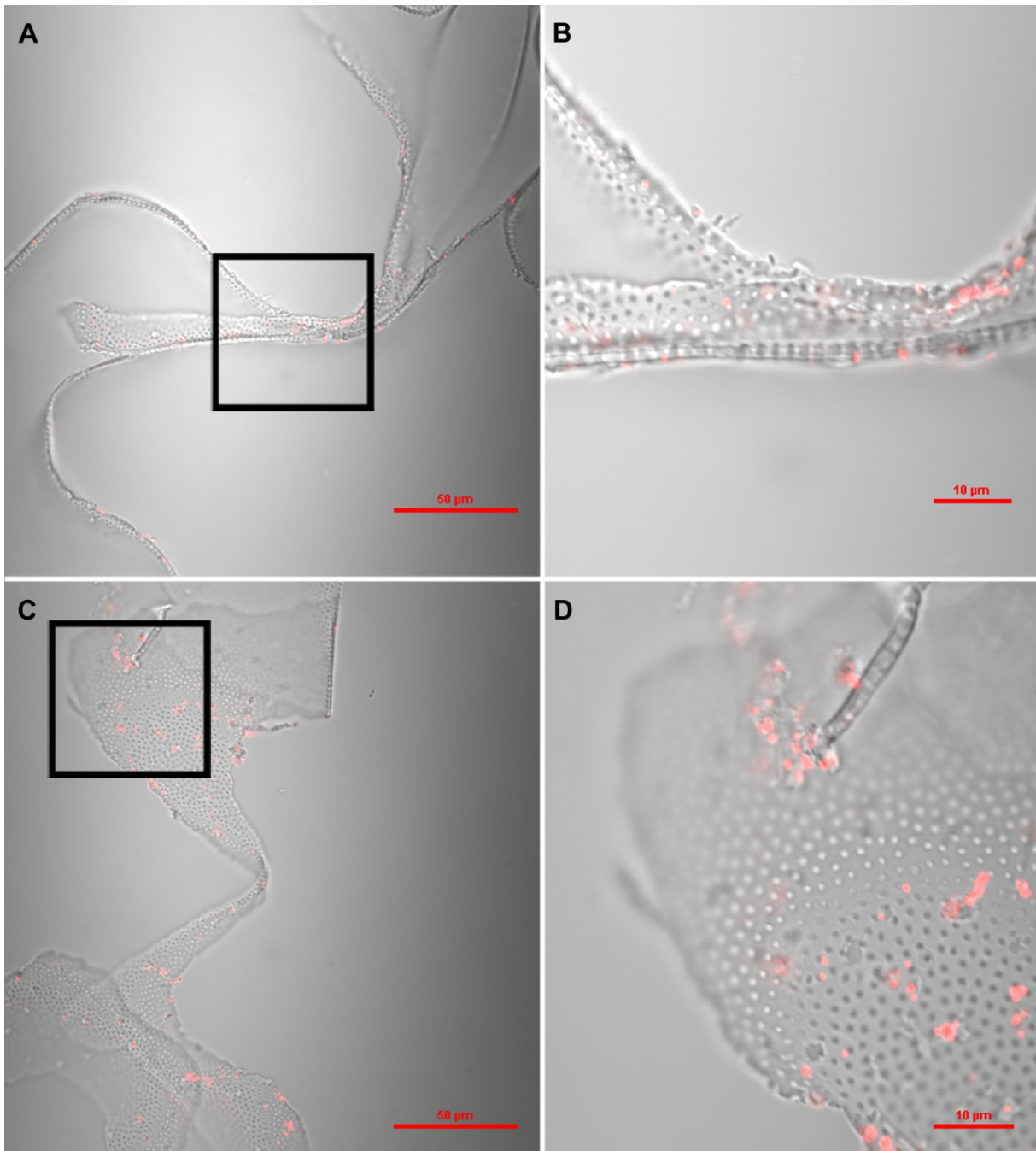


Figure 18: Distribution of 0.2 μm carboxylate-modified microspheres on the chorion surface (18 μm sections) of zebrafish eggs at 24 hpf (A & B) and 48 hpf (C & D). Panel A and C show an overview of the chorion section while panel B and respectively D is a detailed view on the selected area marked in panel A and C. The chorion pores are either dark or light, depending on the optical refraction. Laser power: 100%, HV: 30; TD: 72. Magnification: 60x (A, C) with scale bars: 50 μm ; 60x3.145 (B, D) with scale bars: 10 μm .

2.5 Discussion

During exposure, no precipitations or hints of agglomerations of the differently sized microspheres within the test media were found. Also, no effects on survival of embryos exposed to the microspheres were observed. Due to chorion softening before hatch, the chorion structure at 48 hpf was very fragile and tend to dent when excessive water, transferred with the egg into the glass bottom dishes for microscopy, was removed from the eggs or when embedding in 1% low melting agarose was done. Nevertheless, the eggs were analyzable if their chorion was still intact and no striking differences to normally shaped chorions were detectable. No auto-fluorescence of zebrafish embryos was detected in the negative controls conducted in each test run with the described microscope settings.

None of the chosen microspheres, 0.048, 0.1 and 0.2 μm in size, were taken up across the chorion at 24 and 48 hpf. *Via* laser scanning microscopy, the fluorescent signal of the microspheres was easily detectable and single fluorescent spots were supposed to represent single microspheres. The different optical planes of the eggs showed that the fluorescent signal was only detected at the chorion surface and neither within the perivitelline space nor at or inside the embryo. Images of dechorionated embryos after exposure inside the chorion confirmed these findings, since only very little fluorescent spots were detected. They might have also been transferred by accident, when dechoriation was performed and the embryo might have gotten in contact with the microspheres adhered to the chorion. The same techniques has been applied by Fent et al. (2010), who showed that neither 60 nm nor 200 nm fluorescent silica NPs were detected at or within the exposed embryos. The signal they detected only derived from the chorion surface confirming the barrier function of the zebrafish chorion. In medaka, fluorescent latex nanoparticles with 40 - 500 nm in size, were shown to adhere to the chorion but also to be taken up into the embryo and accumulated in yolk sac, oil droplet and gallbladder (Kashiwada, 2006; Manabe et al., 2011), although the chorion of medaka is thicker than the chorion of zebrafish.

The chorion surrounding the developing zebrafish embryo is pierced by pore canals which are supposed to be important for the exchange of gas and excretion products (Hisaoaka, 1958). Viewed by light microscopy, the pore canals seem to pierce the chorion completely (see Figure 18), leading to the assumption of a sieve-like membrane (Hisaoaka, 1958). The outer diameter of the chorion pores have been measured by Rawson et al. (2000) to be 0.5 – 0.7 μm with a center-to-center distance of 1.5 – 2.0 μm , which has been verified by Lee et al. (2007) in the chorion of living embryos using optical microscopy. The pores are cone-shaped with an even

larger opening in the inside of the chorion. So based on the diameter, the microspheres applied in this study should have been small enough to pass these pore canals. However, on the outside of the chorion, several studies applying electron microscopy have found an electron-dense layer, which at some point appear to completely plug the pores (Hart and Donovan, 1983; Lillicrap, 2010; Rawson et al., 2000). Scanning electron microscopic (SEM) images taken by Lillicrap (2010) at 8 000-fold magnification showed this layer to consist of individual polypeptides covering the outside of the chorion and recessing into the pores. So this outer surface glycoprotein layer might possess a stronger barrier function for the uptake of chemicals and especial of nanoparticles than the diameter of the pores.

Nevertheless, some studies have shown the successful uptake of nanoparticles across the chorion of zebrafish. Live imaging of the uptake across the pore canals were performed by Lee et al. (2007; 2012), documenting the passive diffusion of individual silver nanoparticles (5 – 72 nm sized AgNPs) *via* the chorion canal and into embryos. The time a single AgNP stayed within the chorion canal was determined to 0.1 to 15 s, although some particles extended the time within the pore canal, leading to agglomeration with incoming AgNPs and thus a clogging of the pore canal. Asharani et al. (2008) have shown not only an uptake of 5 – 20 nm sized silver nanoparticles (AgNPs) capped with BSA across the chorion of zebrafish at 48 hpf, but also the uptake into the embryo and even into the nucleolus of cells. Also Felix et al. (2013) visualized negatively charged nanocapsules containing Nile red on the chorion and embryo surface as well as within the yolk at 24 hpf. However, when evaluating the distribution of nanocapsules containing cerium oxide (CeO₂), the majority was associated with the chorion (about 39%) and only 0.07 ± 0.01% was found with the embryo after 48 hours. This reflects the difficulties of studies unraveling the mystery of nanoparticle uptake through observation of toxicity alone. Some researchers have found that the absence or presence of the chorion did not influence the toxicity of AgNPs (Böhme et al., 2015a; Cunningham et al., 2013). However, one of the most discussed problem applying nanoparticles is whether the toxicity in fish embryos derive from the nanoparticles or the release of dissolved ions. In the past, especially metal ions have been shown in several studies to attach to the chorion of different fish species (see for example: Beattie and Pascoe, 1978; Michibata, 1981; Ozoh, 1980; Stouthart et al., 1996) and this binding seems to hold true for metal NPs, the most studied nanoparticles. AgNPs and titanium dioxide (TiO₂) NPs 25 nm in size were found bound to the chorion surface after 24 hours, however the presence of silver ions inside the embryos was supported by the increased toxicity and expression of metallothionein (MT2) in exposed em-

bryos (Osborne et al., 2013). Similar distribution pattern were found by Böhme et al. (2015a) who showed an accumulation of silver at the chorion in normally developed embryos, but also an accumulation at the chorion and within the perivitelline space in sublethally or lethally affected embryos after exposure to silver NPs. They explained the observed toxicity by a local increase of NP concentration at the chorion and a facilitated release of dissolved Ag ions and subsequent uptake across the chorion. Contrarily, Bai et al. (2009) stated that dissolved zinc oxide only partly contribute to the toxicity of zinc oxide (ZnO₂) NPs in zebrafish embryos, which was however refuted by Brun et al. (2014). They also showed the chorion to be an effective barrier for both, the zinc ions and ZnO₂ NPs during the first 48 hpf of zebrafish development. Anionic charged groups of the chorion proteins are suggested to be responsible for this binding (Beattie and Pascoe, 1978; Michibata, 1981; Ozoh, 1980; Stouthart et al., 1996). The molecular constituents of the egg envelope was investigated by Bonsignorio et al. (1996), showing four major polypeptides (116, 97, 50 and 43 kDa) of which the 116 and 50 kDa proteins were stained by lectins, suggesting to be N-linked glycoproteins. Amino acid analysis revealed more serine but less proline content compared to other species. Both of these amino acids are zwitterions, bearing a carboxyl group. Additionally, Pullela et al. (2006) detected thiol-rich proteins in the chorion of zebrafish *via* DSSA probes. All these findings support the explanations why positively charged chemicals, such as metal ions, are bounded to the chorion. In contrast, the applied microspheres containing carboxyl groups themselves therefore are supposed to be negatively charged and were still only detectable at the chorion surface. The hydrophilic carboxylate-modified microspheres are made by grafting polymers containing carboxylic acid groups to sulfate microspheres (Invitrogen, 2004). When ovaries of mature females or ripe eggs are stained by hematoxylin-eosin, the chorion is in all the different steps throughout oogenesis stained pink by the acidic eosin. Usually eosin binds to basic or eosinophilic compounds containing positively charges (Mulisch and Welsch, 2015). It might be possible, that the major components, the polypeptides forming the rigid egg envelope, are indeed positively charged and only the outermost surface layer covering the chorion is negatively charged.

The fluorescent signal of the attached microspheres at the chorion of zebrafish eggs seem to be intensified through extended exposure period. After 48 hpf, the signal and thus the particles attached to the chorion have increased. During embryogenesis, the chorion becomes more permeable from 26 hpf onwards due to the secretion of hatching enzymes (Kim et al., 2004). So the structure of the chorion changes and might also lead to an increase of superficial area,

at which the microspheres can bind to, since still no uptake across the chorion was found. Also, a direct interaction with the pore canals leading to pore clogging as described for AgNPs (Lee et al., 2007) could not be found in higher magnifications.

The uptake of particles across the chorion, which is believed to be driven by kinetically controlled attachment and deposition processes (Praetorius et al., 2014), is also strongly influenced by particle properties - such as size, coating and surface charge. For further testing of nanoparticles with embryonic stages, the determination of actual concentrations in the perivitelline fluid and within the embryos excluding the chorion (Brox et al., 2014) becomes important. Also, a refinement of analytical techniques for a clearer identification of nanoparticles or dissolved parts is necessary. Due to these inconsistencies, several researchers have recommended to test nanoparticle toxicity only in dechorionated embryos to get toxicity driven responses instead of results influenced by the chorion (Kim and Tanguay, 2014; Kim et al., 2014; Meredith et al., 2016; Shaw and Handy, 2011).

2.6 Conclusions

Laser scanning confocal microscopy is suitable to detect the signal of fluorescent polystyrene beads on the chorion of zebrafish embryos. The applied microspheres had diameters of 0.048, 0.1 and 0.2 μm and were thus smaller than the diameter of the chorion pores (0.5 - 0.7 μm). Yet, the chorion of zebrafish seems to be an effective barrier for carboxylate-modified microspheres after 24 and 48 hours of exposure, since the fluorescent signal was only detected on the chorion surface, while no signal was emitted from the embryo within the chorion or from dechorionated embryos. It is assumed that not only the size is important for the uptake across the chorion, but also physical and chemical properties of the nanoparticles. Therefore plain microspheres of similar sizes were tested in zebrafish embryos and the results are shown in the upcoming chapter of this thesis.

Chapter III.

Influence of functional groups displayed on the surface of nanoscale polystyrene particles on the uptake across the chorion

3. Influence of functional groups displayed on the surface of nanoscale polystyrene particles on the uptake across the chorion

3.1 Abstract

As has been shown in Chapter II, carboxylate-modified microspheres were, despite their size of 0.048, 0.1 and 0.2 μm , not able to cross the chorion of zebrafish embryos within the first 48 h of embryonic development. To investigate the influence of the surface properties of nanoparticles on the uptake across the chorion and into the embryo of zebrafish, plain polystyrene microspheres were applied. The chosen microspheres were 0.05, 0.1, 0.2, 1 and 6 μm in size, bearing a yellow-green fluorescent dye and the surface was not modified by additional functional groups. The distribution patterns of the fluorescent microspheres were investigated by laser scanning confocal microscopy (LSCM) *in vivo* at 24 and 48 hpf. No uptake was found for the 1 and 6 μm sized particles, the signal was only detected at the chorion surface. The 0.05 and 0.2 μm sized microspheres were found at the chorion of the eggs, but also within the embryos, mainly within the yolk sac. The 0.2 μm microspheres showed a slower and thus time-dependent uptake across the chorion and within the embryo. The 0.1 μm sized particles showed a different pattern. They were evenly distributed at the chorion surface and the signal deriving from the embryo was very low and had to be strongly multiplied for detection. Hence the properties of the residues on the chorion surface seem to play an important role for the interaction with and the uptake across the chorion surface and embryonic membranes.

3.2 Introduction

Polystyrene nano- and microparticles have a polystyrene core, in which the fluorescent dye can be entrapped. The surface of the beads can display variable functional groups to determine the effective surface charge. Typical cationic microspheres are polystyrene particles displaying amino groups. These cationic particles have been shown to be more toxic compared to the anionic particles of the same size in different cell lines (Anguissola et al., 2014; Bexiga et al., 2014; Foged et al., 2005; Fröhlich, 2012; Kettler et al., 2014; Liu et al., 2011; Wang et al., 2013; Zauner et al., 2001), in sea urchin embryos (Della Torre et al., 2014) and as well as for dendrimers in fish embryos (King-Heiden et al., 2007). Interestingly, King-Heiden et al. (2007) showed an increased toxicity in the presence of the chorion with cationic PAMAM dendrimers G4.0, whereas Bodewein et al. (2016) suggest the chorion to be rather

protective. Cationic particles interact with cellular membranes and the cytotoxic effect might derive from the formation of small holes in the membrane (Bexiga et al., 2014; Foged et al., 2005; George et al., 2012; Kettler et al., 2014; Storm et al., 1995; Wang et al., 2012).

Anionic microspheres have been applied frequently in biological methods due to their broad availability. The surface of these microspheres is highly charged and relatively hydrophilic (Invitrogen, 2004), making them water-soluble, less likely to bind to negatively charged cell surfaces, but more likely to bind proteins and other biomolecules. However, binding is less strong than by hydrophobic microspheres and coupling has to be supported by reagents (Invitrogen, 2004). Anionic microspheres are commonly functionalized with carboxylate or sulfate residues, leading to steric groups on the surface. Plain microspheres, which are not specialized any further, are supposed to bear sulfonated residues due to polymerization reaction during production processes (Anguissola et al., 2014; Della Torre et al., 2014). Although they are also anionic charged, they do not bear any additional functional groups but allow a direct comparison to the carboxylate-modified microspheres.

The first obstacle the nanoparticles have to overcome is the chorion of the fish embryos. The zebrafish chorion has been described in detail in the Introduction of this thesis and its barrier function has been discussed in Chapter I and Chapter II. It is an acellular envelope composed of different *zona pellucida* proteins and a glycoprotein layer as the outer cover. Therefore, active uptake mechanisms as found in several cells cannot be transferred to the chorion uptake of nanoparticles. A passive uptake of nanoparticles has been further investigated in mammalian red blood cells, although the uptake takes place at the lipid bilayers which form the cell membrane. It has been shown, that the nanoparticles enhance the flexibility of the membranes without the formation of persistent holes (Wang et al., 2012).

As has been shown in Chapter II, carboxylate-modified microspheres were, despite their size of 0.048, 0.1 and 0.2 μm , not able to cross the chorion of zebrafish embryos within the first 48 h of embryonic development. The outer diameter of the pores in zebrafish chorions were determined at 0.5 - 0.7 μm (Lee et al., 2007; Rawson et al., 2000) with a center-to-center distance of 1.5 - 2.0 μm . The pores are cone-shaped with an even larger opening at the inside of the chorion. Based on the results obtained in the previous chapter of this thesis with carboxylate-modified microspheres, this chapter focuses on the influence of surface properties of microspheres on the uptake across the zebrafish chorion. Instead of carboxylate-modified surfaces, plain microspheres were applied to freshly fertilized zebrafish embryos. These beads bear no additional functional groups on their surface. However, a comparison to the results

gained in the previous chapter is possible, since the plain particles exhibit a comparable charge, i.e. zeta-potential, as the microspheres used in Chapter II (Anguissola et al., 2014; Lundqvist et al., 2008; Ruenraroengsak and Tetley, 2015). The interaction of nanoparticles with the chorion might as well be especially influenced by surface modifications of the nanoparticles, leading to an uptake across this barrier.

To investigate this interaction, plain microspheres were chosen for uptake-experiments with zebrafish embryos. The microspheres were 0.05, 0.1, 0.2, 1 and 6 μm in size, bearing a yellow-green fluorescent dye, and the surface was not modified by additional functional groups. Thus, the microspheres were anionic and the effective charge is supposed to be almost identical to the carboxylate-modified microspheres tested in chapter II. A restriction of uptake of the 1 and 6 μm sized microspheres is expected simple by the size difference to the chorion pore sizes. The uptake and distribution of the fluorescent signal of the microspheres was observed *via* LSCM in intact eggs as well as dechorionated embryos, which were evaluated at 24 and 48 hpf. Since only the displayed functional groups on the microsphere surface differed, a comparison was possible.

3.3 Materials and methods

3.3.1 Chemicals

All chemicals were of highest purity available and purchased from Sigma-Aldrich (Deisenhofen, Germany). Tests were performed in 24-well polystyrene plates (TPP, Renner, Dannstadt, Germany) covered with self-adhesive foil (Sealing tape SH, 236269, Thermo Fisher Scientific, Waltham, MA) and the lid. Pre-tests had shown no differences in microsphere distribution or fluorescence intensity between pre-saturated polystyrene plates or pre-saturated crystallization dishes made of glass. To avoid any agglomerations or disturbances, the ionic strength of the test medium (dilution water) was set to a minimum. Therefore, the FET dilution water according to TG 236 (OECD, 2013a) was prepared in a 1:5 dilution.

The used microspheres and additional information were generously provided by PhD student E. Malaeksefat of the Saarland University, Germany. They were not functionalized any further, the surface is supposed to display sulfonate residues; thus, they are anionic microspheres. All data obtained are listed in Table 5.

Table 5: Physical and chemical information of the differently sized microspheres.

Microsphere:	0.05 μm	0.1 μm	0.2 μm	1 μm	6 μm
Producer	Fluoresbrite [®] , Polysciences Inc.				
Catalog number	17149	17150	17151	17154	17156
Surface	Plain				
Core	Polystyrene latex bead				
Density of polystyrene	1.055 g/cm ³				
Concentration of particles/mL	3.64×10^{14}	4.55×10^{13}	5.68×10^{12}	4.55×10^{10}	2.10×10^8
Fluorescent dye	Yellow green (441/486)				
Emission maximum	486 nm				
Particle size [nm]	0.0431	0.111	0.22	1	5.841
Microscopy	only very few or no aggregates after sonication				

3.3.2 Fish maintenance and egg production

Wild-type zebrafish (*Danio rerio*, Westaquarium strain) derived from own breeding facilities at the University of Heidelberg. Fish maintenance and egg production have repeatedly been described in detail (Kimmel et al., 1995; Nagel, 2002; Spence et al., 2008) and have been updated for the purpose of the zebrafish embryo acute toxicity test (Lammer et al., 2009). Egg production was performed *via* spawning groups as recommended by the OECD TG 236 (OECD, 2013a) with modifications according to Sessa et al. (2008).

3.3.3 Exposure

All solutions containing microspheres were wrapped in aluminum foil to prevent photo-bleaching. The steps, where light was inevitable (pipetting, transferring of eggs, preparing of eggs/embryos), were kept at a minimum. The microspheres stock suspensions were sonicated for 5 minutes to gain homogenous suspensions before adding to the dilution water. The test concentrations were set to 0.01% and again sonicated for 5 minutes. The test design was basically according to OECD TG 236 (OECD, 2013a): plates were pre-saturated for 24 hours and the medium was renewed before insertion of the eggs and after 24 hours of exposure. The suitability of polystyrene plates was shown in pre-test by comparing the fluorescent signal at the chorion from embryos exposed in commonly used polystyrene plates and glass crystallization dishes. No difference was detected. Incubation of the eggs within the plates was performed in the dark at 26 ± 1 °C for 48 hours. A negative control without microspheres was run and evaluated in each test setup.

3.3.4 Preparation for microscopic evaluation

The distribution of microspheres at and within the zebrafish egg was evaluated at 24 and 48 hpf. Each egg was carefully washed three times with the modified dilution water (1:5). To immobilize the embryo within the egg, each egg was put into a well containing 1 mL of 0.016% tricaine solution (MS-222, ethyl 3-aminobenzoate methanesulfonate), prepared in 1:5 dilution water. At each time point, four exposed eggs were evaluated per microsphere class. Care was taken to avoid the light. Eggs were transferred within one small drop of tricaine solution into glass bottom culture dishes (MatTek Cooperation, Ashland, USA).

After semi-static exposure for 48 hours, four embryos were dechorionated after the washing steps with sharp forceps (DuMont™ No 5) as described by Henn and Braunbeck (2011). After dechorionation, the embryos were immobilized with 0.016% tricaine solution and transferred into glass bottom dishes.

To avoid any movement during laser scanning session, eggs and embryos were embedded in 1% low melting agarose (LMA; SeaPlaque® GTG® Agarose, FMC Bioproducts, Rockland, USA) prepared in 0.016% tricaine solution. Excess tricaine solution was removed from dechorionated embryos, which were orientated on the side within the LMA. Before analyzing under the fluorescence microscope, the embedded embryos were covered by 1 mL tricaine solution to keep the embryo immobilized during scan sessions and to avoid drying-up.

3.3.5 Analysis of the microsphere uptake and distribution

Analysis was performed with Laser Scanning Confocal Microscopy (LSCM, Nikon 90i; Nikon Instruments, Netherlands) and images were taken with a Nikon C1 camera (Nikon Instruments, Netherlands). Laser power was always set to 100%, the high voltage (HV) had to be adjusted individually for each microsphere and is noted under each image. Fluorescent (calcium green) and transmitted light (TD) images of optical section at the widest diameter of the egg are displayed separately and merged, and if available, z-stack images in $-z$ orientation are shown. The images of the dechorionated embryos are either shown as z-stacks in $-z$ orientation or as an optical section to localize the fluorescent signal. All microscope and laser settings are displayed in Table 6. Illustration of the microsphere distribution was performed using the Nikon imaging software NIS-Elements-Viewer (Vol. 4.20, Laboratory Imaging, 1991-2013).

Table 6: Laser and microscope settings for evaluation of fluorescent signal within the chorion

Laser settings		Calcium Green
	Emission wavelength:	515 nm
	Excitation wavelength:	488 nm
	Pinhole radius:	60.00 μm (10x objective) 30.00 μm (4x objective)
	Laser Power	100%
	High voltage (HV)	1 to 25*
	HV transmitted light (TD)	35 to 45*
Microscope settings		
	Objectives:	Fluor 10x W DIC N1 Plan Fluor 4x
	First dichroic mirror:	408/488/543
	First filter cube:	450/35
	Second filter cube:	515/30 605/75

* the exact HV settings of laser and transmitted light (TD) is noted underneath each image

3.4 Results

All tested microspheres showed a well-defined fluorescent signal and during the test, no agglomeration was found in the medium. However, the microspheres tended to bind to feces and fungal hyphae on the chorion surface. At 48 hpf, the chorions were fragile and sometimes covered with fungal hyphae. Care was taken to illustrate the eggs showing less fungal infection. The pictures shown in this chapter illustrate a representative overview of the distribution of microspheres in eggs and embryos at 24 and 48 hpf. HV of the images are noted under each panel.

6 μm microspheres

After 24 hours of exposure, only few microspheres were found at the chorion and the fluorescent signal derived solely from the chorion surface. In Figure 19, the patchy distribution of the microspheres on the chorion is illustrated. At 48 hpf, the microspheres did not cross the chorion; fluorescence was still only found at the chorion surface. As more microspheres were detected at the chorion surface at 48 hpf, a stronger signal was found. Hence, the HV of the laser had to be changed slightly from 15 at 24 hpf to 12 at 48 hpf. Noticeable, the chorion shape at 48 hpf was affected in all exposed eggs. The chorions were

very fragile, making it difficult to embed in agarose, and in some wells the embryo had already ruptured the chorion. Also, fungal hyphae were found on some chorions (see Figure 19 D – E). No z-stacks of eggs at 24 and 48 hpf were prepared.

To clarify, whether the microspheres were able to cross the chorion, also dechorionated embryos were analyzed. After 24 and 48 hours of exposure, no fluorescent signal was found at or within the embryos (not illustrated).

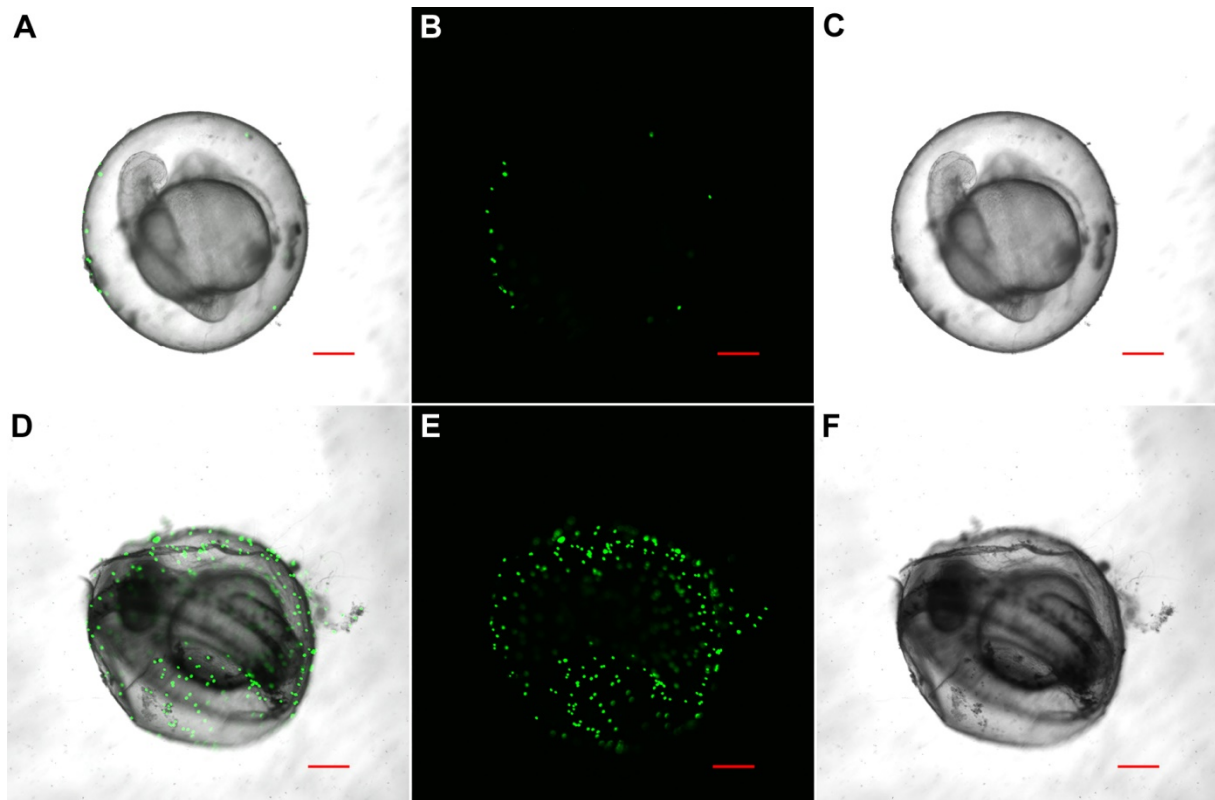


Figure 19: Distribution of 6 μm microspheres on the chorion of zebrafish embryos at 24 hpf (A-C) and 48 hpf (D-F). Merged (A, D), calcium green (B, E) and transmitted light (C, F) images illustrate the attached microspheres to the chorion surface but not within the egg or embryo. At 48 hpf, the chorion is strongly shrunken due to handling and embedding. HV: 15 (A-C); 12 (D-F); TD: 37; 4x magnification; scale bar: 200 μm .

1 μm microspheres

After eggs were exposed to 1 μm sized microspheres, the fluorescent signal was evenly distributed over the whole chorion surface at 24 hpf (Figure 20 A-C) and at 48 hpf (Figure 20 D-E). Differences could be found in the fluorescent signal intensity: more microspheres adhere to the chorion at 48 hpf, hence a stronger signal was detected and the HV needed adjustment (HV: 15 at 24 hpf and HV: 12 at 48 hpf). No signal was detected within the chorion and the embryo (Figure 20 A and D). Moreover, the dechorionated embryos did not reveal any fluo-

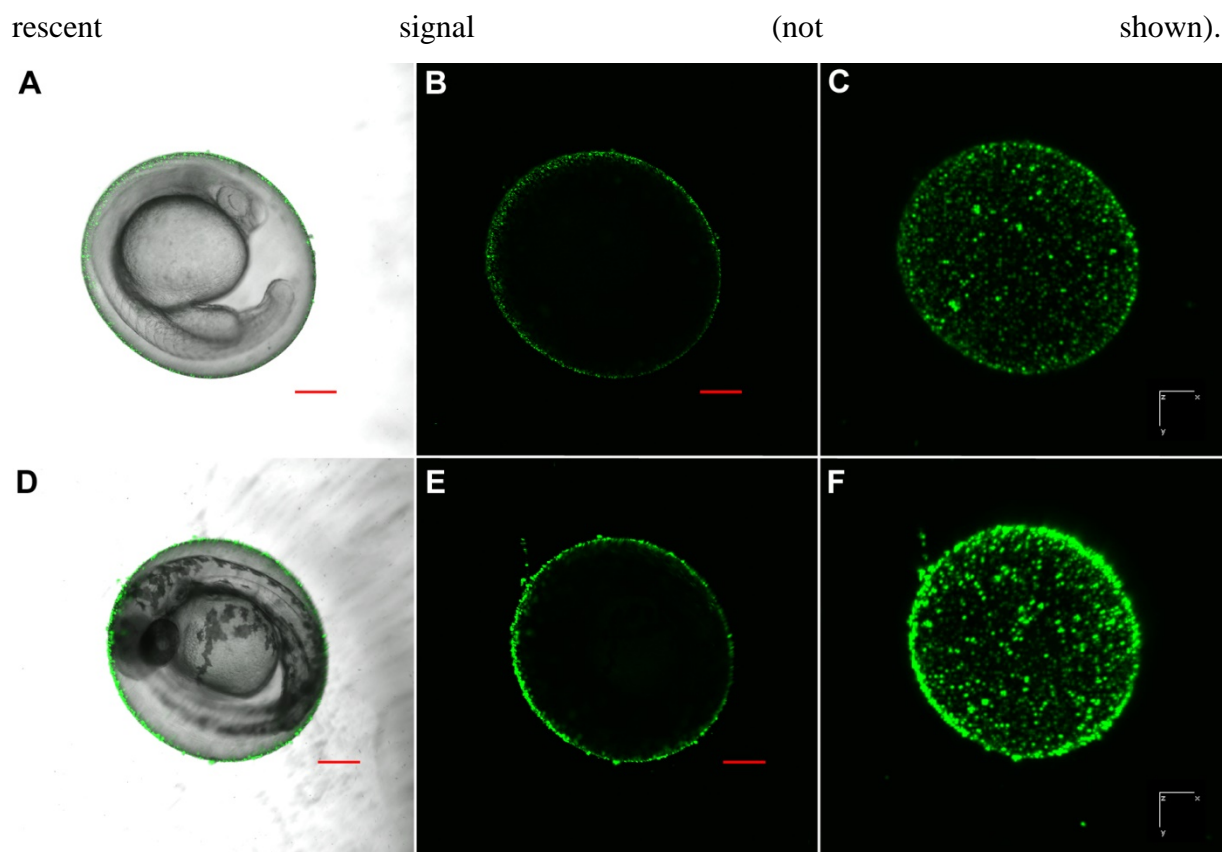


Figure 20: Distribution of 1 μm microspheres on the chorion of zebrafish embryos at 24 hpf (A-C) and 48 hpf (D-F). Merged TD and calcium green (A, D), calcium green (B, E) and z-stack (C, F) images illustrate the attached microspheres to the chorion surface but not within the egg or embryo. HV: 15 (A-C); 12 (D-F); TD: 37; 4x magnification; scale bar: 200 μm .

0.2 μm microspheres

The microspheres were evenly distributed over the chorion surface and the fluorescent signal detected increased with increasing exposure time. Partly stronger fluorescent signals on the chorion surface indicate small agglomerations of microspheres, which were especially found at 48 hpf. Since the fluorescence increased in time, the HV settings for the z-stack image at 48 hpf had to be reduced to HV of 1 to avoid oversaturation. Taking a look on the optical sections of the exposed eggs in Figure 21, no signal can be detected within the eggs at 24 hpf, however at 48 hpf, a very light signal can be seen, adumbrating the shape of the yolk (see arrowheads in Figure 21 E). This signal is very low and in dechorionated embryo at 24 hpf, no signal was detectable inside the embryo at an HV setting of 5. Z-stack images of the individual frames and the enhancement of HV settings to 12 resulted in a light fluorescent signal within the embryo as shown in Figure 22 A, with retraced body shape for better presentation. For a better illustration, the signal was even further intensified; micrograph B in Figure 22 is taken with a HV at 22. At 48 hpf, no intensification was necessary, the fluorescent signal deriving from the embryo was clearly detectable in single optical images taken with the same

settings as the whole eggs (HV: 5). The signal inside the embryo is mainly found within the yolk.

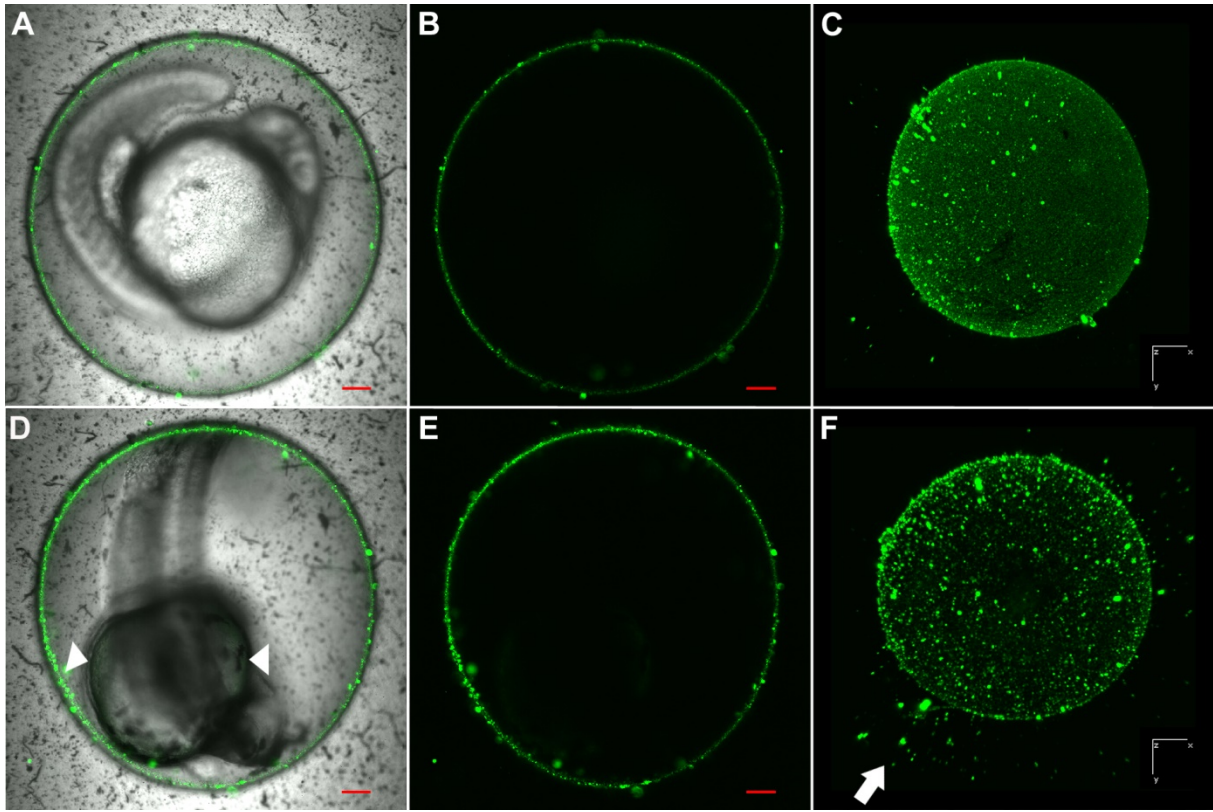


Figure 21: Distribution of 0.2 μm microspheres on the chorion of zebrafish embryos at 24 hpf (A-C) and 48 hpf (D-F). Merged (A, D), calcium green (B, E) and z-stacks (C, F) illustrate the attached microspheres to the chorion surface and very low signals in the yolk (see arrowheads in D). Arrow indicates aggregates of microspheres on fungal hyphae. A-E: HV: 5; F: HV: 1; TD 35; 10x magnification; scale bar: 150 μm .



Figure 22: Embryos exposed within the chorion to 0.2 μm microspheres and dechorionated before analyzing. At 24 hpf (A,B), z-stacks of the embryo were taken at HV: 12 (A) and HV 22 (B) illustrating fluorescent signal within the yolk (y), the yolk extension (ye) and no signal in head (h) and tail (t). At 48 hpf (C) signal was detected within the yolk (optical section) at HV 5. 10x magnification.

0.1 μm microspheres

The 0.1 μm microspheres were attached in an evenly pattern all over the chorion surface after 24 and 48 hours of exposure. Almost no agglomerations of microspheres were found, only at 48 hpf, small, stronger fluorescent projections were found. The signal deriving from the microspheres was very low; the images were taken with comparatively high photomultiplier settings (HV 20-25). Notwithstanding, no signal at all could be detected within the eggs or inside the embryos.

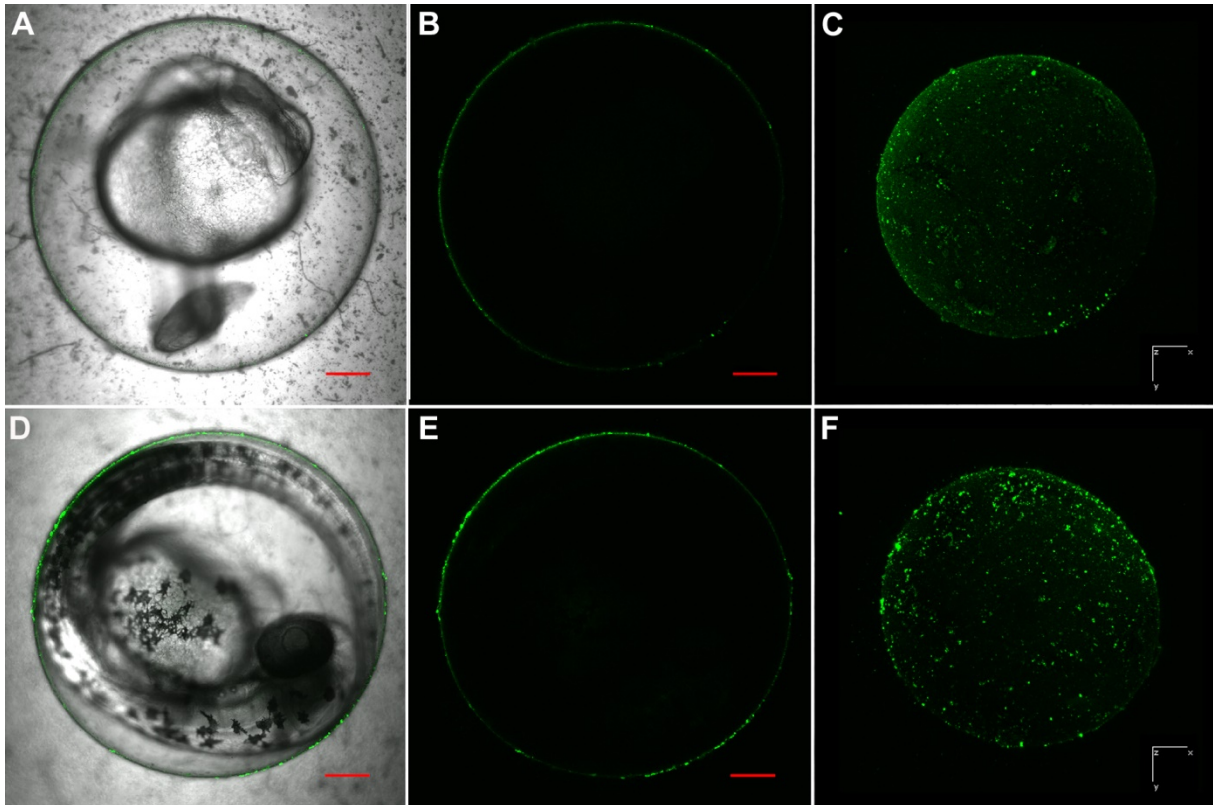


Figure 23: Distribution of 0.1 μm microspheres on the chorion of embryos at 24 hpf (A-C) and 48 hpf (D-F). Merged TD and calcium green (A, D), calcium green (B, E) and z-stack (C, F) images illustrate the attached microspheres to the chorion surface but not within the egg or embryo. A – E: HV: 25; TD: 45; F: HV: 20; 10x magnification; scale bar: 300 μm .

After the embryos were dechorionated and analyzed, the fluorescent signal was detected within the embryos. At 24 hpf, the fluorescent signal in the yolk was very low (HV: 22). At 48 hpf, the microsphere signal was found within the yolk and in the area of the head, however, differences in fluorescent intensity were striking between the different analyzed embryos. Embryos illustrated in panel B and C in Figure 24 were both captured with a very high HV setting of 30. The signal detected in embryo of micrograph C showed an overall fluorescence in the yolk, the head and in the somites. Comparing one optical frame from embryo B in different settings (B1: merged and B2: calcium green), the signal was found mainly in the yolk.

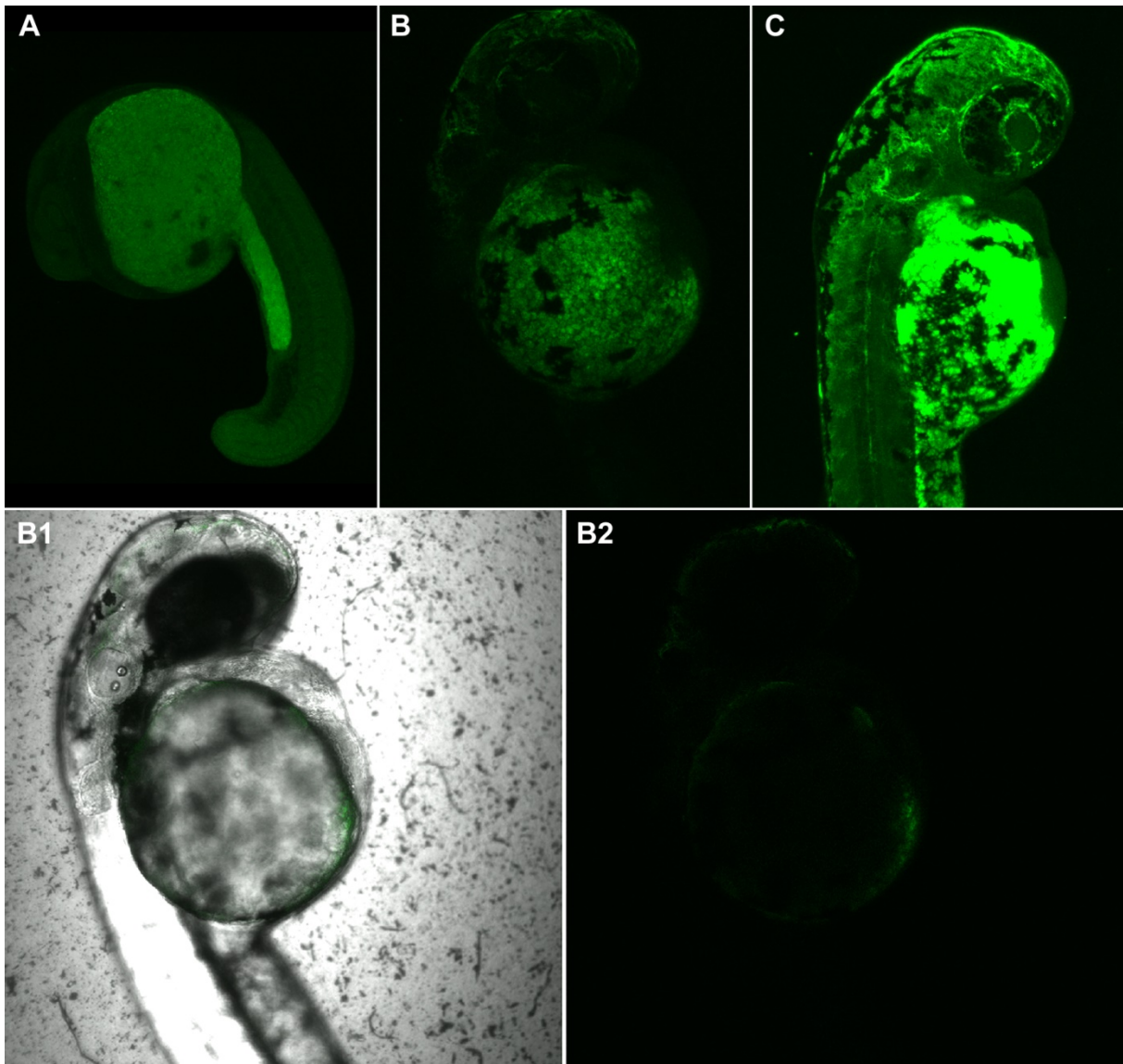


Figure 24: Zebrafish embryos exposed within the chorion to 0.1 μm microspheres and dechorionated before analyzing. At 24 hpf (A), the fluorescent signal can be found in the yolk sack, however, signal is very light although the image was taken with HV 22. At 48 hpf (B, B1-2, C), differences in intensity between the embryos were found. Z-stacks of the images taken with HV 30 (B and C) reveal different signal intensity. A single optical section image taken from the middle of the embryo shown in B, revealed a low signal at the yolk (B1 merged image, B2 calcium green only). B1-2: HV: 30; TD: 45; 10x magnification.

0.05 μm microspheres

Analysis of the fluorescent signal of the 0.05 μm microspheres revealed an even signal, covering the surface of the zebrafish chorion and showing small aggregates at 24 hpf (Figure 25 A-C), dents and fungal infection at 48 hpf (Figure 25 D-F). In the single cross section images taken at the widest diameter of the egg, the fluorescent signal can also be found within the embryo, but not within the perivitelline space. In z-stacks images of 24 and 48 hpf eggs, the embryos were clearly distinguishable within the eggs. Noteworthy, at 48 hpf the signal detected from microspheres inside the embryo was strong, so the HV had to be reduced to 1.

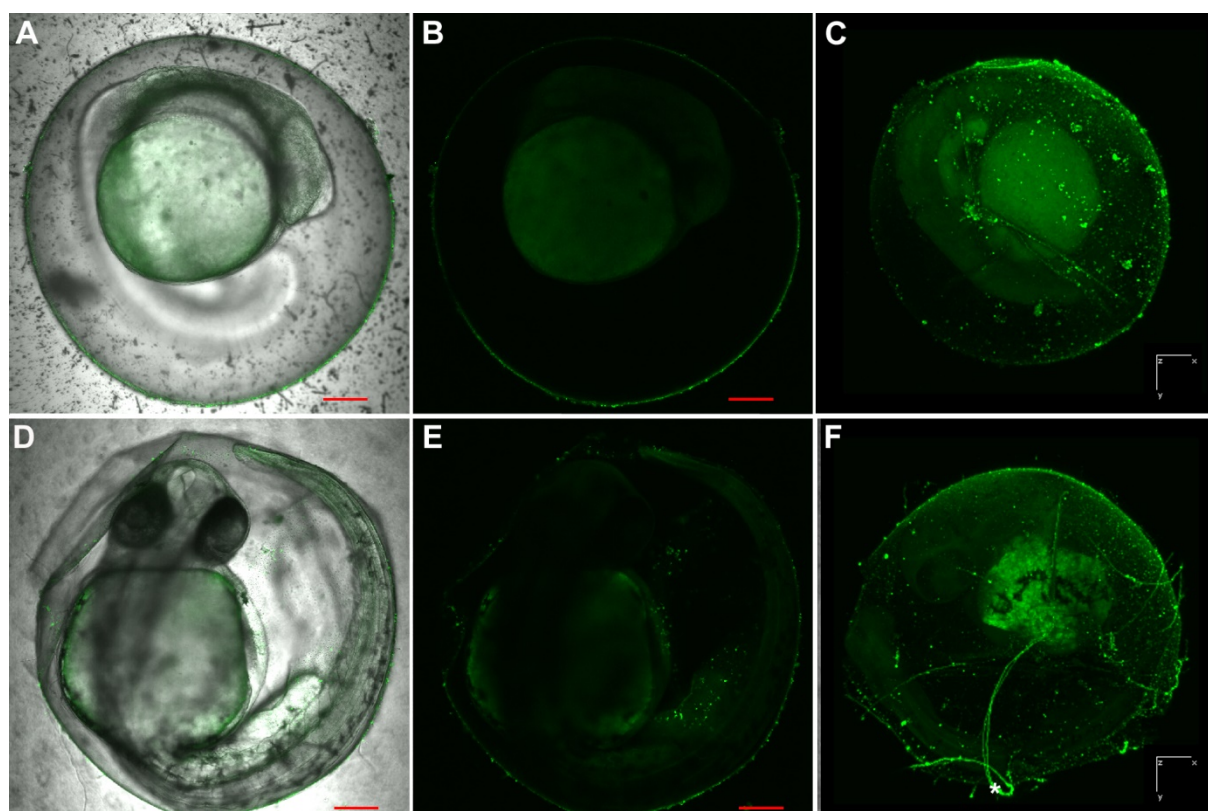


Figure 25: Distribution of 0.05 μm microspheres on the chorion of embryos at 24 hpf (A-C) and 48 hpf (D-F). Merged TD and calcium green (A, D), calcium green (B, E) and additionally z-stacks (C, F) images illustrate the attached microspheres to the chorion surface and within the embryo. At 48 hpf, the chorion is strongly shrunken due to handling and embedding and fungal infection can be found (asterisk). A-C: HV: 5; TD: 35; D-F: HV: 1; TD: 35; 10x magnification; scale bar: 300 μm.

After dechoriation, the main signal was found within the yolk at both endpoints. At 48 hpf, the signal could also be detected in the head region and in a lower extent in the somites (see Figure 26 B). The detected fluorescent signal of the embryos at 24 and 48 hpf was strong and consequently the HV was set to the minimum of 1.

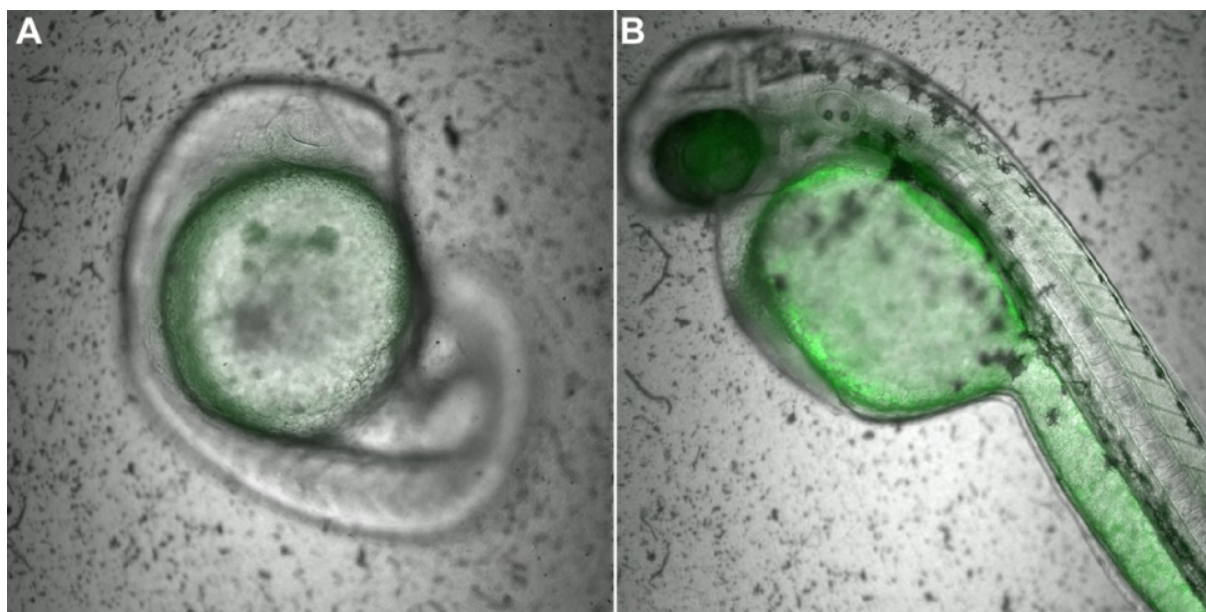


Figure 26: Zebrafish embryos exposed within the chorion to $0.05\ \mu\text{m}$ microspheres and dechorionated before analyzing. At 24 hpf a signal is detected in the yolk (A). The signal increases at 48 hpf (B) and expands to the somites and the head. HV: 1; TD: 35; 10x magnification.

3.5 Discussion

The main purpose of the experiments was to identify the potential implications of microsphere surface properties for an uptake across the chorion. Fluorescent microspheres with plain surface in a size of 6, 1, 0.22, 0.1 and $0.05\ \mu\text{m}$ were applied to freshly fertilized zebrafish eggs, and distribution patterns were recorded in intact eggs and dechorionated embryos. During exposure, no precipitations or hints of agglomerations of the differently sized microspheres within the test media were found. Likewise, no effects on survival of embryos exposed to the microspheres were observed. Due to chorion softening before hatch, the chorion structure at 48 hpf was very fragile and tended to dent when excessive solutions, transferred with the egg into the glass bottom dishes for microscopy, were removed from the eggs or when embedding in 1% low melting agarose was done. Nevertheless, these eggs were analyzable if the chorion was still intact and no differences to normally shaped chorions were detectable. No auto-fluorescence of zebrafish embryos was detected in the negative controls conducted in each test run with the different settings described. However, at HV 30 in some embryos of the negative control an auto-fluorescent signal was detected. This high HV setting was only applied for one illustration of $0.1\ \mu\text{m}$ microspheres in dechorionated embryos to illustrate the differences between embryos of the same batch. However, this strong difference in fluorescent signal between embryos of the same egg batch and test run was an exceptional case.

Simply by the size of the microspheres, an effective barrier function of the chorion and the embryo was expected for 6 and 1 μm sized particles. The outer diameter of the chorion pores have been measured by Rawson et al. (2000) to be 0.5 – 0.7 μm with a center-to-center distance of 1.5 – 2.0 μm , which has been verified by Lee et al. (2007) in the chorion of living embryos using optical microscopy. The pores are cone-shaped with a larger opening at the inside of the chorion. Regarding the pure given physical facts, the microspheres exceeding the size of the pore canal diameter and should clearly be hold back by the chorion. However, the effects of size on the uptake have already been discussed in detail in Chapter II. Further discussion of the distribution of the smaller sized particles will therefore focus on possible influences of surface properties.

Comparing the distribution pattern for the microspheres of 0.1, 0.2 and 0.05 μm it becomes clear that they are all evenly distributed on the chorion surface at 24 and 48 hpf. Hence, the local concentration of the microspheres at the chorion might be almost identical. If compared to the images taken at the carboxylate-modified microspheres of the same size (Chapter II), the distribution pattern is very similar. For all plain microspheres, an increase of particles attached to the chorion was found in combination with a prolonged exposure period (24 < 48 h). In contrast to the observations made for the carboxylate-modified microspheres, an uptake across the chorion and even into the embryos was found for plain microspheres 0.05 to 0.2 μm in size.

A striking inconsistency was found for the results of the 0.1 μm sized microspheres: The uptake of 0.05 and 0.2 μm sized particles suggested the ability of 0.1 μm microspheres to cross the pores of the chorion and reach the embryo. However, the fluorescent signal of the 0.1 μm sized particles was very low at 24 and 48 hpf and the HV had to be set up to 2. A further enhancement of intensity was needed when evaluating the dechorionated embryos (HV: 30). Also an irregularity of the signal intensity was found when comparing the images of different eggs taken with the same HV setting. High HV settings were needed for the detection of very low fluorescent signals, and, as a consequence, unspecific fluorescence signal might be detected. The detection of signal at the HV settings of 30 in control embryos confirmed the unspecific auto-fluorescence provoked at high HV. This might prove a restriction of uptake across the chorion and embryonic membranes for the 0.1 μm microspheres. It is noteworthy that the inconsistency in signal intensity between different individuals was only found in the test runs with 0.1 μm sized microspheres.

To exclude the possibility of fluorescent dye leaking from the inside of the 0.05 or the 0.2 μm beads leading to the detected signal within the embryos, test media of all three nano-sized microspheres were analyzed *via* LSCM. No leakage at all was detected into the media. The fluorescent signal derived exclusively from point-sources representing the single particles. When comparing the size of the fluorescent spots, a consistent increase from 0.05 to 0.1 and 0.2 μm was found.

A clear statement on the uptake can only be made for 0.2 and 0.05 μm microspheres. The 0.05 μm microspheres could easily be detected both inside the embryos within their chorions and inside dechorionated embryos at 24 and 48 hpf (Figure 25 and Figure 26). Notably, the HV were only set to 5 or 1, so the fluorescent signal was strong enough for a clear detection. With such low HV settings, the signal within the embryo at 48 hpf was also detectable in 0.2 μm exposure group. However, at 24 hpf, the fluorescent signal of the microspheres had to be multiplied (HV 12 and HV 22) for a clear signal within the embryo. This indicates a slower and time-dependent uptake across the chorion of the 0.2 μm sized particles compared to the smaller, 0.05 μm microspheres. Surprisingly, no signal at all was found within the perivitelline space.

Manabe et al. (2011) showed *via* fluorescent stereomicroscopy the uptake of plain and carboxylate-modified microspheres (Fluoresbrite[®], 50 nm) across the chorion and into medaka embryos. They found the strongest fluorescent signal within the most lipophilic embryonic compartments, the yolk sac and the oil droplet, and additionally in the gall bladder. In contrast to the complete block of the carboxylate-modified microspheres as presented in Chapter II, Manabe et al. (2011) found a signal of the carboxylate-modified nanoparticles in medaka embryos, albeit weaker than the one detected for plain microspheres. Their findings are presented without any further specifications about fluorescent microscopy settings, nevertheless it confirms the findings made in this thesis: Plain microspheres of 0.05 and 0.2 μm are taken up into zebrafish eggs and embryos, while the uptake of carboxylate-modified nanoparticles are at least restricted by the chorion.

It is well established that living cells incorporate nanoparticles (NPs) by passive penetration of the plasma membrane or actively by exploiting the cellular endocytosis machinery (phagocytosis and pinocytosis). For the passive penetration through cell membranes, NPs were shown to interact with the lipid membranes, inducing the induction of small pores in many cases (Fröhlich, 2012; Kettler et al., 2014; Treuel et al., 2013; Wang et al., 2012). Different surface modifications of polystyrene nanoparticles lead to cationic or anionic charges, affect-

ing the cellular uptake as well as the toxicity in various mammalian cell lines (Anguissola et al., 2014). Besides the already mentioned study by Manabe et al. (2011), this has also been shown in sea urchin embryos (Della Torre et al., 2014). It might be applicable for the uptake at the yolk syncytial layer and at the yolk cell membranes, where the uptake across the embryonic membrane is supposed to happen. However, the chorion is an acellular envelope and an active transport across this first barrier of the unhatched zebrafish can be excluded. The uptake of the microspheres across the chorion might be a combination of the different attractive forces exerted by the different egg compartments: The microspheres attach and deposit by kinetically driven processes (Praetorius et al., 2014) to the chorion surface, leading to an accumulation of the particles. Hence, the local concentration of microspheres increases and since the surface charges of the particles bound to the chorion surface are identical, an interaction between the particles is inevitable when a critical mass of particles is achieved. Consequently, the particles eventually cross the chorion *via* the pore canals. The exact mechanism of uptake across the chorion has not been revealed yet. Lee et al. (2007) postulated the uptake of AgNPs across the chorion to be a passive diffusion process depending on concentration gradients; however, Praetorius et al. (2014) described the behavior of NPs to be driven by kinetically controlled attachment and deposition and not by the formation of a thermodynamic equilibrium. Nevertheless, within the chorion a signal was only detected within the embryo and not within the perivitelline space, thus an (active) uptake across the embryonic membranes into the most lipophilic compartment: the yolk sac has taken place. The lipophilic compartment of the embryo might have a stronger attraction to the microspheres and the uptake across the embryonic membranes might happen faster than the passive uptake across the chorion. This could lead to a lack of fluorescent signal within the perivitelline space.

The involvement of surface properties and reactivity of nanoparticles to zebrafish embryo toxicity was also shown by George et al. (2012), who found cysteine-coated Ag nanoplates to be less toxic compared to plain nanoplates. Labeling nanoplates with RITC (Rhodamine Isothiocyanate) reduced the toxicity and effect rate in zebrafish embryos even more and fluorescence microscopy demonstrated that the nanoplates bind to the chorion without any uptake. Consequently, they assumed a reduction of bioavailability due to a passivation of the Ag nanoplates surface by labeling with RITC (George et al., 2012). Several researchers have shown that the charges (zeta-potential) of plain and carboxylate-modified polystyrene nanoparticles of the same size are almost identical (Anguissola et al., 2014; Lundqvist et al., 2008; Ruenraroengsak and Tetley, 2015). As no uptake of the carboxylate-modified polystyrene

microspheres across the chorion was detected, the mechanisms behind these differences in uptake must be dependent not solely on the charge of the nanoparticles. This means, that the residual groups covering the polystyrene core, might interact with the chorion, the chorion pores and/or the glycoprotein layer covering the whole egg surface. The $-COOH$ groups of the carboxylate-modified microspheres must interact in a more persistent way with the chorion of zebrafish than the groups of the plain polystyrene. The surface of the plain microspheres is supposed to act almost identically to sulfonate-functionalized microspheres ($-SO_3H$), due to sulfonate residues during the polymerization processes (Anguissola et al., 2014; Della Torre et al., 2014). A direct hydroxyl group interaction of graphene oxide with the chorion of zebrafish embryos was shown by Chen et al. (2015b). Besides interaction with the chorion, provoking hypoxia due to chorion pore clogging and a delay in hatching, they also found an incorporation of the about 147 nm sized graphene oxide into embryonic tissue (heart-blood system, muscle, yolk sac), inducing ROS (reactive oxygen species). It was shown that polyethylene glycation of nanodots cover abundant carboxyl and amidogen groups on the surface. This was shown to decrease the sublethal and lethal effects found in zebrafish embryos at 24 and 48 hpf (Chen et al., 2015a), indicating a restricted bioavailability of these nanodots.

Several studies with polymeric dendrimers have ascertained contrary relations between toxicity and increasing number of terminal groups characterizing the different generations of dendrimers and thus a higher charge of the dendrimers. Harper et al. (2015) and Bodewein et al. (2016) found a decreased toxicity of anionic and cationic dendrimers in zebrafish embryos with increasing members of terminal groups, regardless if tested with or without the chorion. They assumed the positively charged dendrimers to interact with the negatively charged chorion, resulting in a hindered uptake. Contrary, King-Heiden et al. (2007) reported an increase of zebrafish toxicity with increasing number of reactive moieties on the surface of the tested cationic dendrimers, which they explained by an increase of effective concentration due to the attractiveness of the negatively charged chorion to the positive dendrimers. Hence, the plain charge of a particle or molecule might not be solely responsible for an uptake or a block.

The chemical residues covering the surface of nanoparticles might display the most important key factor for an uptake across not only the chorion, but also across the embryonic membranes. However, the mechanism behind interaction with chorion and embryonic membranes seems to be dependent on many other factors. Further investigations with determination of nanomaterial characteristics in FET water are necessary to get further insights in uptake mechanisms across the chorion of zebrafish embryos. Also the application of electron micros-

copy might be considered to elucidate the interaction of nano-sized particles with the chorion, embryonic membranes and tissues.

3.6 Conclusions

Plain 0.05 μm and 0.2 μm sized polystyrene beads were found to cross the chorion and the embryonic layers of zebrafish embryos. Comparing these results to the results derived with almost identically sized carboxylate-microspheres as presented in Chapter II, it becomes clear that the residual groups covering the polystyrene play the key role for uptake mechanism. The carboxylate-modified microspheres interact in a more persistent way with the zebrafish chorion, the pores and/or with the glycoprotein layer of the chorion than the plain microspheres.

Chapter IV.

**Permeability of the chorion of the fathead minnow,
*Pimephales promelas***

4. Permeability of the chorion of the fathead minnow, *Pimephales promelas*

4.1 Abstract

Early life stages of fish represent an alternative model to adult fish used for ecotoxicological studies to assess the potential risk of chemicals. During the first days of embryogenesis the embryo is surrounded by an acellular envelope, the chorion, which has repeatedly been discussed as a potential barrier for chemicals. In this study, the uptake across the chorion of fathead minnows has been studied by two different approaches:

(1) High solutes of differently sized polyethylene glycols (PEGs) were used to evoke osmotic pressure. Exposure to molecules of a size not able to cross the chorion should result in an efflux of water and a reduced reflux, indicated by deformations of the chorion. An uptake was assumed for PEGs $\leq 4,000$ Da since no chorion deformations were found. PEGs of a molecular size of 6,000, 8,000 and 12,000 Da were restricted in uptake across the chorion; no equilibrium could be found and the chorions remained deformed.

(2) Fluorescent microbeads were applied to freshly fertilized eggs and the distribution pattern of these beads was illustrated by laser scanning confocal microscopy (LSCM). The carboxylate-modified fluorescent microspheres 0.048 μm in size were detected on the chorion surface and especially at the adherends of the fathead minnow eggs, but not inside the perivitelline space or the embryos. No time-dependent uptake could be found, although the chorion is supposed to soften and permeability thus increasing.

The results suggest that not only the size of a chemical, but also its chemical and physical properties play a major role for uptake across the chorion of teleost fish. Likewise, the properties of the chorion itself might influence the uptake of a chemical due to binding.

4.2 Introduction

The fathead minnow for ecotoxicological testing of chemicals

The fathead minnow, *Pimephales promelas*, is the most common laboratory fish in the United States of America and has been used for (eco-)toxicological studies since the 1950ies (Ankley and Villeneuve, 2006). An enormous database regarding toxicity tests with the fathead minnow was established by the U.S. EPA and can be found on their webpage (access under <http://cfpub.epa.gov/ecotox/>), however, data about developmental toxicity in the fathead min-

now embryos are scarce. In July 2013, the OECD has approved the new guideline 236 “Fish Embryo Acute Toxicity Test (FET)” for the testing of chemicals with embryos as an alternative to the acute fish toxicity tests like TG 203 and 210 (OECD, 1992, 2013b). As Braunbeck et al. (2005) showed, the principles of the FET are - with minor modifications - transferable to other OECD fish species like the medaka or the fathead minnow. To propagate and establish the fish embryo acute toxicity test (FET) with fathead minnow, more information about developmental sublethal and acute effects is needed.

The fathead minnow develops slightly slower compared to zebrafish development and to understand chemical alterations in development, a profound knowledge is essential. The following passage summarizes the early development of fathead minnow embryos at 25 °C according to the works by Devlin et al. (1996) and Böhler (2012).

The 1-cell stage of a freshly spawned fathead minnow egg appears approximately 40 minutes after fertilization and the first cleavage, which takes about 5 – 7 minutes, results in 2 equal sized blastomeres at 1 hpf. Further synchronous, meridional cleavages every 15 – 25 minutes results in rows of equal sized cells. At the 32-cell stage (at 1:55 h), the cleavage becomes asynchronous and difficult to follow, since the cleavage planes are no longer perpendicular to the yolk body. According to Devlin et al. (1996), the chorion hardens at this stage and is about 1.4 mm in diameter. At 3:30 hours, the late cleavage stage can be distinguished as the cells form an elevated cap upon the yolk and the outermost very closely packed cells form the early epidermal stratum. During the next 4:30 hours, the blastula expands (high blastula stage), flattens (flat blastula stage) and starts the gastrulation in which the edge of the blastoderm becomes elevated and forms the early germ ring. This germ ring starts to migrate over the yolk body, and as the extensions of the germ ring meets, the end of the epiboly stage is marked at 13:00 hours. At this stage, the optic anlagen become visible as two lateral enlargements of the head region. The first five somites appear 3 hours later, and the different brain regions, the notochord, the optic anlagen and the beginning of the pericardial coelom can be distinguished. Also, the Kupffer’s vesicle becomes present, an important factor for the left-right development of the organs of the fathead minnow embryo. The first neuromeres are visible after 20 hours (14 somites pairs) and at 22:00 hpf, the otic vesicles have formed. At 24 hpf, the tail bud stage is reached, in which the embryo has formed about 20 somites pairs and the tail starts to detach from the yolk. Also at this stage, the olfactory placodes are visible and the lens placodes extend into the optic cup. First movements of the embryo are visible from 25.5 hpf onwards and the tail becomes completely detached from the yolk about one hour later.

The heart forms parallel to the tail detachment and sporadic beating becomes visible from 27 hours onwards. A constant heartbeat is visible at 30 hpf, which leads to the circulation of pigmented blood cells from 35 hpf onwards. From this time point on, the embryo elongates and grows, consuming the yolk, which becomes steadily smaller. Retinal pigmentation starts at 40 hpf, the blood starts running through the intersegmental arteries about 10 hours later (50 hpf). At 72 hpf, the embryonic body becomes curved around the yolk, tail and pectoral fins start to grow and at the yolk sac, the body pigmentation starts spreading over the body. At 96 hpf, the swim bladder becomes visible, the embryo straightens and the yolk is almost completely absorbed. At 120 hpf, the gill starts ventilation, eyes begin to move and the embryo is ready to hatch. The swim bladder darkens and the bile bladder can be easily distinguished by its bright yellow color. Hatch occurs between 96 and 144 hpf.

One of the most discussed potential barriers for chemical substances in the fish embryo toxicity test is the egg envelope, the chorion. Reproduction in fathead minnow is slightly different than in zebrafish, thus the chorion structure of fathead minnow eggs also differs compared to zebrafish chorion. Fathead minnows spawn beneath floating or submerged objects. The territorial males clean and prepare a nesting site with their tubercles around the mouth. Egg deposition takes place underneath this site, to which the male lifts the female. The buoyant and adhesive eggs stick to the substrate as well as to other eggs. Several females can contribute to an egg batch, and the male will remain at the nest site to guard and clean the eggs until the embryos hatch (Denny, 1987). Hardening of the chorion takes place at multicellular stage (Braunbeck et al., 2005; Devlin et al., 1996) and thereafter, the chorion of the fathead minnows show flat areas, the adherends. At these sites, the eggs are glued to the underground or to neighboring eggs.

Is the chorion a barrier?

Given the extensive database on toxicity in fathead minnows, surprisingly few studies have investigated the uptake of chemicals across the chorion and into the embryo. An almost linear increase of ^3H -uridine within the first 4 days of fathead minnow development was detected by Manner and Muehleman (1976). However, time-dependency in the uptake was recorded by a very rapid uptake of methyl-mercury across the chorion of one-cell fathead minnow eggs within the first 12 hours of exposure and a subsequent slower uptake for the next hours (Devlin, 2006). This might indicate an age-dependent change in permeability of the chorion due to the chorion hardening processes, which can be supported by the findings of an uptake of silver nanoparticles across the chorion and inside the embryo within the first 24 hours of

development (Laban et al., 2010). Also highly lipophilic substances, like TCB (3-3'-4-4'-tetrachlorobiphenyl) have been found in high levels in eggs spawned under exposure (Lindstrom-Seppa et al., 1994). However, this uptake is rather based on the maternal transfer of the toxin inside the eggs and might only partly results from a direct uptake across the chorion after spawning. Generally, the mechanisms of hardening after spawning and softening before hatch in conjunction with a changing permeability might be comparable to mechanisms found for the zebrafish chorion. Nevertheless, very little is known about the structure, properties and composition of the fathead minnow chorion.

The fathead minnow chorion of 4 hpf eggs was briefly described by Lillicrap (2010), who found a very smooth and lustrous appearance of the egg outside in SEM images (Figure 27 A). Considerably less particulates and microorganisms stuck to the outside of the chorion compared to the chorion of zebrafish embryos. With higher magnification, he found evidence of the pore openings, 0.2 μm in size, on the outside of the chorion (Figure 27 B). More or less by accident, he also presented the adherent of the eggs (arrow in Figure 27 A), which appears to be a plane area with a smooth surface, covered by small scratches. The edge of the plane area, however, might possess different structural properties, since it appears fringed.

Manner et al. (1977) investigated the ultrastructure of the chorion, showing that it is about 10 μm thick and composed of 21 layers. He described the chorion to consist of the outer layer with ridges covering 19 lamellar layers showing all different fiber orientation, beneath which an electron-dense inner layer is found (Manner et al., 1977). Only recently, Böhler (2012) confirmed the layering, however in a different orientation: The outer layer of the chorion is the electron dense one (see C and D in Figure 27), covering the multi-orientated layers. The different orientations of these layers are thought to contribute to the stiffness of the egg envelope of the fathead minnow. The chorion is pierced by small pores which are regularly distributed all over the chorion (Manner and Dewese, 1974; Manner et al., 1977) and meander through the different layers. As a sperm-entering site of the egg, one star-shaped micropyle can be found. While embryogenesis takes progress, the layers become thinner, contributing to an increase in permeability (Manner and Muehleman, 1976; Manner et al., 1977).

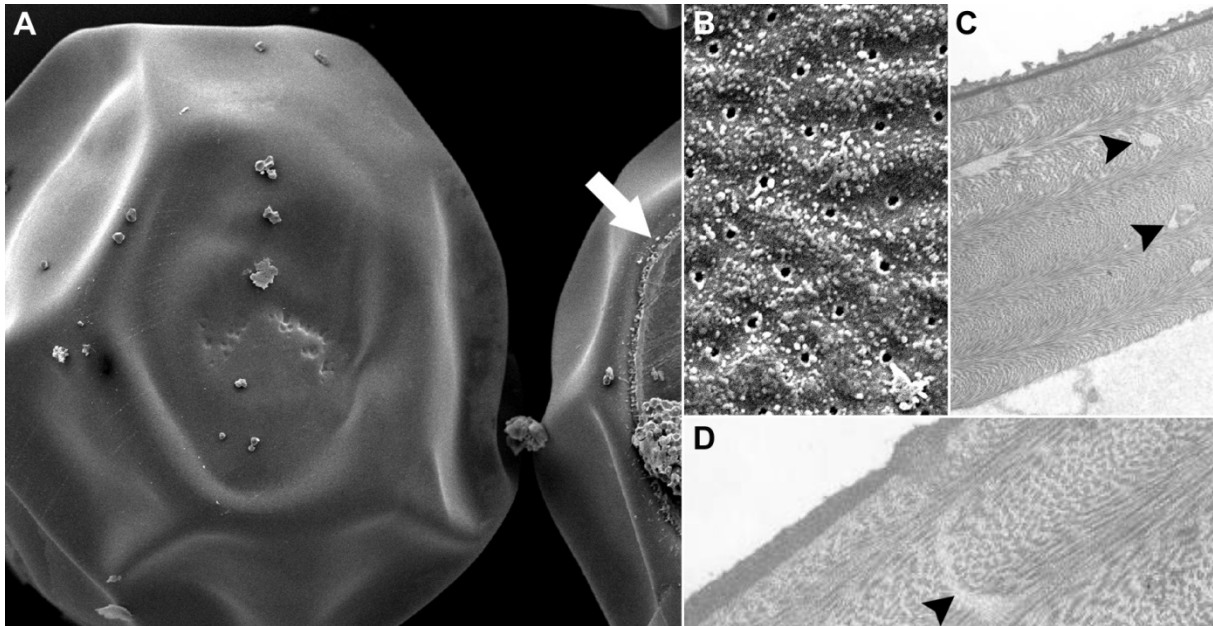


Figure 27: An overview of the fathead minnow chorion. SEM images of the outside (A and B) taken by Lillicrap (2010) show a very smooth and lustrous surface of the chorion (A; 80x magnification) in which the outer pore openings can be discovered (B; magnification: 8000x). TEM images of the chorion (C and D) taken by Böhler (2012) show the outer surface of the chorion to be electron-dense, while the thickest part of the chorion is made of different orientated layer, through which the pore canals (arrowheads D; 16000x magnification) meander and form little lacunae (arrowheads in C; 6200x magnification).

In the Introduction of this thesis, the properties and structures of zebrafish chorion have been described in detail, and the two striking differences in chorion properties of the fathead minnow are as followed: (1) the most prominent differences are the thickness and the stiffness of the fathead minnow chorion compared to the rather fragile chorion of the zebrafish; (2) taking a closer look on embryonic development, a striking difference is found in the time spent within the chorion: Hatching occurs between 52 and 96 hours post fertilization (hpf) in zebrafish, while the fathead minnow is slower in development and hatching occurs between 72 and 120 hpf. Also the criteria of the zFET had to be adjusted to the slightly slower development of the fathead minnow embryos as described above.

A brief overview about the most important facts of the chorion of the zebrafish and the fathead minnow are summarized in Table 7.

Table 7: The most important facts about spawning and the chorion of the two common OECD fish species for chemical testing, the zebrafish and the fathead minnow

	Zebrafish	Fathead minnow
	<i>Danio rerio</i>	<i>Pimephales promelas</i>
Spawning	flooded vegetation in still, shallow water with silt-covered bottoms	underneath submerged substrate (stone, woods, leafs, etc.)
Egg shape	round, 1 mm, translucent	1 mm, translucent, stick to surface (adherends are flat)
Chorion thickness	1.5 – 2.5 μm	10 μm
Chorion layers:		
outside	smooth, electron-dense	electron-dense*
middle	electron-lucent	19 layers of different fiber orientation
inside	electro- dense, thickest layer	honeycomb-like structure*
Pores	distributed all over the chorion, size: 0.5 - 0.7 μm , corkscrew, ridged walls	distributed all over chorion, size: 0.2 μm , in loops through the chorion
Micropyle	yes, round	yes, star-shaped
Surface	small depositions all over surface	smooth, clean surface; males clean eggs, deposition of anti-fungal secrete
Handling	soft structure, easy manipulated and ruptured	stiff and robust, strong appearance

* since the orientation in Manner et al. 1977 is apparently inverted, the description in this table is adjusted accordingly.

Aims of the tests with the fathead minnow embryo

These differences are important regarding the testing of potential toxic substances and the evaluation of data obtained with embryonic stages. No concrete conclusion can be drawn whether or not a substance is able to cross the chorion. For this purpose, the same approach was chosen for the investigation of the uptake across the chorion of the fathead minnow embryo as described for the zebrafish (see Chapter I and Chapter II).

- (1) In order to gain more information about the upper limit of the molecular size of chemicals to cross the chorion, differently sized, non-toxic polymers, the hydrophilic polyethylene glycols (PEGs) were applied to fathead minnow eggs. In the present study, PEGs in a molecular weight range of 2 000 – 12 000 g/mol were applied at a concentration of 20 g/L. This concentration is able to evoke osmotic effects and will lead to a deformation of the chorion if no uptake is possible. The molecular weight of the PEG solution, in which the chorion shape was not influenced or was able to be regained during the exposure time of 120 hours post fertilization (hpf), is equivalent to the *critical molecular size* to cross the chorion.

To ascertain a possible time-dependent increase in permeability of the chorion, the exposure periods were: (1) 0 – 120 hpf; (2) 24 – 120 hpf and from (3) 48 – 120 hpf.

- (2) The uptake of small particles across the chorion was investigated by the distribution pattern of 0.048 μm sized carboxylate-modified microspheres (FluoSpheres[®], Invitrogen). These microspheres are small manufactured ultraclean polystyrene particles, loaded with a red fluorescent dye and are easily located at or within the chorion and the embryo *via* laser scanning confocal microscopy (LSCM). Distribution patterns of the fluorescent particles were evaluated at 24, 48 and 72 hpf.

In the following sub-chapters (4.3 and 4.4), the two approaches are described and the results are presented and discussed separately. All findings with the fathead minnow are summarized in a joint conclusion (4.5).

4.3 The critical molecular size of polymers to cross the chorion of fathead minnow

4.3.1 Materials and methods

4.3.1.1 Chemicals

All chemicals were of highest purity available and purchased from Sigma-Aldrich (Deisenhofen, Germany). Tests were performed in 24-well polystyrene plates (TPP, Renner, Dannstadt, Germany) covered with self-adhesive foil (Sealing tape SH, 236269, Thermo Fisher Scientific, Waltham, MA) and the lid.

The PEGs (CAS 25322-68-3) used were: PEG 2 000 (average MW 2 050), PEG 3 000 (average MW 3 015 - 3 685), PEG 4 000 (average MW 3 500 - 4 500), PEG 6 000 (average MW 5 000 - 7 000), PEG 8 000 (average MW 8 000), and PEG 12 000 (average MW 11 000 - 15 000). All stock solutions and test concentrations were prepared in dilution water (294.0 mg/L $\text{CaC}_2 \times 2 \text{H}_2\text{O}$; 123.3 mg/L $\text{MgSO}_4 \times 7 \text{H}_2\text{O}$; 64.7 mg/L NaHCO_3 ; 5.7 mg/L KCl) according to OECD TG 236 (OECD, 2013a). Before use, the pH value of the dilution water was adjusted to 7.7 ± 0.2 . For each test run, a stock solution of the respective PEG was prepared at a concentration of 100 g/L. To correct the volume, the volume of the stirring bar was added after completed preparation of the solutes in volumetric flasks. Stock solutions were stored in the dark at room temperature and stirred thoroughly before usage. The PEG test concentration was set to 20 g/L, and the test medium was prepared daily from the stock solutions.

4.3.1.2 Fish maintenance and egg production

Wild-type fathead minnow, originating from R. Lange (Schering AG, Berlin, Germany) derived from own breeding facilities at the University of Heidelberg. Holding tanks with black glass walls were 10 L or 40 L flow-through aquaria, in which either one or two spawning groups were held. Spawning groups consist of 1 male and 2 female fathead minnows, and each group had access to a spawning substrate made of PVC tube halves with a plastic tray. Temperature was kept 25 ± 1 °C and the photo period was set to 16 hours light - 8 hours dark. Constant water aeration kept oxygen > 90%, water hardness was about 20 °dH (356 mg CaCO_3). Other water parameter (pH, conductivity as well as nitrate, nitrite and ammonium) were all in adequate range for fathead minnows (Braunbeck et al., 2005; Denny, 1987). Fish were fed twice daily with dry flakes *ad libitum* and additionally once daily with freshly defrosted brine shrimps (Kordon's Golden Gate® Frozen Brine Shrimp, Kordon LLC, Hayward, USA.).

Each morning and afternoon, spawning substrates were checked for eggs. If eggs were present, the PVC-houses were removed and eggs were carefully scratched with a spatula from the spawning substrates. Egg clutches were separated carefully with forceps using a stereo microscope. Developmental stages of the eggs were determined according to Devlin et al. (1996).

4.3.1.3 Egg exposure

Only fertilized and regularly divided eggs were used for tests. After separating the egg clutches they were directly transferred into PEG solutions or incubated in dilution water until exposure started at 24 or 48 hpf. Eggs were incubated (Memmert, Schwabach, Germany) at 25 ± 1 °C and a 16 h light : 8 h dark regime.

Exposure was performed in triplicates with 10 eggs each due to the small clutch sizes, and started at 0-5 hpf, 24 hpf and 48 hpf. To assure a comparable start of exposure, the eggs were transferred into 4 mL of the PEG solutions subsequently after checking the egg quality and developmental stage. Thereafter, eggs were transferred into 24 well plates, which had been pre-saturated for 24 hours and were refilled with 2 mL of the respective PEG solution. A negative control (dilution water) was performed with 12 eggs. An internal negative control on each plate was only conducted, if enough eggs were available. However, an internal negative control was not taken into consideration when evaluating the chorion shape. Since only one concentration (20 g/L) of the different PEGs were tested, no positive control was performed. To minimize evaporation, the 24 well plates were closed with a self-adhesive tape and the lid and placed in the incubator. All tests were performed semi-static; the medium was renewed every 24 hours after recording effects.

4.3.1.4 Endpoints and evaluation

Evaluation of effects on chorion and embryos were performed every 24 hours using an inverted microscope (Olympus CKX41, Olympus, Hamburg, Germany). To illustrate effects, micrographs were taken (AxioCam ICc1, Zeiss, Oberkochen, Germany). Effects on the embryos were observed and recorded according to OECD TG 236 (OECD, 2013a). Lethal endpoints were coagulation, non-detachment of the tail, non-formation of the somites and lack of heart-beat. However, the times for the lethal criterion “non-detachment of the tail” had to be adjusted the slightly slower embryonic development of the fathead minnow compared to the zebrafish (see Figure 8). Additionally, every abnormality in development was recorded until the end of the tests at 120 hpf. Also all hatched fish were recorded.

Table 8: Summary of the lethal and sublethal endpoints of the FET determined according to OECD TG 236 adjusted to the development of the fathead minnow according to Devlin et al. (1996) and Böhler (2012)

Toxicological endpoints		Exposure time (hpf)				
Lethal endpoints		24	48	72	96	120
	Coagulation	*	*	*	*	*
	Non-detachment of the tail		*	*	*	*
	Lack of somites	*	*	*	*	*
	Lack of heartbeat		*	*	*	*
Sublethal endpoints						
	Lack of spontaneous movement		*	*		
	Reduced heartbeat rate		*	*	*	*
	Reduced or lack of blood circulation		*	*	*	*
	Reduced or lack of pigmentation			*	*	*
	Affected eye development	*	*	*	*	*
	Edema formation (yolk sack or pericardium)		*	*	*	*
	Tail deformation ^a	*	*	*	*	*
	Spine deformation ^a	*	*	*	*	*
	Somite deformation	*	*	*	*	*
	Head deformation	*	*	*	*	*
	Retardation in development	*	*	*	*	*

^a might be difficult to see within the chorion

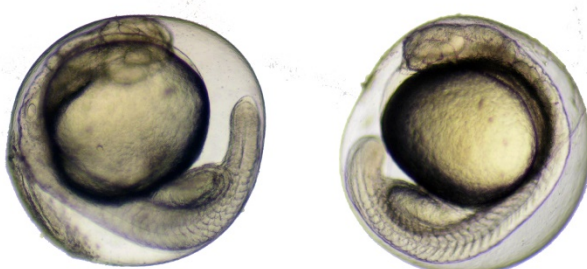
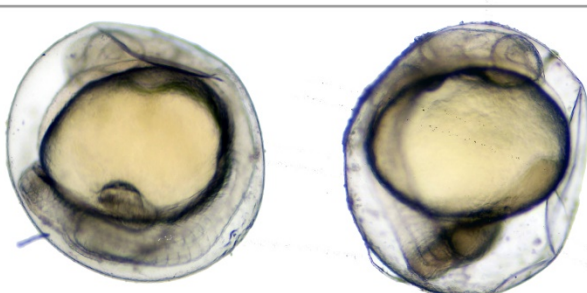
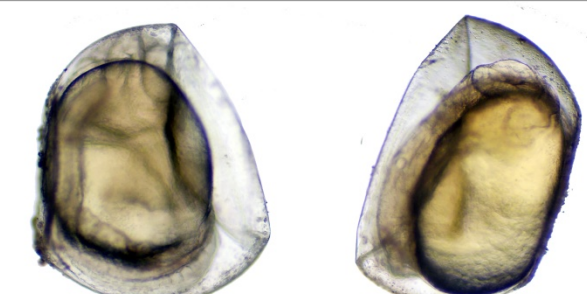
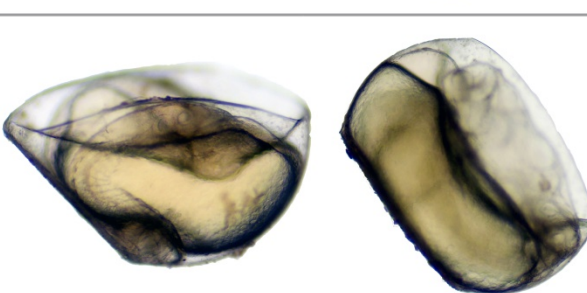
Due to the structure and stiffness of the fathead minnow chorion, deformations of the chorion were rated from 0 (no effects) to 3 (strong deformation of the chorion). Care has been taken to count only deformations caused by the PEG solutes and differentiate these effects from the adherends of the fathead minnow eggs.

To see and evaluate all deformations of the chorion, it was necessary to shake the eggs, as they tend to lay on flat sections or on big chorion deformations. While swirling in the test medium, all sides of the egg could be evaluated. The rating system of fathead minnow chorions is illustrated with representative pictures and a short description in Table 9. To get clearer results of the deformations, intermediate grades of 0.5 were given. Coagulated eggs were not taken into account for the evaluation of the chorion deformations, since the degradation process and the fungal infestation might influence the grade of deformation.

All illustrations were prepared using Sigma Plot 12.0 (Systat Software, San Jose, California, USA). For statistical analysis, one-way analysis of variance (One-way ANOVA) with multi-

ple comparisons *versus* control group (Dunnett's Method) was performed, regardless if normality tests failed.

Table 9: Rating system for the different chorion deformations as a result of PEG-induced osmotic effects. Effects were rated from 0 = no deformation with glue-patches visible to 3 = very strong deformations of the chorion with no or only little room for the embryo. Pictures taken by A. Keck.

Grade	Examples at 24 hpf	Short description
0		<ul style="list-style-type: none"> - no deformation of the chorion - straight areas are the adherends, where eggs are glued to spawning substrate or neighboring eggs
1		<ul style="list-style-type: none"> - small deformations of the chorion, mainly at the adherends of the chorion - enough place to move within the chorion
2		<ul style="list-style-type: none"> - prominent deformations of the chorion - embryo can move within the chorion, but might be touched by the deformations
3		<ul style="list-style-type: none"> - very strong deformations - embryo often touched by the chorion - embryo might be squeezed by the chorion - no or very little room to move within the chorion

4.3.2 Results

4.3.2.1 Effects of differently sized PEG on embryonic development

Across the different approaches, the effects on embryos exposed to differently sized PEG were quite similar. Only few embryos were coagulated or showed other lethal effects. The most prominent alterations in embryonic development were effects on the cardiovascular system and deformations of the head (see all examples in Figure 28). The morphology of the head could be extremely altered and especially eye formation was severely affected (see arrow in Figure 28). Common sublethal effects in fathead minnow embryos were a reduced heartbeat with a reduction or a complete lack of blood-flow. Moreover, accumulation of blood cells (arrowheads in Figure 28), the formation of edemata of the pericardium and above the yolk (see asterisks in Figure 28) as well as general deformations of the yolk were found in exposed embryos. Some of the sublethal effects on the spine like scoliosis or sharply bent tails (Figure 28 A, C and D) could only be evaluated in detail after hatch.

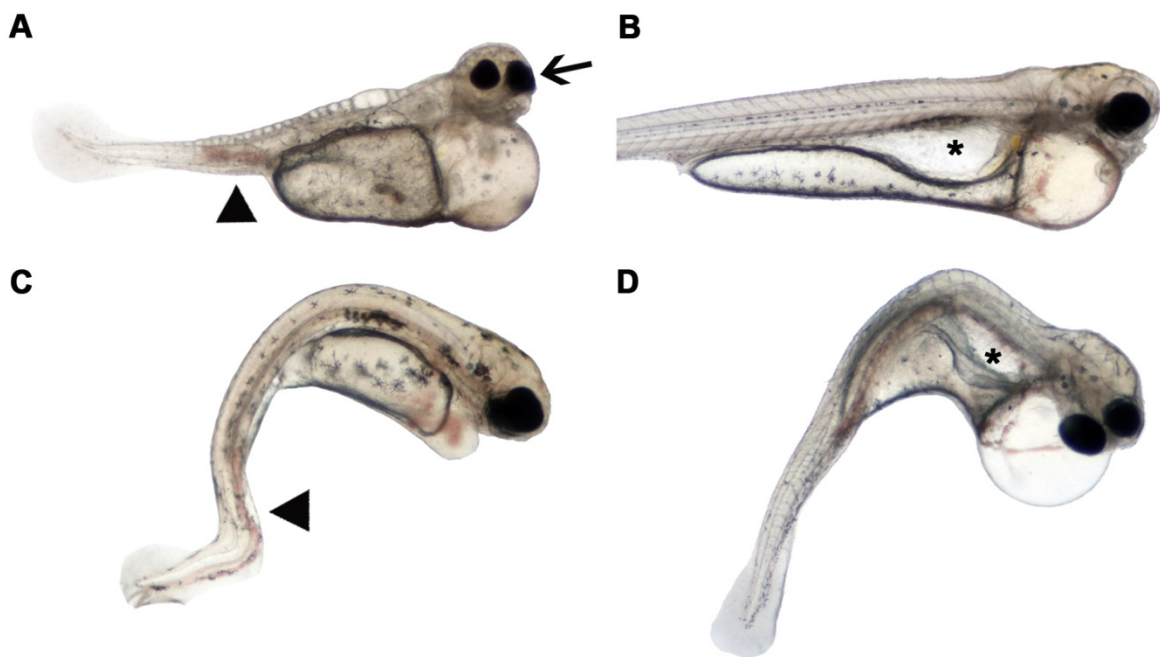


Figure 28: Sublethal effects in fathead minnow embryos at 120 hpf exposed to 20 g/L PEG 3,000 (A), PEG 6,000 (B) and PEG 12,000 (C, D). Note the effects on eye development (arrow), blood accumulation (arrow-head) and the edema above the yolk (asterisk) and deformation of the yolk itself. Also very prominent are the deformations of the head (A-D) and the formation of pericardial edema (A, B and D) and the bent tails (A, C, D). Pictures taken by A. Keck.

All effects (lethal and sublethal effects) were analyzed in 3 runs, each with 10 embryos. To get an impression of the effects of 20 g/L PEG in fathead minnow embryos, the percentage of all lethally and sublethally affected embryos were summed up and are illustrated in Figure 29,

Figure 30 and Figure 31. The exact percentages of coagulated or affected embryos can be found in the Annex. All conducted tests were valid, since less than 10% of the embryos of the negative control showed any effects. Exposure started directly after fertilization (approximately 0 - 3 hpf), 24 hpf and 48 hpf and each test was run until 120 hpf.

Exposure start from 0 hpf onwards

When exposure started directly after fertilization, the embryos showed an increase of effects correlated to the size of PEG they were exposed to (see Figure 29). Only a minor time-dependent increase of affected embryos was observed. Only few affected embryos were found in PEG $\leq 4,000$ Da throughout exposure time. At the end of exposure, the percentages of affected embryos exposed to PEGs $\leq 4,000$ were between 10 and 16.7% and hence only slightly elevated compared to control group (5.5%).

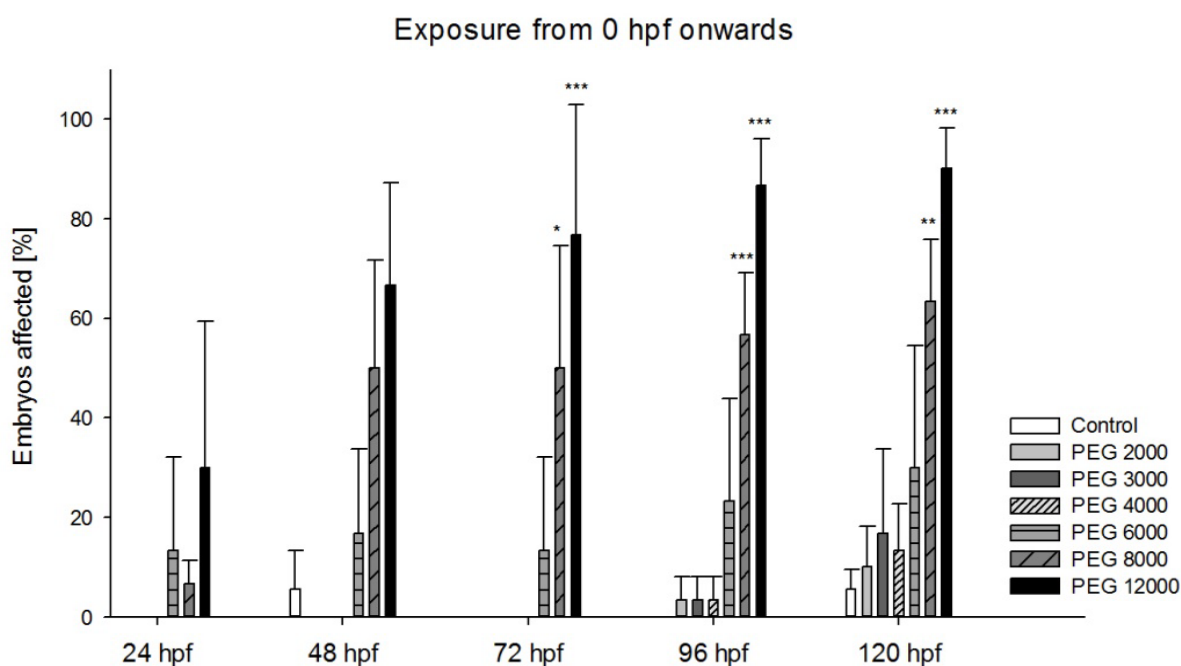


Figure 29: Effects in fathead minnow embryos exposed from 0 hpf to 120 hpf to differently sized PEGs at 20 g/L. A size-dependent increase in affected embryos could be found for PEGs $\geq 6,000$ Da. ANOVA with comparison to control group (Dunnett's method; * $P < 0.1$, ** $P < 0.01$, *** $P < 0.001$). $n = 3$ runs à 10 embryos. Data produced jointly with A. Keck.

Effects in embryos exposed to PEGs $\geq 6,000$ Da were found very early in development and became manifested over the course of exposure. Whereas embryos exposed to PEG 6,000 showed effects between 15 and 30% throughout exposure, effect levels in PEG 8,000 and 12,000 were always higher. From 72 hpf onwards, tremendous effect rates with statistically significant differences to control ($P < 0.05$) were found in embryos of those two treatments.

At 120 hpf, 63.3% embryos exposed to PEG 8,000 and 90% exposed to PEG 12,000 showed alterations in embryonic development.

Exposure start from 24 hpf

Exposure from 24 hpf until 120 hpf showed almost identical effect rates than exposure starting from 0 hpf onwards. Again, no significant changes in percentage of affected embryos exposed to the different PEGs could be found over the exposure period of 96 hours (120 hpf). However, the effect rates of PEG 12,000 showed statistical significances to control group ($P < 0.001$) at each time point of evaluation. At the end of the test, after 96 hours of exposure, 57% of the embryos exposed to PEG 8,000 and 90% of the embryos exposed to PEG 12,000 showed effects. At this time point, PEG 6,000 caused in approximately 20% of the introduced embryos effects, while at the same time PEG 3,000 and PEG 4,000 showed 6.7% affected embryos. No effects were found in embryos exposed to PEG 2,000 during the whole period of exposure.

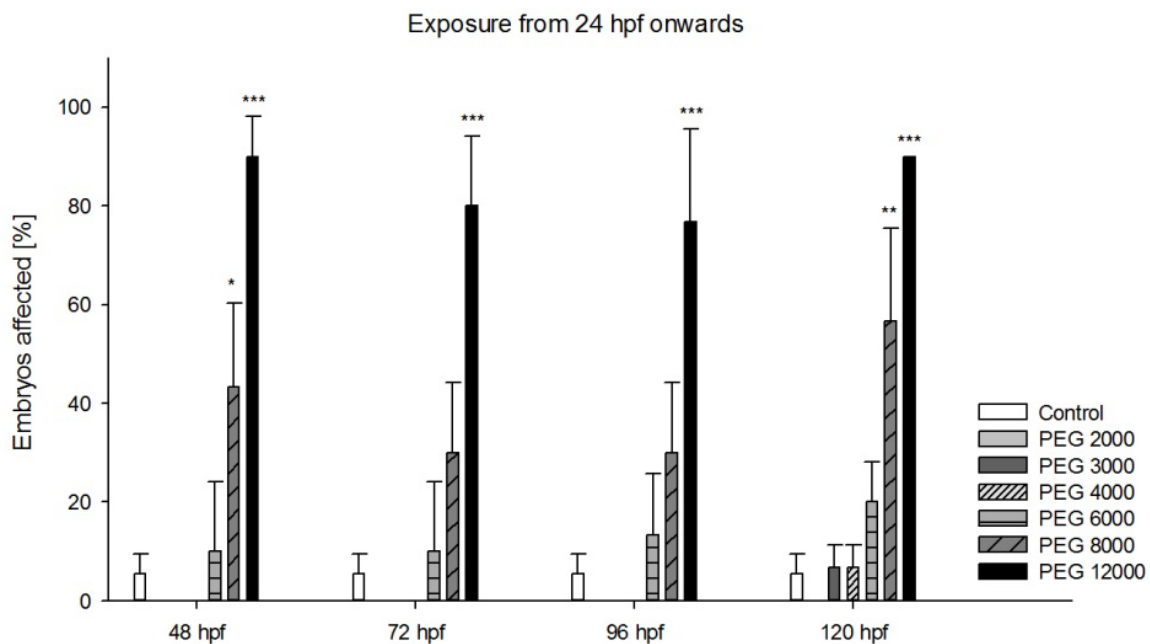


Figure 30: Effects in fathead minnow embryos exposed from 24 hpf to 120 hpf to differently sized PEGs at 20 g/L. A size-dependent increase in affected embryos could be found for PEGs $\geq 6,000$ Da, however only PEG 8,000 and 12,000 revealed statistical significances in affected embryos compared to control (ANOVA with comparison to control group (Dunnett's method; * $P < 0.1$, ** $P < 0.01$, *** $P < 0.001$). $n = 3$ runs à 10 embryos. Data produced jointly with A. Keck.

Exposure start from 48 hpf

When exposure started at 48 hpf, a maximum effect rate of 55% could be found. Throughout the test, only few embryos of the control group showed effects. A minor time-dependent increase of affected embryos was found in PEG 2,000 with 6.7% affected embryos at 72 hpf and 26.7% at 120 hpf. Embryos exposed to PEG 3,000 – 8,000 showed similar effect ranges between 6.7% for PEG 4,000 and 20% for PEG 8,000. Statistical differences to control group ($P < 0.01$) were found for embryos exposed for 48 hours (96 hpf) and 72 hours (120 hpf) to PEG 12,000.

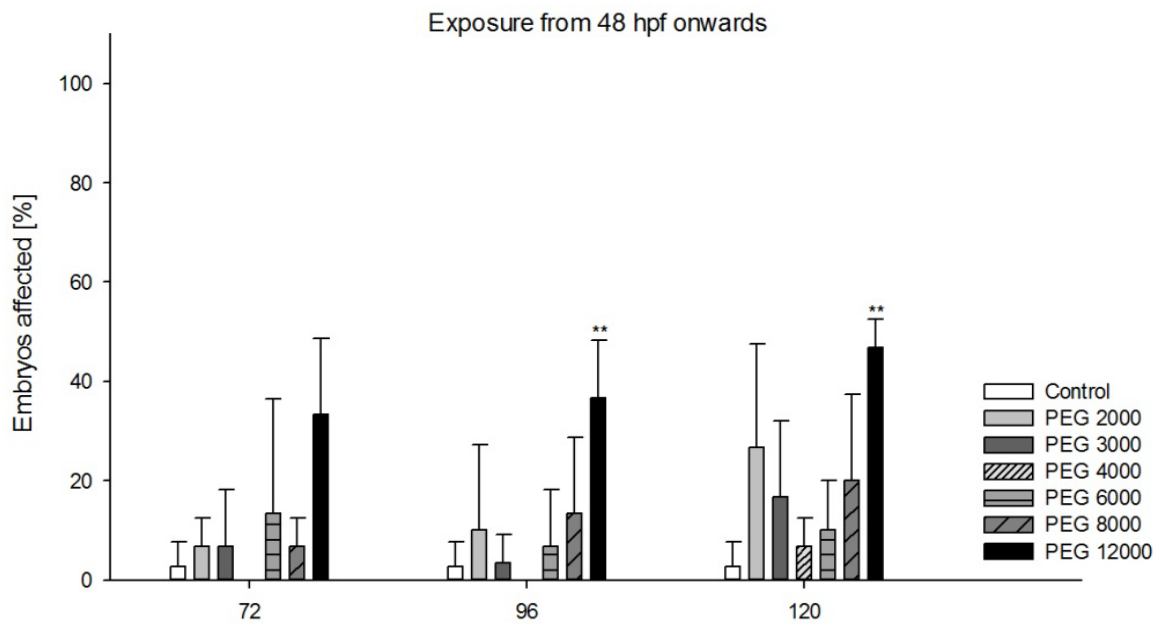


Figure 31: Effects in fathead minnow embryos exposed from 48 hpf to 120 hpf to differently sized PEGs at 20 g/L. Overall response of embryos to the different PEG did not exceed 60% threshold. Only PEG 12,000 revealed statistical significances in affected embryos after 48 and 72 hours of exposure (at 96 hpf and 120 hpf) compared to control (ANOVA with comparison to control group (Dunnnett's method; * $P < 0.1$, ** $P < 0.01$, *** $P < 0.001$). $n = 3$ runs à 10 embryos. Data produced jointly with A. Keck.

4.3.2.2 Effects on chorion shape of fathead minnow embryos

The chorion of the controls and PEG < 4,000 showed no deformations at all during exposure to 20 g/L. However, minor to strong effects of PEG \geq 4,000 on the chorion shape were found and rated according to the system described in Table 9. The effects on chorion shape were only evaluated for non-coagulated embryos. Detailed tables listing all affected and coagulated embryos as well as the deformations of the chorion per run are attached in the Annex of this thesis.

Exposure start from 0 hpf

With rising molecular size of PEGs, more and especially stronger deformations of the chorion were observed throughout exposure period. Only a small percentage (10%) of eggs exposed to PEG 4,000 for 24 hours showed effects classified as 1, 1.5 and 2 (each 3.3%). This even decreased after 48 and 72 hpf to 3.3% of deformations rated a 0.5. As the embryos of negative control, embryos exposed to PEG 4,000 started hatching gradually at 96 hpf.

PEG 6,000 showed very strong chorion deformations after 24 hpf, of which 66.7% were classified grade 2, 23.3% grade 2.5 and 10% grade 3. During exposure, the percentage of eggs with chorion deformations and the severity of deformations declined. At 48 hpf, no chorion was rated a grade 3, however, 10% were rated a grade 1, 20% a 1.5 and 2 and 16.67% a 2.5. Steadily, the percentage of eggs showing deformed chorion decreased and hence eggs showing no deformations at all increased from 30% at 48 hpf to 76.67% at 72 hpf. Together with the hatched embryos, the eggs with no deformations or very small deformations (grade 0.5 and 1) were the majority at 96 and 120 hpf.

Eggs exposed to PEG 8,000 showed very strong deformations of the chorion. Only few eggs were rated as normal (3.3%), while the majority was rated a 2.5 (53.3% at 24 hpf) and 3 (43.3% at 24 hpf). Further exposure revealed a slight shift to less deformed chorions (about 20% grade 2 at 72 hpf and grade 1 – 2 at 96 hpf). Percentage of hatched embryos stayed in the range found in the other treatments, starting from 96 hpf onwards.

The strongest effects in chorion shape were found in the PEG 12,000 treatment. During the first 72 hours of exposure, the majority of the chorions were rated 2.5 (approx.15%) and 3 (86.7 to 63.3%). Hatching was observed very early, starting with 3.3% hatched embryos at 48 hpf. However, at the end of the test the percentage of hatched embryos did not differ from the other treatments.

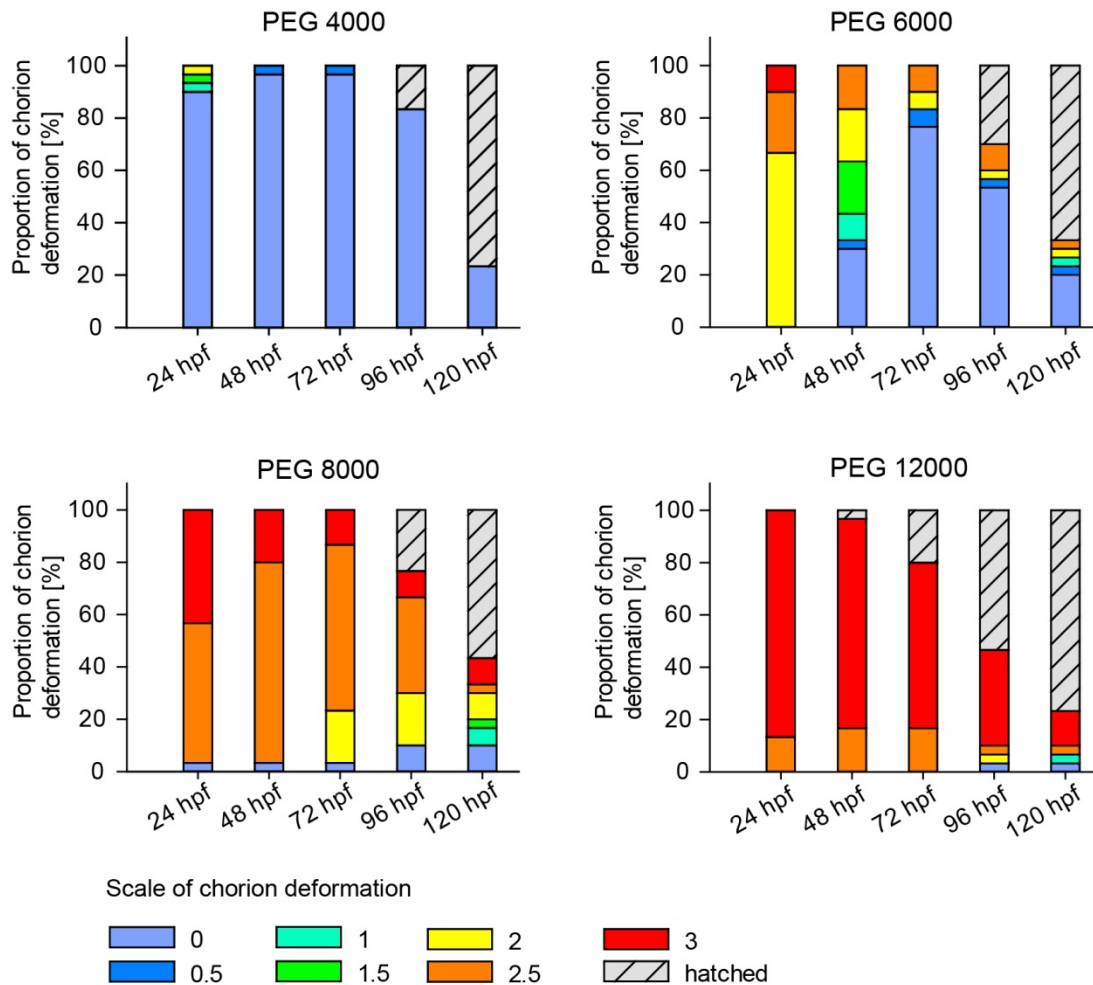


Figure 32: Percentage of fathead minnow eggs showing chorion deformations exposed from 0 hpf onwards to PEG 4,000 – 12,000. Deformation of the chorions was rated according to a scale from 0 (no deformation) to 3 (very strong deformation) and are given as the mean. n=3 runs à 10 eggs, except for PEG 12,000 at 120 hpf: 2 runs à 10 eggs, 1 run à 9 eggs. Data produced jointly with A. Keck.

Exposure start from 24 hpf

At PEG 4,000, the eggs exposed from 24 hpf onwards revealed almost no deformation. 3.3% of the introduced eggs had deformations of grade 2 after 24 h (48 hpf) and grade 1 after 48 hours (72 hpf). However, majority of eggs (96.7%) showed no change in chorion shape at all and at 120 hpf 96.7% of the embryos have hatched.

Treatment with PEG 6,000 for 24 hours (48 hpf) showed that about 60% of the introduced eggs showed no (20%) or only minor deformations rated grade 0.5 and 1 (each 6.7%) and grade 1.5 (24.2%). About 40% were found to have strong deformations of the chorion (31.7% grade 2; 10.8% grade 2.5). In the course of treatment, the strong deformations of the chorion almost disappeared and no (approx. 60%) or very few deformations (grade 0.5 – 1.5) were found besides hatched embryos at 72 and 96 hpf. At the end of the test after 96 hours of expo-

sure (120 hpf), 92.5% of the introduced embryos have hatched while the rest showed no deformations.

Again PEG 12,000 showed the strongest effects on chorion shape of fathead minnow eggs (grade 2.5 and 3) until 96 hpf (72 hours exposure). At 120 hpf, the 54.3% of the embryos have hatched but the rest still showed strong (3.3% grade 2) and very strong (8.1% grade 2.5 and 34.3% grade 3) deformations.

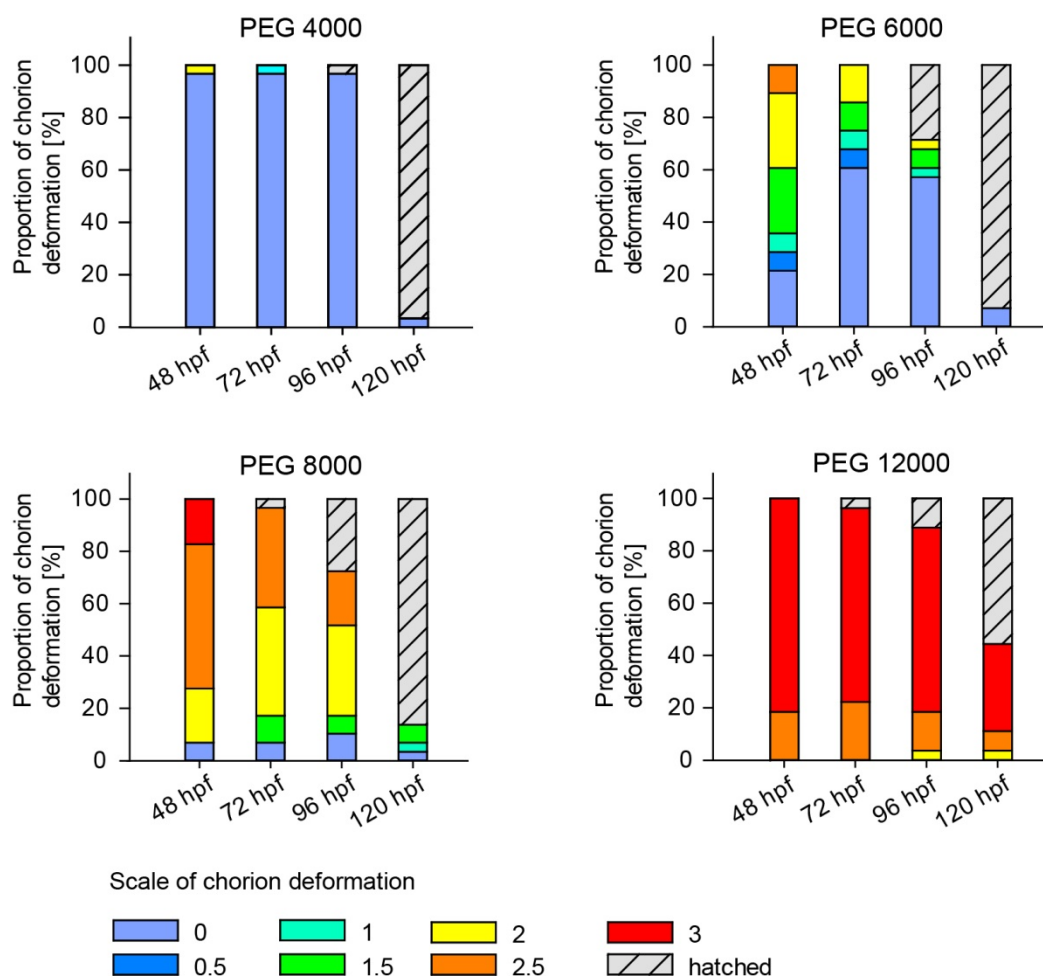


Figure 33: Percentage of fathead minnow eggs showing chorion deformations exposed from 24 hpf onwards to PEG 4,000 – 12,000. Deformation of the chorions was rated according to a scale from 0 (no deformation) to 3 (very strong deformation) and are given as the mean. n=3 runs à 10 eggs, except for PEG 6,000: 1 run à 8 eggs; PEG 8,000: 1 run à 9 eggs; PEG 12,000: 1 run à 7 eggs. Data produced jointly with A. Keck.

Exposure start from 48 hpf

When exposure started at 48 hpf, only 3.3% (= one embryo) exposed to PEG 4,000 showed chorion deformations of grade 2 after 24 hours (72 hpf). Until the end of the test, 53.3% of the embryos have hatched, whereas the rest of the eggs were normally shaped.

At 72 hpf, half of the introduced eggs to PEG 6,000 showed no deformations, while the chorions of the other half were deformed mainly to grade 2 (40%). In the course of the test, the

percentage of deformed chorions decreased steadily until 120 hpf and up to 83.3% embryos hatched. The rest of the introduced embryos showed only slight deformed chorions (at 96 hpf) or no deformation of the chorion (at 120 hpf).

At 72 hpf (24 hours of exposure), about 80% of the eggs exposed to PEG 8,000 showed strong deformations rated 2 – 3, which gradually decreased to approximately 20% while the amount of hatched embryos and non-deformed chorions rose steadily until 120 hpf.

Exposure to PEG 12,000 from 48 hpf onwards showed the strongest effects on chorion shape. After 24 hours of exposure (72 hpf), 73.3% of the introduced eggs showed deformations evaluated grade 3 and 23.3% grade 2.5. This pattern did not change over the next 48 hours until end of test, however, hatching increased at 96 hpf (43.3%) and 120 hpf (53.3%).

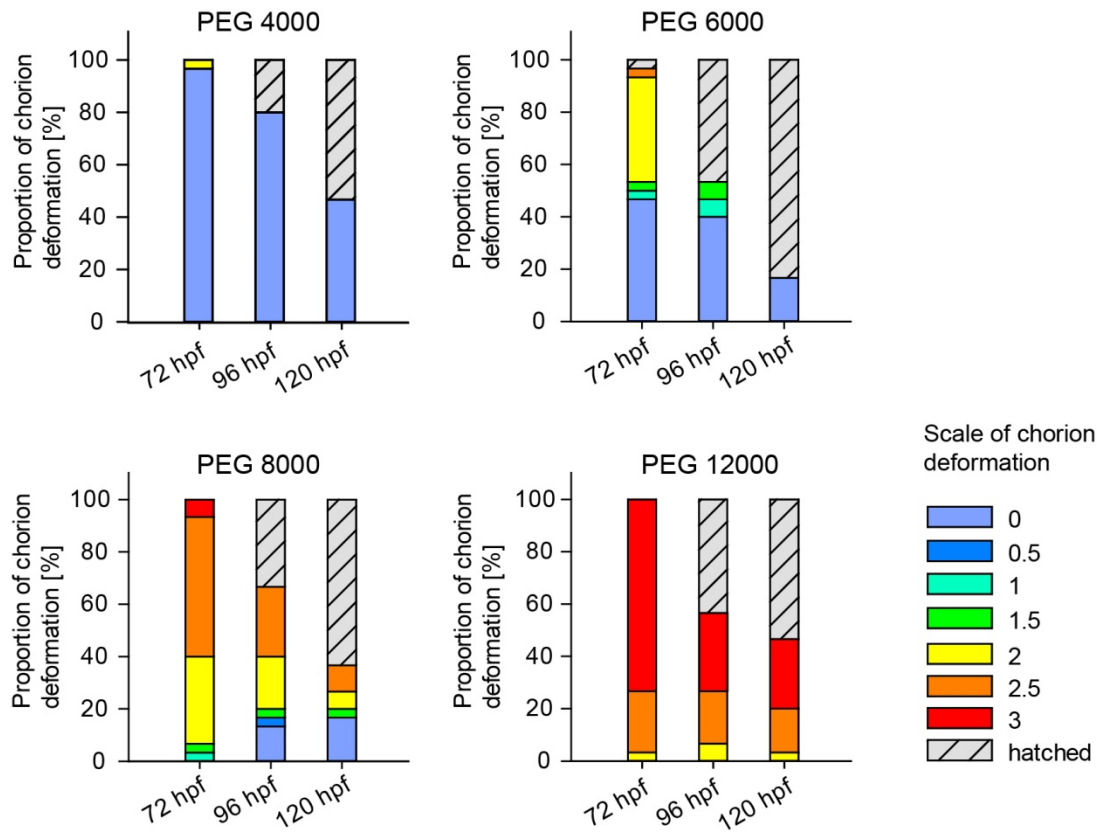


Figure 34: Percentage of fathead minnow eggs showing chorion deformations exposed from 48 hpf onwards to PEG 4,000 – 12,000. Deformation of the chorions was rated according to a scale from 0 (no deformation) to 3 (very strong deformation) and are given as the mean. n=3 runs à 10 eggs. Data produced jointly with A. Keck.

4.3.3 Discussion

Analogously to the study with zebrafish embryos described in Chapter I, the osmosis-evoking effects of PEG were used to study the permeability of the chorion of fathead minnow embryos. The relatively low toxicity found in zebrafish embryos showed differently sized PEGs suitable for testing the size-dependent uptake even at very high concentrations.

High standard deviations throughout the tests indicate differences in sensitivity of the used eggs. The quality of fathead minnow eggs is hard to maintain at a high level, due to the differences in spawning compared to, for example, zebrafish. The fathead minnow is a fractional spawner, and the reproductive cycle can be controlled *via* photoperiod and water temperature (Jensen et al., 2001). Females can produce 50 – 100 eggs every 3-5 days (Jensen et al., 2001), however such high numbers of eggs clutch size have not been observed in the breeding facility at the University of Heidelberg. Age, size and condition of females have a major impact on reproductive fitness (Gale and Buynak, 1982) and consequently on quality of produced embryos and egg envelopes. Since the used breeding fish derived from a group obtained several years ago, the genetic variety in the fathead groups might have been reduced with influences in egg envelope quality and embryonic alterations. No specifications on genetics stocks of fathead minnow used in the various laboratories are available at all (Ankley and Villeneuve, 2006). Differences in effects on chorion shape and embryonic development between the different runs might be a consequence due to differences in egg quality. However, all tests conducted were valid according to test guidelines on toxicity, since less than 10% of the embryos in the negative control showed effects. Since there is no standardized method to describe the chorion properties during a test run, the high standard deviations should be taken as biological variability as found in the field.

Effects on fathead minnow embryos were found throughout the different treatments, although the percentage of affected embryos in control groups as well as in treatment groups exposed to PEGs $\leq 4,000$ Dalton could not be correlated to chorion deformations. At the tested PEG concentration of 20 g/L, no effects on chorion shape were found for PEG $< 4,000$. Rates of affected embryos at PEG 4,000 were only slightly elevated compared to baseline effects found in control and PEG 2,000 and 3,000. In all treatments with PEGs $\geq 6,000$ Da, an increase in number of affected embryos could be found with rising exposure period until the end of the test at 120 hpf. The increased percentage of affected embryos exposed to PEG 6,000 – 12,000 was found to be approximately the same for treatments starting from 0 and 24 hpf onwards. In treatment with exposure from 48 hpf onwards, this rate was reduced to

about 30% of the values found in treatments with exposure starts at 0 or 24 hpf for PEG 6,000 and 8,000 and to about 50% for PEG 12,000. Within the first 33 hpf the complete organogenesis is finalized, so alterations in development might not be as prominent when exposure started beyond this time point.

Nevertheless, a clear correlation of chorion deformations and affected embryos can be drawn when regarding the results of this study. An increase in chorion deformation was found with rising molecular size of the tested PEGs. The more chorion deformations were found, the more affected embryos were observed. The strongest effects on both, chorion and embryonic development, was found for PEG 12,000 regardless of exposure start. Hence, when exposure started at 48 hpf, the sensitive window for mechanical effects due to chorion deformation might have been skipped. On the other hand, the water efflux out of the chorion might also influence the water household of the cells. After 48 hpf, the embryonic membranes surrounding the embryo have become stronger and more resistant to influences, therefore older embryonic stages are assumed to be less sensitive to chemicals than younger stages, which has been found for sub-chronic effects in the fathead minnow (Pickering et al., 1996).

Deformations of the fathead minnow chorion were found subsequently to transfer into the PEGs $\geq 4,000$ Da solutions. Different severities could be found and were rated with a special system. Small deformations were mainly recorded at the adherends which seemed to dent, while at prominent to very strong deformations, the chorion dented from all sides of the egg. Fathead minnows deposit their adhesive eggs on the surface of spawning substrate (Denny, 1987) where the hardening process takes place after fertilization in multicellular stage (Braunbeck et al., 2005). Hence, the contact area to the substrate or neighboring eggs of the initially round egg becomes flat. One egg might have more than one of these flat areas, since they also might stick to several neighboring eggs. The chorion of the fathead minnow is a strong, quite stiff structure of 10 μm thickness pierced by meandering pore canals (Böhler, 2012; Manner et al., 1977). It is composed of approximately 20 layers of different orientation and it seems like these crossed layers provide the high stability of the chorion. This stability was forced to dent by osmotic pressure generated by the high concentration of the PEG solutions the eggs were exposed to. The flat areas seem to be the weakest part of the chorion of the fathead minnow, since the deformations always occurred first at these adherends. The usually round shape of a fish egg is almost identical to a sphere – hence, tensile stresses inside can be distributed uniform in all directions. When internal pressure decreases due to water efflux out of the body (= the egg), the middle of flat areas in an otherwise spherical body is

not able to re-distribute the pressure from the surrounding areas. Hence the flat areas give in first, resulting in dents of different severity, which always start from the middle of the adherends of the fathead minnow eggs.

For PEGs $\leq 4,000$ Da no or only very small chorion deformations were found, indicating an uptake across the chorion within several hours. The stability of the chorion might not be the key factor for the unchanged chorion shape. Money (1989) stated that at equivalent weights the lower molecular weighted PEGs generate a higher osmotic pressure than higher molecular weighted PEGs. The osmotic pressure correlates not only to the molecular weight (=size) of the solute, but also to the concentration. In relation to the normal shaped eggs exposed to PEGs $< 4,000$ Da, this means that although the generated osmotic pressure was higher than in solutions of $> 4,000$ Da, equilibrium was achieved. This shows a quick reflux of water with dissolved PEGs has taken place to balance the internal pressure with no effects on chorion shape. However, the stiffness of the chorion might have been beneficial for just “popping” back into the normal, more or less round shape.

At the same time, low osmotic pressure in high MW PEGs (= larger molecules) lead to strong deformations of the chorion illustrating the water efflux out of the perivitelline space but no process of equilibrium. In all three approaches, the effects on chorion shape increased with rising PEG size. However, the severity of chorion deformations decreased when exposure started delayed (0 hpf $>$ 24 hpf $>$ 48 hpf). Only the proportions of chorion deformations found in PEG 12,000 were found to be the same, no matter when exposure started. Nevertheless, the percentage of eggs showing chorion deformations stayed at the same level, especially when regarding the actual age of the eggs. The decrease in severity of chorion deformations might also arise from the advanced development of only slightly affected embryos. The embryos were able to move within the chorion and might have induced a bulging of the dented chorions. Also, permeability of the chorion rises with development (Manner and Muehleman, 1976; Manner et al., 1977), encompassing hatch. In all treatments hatching was found to be very similar and occurred in the range between 72 – 120 hpf. A clear correlation of chorion deformations and affected embryos can be drawn when regarding the results of this study. Also, a time-dependency was found during each treatment but also between the different starting points in a reduced severity of chorion deformations and a slightly increase in affected embryos. When exposure started at 48 hpf, the percentages of chorion deformation and affected embryos were reduced after 24 hours. However when comparing the percentage of deformed chorions at the actual age of the eggs, the differences were marginal.

4.4 The permeability of the fathead minnow chorion to fluorescent microspheres

4.4.1 Materials and methods

4.4.1.1 Chemicals

All chemicals were of highest purity available and purchased from Sigma-Aldrich (Deisenhofen, Germany). Tests were performed in 24-well polystyrene plates (TPP, Renner, Dannstadt, Germany) covered with self-adhesive foil (Sealing tape SH, 236269, Thermo Fisher Scientific, Waltham, MA) and the lid.

All test concentrations were prepared in a 1:5 dilution of the OECD dilution water (294.0 mg/L $\text{CaCl}_2 \times 2 \text{H}_2\text{O}$; 123.3 mg/L $\text{MgSO}_4 \times 7 \text{H}_2\text{O}$; 64.7 mg/L NaHCO_3 ; 5.7 mg/L KCl) according to TG 236 (OECD, 2013a). Before use, the pH was adjusted to 7.7 ± 0.2 . The microspheres used are carboxylate-modified and had a size of 0.048 μm (FluoSpheres[®]; F8793; Invitrogen, Life Technologies[™] GmbH, Frankfurt, Germany). The test concentration was prepared at 0.01% microspheres in 1:5 diluted OECD water. A detailed description and characterization of the 0.048 μm microspheres can be found in Chapter II.

4.4.1.2 Exposure and microscopically evaluation

Egg production and handling of the eggs were performed as described in Chapter II. Eggs were exposed continuously for the time within the chorion (24 to 72 hpf). Incubation was performed in the dark at 25 ± 1 °C. Exposure was done semi-static, test medium was exchanged daily. Before analysis under laser scanning confocal microscopy (LSCM), each egg was washed twice for about 5 minutes in 1:5 OECD water to avoid any disturbing external signal. Eggs were handled with extreme care to avoid any rupture of the chorion. For anesthesia, each egg was put into a well containing 1 ml of 0.016% tricaine solution (MS-222, ethyl 3-aminobenzoate methanesulfonate), prepared in 1:5 dilution water. At each time point 4 eggs were evaluated. Care was taken to avoid light, therefore, everything was covered by aluminum foil, and all the steps in the light were minimized.

Eggs were transferred within one small drop of tricaine solution into glass bottom culture dishes (MatTek Cooperation, Ashland, USA). To avoid any movement during laser scanning session, eggs were embedded in 1% low melting agarose (LMA; SeaPlaque[®] GTG[®] Agarose, FMC Bioproducts, Rockland, USA) prepared in 0.016% tricaine solution.

The distribution of the microspheres was analyzed with Laser Scanning Confocal Microscopy (LSCM, Nikon 90i; Nikon Instruments, Netherlands) and images were taken with a Nikon C1 camera (Nikon Instruments, Netherlands). All settings are given in Table 10. Illustration of the microsphere distribution was performed using the Nikon imaging software NIS-Elements-Viewer (Vol. 4.20, Laboratory Imaging, 1991-2013).

Table 10: Laser and microscope settings for evaluation of fluorescent signal within the chorion

Laser settings	Texas Red	
	Emission wavelength:	605.0 nm
	Excitation wavelength:	543.5 nm
	Pinhole radius:	60.00 μm
	Laser power	100%
	High voltage (HV)	12
Microscope settings		
	Objective:	Plan Fluor 10x DIC L
	First dichroic mirror:	408/488/543
	First filter cube:	450/35
	Second filter cube:	515/30
		605/75

4.4.2 Results

To compare the fluorescent signal of the microspheres across the chorion, all images were taken with the same settings: laser power was set to 100% and High Voltage (HV) at 12. No agglomerations or precipitations of the tested microspheres were found in the medium.

The fluorescent microspheres were detected all over the chorion surface; however, the distribution pattern was strongly influenced by the characteristics of the fathead minnow chorion. Representative optical cross sections (A, C and E) of the eggs revealed irregular distribution of the fluorescent signal. Some areas (indicated by arrows in Figure 35 A, C and E) emitted a strong and even fluorescent signal, while the rest of the chorion showed a weaker fluorescent signal. The three-dimensional images (B, D and F in Figure 35) of the selected cross-sections revealed that the strongly fluorescent areas were the adherends of the fathead minnow eggs (arrows in Figure 35). The plane area of the adherends can be clearly distinguished from the otherwise more or less spherical shape of the egg. Also small projections on the chorion surface like rotifers or bacteria showed a strong fluorescent signal.

Signals of less intensity were found at the whole surface of the fathead minnow chorions. This signal increased with rising exposure period. Whereas almost no signal at the chorion was found at 24 hpf (A and B in Figure 35), the signal got stronger at 48 hpf (C and D in Figure 35) and 72 hpf (E and F in Figure 35). Especially after 48 hpf, the fluorescent molecules were evenly distributed all over the chorion surface.

No evidence of the 0.04 μm carboxylate-modified microspheres was found within the eggs or within the embryos at any time point.

Taking a closer look on the chorion surface where the adherend is located, the differences of the chorion structures becomes clear (Figure 36). The round areas of the chorion seemed to be smooth and were more or less evenly fluorescent, whereas the adherend were sharply formed structures showing a strong signal of fluorescent and areas of single distinct signals. These spot-fluorescent signals each represented one microsphere. Agglomerations of microspheres in the test medium or precipitations at the chorion were excluded.

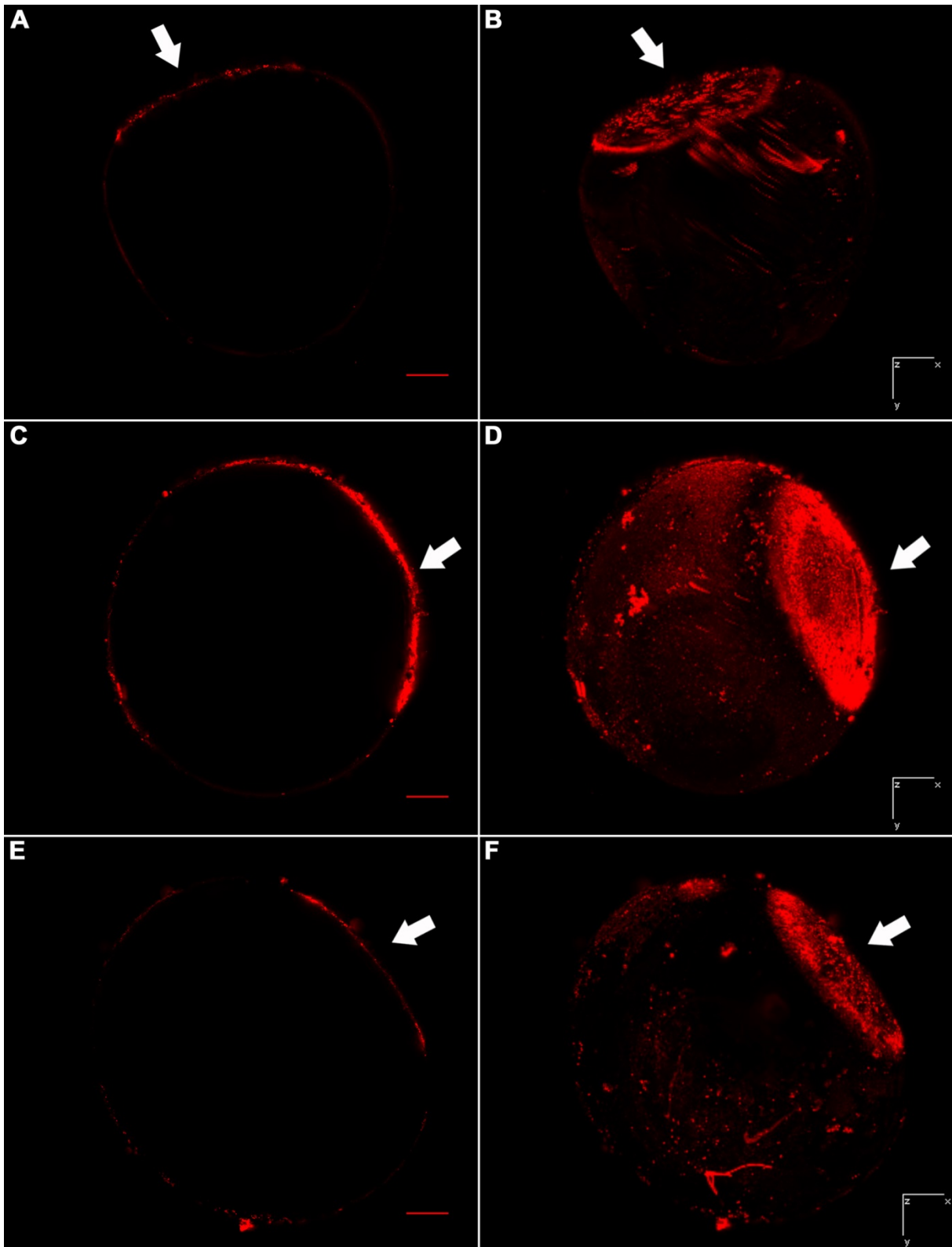


Figure 35: The distribution pattern of 0.048 μm carboxylate-modified microspheres across the chorion of fathead minnow eggs at 24 hpf (A, B), 48 hpf (C, D) and 72 hpf (E, F). The left pictures (A, C, E) show one plane cross section of the egg and the right pictures (B, D, F) illustrate the 3D picture of the same eggs (all z-stacks). The main fluorescent signal can be found in the adherends of the eggs (arrows) and some fluorescent signal can be found across the chorion. However, no fluorescent signal is found within the egg and the embryos. Scale bars in A, C and E are 300 μm .

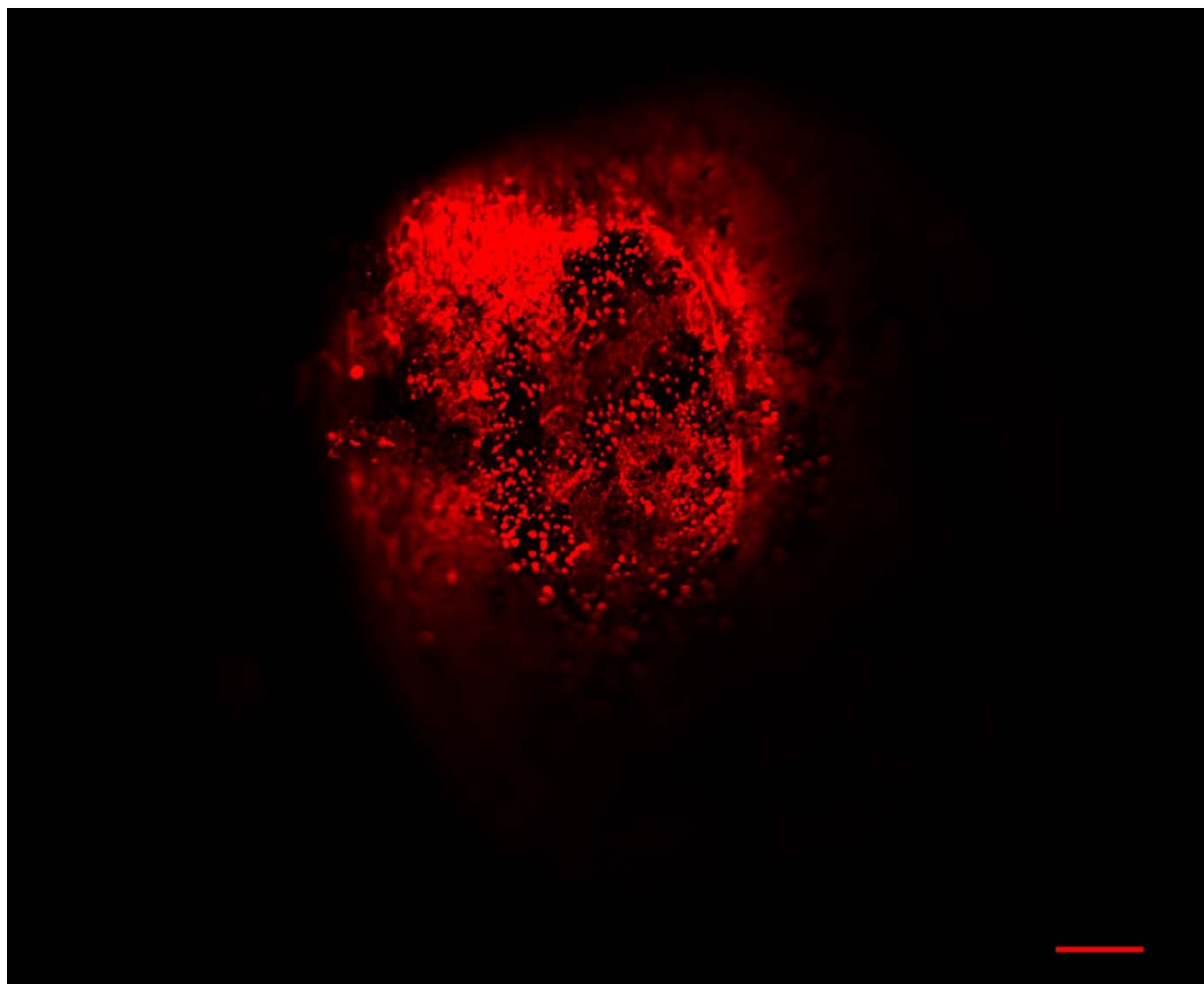


Figure 36: Optical cross section of the surface of the chorion of a 24 hpf egg exposed to 0.048 μm microspheres showing the adherend. The adherend is not smooth, each distinct fluorescent signal is supposed to represent one microsphere. Scale bar: 150 μm .

4.4.3 Discussion

Studies on uptake mechanisms of chemicals across the chorion and in the embryo of fathead minnows are rare and no general assumption about the uptake can be made. Lindstrom-Seppa et al. (1994) showed the incorporation of 3-3'-4-4'-tetrachlorobiphenyl (TCB) into the eggs spawned during parental exposure. Similar concentrations inside the eggs as in ovaries of the respective exposure treatment were found, indicating a maternal elimination of TCB *via* oocytes. An uptake of ^3H -uridine through and the retention within the chorion was shown by Manner and Muehleman (1976). Co-exposure to linear alkyl benzene sulfonate (LAS) decreased the uptake which was explained by an influence of the surfactant properties of LAS to the chorion membrane. A similar approach with showing the bioaccumulation of methylmercury inside fathead minnow eggs was pursued by Devlin (2006). However all these studies homogenized whole eggs without dechoriation and the chemicals might as well be associated to the chorion without crossing it. No differentiation had been made between the com-

partments embryo, perivitelline fluid and chorion, which has been shown to be important when regarding the real internal concentrations (Brox et al., 2014).

Laban et al. (2010) tested silver nanoparticles (AgNPs) in fathead minnow embryos, 31 - 61 nm in size and thus comparable to the size of the applied microspheres in this study. They found single and agglomerations of AgNPs on the chorion surface, but also engulfed by a sac inside the embryos. They suggest an uptake *via* diffusion across the pores in the chorion facilitated by the accumulation of particles on the chorion surface and a following endocytosis into the embryos (Laban et al., 2010).

So far, this has been the first study implying well-defined, fluorescent microspheres in nano-scale size to study the uptake across the chorion of fathead minnow eggs. The data presented show that exposure to microspheres 0.048 μm in size did not lead to an uptake across the chorion of fathead minnow eggs at an exposure for 24, 48 and 72 hours. A fluorescent signal was only detected on the chorion surface and especially at the adherends of the chorion. The chorion of fathead minnows is about 10 μm thick and several pore canals pierce the chorion (Böhler, 2012; Manner et al., 1977). Only Böhler (2012) measured the pore sizes of air-dried native chorions under light microscopy and estimated the diameter of the outer chorion pores to about 0.2 μm . Although these values might not correctly represent the actual pore size due to handling of the chorion (stretching on the slides, drying), it gives an idea about the pore diameter exceeding the diameter of the applied microspheres. Actually, the pore size might not be limiting factor for an uptake across the chorion.

Egg production in fathead minnows starts at the age of about 4-5 months (Jensen et al., 2001; Leino et al., 2005). Under the influence of estrogens, the female produces in its liver vitellogenin which accumulates in the maturing oocyte as the yolk. The proteins to form the egg envelope derive from the follicular epithelium or the oocyte itself (Guraya, 1986). Since these chorion-forming proteins, also called *zona radiata* (*zr-*) proteins, are found to be homologous to mammalian *zona pellucida* proteins (Del Giacco et al., 2000; Murata, 2003; Wang and Gong, 1999) and are clearly conserved among teleostean fish (Arukwe and Goksoyr, 2003), they might also certainly be part of the fathead minnow chorion. In histopathological studies, the chorion is usually pale to dark eosinophilic and refractive when treated with hematoxylin and eosin (US EPA, 2006), indicating positively charged proteins and polysaccharides. The positively charged surface might bind the carboxylate surface of the microspheres, leading to an accumulation of the fluorescent beads. However, binding is supposed to be less strongly than by hydrophobic microspheres and coupling has to be supported by reagents (Invitrogen,

2004). Contrarily, different authors suggest that in particular the chorions of several teleost fish act as a sink for metals and anionic charged groups of the chorion proteins are responsible for this binding (Beattie and Pascoe, 1978; Michibata, 1981; Ozoh, 1980; Stouthart et al., 1996). In zebrafish chorion, Pullela et al. (2006) detected thiol-rich proteins in the chorion *via* DSSA probes, confirming the assumptions.

Since the fluorescent signal of the chorion is scarce compared to the fluorescent signal of the adherends, the binding by the chorion itself might not be very strong. A similar distribution pattern was found by Böhler (2012) who showed an accumulation of 2,7-dichlorofluorescein at the adherends, but no signal in the chorion or in the embryo at 48 and 72 hpf after 24 hours of exposure. The adherends seem to possess a stronger binding affinity caused by a different molecular composition than the rest of the chorion. During oogenesis, the oocyte forms within follicular vesicles, with components produced by the liver and transported *via* blood vessels. In cortical alveolus oocytes the *zona radiata* becomes visible and is thickening during maturation of the oocyte (Leino et al., 2005; US EPA, 2006). The follicle epithelium does not form different areas of the chorion *per se*, so the adherends do not form until the chorion is attached to submerged objects or neighboring eggs and hardened. Despite extensive literature research, no other study could be found to confirm this assumption and there is an immense lack of knowledge of the exact chorion composition and especially of the differences of the adherends to the rest of the fathead minnow chorion. Only a small image section of the ultrastructure of the adherend of the fathead minnow chorion was found in chapter 3 (image 3.8) of the master thesis by Lillicrap (2010). Next to a SEM image of a whole 4 hpf egg, the surface of an egg showing a plane area, with a smooth surface, but a roughened outer edge. Compared to the other normally round surface of the egg, the plane and the edge of the plane area might possess different structural properties. They seemed not as smooth and unstructured as the rest of the surface. The plane area seemed to be covered with scratches, while the edge appeared fringed. These structural differences illustrated by SEM micrographs, support the assumption gained by the differences in distribution pattern of the 0.048 nm microspheres.

4.5 Conclusions

Fathead minnow eggs are surrounded by a strong, 10 μm thick chorion. The egg shape is not perfectly spherical, since the adhesive eggs stick to the spawning substrate and neighboring eggs, leading to flat areas, the adherends. In this chapter, the uptake across the fathead minnow chorion was investigated following two experimental approaches:

(1) The critical molecular size was determined by evoking effects similar to osmosis. PEGs < 4,000 Da were able to cross the chorion since no chorion deformations were found when exposed to high solute strength, although the osmotic pressure generated by small molecular sized PEGs is supposed to be higher than the ones generated by larger molecular sized PEGs. PEG 4,000 showed slight deformations of the chorion; however, these effects were marginal, indicating a critical size for polymers to cross the chorion of fathead minnows to be approximately 4,000 Dalton. Throughout exposure, no changes in chorion deformations were found at PEG 12,000, while the severity of chorion deformations at PEG 6,000 and 8,000 decreased. This is supposed to be a combination of an increase in chorion permeability and the moving embryo inside the chorion.

(2) Fluorescent microspheres, 0.048 μm in size, were applied to freshly spawned eggs. No uptake across the chorion could be illustrated. Fluorescent microscopy revealed a strong accumulation of microspheres at the adherends of the chorion, at which they were glued to neighboring eggs or the spawning substrate. Different assumptions about the chorion properties of teleost fish have been made. On the one hand, the chorion is stained by the negatively charged eosin, indicating positive structures. On the other hand, some authors suggest negatively charged chorion proteins, since the chorion has repeatedly been shown to accumulate positively charged metals.

Chapter V.

Potential of fish embryo toxicity test (FET) to detect the varying toxicities of highly reactive substances

5. Potential of the fish embryo toxicity test (FET) to detect the varying toxicities of highly reactive substances

5.1 Abstract

Hair coloring has been carried out for more than 2000 years using various natural dyes such as vegetable-/plant-based colors, minerals or animal-borne substances. To provide a long-lasting hair color, oxidative hair dyes have been developed which contain highly reactive molecules: dye precursors, i.e. a combination of primary intermediates and couplers, and oxidants. The final hair color forms upon mixture of the components directly in the hair fiber. Side effects of these reactive molecules have been studied with regards to consumer safety and health. Environmental safety assessments have been built up on the knowledge of ecotoxicity of the precursors, couplers and their relevant metabolites. These reactive components can be oxidized by oxygen from the medium, i.e. water or air. The effects of this auto-oxidation as a time-dependent phenomenon was investigated for the most commonly used hair dye precursors, the primary intermediates *para*-phenylenediamine (PPD) and toluene-2,5-diamine sulfate (PTD) as well as for the newly developed 2-methoxymethyl-*para*-phenylenediamine (MBB) in zebrafish embryos. Additionally, the modulation of toxicity by the well-known scavenger ascorbic acid has been elucidated.

Overall, the three precursors showed dose-dependent effects in zebrafish embryos, the higher the tested concentration of the precursors, the higher the percentage of affected embryos. Differences in toxicity were found between the different ages of stock solutions. The most toxic aged stock solution were found to be 16 hours for PPD ($LC_{50} = 0.92$ mg/L), 8 hours for PTD ($LC_{50} = 0.45$ mg/L) and 16 hours for MBB ($LC_{50} = 4$ mg/L). In all experiments with the amendment of 0.04% ascorbic acid, the toxicity was strongly reduced, indicating that ascorbic acid is able to prevent the auto-oxidation and further reactions of the precursor molecules by reacting with oxygen and/or radical oxygen species (ROS) produced during oxidation of precursors. Hence it can be concluded that the toxicity of the three precursors is strongly dependent on the formation of free radicals and also on the different products formed by auto-oxidation and further reactions (i.e. self-coupling).

5.2 Introduction

Hair is one of the unique features of mammals, and in humans there are three different hair types: the fine and straight to slightly curly Caucasian hair with a nearly circular cross section, the coarse and straight to wavy Mongolian hair with a quite similarly shaped cross section, and the coarse and wavy to wooly Ethiopian hair with a slightly oval cross section (Morel and Christie, 2011). The hair grows from elongated sacs in the epidermis, the follicles. Near in the center of the bulb, the dermal papilla is found which is involved in growth functions. A basal layer of cells surrounds the papilla and produce the hair cells. The hair fiber is composed of dead skin cells with keratin as the main component produced by keratinocytes in the epithelial tissue. Blood vessels leading to the papilla nourish the growing hair fiber. The hair fiber can be divided into the cuticle, the cortex, the cell membrane complex (CMC) and the medulla in the center of the hair.

The cuticle is the outer part of the hair and regulates the amount of water inside the hair fiber. Cuticle damage is usually due to weathering or mechanical damages caused by e.g. brushing, excessive use of shampoo and inappropriate treatments. The cuticle consists of flat overlapping cells (scales) surrounding the central fiber core (see Figure 37). These cells form 6-10 layers and the edges of the scales run circumferentially around the fiber attached to the root and pointing to the tip of the hair. Each cuticle cell contains a thin outer membrane, the F-layer or epicuticle, which is formed by a layer of fatty acids linked to a protein layer through thioester linkage to cysteine residues (Morel and Christie, 2011). This makes the hair fiber hydrophobic and is important for the hair dyeing process. Beneath the F-layer, three other layers can be found: the A-layer (120 nm), high in cysteine content and strongly cross-linked, the B-layer (exocuticle) also rich in cysteine and the endocuticle, with low cysteine but relatively high levels of dibasic and diacidic amino acids (Morel and Christie, 2011).

The major part of the hair is the cortex, formed by 1-6 μm thick and about 20 – 100 μm long cells and intercellular binding material (Randbrook, 1964). Compared to the cuticle, the cortex is richer in cysteine, diacidic amino acids, lysine and histidine. The cells contain pigment granules, nuclear remnants and bear pronounced substructure, the macrofibrils composed of intermediate filaments (IFs) or microfibrils, which are embedded in the less structured matrix (see Figure 37). The IFs contain precise arrays of low-sulfur proteins with coiled sections (α -helical form = α -keratin). The largest subunit of the cortex is the matrix, which contains the highest concentration of disulfide bonds and contributes significantly to the swelling behavior of the hair (Morel and Christie, 2011). Also melanin is found in the cortex, which gives the

hair its natural color and serves as photo-protection. Only hairs with large cross section have a third structure, the medulla. The medulla is the inner region and can be empty or filled with sponge keratin, can serve as a pigment reservoir and can contribute to the brightness of the hair. It has a very high lipid concentration. Between the cuticle and cortex cells, the cell membrane complex can be found, which link these two cell layers. It is composed of polysaccharides, proteins and ceramides and commonly a low level of sulfur-containing amino acids (da França et al., 2015; Morel and Christie, 2011). Its outer lipid layer forms the epicuticle, while its inner lipid layer is the intercellular cement (Figure 37), connecting the cells.

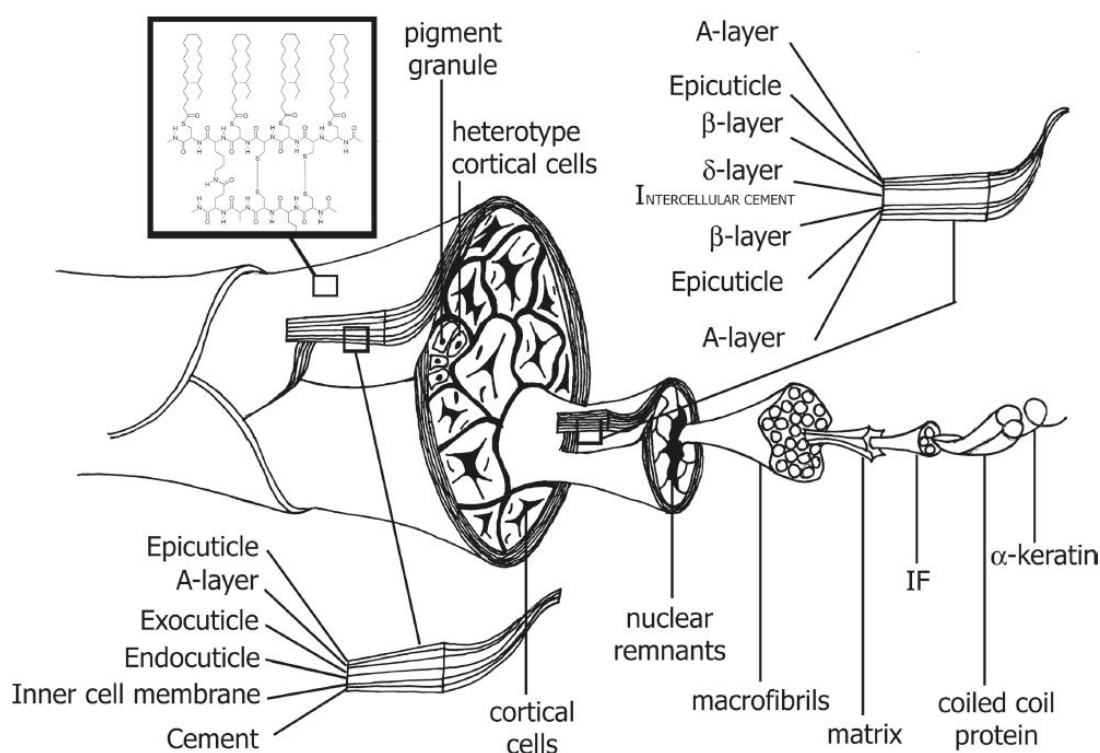


Figure 37: Structure of the human hair. The outer cell layer is formed by overlapping cuticle cells, which are composed by the epicuticle, the A-layer, exo- and endocuticle. The cuticle cells surround the cortex. Corticle cells contain pigment granula and nuclear remnants. Their substructures are: macrofibrils composed of intermediate filaments (IF) and the matrix. The further substructures of the IF are coiled coil proteins formed by α -keratin. Scheme taken from Morel and Christie (2011)

Hair coloring has been carried out for more than 2000 years using various natural dyes such as vegetables/plant based colors, minerals or animal substances. There are three ways to modify the hair color: (1) bleaching to get lighter hair color, (2) adding artificial color to the hair or (3) a combination of both. Hair dyes can be divided based on their coloring mechanism into two main categories: oxidative or non-oxidative dyes and can be further classified based on their color duration in the hair into: temporary dyes or color rinses; semi-permanent dyes; and permanent (oxidative) dyes. Temporary and semi-permanent hair dyes contain direct

dyes, i.e. colorful molecules, which will interact with the cuticle of the hair. They are not transformed into other dyes or shades of dyes and to achieve differentiated shade of the hair color, four to five dyes are mixed (Robbins, 2012). They do not (temporary) or only slightly (semi-permanent) penetrate into the cortex of the hair (Corbett, 1973; da França et al., 2015). Temporary dyes are composed of acid dyes characterized by anionic properties and are carefully selected to allow a maximum of water solubility and a minimum of penetration. Application can be singly or continuously (progressive) *via* shampoo, gel emulsion or solution. The color coats the hair surface without penetrating the cuticle, hence the temporary dye is easily washed out of the hair after a single shampoo (da França et al., 2015; Robbins, 2012).

Semi-permanent dyes are commonly cationic molecules of a low molecular weight and with high affinity to hair keratin. Small hair dyes might slip in the hair cortex and often a high pH value promoted opening of the cortex for a better penetration of the hair dye. The hair color is applied as lotion, shampoo, mousse and emulsion and has to be applied to the hair for 10 – 40 minutes (Corbett, 1976; da França et al., 2015). The color last for three to six washes and in case oxidative precursors and hydrogen peroxide is included for up to 20 washes (demi-permanent dyes). Other dyes such as plant-based dyes, e.g. henna and chamomile flowers, or metal salts, e.g. lead, silver salts and bismuth, are also categorized as semi-permanent hair dyes (Corbett, 1976; Nohynek et al., 2010; Robbins, 2012).

Permanent or oxidative hair dyes are the most common used hair dyes and have a market share in the EU or the US of about 80% (Corbett, 1999). They offer a wide spectrum of color shades, which can lighten the hair up to three levels, change the color subtle or dramatic, and provide a long-lasting hair color and 100% gray coverage (Draelos, 2005; P&G, 2015). The process of oxidative hair color is based on an observation made by Hofmann (1863) that the colorless *para*-phenylenediamine (PPD) produces brown shades on a variety of substrates when an oxidizing agent, including atmospheric oxygen, is available. This exact process still holds true for modern hair color formulations. The color formation happens upon mixture of the required components directly in the hair fiber.

The first component is the primary intermediate, also referred to as oxidation base or developer, which is commonly *para*-diamine or *para*-aminophenol and occasionally their *ortho* isomers (Corbett, 1973; Corbett, 1999). These hydroxy- or amino- groups in *para* or *ortho* position serve as electron donors and the primary intermediates include *p*-aminophenol and its derivatives as well as the compounds tested in this thesis, *para*-phenylenediamine (PPD), toluene-2,5-diamine sulfate (PTD) and 2-methoxymethyl-*para*-phenylenediamine (MBB).

The second component is the coupler, an aromatic compound with two electron donor groups (-NH₂ or -OH) arranged in *meta* position. These couplers do not produce significant color when oxidized alone, however in combination with primary intermediates a variety of color shades are possible (Corbett, 1999). Couplers include *m*-phenylenediamine, *m*-aminophenol resorcinol, naphthols and their derivatives.

The third component is the oxidant, which is almost exclusively hydrogen peroxide, added with an alkali, usually ammonia or an ammonia substitute such as monoethanolamine (MEA). The alkalizing agent is required to promote the pH value at which the oxidation of the precursors can take place. These reactions are usually carried out at a pH from 8 to 10 (Robbins, 2012). Additionally, alkalizing agents help to swell the hair fiber, making it easier for the precursors to diffuse into the hair (P&G, 2015). MEA is not able to completely oxidize natural hair pigments, such as melanin, thus products containing MEA are used to dye hair in similar or darker shades of the natural hair color (da França et al., 2015). To remove melanin, ammonia is used for achieving a lighter hair color. The bleaching process by ammonia takes place in combination with the oxidant, hydrogen peroxide and the natural hair pigment is dispersed and solubilized.

As illustrated in Figure 38 for PPD, the second and main purpose of the oxidant however, is the oxidation of the primary intermediates to produce benzoquinonediimine or monoamine which further react with present couplers (Corbett, 1999; Morel and Christie, 2011). The produced dimers, such as diphenylamine or leuco-dye (see Figure 38, pathway A), can be further oxidized to brightly colored binuclear indo dye or with the suitable coupler to trinuclear or polynuclear compounds (Corbett, 1999; Morel and Christie, 2011; Robbins, 2012). Although hydrogen peroxide is the oxidative agent of choice for oxidative hair dyeing, the processes of auto-oxidation (the oxidation by oxygen in air) can be used for oxidization of the precursors to form the desired hair color (Morel and Christie, 2011; Robbins, 2012).

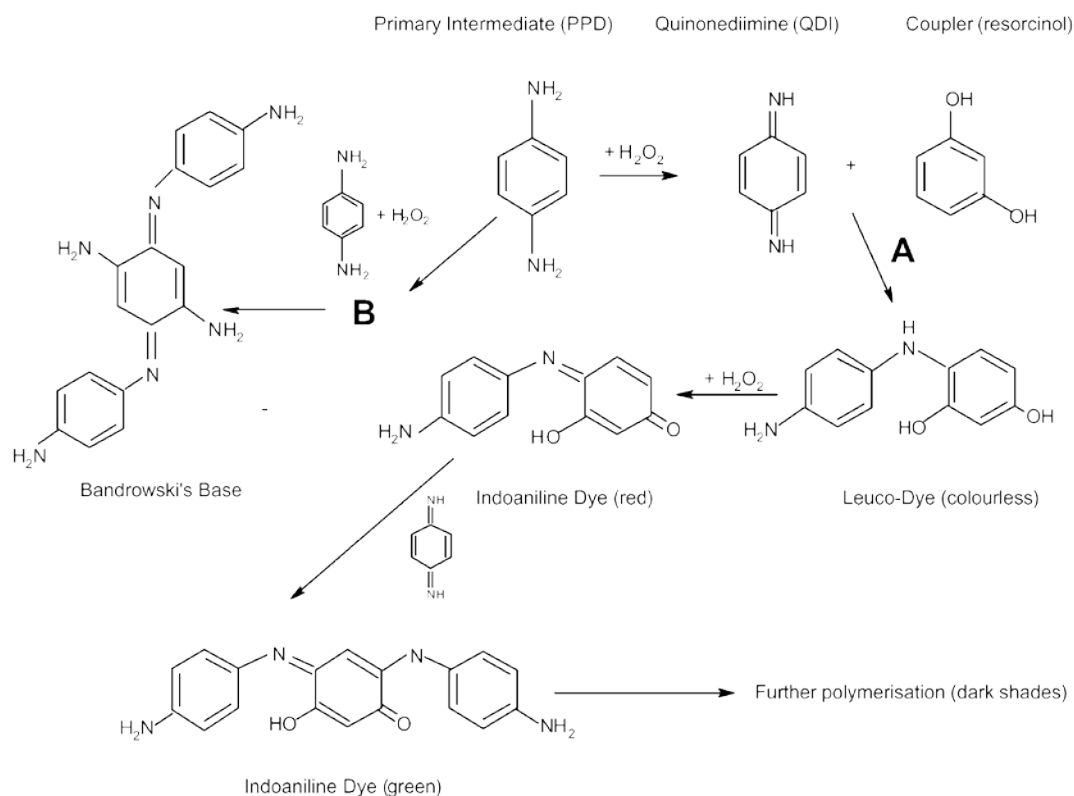


Figure 38: Reaction scheme of the oxidation of *para*-phenylenediamine (PPD) by hydrogen peroxide (H_2O_2) and possible coupling processes. Pathway A: In a first oxidation of PPD, quinonediimine (QDI) is formed which further reacts with a present coupler (here: resorcinol) to form a colorless dimer (leuco-dye). In further oxidative coupling reactions, trinuclear (here indoaniline dye) or polynuclear compounds are formed, resulting in the desired color range. Pathway B: in the absence of couplers, PPD is able to form Bandrowski's base as a result of self-coupling, oxidized by hydrogen peroxide. Scheme taken from Nohynek et al. (2004), adopted from Spengler and Bracher (1990).

The variety of possible hair colors and shades is achieved by a careful choice of the used bases and couplers, their ratio and competing reactions inside the hair fiber (da França et al., 2015; P&G, 2015). This is influenced by the total concentration of the various precursors, the pH and the diffusion rates (Morel and Christie, 2011). Especially the coupler selection seems to be a critical point in hair dye formulations, since the substitution pattern of the precursors as well as their oxidative products can be important for their reactivity and the final color (Morel and Christie, 2011). The clue of oxidative hair color is that the precursors are very small molecules, able to penetrate into the cortex of the hair. The oxidation and subsequent dimer and trimer formation due to coupling reactions takes place inside the hair and these formed molecules are bigger and hence trapped inside the cortex (da França et al., 2015; P&G, 2015; Robbins, 2012). Also the charge of the final products leads to binding to the keratin of the hair. In hair dye formulations, a slightly acid conditioner is used for the re-attachment of the cuticle layer, to restore the outer f-layer, reduce hair fiber damage and lead to a nice hair feel (P&G, 2015).

One of the most often used primary intermediates are *para*-phenylenediamine (PPD) and related hair dye components, such as toluene-2,5-diamine (PTD) and its sulfate. For PPD and, to a lesser extent also for PTD, a variety of relevant oxidation products as well as their formation conditions are documented in literature (e.g. Corbett, 1972; 1999; Dolinsky and Wilson, 1968; Robbins, 2012) and have been summarized by Meyer and Fischer (2015). Due to their structural and electronic relationship to PPD (see Figure 39), comparable reactivity can be expected for PTD and MBB, varying from PPD by an additional methyl group (PTD) or methoxymethyl group (MBB). Nonetheless, these additional groups might influence the reaction and hence the resulting coupling products.

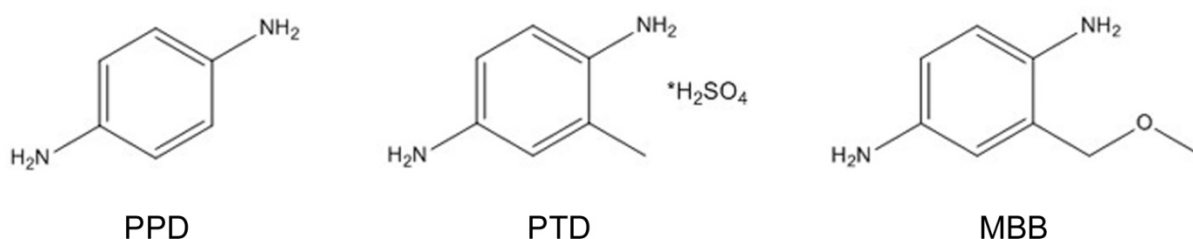


Figure 39: Structural formula of *para*-phenylenediamine (PPD), toluene-2,5-diamine sulfate (PTD) and 2-methoxymethyl-*p*-phenylenediamine (MBB) to illustrate the structural relationship of the three precursor molecules. PTD differs from PPD by an additional methyl group, while MBB is substituted by an additional methoxy-methyl group. Formulas illustrated using PerkinElmer, ChemDraw Professional 15.0 (1998-2015 PerkinElmer Informatics, Inc.).

The potential of PPD and PTD to cause and elicit contact allergies and skin sensitizing has been confirmed by numerous animal and human studies (e.g. Diepgen et al., 2016; Picardo et al., 1992; SCCP, 2006, 2007; White et al., 2006; Young et al., 2016). The allergic potential is most likely due to the formation of oxidized products caused by oxidation *via* air exposure (Aeby et al., 2009). Especially the auto-oxidation of PPD in the absence of couplers (see pathway B in Figure 38) results in the formation of the mutagenic compound Bandrowski's base (Altman and Rieger, 1968; Corbett, 1972; Heilingötter, 1968), which is believed to be the driving force to cause contact allergies. Hence the developing of new dye precursors is an intensive field in cosmetic research. Only recently, the coupler MBB was developed by Procter and Gamble and is believed to promise a combination of excellent permanent color performance with a reduced risk of developing allergies (Blömeke et al., 2015; Goebel et al., 2014; SCCS, 2013).

In Europe, the regulatory framework for cosmetic products is the Regulation (EC) 1223/2009 (EU, 2009), replacing the Directive 76/768/EC (EU, 1976) which was adopted in 1976. In the process of registration and submission of personal products, the primary intermediates, cou-

plers as well as their relevant metabolites and final products need to be evaluated for consumer safety according to the guidance document SCCS/1564/15 by the Scientific Committee on Consumer Safety (SCCS, 2016). However, this only concerns testing to provide facts on human safety. Environmental safety assessments have been built up on the knowledge of ecotoxicity of the precursors, couplers and their relevant metabolites, which have to be registered and authorized according to EC 1907/2009 (EC, 2007). These data can be found in the registration dossier of the respective chemical, which is accessible *via* the homepage of the European Chemicals Agency (ECHA, <http://echa.europa.eu/>). Traditionally, the ecotoxicology to aquatic organisms are performed in standard toxicity tests in fish (e.g. rainbow trout, zebrafish and fathead minnow), invertebrates (e.g. daphnids, chironomids) and algae (e.g. green algae). Ethical concerns and animal welfare restrictions require the development of non-animal testing strategies. To replace the acute toxicity tests with fish, e.g. OECD TG 203 (OECD, 1992), the use of fish embryos, especially zebrafish *Danio rerio* embryos (Busquet et al., 2014; Lange et al., 1995; Nagel, 2002) have been proposed as a suitable alternative and the guideline 236 “*Fish Embryo Acute Toxicity Test (FET)*” for the testing of chemicals (OECD, 2013a) has been assembled. Previously, Belanger et al. (2013) have well established the relationship between FET and classical acute fish toxicity *in vivo* including some oxidative dyes.

In this study, zebrafish embryos were used to understand the age-dependent toxicity of PPD, PTD and MBB, and to elucidate the influences of air- and waterborne oxygen on toxicity. For this purpose, the stock solutions of the precursors were aged for time periods of 1, 4, 8, 16, 24, 48 and 72 hours before initiating the exposure. Thus, the impact of the oxidized products and metabolites formed in the absence of developer (oxidation bases) to zebrafish embryo toxicity can be investigated.

To provide additional information on the mechanisms driving the toxicity and especially whether it is solely driven by the reactivity of the three precursors to air- and waterborne oxygen, the aged stock solutions were combined with a well-known scavenger, ascorbic acid. Ascorbic acid (AA), also known as vitamin C, is naturally occurring in fruits and vegetables and its deficiency is linked to scurvy in humans. After its discovery in the late 1920s by Albert von Szent Györgyi, vitamin C became one of the most celebrated nutrient supplements known to effectively scavenge free radicals and reactive oxygen species (ROS). AA is an excellent electron donor, stabilizing free radicals inside and outside the cells and thus quenching their reactivity (Bendich, 1990; Bindhumol et al., 2003). These antioxidant properties have made ascorbic acid an important additive and active ingredient in food and cosmetics

(Arrigoni and De Tullio, 2002; Balaguer et al., 2008; Bendich et al., 1986; Frankel, 1996; Raschke et al., 2004). AA was added to the FET medium before aging of stock solution was performed. By this, the auto-oxidation of the precursors and consequently the formation of ROS or other radicals or at least their availability might be decreased.

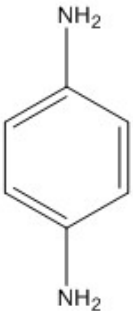
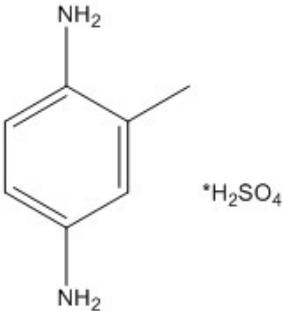
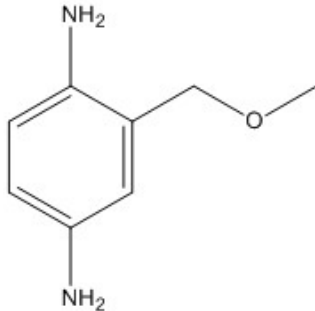
5.3 Material and methods

5.3.1 Chemicals

All chemicals were purchased from Sigma Aldrich (Deisenhofen, Germany) at the highest purity available, unless noted differently. Dilution water (294.0 mg/L $\text{CaC}_2 \times 2 \text{H}_2\text{O}$; 123.3 mg/L $\text{MgSO}_4 \times 7 \text{H}_2\text{O}$; 64.7 mg/L NaHCO_3 ; 5.7 mg/L KCl) was prepared according to OECD Test Guideline 203 (OECD, 1992), pH was adjusted to 7.7 ± 0.2 . All stock solutions and test solutions as well as the positive control 3,4-dichloroaniline (CAS 95-76-1) and ascorbic acid (CAS 50-81-7) were prepared in dilution water.

The aromatic amine precursors *p*-phenylenediamine (PPD; CAS 106-50-3), toluene-2,5-diamine sulfate (PTD; CAS 615-50-9) and 2-methoxymethyl-*p*-phenylenediamine (MBB; CAS 337-906-36-2) were provided by Procter & Gamble (Cincinnati OH, USA). The analytical purity of PPD was 100% (HPLC; QS-Laboratory A. Sauer). Analytical purity of the used PTD batch was 99.9% at 254 nm (HPLC, Procter & Gamble, Hünfeld, Germany), with 54.0 weight% calculated as free base and 97.4 weight% calculated as sulfate (by Spectral Service, Köln. Study No. SSL03511). The analytical purity of MBB was determined to be 100.0% by H-NMR (spectral service, Köln. Study No. WLD24148). Details on the different chemical names, trade names, structures and properties are listed in Table 11. All test materials were stored in glass vessels in the dark under vacuum at room temperature. Handling of open vessels was kept to a minimum to avoid oxidation by air before testing.

Table 11: Chemical names, structures and properties of the tested hair dye precursors PPD, PTD sulfate and MBB. Structural formula illustrated using PerkinElmer, ChemDraw Professional 15.0 (1998-2015 PerkinElmer Informatics, Inc.).

	PPD	PTD (sulfate)	MBB
INCI name	<i>p</i> -Phenylenediamine	Toluene-2,5-diamine sulfate	2-Methoxymethyl- <i>p</i> -phenylenediamine
Chemical names	1,4-Diaminobenzene; <i>para</i> -Benzenediamine; 1,4-Benzenediamine; <i>para</i> -Aminoaniline; 4-Aminoaniline; <i>para</i> -Diaminobenzene	2,5-Diaminotoluene sulfate; 2-Methyl- <i>p</i> -phenylenediamine sulfate; <i>p</i> -Toluenediamine sulfate; <i>p</i> -Toluylenediamine sulfate;	1,4-Benzenediamine,2-(methoxymethyl); 2-(Methoxymethyl)benzene-1,4-diamine; 1,4-Diamino-2-methoxymethyl-benzene
Trade names	PPD	Rodol; Colorex; Jarocol	MBB; ME+
CAS no.	106-50-3	615-50-9 (sulfate 1:1)	337906-36-2
Structural formula			
Empirical formula	C ₆ H ₈ N ₂	C ₇ H ₁₀ N ₂ × H ₂ SO ₄	C ₈ H ₁₂ N ₂ O
Mol weight	108.15 g/mol	218.23 g/mol 122.19 g/mol (PTD only)	152.2 g/mol
Appearance	beige to light brown crystalline powder	slightly reddish, fine-crystalline powder	slightly brownish, crystalline powder

5.3.2 Zebrafish maintenance and egg production

Wild-type zebrafish (Westaquarium strain) derived from own stock facilities at the University of Heidelberg were kept under conditions described in detail by Lammer et al. (2009). Breeding conditions were as follows: oxygen contents $\geq 90\%$; water temperature 26.0 ± 1.0 °C, pH 8.0 ± 0.2 , conductivity 600 – 800 $\mu\text{S}/\text{cm}$; ammonia < 5 mg/L, nitrite < 1 mg/L; nitrate < 25 mg/L, 13 – 16 °dH (214.5 – 286 mg/L CaCO₃) total water hardness and a photo period of 16 h light – 8 h dark. Fish maintenance and egg production have repeatedly been described in detail (Kimmel et al., 1995; Nagel, 2002; Spence et al., 2008) and have been updated for the purpose of the zebrafish embryo acute toxicity test (Lammer et al., 2009). Egg production was

performed *via* spawning groups as recommended by the OECD TG 236 (OECD, 2013a) with modifications according to Sessa et al. (2008).

5.3.3 Acute toxicity in the zebrafish embryo test (FET)

All tests were performed according to the OECD TG 236 – Fish Embryo Acute Toxicity Test” (FET) (OECD, 2013a). Dilution water was used as a negative control (both internal plate controls and external negative control), 4 mg/L 3,4-dichloroaniline prepared in dilution water served as a positive control.

The FET was conducted in 24-well polystyrene plate (TPP, Renner, Dannstadt, Germany), which had been pre-incubated for 24 h prior to the test start with the respective test concentrations. The 24-well plates were covered with self-adhesive foil (Sealing tape SH, 236269, Thermo Fisher Scientific, Waltham, MA) and the lid and incubated at 26.0 ± 1 °C. Photoperiod was 14 h light – 10 h dark. Exposure was semi-static with daily exchanges of the entire volume of the test solutions after assessment of changes in embryonic development.

Only egg batches with a fertilization rate $\geq 80\%$ were used. A test was considered valid, if a mortality rate of $\leq 10\%$ in the negative control (plus ascorbic acid or humic acids control) and $\geq 30\%$ in the positive control could be observed at the end of the test. In case of two controls during a test run, both were included in ToxRat[®] analysis. Embryos were examined after 24, 48, 72 and 97 hours post fertilization (hpf) for the following lethal effects: non-detachment of the tail, non-formation of the somites, coagulation and, from 48 hpf onwards, lack of heart-beat. Besides lethal effects, every aberration in normal development (e.g. edema formation, underdevelopment, reduction or lack of blood circulation) was recorded according to Bachmann (2002) and Nagel (2002).

5.3.4 Preparation of test solutions

During the entire experiment, the PPD, PTD and MBB stock solutions were prepared daily by direct dissolving in dilution water at a concentration of 40 mg/L. During the aging experiments, the stock solutions were protected from light by aluminum foil and kept at room temperature. Solutions were mildly agitated until usage for the preparation of the final test concentrations. The time period until use of the final test solutions was equivalent to the desired period of aging of the stock solutions, namely <1 h, 4 h, 8 h, 16 h, 24 h, 48 h or 72 h. Before preparing of the final test concentrations, the pH of the stock solution was checked, but no adjustment had to be made for the FET (pH 7.7 ± 0.3). Nominal final PTD and PPD test concentrations can be found in Table 12.

5.3.5 Supplementation of the test solutions by ascorbic acid

In order to prevent auto-oxidation, the stock solutions were supplemented by addition of 400 mg/L ascorbic acid (AA) in dilution water. Stock solutions were prepared as described above and aged in the presence of ascorbic acid.

In addition, a 4 g/L AA stock solution was prepared by direct solution in dilution water for supplementation of the different test concentrations to arrive at identical final concentration of 0.04% AA. AA stock solutions were protected from light by aluminum foil and stored at room temperature. The pH of the AA stock solution was adjusted to 7.7 and checked prior use. Since AA stock solutions were found to be stable, they were used for up to 3 months. After appropriate periods of aging, pH of the stock solutions plus AA were adjusted with 1 M NaOH in *Aqua bidest.* from pH 3 to 7.7 ± 0.1 . All final test concentrations were checked and adjusted if necessary. The final nominal test concentrations of PPD, PTD and MBB supplemented by 0.04% AA are listed in Table 12. In addition to normal negative and positive controls, an ascorbic acid control at 0.04% was run

5.3.6 Statistical analysis

At the end of the test at 96 hpf, the LC_{50} (concentration at which 50% of the exposed embryos showed lethal effects) and the EC_{50} (concentration at which 50% of the exposed embryos showed lethal and sublethal effects) values were calculated using ToxRat[®] version 2.10 probit analysis using linear maximum likelihood regression. Cumulative mortalities of zebrafish exposed to PPD, PTD and MBB were illustrated with SigmaPlot 12.0 (Systat Software, San Jose, CA).

Table 12: All concentrations of the tested PPD, PTD and MBB solutions, their aging process, the amendments with ascorbic acid (AA), the stock solutions and the final concentrations tested in the FET with zebrafish embryos. All concentrations are nominal concentrations.

	Age of stock solution	Nominal concentrations (mg/L)	
		stock solution	test solutions
PPD	1 hour [#]	40	0.0625, 0.125, 0.25, 0.5, 1, 2, 4, 8
	4 hours	40	0.0625, 0.125, 0.25, 0.5, 1, 2, 4, 8
	8 hours	40	0.0625, 0.125, 0.25, 0.5, 1, 2, 4, 8
	16 hours	40	0.125, 0.25, 0.5, 1, 2, 4, 8
	24 hours	40	0.125, 0.25, 0.5, 1, 2, 4, 8
plus 0.04% AA	1 hour	100	0.5, 1, 2, 4, 8, 16, 32
PTD	1 hour	40	0.0625, 0.125, 0.25, 0.5, 1, 2
	4 hours	40	0.25, 0.5, 1, 2, 4, 8
	8 hours	40	0.25, 0.5, 1, 2, 4, 8
	16 hours	40	0.0625, 0.125, 0.25, 0.5, 1, 2, 4
	24 hours	40	0.0625, 0.125, 0.25, 0.5, 1, 2, 4
	48 hours	40	0.5, 1, 2, 4, 8, 16
	72 hours	40	0.5, 1, 2, 4, 8, 16
plus 0.04% AA	1 hour	40	0.0625, 0.125, 0.25, 0.5, 1, 2
	4 hours	40	0.5, 1, 2, 4, 8, 16
	8 hours	40	0.5, 1, 2, 4, 8, 16
	16 hours	40	0.5, 1, 2, 4, 8, 16
MBB	1 hour	100	1, 2, 4, 8, 16, 32, 64
	4 hours	100	1, 2, 4, 8, 16, 32, 64
	8 hours	100	1, 2, 4, 8, 16, 32, 64
	16 hours	100	1, 2, 4, 8, 16, 32, 64
	24 hours	100	1, 2, 4, 8, 16, 32, 64
	48 hours	100	1, 2, 4, 8, 16, 32, 64
plus 0.04% AA	1 hour	100	1, 2, 4, 8, 16, 32, 64

[#] test was performed in complete darkness

5.4 Results

5.4.1 Age-dependent toxicity of PPD, PTD and MBB in zebrafish embryos at 96 hpf

Freshly prepared PTD stock solutions were first clear, but turned brownish-red within 1 hour. This effect was also observed with PPD stock solutions, as they were clear with a slight hint of pink and turned brownish-red within 1 hour. PTD and PPD stock solutions turned dark brown at ages ≥ 4 hours. Freshly prepared MBB stock solutions were clear but turned brownish after a couple of hours. Also, as the solution turned older, a brownish adsorption on the glass bottle and on the magnetic stir bar was observed.

All FETs were valid, since mortality in negative controls were $< 10\%$, total hardness was 13 – 16 °dH, test temperature was 26 ± 1 °C and dissolved oxygen never fell below 80%. Determined pH values of the different test concentrations ranged between 7.5 ± 0.2 for PPD and 7.7 ± 0.2 for PPD + AA; 7.6 ± 0.2 for PTD, 7.3 ± 0.6 for PTD +AA; 7.7 ± 0.1 for MBB and 7.6 ± 0.2 MBB +AA.

All three hair dye precursors showed coagulation-based mortalities of zebrafish embryos from 24 hpf onwards. The mortality rate in each of the test runs did not rise with increasing exposure period. Hence, only the results at the end of the test at 96 hpf are illustrated and described further. Clear dose-dependent increases in toxicity were found in all test runs. The main toxic effect was coagulation of embryos.

P-Phenylenediamine (PPD) While the dose-related curves of PPD solutions aged for 16 and 24 h showed a very steep increase in toxicity at 96 hpf, the curves for PPD solutions aged for ≤ 8 h displayed a more sigmoidal shape (Figure 40). Independent of stock solution aging processes, 100% of the zebrafish embryos were coagulated at 4 and 8 mg/L PPD. In contrast, mortalities at 1 mg/L and 2 mg/L PPD varied with aging: whereas 75, 40, 45 and 30% of the embryos were lethally affected by 2 mg/L PPD aged for 1, 4, 8 and 24 h, respectively, all embryos died within 96 h of exposure to 2 mg/L PPD aged for 16 h (80% at 1 mg/L PPD aged for 16 h). The corresponding 96 h LC₅₀ values for PPD could be determined at 1.32, 1.82, 1.86, 0.92 and 2.13 mg/L for solutions aged for 1, 4, 8, 16 and 24 h (see filled dots of insert in Figure 40).

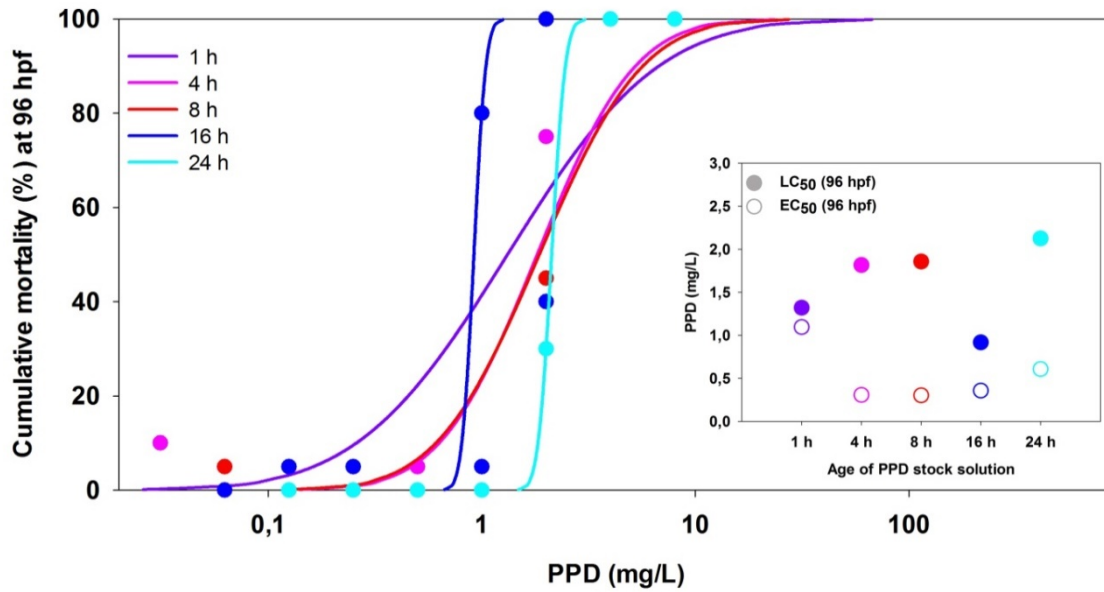


Figure 40: Cumulative mortality (%) of zebrafish embryos exposed for 96 hours to differently aged PPD solutions. PPD solutions aged for 16 hours (blue line) showed the highest toxicity. Insert illustrates LC₅₀ (filled dot) and EC₅₀ (empty dot) values determined for PPD solutions aged between 1 and 24 h. Graphs based on ToxRat[®] calculations and illustrated with SigmaPlot 12.0.

The most conspicuous sublethal effect in early embryos exposed to PPD was a reduction of body pigmentation. At 48 hpf, the lack of body and eye pigmentation was striking (see embryos in Figure 41) and with rising exposure time, this retardation in pigmentation of the body and the eyes was almost compensated. However, an increase of a well-defined brownish accumulation in PPD-exposed embryos above the yolk and the digestive tract but underneath the developing swim bladder (see asterisk in Figure 41 exposed to 2 mg/L PPD) was detected from 72 hpf onwards. These were the main effects in embryos leading to almost identical EC₅₀ values in 1, 4, 8 and 16 hours aged PPD solutions at a range between 0.30 and 0.36 mg/L PPD (see empty dots of insert in Figure 40). Only the PPD stock solution aged for 1 and 24 h showed less prominent effects with EC₅₀ value of 1.09 and 0.61 mg/L.

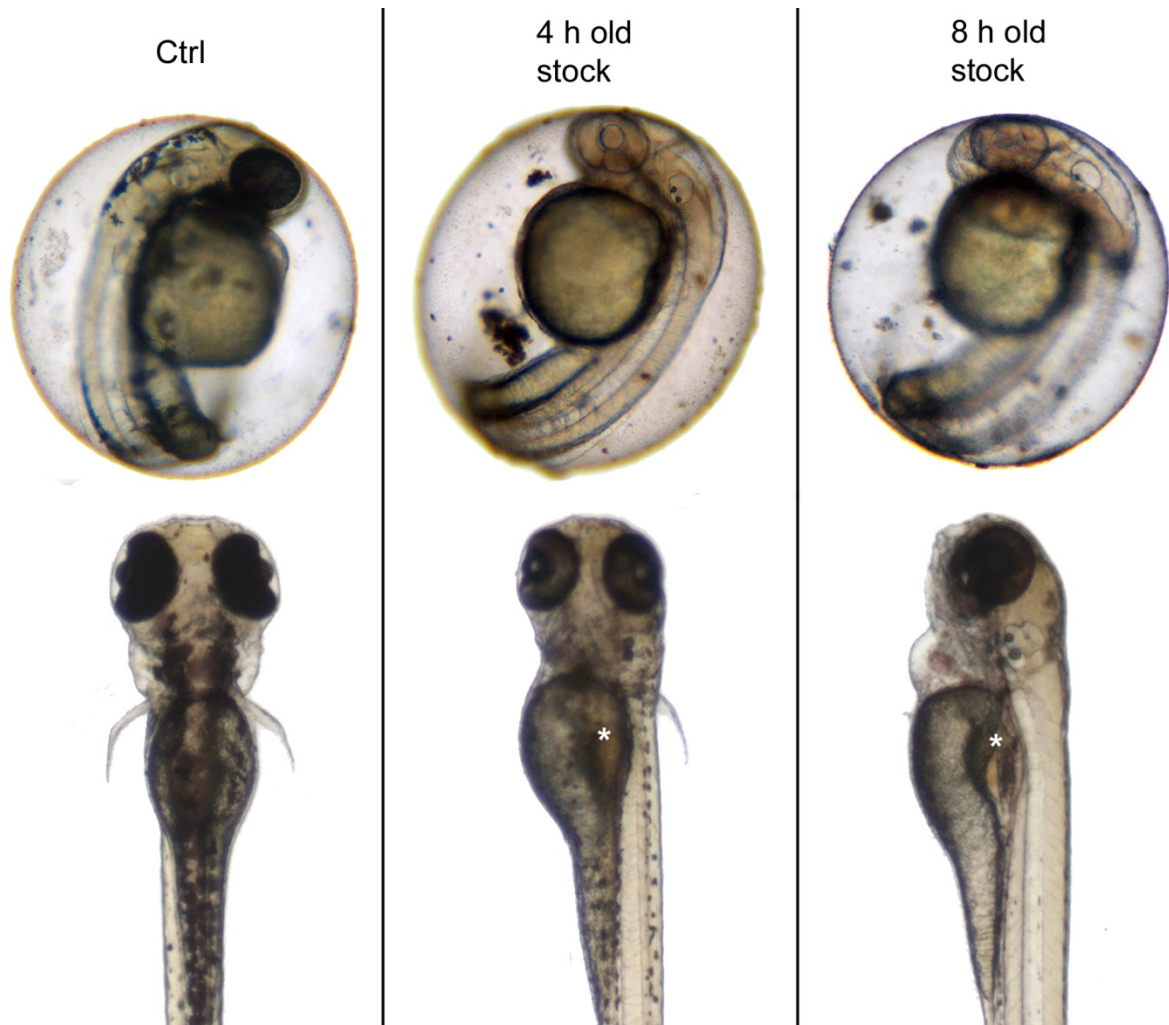


Figure 41: Phenotypes of 48 hpf embryos inside the chorion and hatched larvae at 96 hpf exposed to PPD. Column 1 shows the control embryos; column 2 represents 2 mg/L of 4 hours aged PPD stock solution; 3 column shows embryos exposed to 2 mg/L of the 8 hours aged PPD stock solution. Differences in whole body but especially in eye pigmentation can be seen in the PPD treated embryos. A brownish accumulation, indicated by asterisks, in a well-defined area above the gut and the yolk sac is seen.

Tuolene-2,5-diamine sulfate (PTD)

The cumulative PTD mortality of zebrafish embryos exposed to differently aged stock solutions was strongly dose-dependent (see toxicity curves in Figure 42). Especially the mortality rates found for 48 and 72 h old PTD stock solutions were shifted to higher tested concentrations. Whereas at a concentration of 1 mg/L 95% (16 h PTD) or 100% (1, 4 and 8 h PTD) of the introduced embryos were coagulated, only 25% in the 24 h old solution died and no mortality at all was found at 1 mg/L PTD aged for 48 and 72 hours. The most toxic PTD stock solution was the one aged for 8 h with a LC_{50} value determined at 96 hpf at 0.45 mg/L PTD. The LC_{50} values determined for stock solutions older than 8 h increased steadily (see insert Figure 42), and a significant reduction of cumulative toxicity became evident for solutions older than 24 h. Since embryos exposed to PTD did not show any sublethal effects in addition to acute lethal effects, EC_{50} and LC_{50} values were almost identical (see Table 13) and thus, only the corresponding LC_{50} values are shown in the insert of Figure 42.

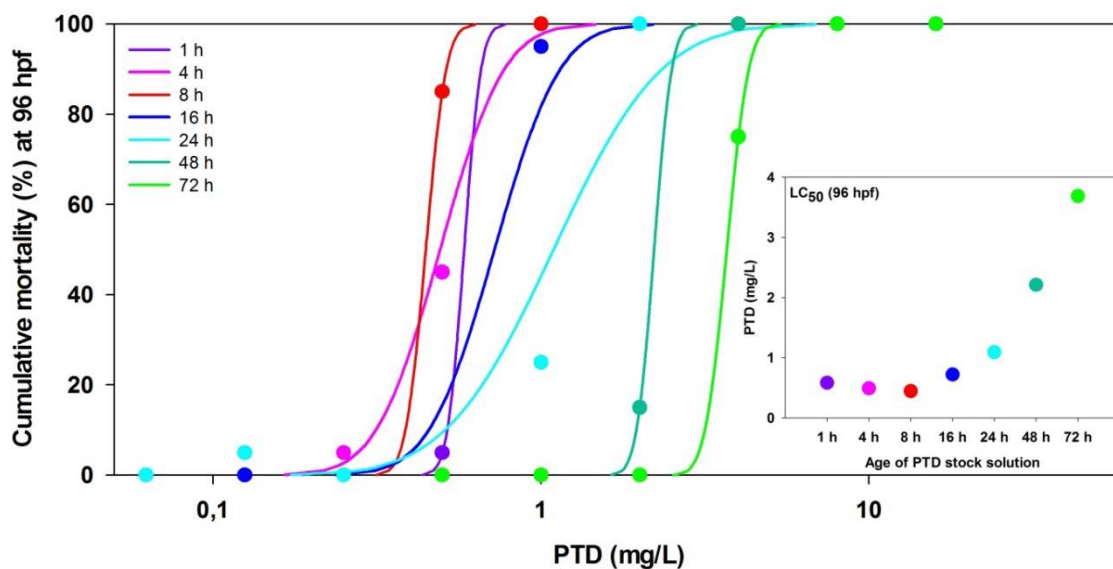


Figure 42: Cumulative mortality (%) of zebrafish embryos exposed for 96 hours to differently aged PTD solutions. Stock solution aged for 8 hours showed the highest toxicity (red line), while stock solutions aged for more than 24 hours resulted in lower toxicity (blue-green, green and bright green functions). The insert illustrates the concentration at which 50% of the introduced embryos were lethally affected (LC_{50} values) as determined via ToxRat[®] probit analysis. A clear reduction of toxicity with LC_{50} values above 1 mg/L could be shown for PTD solutions aged ≥ 24 h. Graphs based on ToxRat[®] calculations and illustrated with SigmaPlot 12.0.

2-Methoxymethyl-p-phenylenediamine (MBB)

Within the single test runs, the toxicity of MBB in zebrafish embryos was strongly dose-dependent. Differences between the tested concentrations per run were found, resulting in variable curve progressions. Quite similar steep cumulative mortality curves are found for MBB stock solutions aged for 8, 16 and 24 h, while for all other stock solutions, the toxicity rate increased slower with rising concentrations.

The toxicity of MBB to zebrafish embryos was also influenced by age of stock solutions. However no clear statement can be made about increase or decrease of toxicity with rising age of MBB stock solutions: When comparing the determined LC_{50} values (filled dots in insert of Figure 43), no pattern of toxicity can be found with rising age of MBB stock solutions. The stock solution aged for 1 h and 16 h showed similar mortality rates, with the lowest determined 96 h LC_{50} values at 4.03 mg/L and 4.00 mg/L, respectively (see also Table 13). All other LC_{50} values found for the differently aged MBB stock solutions ranged between 5.46 mg/L (8 h MBB) and 8.92 mg/L (4 h MBB).

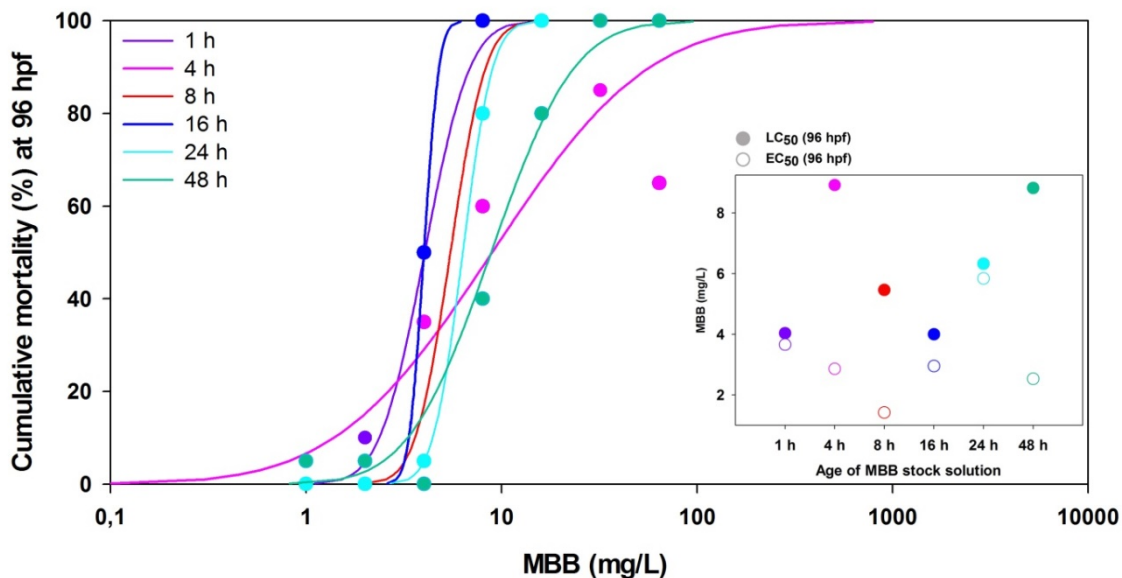


Figure 43: Cumulative mortality (%) of zebrafish embryos exposed for 96 hours to differently aged MBB solutions. All stock solutions showed similar responses in zebrafish embryos. Stock solution aged for 16 hours showed the highest toxicity (blue line). Insert illustrates LC_{50} (filled dot) and EC_{50} (empty dot) values determined for MBB solutions aged between 1 and 48 h. Graphs based on ToxRat[®] calculations and illustrated with SigmaPlot 12.0.

Exposed embryos showed a dose-dependent increase in effects on embryonic development. As a main effect, embryos showed no or reduced pigmentation at every time point of observation from 48 hpf onwards, which could not be compensated until the end of the test. Stock

solution aged for 8 h showed the most affected embryos at 96 hpf, resulting in the lowest EC_{50} value at 1.42 mg/L MBB (see empty dots in insert of Figure 43 and Table 13).

Also, embryos showed a brownish accumulation between the yolk/intestine tract and the notochord/swim bladder (Figure 44) from 72 hpf onwards. The accumulation of brownish material, as found in PPD-exposed embryos, was well-defined and increased with rising test concentrations. Selected images of embryos treated with 4 h old MBB stock solution at different test concentrations showed a dose-dependent increase of accumulation between 2 and 8 mg/L, while in embryos treated with higher concentrations no differences in intensity could be found.

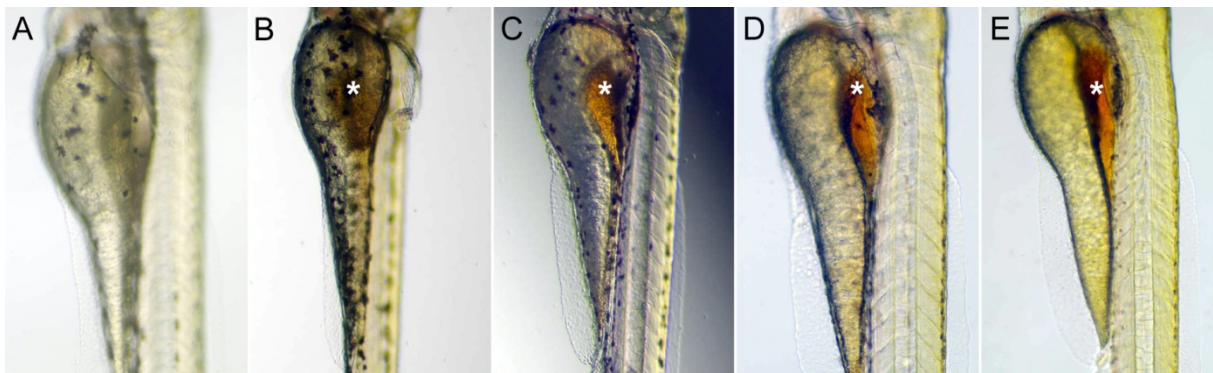


Figure 44: Dose-dependent increase of brownish accumulation in 96 hpf zebrafish embryos exposed to MBB solutions aged for 4 hours. The accumulation is found in a distinct area between yolk/intestine tract and swim bladder/notochord (see asterisks). Embryos were exposed to 2 mg/L (A), 4 mg/L (B), 8 mg/L (C), 32 mg/L (D) and 64 mg/L (E) MBB for 96 hours. The accumulation increases between 2 and 8 mg/L, all embryos exposed to higher concentrations showed similar intensity of the accumulation. With rising exposure concentration, also a reduction of body pigmentation can be found.

5.4.2 Influence of ascorbic acid on toxicity of PPD, PTD and MBB as determined in zebrafish embryos

No age-dependent change of stock solution color as described for the standard FETs was observed upon supplementation with ascorbic acid. PPD, PTD and MBB stock solutions with ascorbic acid remained clear for at least a week; nevertheless the tested stock solutions were prepared daily to ensure the different aging points. All tests were valid, since mortality in negative and ascorbic acid controls were < 10%.

The addition of 0.04% ascorbic acid to PPD stock solution aged for 1 h resulted in a 50% reduction of the LC_{50} value from 1.32 mg/L to 3.55 mg/L. No further tests were performed, due to this reduction in toxicity.

Also for PTD, toxicity was extremely reduced by addition of ascorbic acid, resulting in a complete lack of embryo mortality in all concentrations tested of stock solutions aged for 1, 4, 8 and 16 h (Table 13). However, sublethal effects such as reduction of pigmentation and edema formations could be detected, resulting in EC_{50} values of 5.1 - 5.2 mg/L PTD supplemented with 0.04% ascorbic acid aged for 4, 8 and 16 h (for details see Table 13). Nevertheless, no effects on embryos were seen for PTD with 0.04% ascorbic acid aged for 1 h.

Compared to the toxicity data gained with the standard FET (LC_{50} at 4.03 mg/L) for MBB stock solution aged 1 hour, no toxicity could be observed in the same range of MBB concentrations with the addition of 0.04% ascorbic acid. Hence, no LC_{50} value could be determined ($LC_{50} > 64$ mg/L MBB + 0.04% AA). Nevertheless, developmental effects in embryos exposed to MBB + AA were found. Again, the main sublethal effect was a strong reduction of pigmentation and a dose-dependent brownish accumulation between the yolk and the notochord/the swim bladder. The EC_{50} value was determined at 20.01 mg/L. The ascorbic acid therefore strongly reduced MBB toxicity and no further test with the addition of AA was performed. A summary of all LC_{50} and EC_{50} values determined in the standard fish embryo acute toxicity test and with the addition of 0.04% ascorbic acid (AA) is found in the Table 13.

Table 13: Toxicity of the tested hair dye precursors to zebrafish embryos at 96 hpf in the standard fish embryo toxicity (FET) test and with the addition of 0.04% ascorbic acid (AA). A strong reduction of toxicity is found with AA, hence only one LC₅₀ value could be determined. All listed LC₅₀ and EC₅₀ values determined via Tox-Rat[®] probit analysis.

Age of stock solution	Standard FET		FET + 0.04% AA		
	LC ₅₀ (mg/L)	EC ₅₀ (mg/L)	LC ₅₀ (mg/L)	EC ₅₀ (mg/L)	
PPD	1 hour	1.32 [#]	1.09 [#]	3.55	2.06
	4 hours	1.82	0.31	n.t.	n.t.
	8 hours	1.86	0.30	n.t.	n.t.
	16 hours	0.92	0.36	n.t.	n.t.
	24 hours	2.13	0.61	n.t.	n.t.
	72 hours	3.69	3.69	n.t.	n.t.
PTD	1 hour	0.58	0.58	> 2.00	> 2.00
	4 hours	0.49	0.47	> 16.00	5.19
	8 hours	0.45	0.45	> 16.00	5.13
	16 hours	0.72	0.70	> 16.00	5.06
	24 hours	1.09	1.04	n.t.	n.t.
	48 hours	2.21	2.21	n.t.	n.t.
	72 hours	3.69	3.69	n.t.	n.t.
MBB	1 hour	4.03	3.66	> 64.00	20.01
	4 hours	8.92	2.86	n.t.	n.t.
	8 hours	5.46	1.42	n.t.	n.t.
	16 hours	4.00	2.95	n.t.	n.t.
	24 hours	6.32	5.84	n.t.	n.t.
	48 hours	8.82	2.53	n.t.	n.t.

[#] test was performed in complete darkness; n.t. – not tested,
LC₅₀ values shown in **bold** indicate the most toxic ages of stock solutions.

5.5 Discussion

Hair dyes have been used for decades to cover up grey hair or for fashion statements. Permanent or oxidative hair dyes are the most common used hair dyes and the process is based on a centuries-old observation made by Hofmann (1863): The colorless *para*-phenylenediamine (PPD) produces brown shades on a variety of substrates when an oxidizing agent, including air oxygen, is available (Morel and Christie, 2011). Until today, PPD is the most common used hair color ingredient, although it has been shown to form by-products associated to its skin sensitization potential (Aeby et al., 2009; Chung et al., 1995; Nohynek et al., 2004; Nohynek et al., 2010; Picardo et al., 1992; White et al., 2006). Environmental safety assessments have been built up on the knowledge of ecotoxicity of the precursors, i.e. the primary intermediates and the couplers as well as their relevant metabolites. The main focus of the conducted tests was the identification of effects of commonly used hair-dye primary intermediates, *para*-phenylenediamine (PPD), toluene-2,5-diamine (PTD) sulfate and 2-methoxymethyl-*para*-phenylenediamine (MBB) in zebrafish embryos. Since air- and water-borne oxygen is able to oxidize the reactive precursors, various periods of time ranging from 1 to 72 hours were chosen as pre-incubation, allowing the formation of metabolites. Hence, not only the toxicity of the parent substance, i.e. the precursors, was investigated by applying 1 hour old test-solutions, but also the toxicity of aged solutions containing all possible oxidized metabolites. To verify if the oxidative products are responsible for the toxicity in zebrafish embryos, the well-known scavenger ascorbic acid was used to prevent oxidation. This testing strategy has not been applied for toxicity testing of hair dye molecules in zebrafish embryos before.

Overall, the three primary intermediates showed dose-dependent effects in zebrafish embryos: the higher the tested concentration, the higher the percentage of affected embryos. One very prominent effect in surviving embryos was the reduction or lack of body and eye pigmentation, which is a very universal effect and frequently found in phenol- and aniline-exposed embryos (Keth, 2012; Schulte and Nagel, 1994; Schulte, 1997). The exact mechanism of interference of the tested compounds with the melanophores in the skin or retina of zebrafish embryos is not known. Pigmentation in zebrafish embryo starts at 30 hpf, first appearing in the pigmented layer of the retina and as distinctive clusters of melanophores in the skin dorsal and anteriorly in the head (Kimmel et al., 1995). The reduction or lack of pigmentation is found between 48 - 72 hpf, while at 96 hpf, a pigmentation can be found in embryos and in

some cases only with minor reductions compared to negative control embryos. Hence, the embryo seems capable catching up this retardation in development.

The reactivity of the precursors in the FET medium and the formation of various products by self-coupling processes is visualized by the change in color of the aged PPD-, PTD- and MBB-stock solutions (Meyer and Fischer, 2015). First, the stock solutions were clear with a slight hint of brownish-red and became dark brown at ages ≥ 4 hours. In solutions aged for longer periods (16 – 72 hours), some adsorption of brown material to the glass bottoms and the stirring bars was found. Hatched embryos exposed to solutions aged for ≥ 4 hours showed an accumulation of brownish material between the yolk/intestine tract and the developing swim bladder/notochord. The prevalence and intensity of this effect increased with rising ages of stock solutions and rising test concentrations. Thus it appears that the formed oxidized products of PPD, PTD and MBB are taken up *via* the mouth and subsequently accumulate in the intestine and hindgut lumen. In zebrafish embryonic development, the intestine and hindgut appears under the light microscope shortly between 42 and 60 hpf and the lumen becomes more prominent at 72 hpf (Kimmel et al., 1995), correlating with the appearance of brown material inside the embryo at 48 hpf and an increase until the test end at 96 hpf. Hence, the shades of brown in the test solutions as well as the accumulation within the embryos are an indicator of the successful oxidation of the respective precursors, PPD, PTD or MBB, by oxygen in the air and within the medium and also of a subsequent and time-depending coupling process.

Aeby et al. (2009) found PPD to be initially stable in constantly air saturated aqueous medium. However after 30 minutes, a peak of a second monomer was detected via liquid chromatography, indicating auto-oxidation. After approximately 5 hours, the presence of PPD has dropped to about 50%, while in the meantime, these monomers had polymerized and formed dimeric and trimeric auto-oxidation products as well as Bandrowski's Base (Aeby et al., 2009). They also found 8 hours after the PPD addition substantial amounts of dimer, BB and second trimer. For PTD auto-oxidation in aqueous medium, analogous products have been detected by Goux et al. (2007) via spectroelectrochemical methods. Therefore, similar processes of auto-oxidation and formation of self-coupled products can be assumed for MBB based on their structural similarities.

In the standard FETs with zebrafish embryos, the ranges of LC_{50} values determined with the stock solutions aged for 1 to 48 hours were 0.92 – 2.13 mg/L for PPD (1 h - 24 h), 0.45 – 2.21 mg/L for PTD and 4.0 – 8.82 mg/L for MBB. Comparing these ranges with the LC_{50}

endpoints submitted by registrants in the ECHA registration dossier (access *via* ECHA webpage: <http://echa.europa.eu>, accessed June 2016), the determined endpoints were found in similar ranges. The accepted endpoints for acute toxicity in fish derived from key studies as follows. The LC₅₀ submitted for PPD was determined in a flow-through study with rainbow trout fingerling at 3.9 mg/L (nominal, dossier PPD). For PTD a LC₅₀ (96 h) value was determined in a flow-through study with zebrafish (OECD, 1992) at 1.08 mg/L (nominal, dossier PTD). For MBB, the 72 h LC₅₀ value was determined in an FET study based on the OECD draft guideline (OECD, 2006) with zebrafish embryos to be > 5.69 mg/L (mean-measured, dossier MBB).

In all performed FETs, the main lethal effect in all tests was coagulation, and when comparing the percentage of embryos coagulated at 24 hpf with the ones coagulated at the end of the test (96 hpf), no increase was found. The most toxic aged stock solution were found to be 16 hours for PPD (LC₅₀ = 0.92 mg/L), 8 hours for PTD (LC₅₀ = 0.45 mg/L) and 16 hours for MBB (LC₅₀ = 4 mg/L). Correlating the formation of possible reactive products in air saturated medium as described above to the strong embryotoxic response of the tested precursor solutions aged for ≥ 8 hours, it becomes clear that the concentration and the accumulation of the formed products drives the reaction in the embryos.

The effects of PPD auto-oxidation has been studied in various approaches in e.g. human immortalized keratinocytes (Kawakubo et al., 2000; Picardo et al., 1992; Zanoni et al., 2015), reconstituted human epidermis and hepatocytes (Nohynek et al., 2005; SCCP, 2006), dendritic cells (Aeby et al., 2009) or in various laboratory animals (Bharali and Dutta, 2009; SCCP, 2006) - however always under the aspect of skin sensitization (see also Diepgen et al. (2016); Pot et al. (2013)). One major discussed pathway for the allergic potential of the precursors is the formation of reactive oxygen species (ROS) and free radical cations. Although ROS is important in normal embryonic development and the regeneration of complex structure, an excess of oxidative stress is associated with embryotoxicity (Dennery, 2007; Gauron et al., 2013; Hahn et al., 2014). ROS and reactive cations as products of PPD, PTD and MBB oxidation can bind to DNA, proteins and lipids and hence, lead to cell death (O'Brien, 1985). In the conducted FETs, the course of survival or coagulation of the embryo seems to be settled within the first hours of exposure. Directly after fertilization, the developing embryo consists of only a small amount of cells and is strongly vulnerable for interferences with DNA, proteins and other biomolecules by ROS or reactive cations formed by the oxidation of PPD, PTD and MBB. For PPD, an interaction with small peptides containing one of the nucleophilic amino

acids cysteine, lysine, histidine or arginine has been shown by Aleksic et al. (2009), and the selective binding of PPD to cysteine residues in the synthetic peptide DS3 was verified by Jenkinson et al. (2009). Especially the auto-oxidation products *p*-benzoquinonediimine, *p*-benzoquinones and Bandrowski's Base interact with proteins to form adducts or be involved in complex reduction reactions (Aleksic et al., 2009; Jenkinson et al., 2009; Pot et al., 2013). In HaCaT cells, Zanoni et al. (2015) showed the capability of auto-oxidation of PPD to induced DNA oxidation at levels similar to positive control (10.5 µg/ml H₂O₂). Due to structural and chemical similarities, these mechanisms can be assumed for the oxidized products of PTD and MBB.

An additional influence in toxicity might be the bioavailability of the parent substances and their oxidized metabolites: PTD is methylated and might be more bioavailable than PPD as the basic molecule. The less toxic tested substance is MBB bearing a bigger and more steric residue (-C₂H₅O₂).

To investigate whether the formation of reactive oxygen species (ROS) and the different oxidized and self-coupled products are responsible for the toxicity of the aged precursor to zebrafish embryos, the scavenger ascorbic acid (AA) was added to the FET medium. AA is supposed to inhibit the auto-oxidation of PPD, PTD and MBB as well as to decrease levels of produced ROS and other free radicals produced in the oxidation process. Visually, a clear indication of the successful prevention of auto-oxidation of the three precursors was the absence of a color change of the prepared stock solutions and test solutions. All solutions were clear throughout the aging process and the subsequent FET procedure. Since the color formation is caused by the formation of various self-coupling products due to auto-oxidation of the precursors (Aeby et al., 2009; Corbett, 1972; Goux et al., 2007; Meyer and Fischer, 2015), AA is able to reduce or even prevent these two successive reactions.

Regarding the effects of PPD, PTD and MBB in zebrafish embryos, lethality and deformations were effectively reduced in all performed experiments with the amendment of 0.04% ascorbic acid. Exposed embryos in the highest tested concentrations of all runs showed a reduced pigmentation. Nevertheless, the rate of affected embryos was lower with the amendment of AA. Comparing the resulting EC₅₀ values in the standard FET to the ones determined with the addition of 0.04% AA, the effect rate was reduced by a factor of approximately 2 (PPD), 5.4 (MBB) and 7 (PTD). The reduction in pigmentation was only seen in embryos of the treatments, not in the AA-control, hence a whitening effect of AA due to melanocyte in-

teraction as seen in humans (Balaguer et al., 2008; Raschke et al., 2004) can be fairly excluded.

The toxicity of the three precursors was strongly reduced by AA in all treatments and test runs. AA is assumed to react with the oxygen in water itself, to scavenge effectively ROS and to chelate radicals (Bendich et al., 1986; Bodannes and Chan, 1979), which might also held true for oxidized precursors formed by - a presumably lower rate of - auto-oxidation. Consequently, less reactive molecules lead to a decrease in self-coupling processes triggering a reduction of toxicity. The protective effects of AA has been mainly studied in mammals, but also in fish exposed to ethanol (Reimers et al., 2006) and pesticides e.g. organochlorine (Agrawal et al., 1978), deltamethrin (Datta and Kaviraj, 2003) and ethyl methane sulfonate (Guha and Khuda-Bukhsh, 2002). Although in zebrafish embryos no prevention of ethanol-induced pericardial edema were found (Reimers et al., 2006), the other authors demonstrated with an AA supplementation a reduced stress response caused by pesticides (Agrawal et al., 1978; Datta and Kaviraj, 2003) and the inhibition of the oxidative metabolism of the genotoxic ethyl methane sulfonate (Guha and Khuda-Bukhsh, 2002). The effectiveness of a pretreatment with AA to reduce oxidative stress was shown by El-Gendy et al. (2010) in imidacloprid-exposed mice. For PPD, Coenraads et al. (2016) demonstrated an attenuating effect on the elicitation reaction in sensitized individuals by pretreatment with AA.

5.6 Conclusions

Since the FET is already being used for the assessment of chemical safety and should be applied to an even wider range of applications, the possibility of variations in the test performance to address the toxicity of rapidly changing substances has been evaluated. The toxicity of strongly reactive oxidative hair dye precursors has been assessed in the standard FET according to TG 236 (OECD, 2013a). To cover the ability of auto-oxidation and self-coupling of these reactive molecules, the process of aging of the stock solution before introducing the test organisms, freshly fertilized fish eggs, has been successfully applied. With small modifications of the standard procedure, the transformation of the precursors to various products, such as reactive oxygen species and reactive self-coupling products (dimers, trimers, and Bandrowski's base) can be assessed in the FET. Moreover, the amendment of ascorbic acid at 0.04% has been found to inhibit successfully the formation of these reactive products. No transformation of color in the aqueous medium as an indicator of the self-coupling products was found. Also, in the FET with ascorbic acid the toxicity in zebrafish embryos was strongly reduced over the course of the test period.

Overall, the FET standard test design can be easily modified in the laboratory to learn more about the mode of action of a reactive substance, the modifications by other substances and the toxicity. To investigate whether a more realistic environmental aspect can be transferred into the laboratory, the next chapter describes the performance of the FET with PTD in native river water and the involved influences of dissolved humic materials on the toxicity in zebrafish.

5.7 Acknowledgement

The performed tests were conducted in collaboration with the Procter & Gamble Company, Cincinnati OH, USA. The results of the performed FET studies with PTD have been submitted as supporting studies by the Procter & Gamble Company for the registration of PTD. Additionally, results of FET studies performed with Bandrowski's base (data not shown) were submitted for the registration of PPD.

Chapter VI.

Influences of humic acids and native river water on the toxicity of toluene-2,5-diamine sulfate (PTD)

6. Influences of humic acids and native river water on the toxicity of toluene-2,5-diamine sulfate (PTD)

6.1 Abstract

For the investigation how heterogeneous matrices might influence the behavior and consequently the toxicity of the hair dye precursors PTD, the fish embryo toxicity test (FET) was performed in an environmentally more realistic scenario under controlled conditions in the laboratory. The FET dilution water was (a) amended with Suwannee River Standard II humic acids (HA) at 2 or 8 mg/L and (b) substituted by native river water sampled from a German river. The Neckar River was chosen as a typical German river, heavily anthropogenic influenced by urban water purification plants clearing the sewage of about 11 million people and several direct immissions from industrial sewage treatment plants (LUBW, 2007). Sampling occurred at two different flow rates: normal and during a flood.

The amendment with humic acids only slightly reduced the toxicity of PTD to zebrafish embryos. LC_{50} values for PTD with 2 mg/L and 8 mg/L humic acids could be determined at 0.711 and 1.12 mg/L PTD, respectively, while the LC_{50} without any amendment was found to be 0.85 mg/L PTD. In contrast, the toxicity of PTD in natural river water was lowered, although no difference could be found between toxicity in river water at normal and elevated flow rate. In comparison to the standard FETs, the LC_{50} values (96 hpf) were lowered approximately 2 times for the 4 hours aged PTD solution, 3 times for the 8 hours aged PTD solution and 5 times for the 16 hours aged PTD solutions.

This study showed that the organic matrix within the native river water needed some time to react with the PTD molecules as well as with possibly emerging products. The amendment with humic acids cannot fully display the natural occurring complexity of aggregation, disaggregation and formation of complexes with the reactive hair dye primary intermediate PTD. Nevertheless, the FET can be modified to address a more realistic approach of toxicity.

6.2 Introduction

In Chapter V of this thesis, the toxicities of oxidative hair dye primary intermediates PTD, PPD and MBB as well as their self-coupling products formed within several hours, have successfully been assessed in the standard FET according to TG 236 (OECD, 2013a). With only small aberrations from the standard protocol, the transformation of hair dye precursors in the presence of oxygen to a broad range of reactive products, i.e. reactive oxygen species and

self-coupling products like dimers, trimers and Bandrowski's base, can be assessed in the FET. One of the most commonly used hair dye precursors, the primary intermediate PTD, showed in the standard FET the strongest toxicity in solutions aged for 8 hours ($LC_{50} = 0.45 \text{ mg/L}$). The LC_{50} values determined for stock solutions older than 8 h increased steadily and a significant reduction of cumulative toxicity became evident for solutions older than 24 h. With the amendment of 0.04% ascorbic acid, this transformation and the reactivity of the products were prevented and a decrease of toxicity to zebrafish embryos was observed. In PTD treatments, no embryotoxic effects were found in solutions aged for 1, 4, 8 and 16 hours.

To investigate whether a more environmentally realistic aspect can be transferred into the laboratory and how the heterogeneous matrices might influence the behavior, the toxicity of

PTD to zebrafish was determined in standard dilution water amended with humic acids (HA) and in a further step in native river water.

The Neckar River was chosen as a typical German river, heavily anthropogenic influenced. With 367 km, the Neckar River is the 10th longest river of Germany. It rises in the Black Forest at 706 m above sea level and winds its way through the German Federal Land of Baden-Württemberg (see Figure 45), passing the cities Stuttgart, Heilbronn and Heidelberg until it joins the Rhine River in the largest city Mannheim at about 85 m above sea level (LUBW, 2007). The Neckar passes through the typical southern German escarpment landscape with Keuper, Muschelkalk, bunter and granite (LUBW, 2007).

The outlet of the Neckar at Mannheim averages $145 \text{ m}^3/\text{s}$. The catchment area covers $13\,985 \text{ km}^2$ with 18 inflows and collects the sewage of about 5 million inhabitants (LUBW, 2007). The first 203 km upstream, from its mouth to the last lock at Plochingen, the Neckar

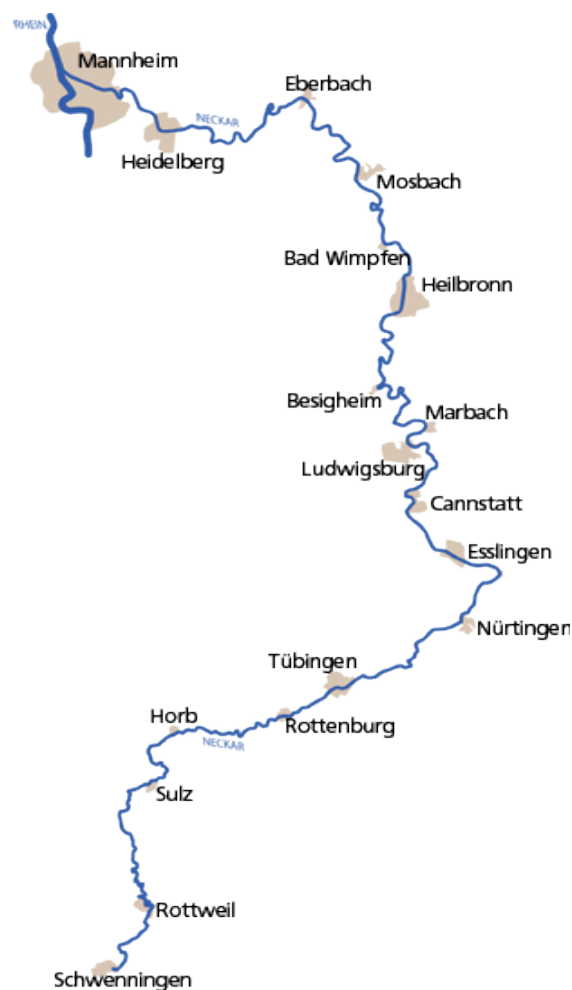


Figure 45: Course of the Neckar River through the German Federal Land of Baden-Württemberg (www.Fahrrad-Tour.de, 2013)

River is used as a Federal Waterway. To enable the navigability on the waterway at any water level, locks, weirs and channels were built. Today there are 27 locks operating between Mannheim and Plochingen.

In 2007, there were 588 urban sewage plants for about 11 million people (LUBW, 2007). Besides those, there are 37 direct pipes of industrial sewage plants joining the river. Compared to the length of the stream, the Neckar River thus shows a high density of sewage plants in Germany.

In natural waters, one major characteristic is the freight of organic matter which can be analyzed by determining the biochemical oxygen demand (BOD), the chemical oxygen demand (COD) and the total organic carbon (TOC). The total organic carbon is typically classified according to the solubility, as measured by particle size. Particles under 0.45 μm are classified soluble and form the group of “dissolved organic carbon” (DOC), while the particles of a size above 0.45 μm are classified as “particulate organic carbon” (POC). Riverine vegetation, soil and landscape composition as well as anthropogenic influences and seasonal variations have major impacts on TOC in aquatic systems. As a matter of fact, DOC is the carbon content found in the water column and hence the focus of interest for the present test procedure. A further classification of DOC can be made into humic substances and a variety of labile, chemically well-defined compounds, such as polysaccharides, low weight acids and other low weight substances (Sachse et al., 2005; Thomas, 1997). Humic substances are a complex and heterogeneous mixtures of a variety of materials, formed by a process called humification, in which plant and microbial remains are decayed and transformed (IHSS). They account for up to 80% of the organic carbon in freshwaters including organisms (Steinberg et al., 2007). According to their solubility in water, humic substances can be separated into humin (insoluble), humic acids (soluble at a $\text{pH} > 2$) and fulvic acids (soluble under all conditions; McDonald et al., 2004). Since 1981, the International Humic Substances Society has collected and distributed standard and reference samples of various natural humic substances, allowing the comparison of experiments conducted with humic substances. In the present study, the used humic acid was collected from the Suwannee River (IHSS Code: 1S101H), in southeast Georgia, USA. Ritchie and Perdue (2003) determined the concentration of carboxyl and phenolic functional groups in a variety of standard and reference materials from IHSS, including the used Suwannee humic acids. They estimated the mass carbon to 52.55% on a dry, ash-free basis, with a carboxylic content of 9.59 meq g/C and a phenolic content of 4.24 meq g/C.

The main focus of aquatic ecotoxicology research on organic content has been the binding properties, especially the ones of humic acids, and the resulting impact on bioavailability in aquatic organisms. It is well established, that organic and lipophilic substances tend to bind and adsorb to organic carbon, forming complexes resulting in a reduced bioavailability (Bollag and Myers, 1992; Fent and Looser, 1995; Haitzer et al., 1998; Meinelt et al., 2006; Thorn et al., 1996). The precise mechanisms on which the decrease in toxicity in presence of humic acids is based on, has not yet been elucidated. However, some studies showed an enhancement of bioconcentration at low concentration of DOC (0.5 – 4 mg/L) as has been reviewed by Haitzer et al. (1998). Only in the last years, nanotechnology makes use of low concentrations of humic acids to stabilize nanoparticles (NPs) in aquatic media and the influences on aggregation and disaggregation of NPs (Mohd Omar et al., 2014). Gao et al. (2012) showed an increase of total silver (Ag) content in aquatic system with concentrations of < 10 mg/L humic acids, while a decrease of Ag content was found at higher carbon concentrations, due to increased bridging processes and settling of the Ag NP-TOC-complexes. Nevertheless, toxicity of these suspensions to *Daphnia* decreased almost linear with increasing humic acids concentrations (< 20 mg/L). These observations have also been made in zebrafish embryos: despite a lower body burden due to complexation, titanium dioxide nanoparticles (TiO₂ NPs) have been shown to be more toxic to zebrafish embryos in the presence of humic acids (Yang et al., 2013). It has been postulated, that humic acids or other natural organic matters may serve as a free radical scavenger (Fabrega et al., 2009; Goldstone and Voelker, 2000; Wang et al., 2001). Besides the positive effects of stabilizing solutions, several hints of xenobiotic character of humic substances have been postulated with potential of herbicidal mode of actions, membrane-irritations and interferences with DNA (see for example Steinberg et al., 2004; Steinberg et al., 2007; Wolf et al., 2016). Especially in combination with UV light, DOC has been shown to induce reactive oxygen species and free radicals (Cooper and Zika, 1983; Fede and Grannas, 2015; Vaughan and Blough, 1998).

As has been shown in Chapter V, the auto-oxidation of the hair dye precursors, the primary intermediate PTD, PPD and MBB, led to an increase of toxicity in zebrafish embryos, which has been explained partly by the formation of free radical species, such as radical oxygen species and radical by-products during the self-coupling process. A clear reduction was found with an ascorbic acid supplementation, and for a better understanding of the behavior of precursors and their self-coupling products in sewage treatment plants and natural waters, this

chapter elucidates the impact of humic acids solely and as part of the complex matrix of natural river water.

The toxicity of PTD was assessed in two different approaches in the laboratory:

(1) The modulation of toxicity by humic acids:

In order to mimic the complex impact of dissolved organic carbon in the environment, humic acids (HA) at concentrations of 2 and 8 mg/L were selected as an additional supplement in the FET. For a direct comparison, a standard test was also performed.

(2) The influence of native river water on toxicity:

The standard FET protocol was performed, however, native river water as an ecological relevant matrix was used instead of dilution water as recommended by TG 236 (OECD, 2013a). Two different samplings were performed in summer 2013, the first one during normal stream stage, the second one during the event of a flood. This allows the comparison of influences due to a higher content of organic matters in the water column.

6.3 Material and methods

6.3.1 Chemicals

All chemicals were purchased from Sigma Aldrich (Deisenhofen, Germany) in highest purity available, unless noted differently. Suwannee River Humic Acid Standard II was obtained from the International Humic Substances Society (IHSS; St. Paul MN, USA).

Toluene-2,5-diamine sulfate (PTD; CAS 615-50-9) was provided by Procter & Gamble (Cincinnati OH, USA). The analytical purity of PTD was 99.9% at 254 nm (HPLC, Procter & Gamble, Hünfeld, Germany), test material was stored in glass vessels in the dark under vacuum at room temperature. For details on chemical and physical properties, please refer to Chapter V, Table 11.

Dilution water (294.0 mg/L $\text{CaC}_2 \times 2 \text{H}_2\text{O}$; 123.3 mg/L $\text{MgSO}_4 \times 7 \text{H}_2\text{O}$; 64.7 mg/L NaHCO_3 ; 5.7 mg/L KCl) was prepared according to OECD Test Guideline 203 (OECD, 1992), pH was adjusted to 7.7 ± 0.2 . Dilution water served as a negative control the standard FET (0 mg/L HA) and the FET with the amendment of humic acid. As a positive control, 4 mg/L 3,4-dichloroaniline (CAS 95-76-1) was prepared either in normal dilution water or in native river water.

6.3.2 Zebrafish maintenance and egg production

Wild-type zebrafish (Westaquarium strain) derived from own breeding facilities at the University of Heidelberg and were kept under conditions described in detail by Lammer et al. (2009). Breeding conditions were as follows: oxygen contents $\geq 90\%$; water temperature 26.0 ± 1.0 °C, pH 8.0 ± 0.2 , conductivity 600 – 800 $\mu\text{S}/\text{cm}$; ammonia < 5 mg/L, nitrite < 1 mg/L; nitrate < 25 mg/L, 13 – 16 °dH (214.5 – 286 mg/L CaCO_3) total water hardness and a photo period of 16 h light – 8 h dark. Egg production was performed *via* spawning groups as recommended by the OECD TG 236 (OECD, 2013a) with modifications according to Sessa et al. (2008).

6.3.3 Fish embryo toxicity test (FET)

All tests were performed according to the OECD TG 236 – Fish Embryo Acute Toxicity (FET) Test (OECD, 2013a). The FET was conducted in 24-well polystyrene plate (TPP, Renner, Dannstadt, Germany), which had been pre-incubated for 24 h prior to the test start with the respective test concentrations. The 24-well plates were covered with self-adhesive foil (Sealing tape SH, 236269, Thermo Fisher Scientific, Waltham, MA) and the lid and incubated

at 26.0 ± 1 °C. Photoperiod was 14 h light – 10 h dark. Exposure was semi-static with daily exchanges of the entire volume of the test solutions after assessment of embryonic development.

Only egg batches with a fertilization rate $\geq 80\%$ were used. Embryos were examined after 24, 48, 72 and 97 hours post fertilization (hpf) for the following lethal effects: non-detachment of the tail, non-formation of the somites, coagulation and, from 48 hpf onwards, lack of heart-beat. Besides lethal effects, every aberration in normal development (e.g. edema formation, underdevelopment, reduction or lack of blood circulation) was recorded according to Bachmann (2002) and Nagel (2002).

A test was considered valid, if a mortality rate of $\leq 10\%$ in the negative control (plus respective humic acids control) and $\geq 30\%$ in the positive control could be observed at the end of the test.

6.3.4 Modulation of PTD toxicity by addition of humic acids

In order to mimic the complex impact of dissolved organic carbon in the environment, humic acids (HA) at concentrations of 2 and 8 mg/L were selected as an amendment of dilution water in the FET. As a control, a FET was run in parallel without addition of humic acid (0 mg/L HA). All stock solutions and test solutions as well as the positive control 3,4-dichloroaniline and humic acid were prepared in dilution water.

A HA stock solution of 40 mg/L was prepared by directly dissolving HA in dilution water. Stock solutions of 40 mg/L PTD and final PTD test solutions were prepared freshly on each day of the experiments with dilution water or humic acid-complemented dilution water (2 mg/L or 8 mg/L HA). PTD stock solutions were adjusted to $\text{pH } 7.7 \pm 0.2$ and used immediately after preparation (aging < 1 h). Final nominal test concentrations can be found in Table 14. In addition to regular negative and positive controls, HA control runs without PTD were performed at 2 and 8 mg/L, respectively.

Table 14: The concentrations used in the FETs to investigate the influences of 0, 2 or 8 mg/L humic acids (HA) on the toxicity of PTD in zebrafish embryos. Stock solutions and the final test concentrations are listed as nominal concentrations.

		Age of stock solution	Nominal PTD concentration (mg/L) of	
			stock solution	test solutions
	0 mg/L humic acid	1 hour	40	0.25, 0.5, 1, 2, 4
PTD plus	2 mg/L humic acid	1 hour	40	0.25, 0.5, 1, 2, 4
	8 mg/L humic acid	1 hour	40	0.25, 0.5, 1, 2, 4

6.3.5 FET in native river water

To simulate the behavior of PTD under natural conditions, FETs were performed in natural water collected from the Neckar River at Heidelberg (Southern Germany). At the sampling site (49°24'41.48"N / 8°40'18.62"E) the river is canalized, hence the riverine vegetation as well as sediment deposition did not have a significant impact on the water. Sampling was performed by direct immersion of the sampling vessels at a depth of about 30 cm. In order to avoid major derogations of the water by air, sampling vessels were filled until overtopping.

For each day of the subsequent FETs, one aliquot of the unfiltered river water and another two aliquots for the dilution to the final test solutions were stored at -20 °C. All PTD stock and test solutions were exclusively prepared in river water thawed and heated in a water bath until temperature had reached 26 °C. Details on test design, concentrations of stock solution and test solutions can be found in Table 15.

Table 15: Test design and nominal concentrations of PTD tested in zebrafish FET under supplementation by Neckar River water.

	Normal Neckar River water	Flood Neckar River water
Dilution water	Neckar River water sampled under normal flow conditions	Neckar River water sampled during a flood
Stock solution	100 mg/L	100 mg/L
Test concentrations (mg/L)	0.25; 0.5; 1; 2; 4; 8; 16; 32	0.25; 0.5; 1; 2; 4
Age of stock solution	8 h	4, 8, 16 h
Embryos/run	20 (controls: 24)	10 (controls: 12)
Negative controls	Neckar River, normal water	Neckar River, flood water

6.3.6 Characterization of the river water

Total organic carbon (TOC) and dissolved organic carbon (DOC) were analyzed according to DIN (1997). Additionally, the total carbon (TC) and the inorganic carbon (IC) were determined. The chemical oxygen demand (COD) was performed according to ISO (2012) and DIN (1980) with LCK414 COD cuvette (suitable in a range of 5 - 60 mg/L). Due to the turbidity of the river water, the COD was determined for the thoroughly mixed river water and for the supernatant after sedimentation of the particles in the water column. The biological oxygen demand (BOD) was performed according to the "Determination of biochemical oxygen demand after n days (BOD_n) – Part 2: Method for undiluted samples (modified ISO, 1998)", with $n = 5$ days. As an indication of the total freight of dissolved aromatic moieties,

the SAC₂₅₄ was determined photometric (Ultrospec 2100 pro; Amersham Bioscience). The river water was also analyzed for nitrate, nitrite, ammonium, total hardness, chloride and phosphate (all tested with Aquamerck[®] test kits; Merck, Darmstadt, Germany). Also, the following standard water parameters were tested: pH (Knick pH Meter 765, Berlin, Germany); oxygen content (wtw Cell Ox325 with Multiline P4; wtw Weilheim, Germany); conductivity (wtw, Con Ox OxiCal with Multi 350i; wtw, Weilheim, Germany) and temperature (ama digit, ad. 15th).

6.3.7 Statistical analysis

At each time point of evaluation, the LC₅₀ (concentration at which 50% of the exposed embryos showed lethal effects) and the EC₅₀ (concentration at which 50% of the exposed embryos showed lethal and sublethal effects) values were calculated using ToxRat[®] version 2.10 probit analysis using linear maximum likelihood regression.

In case of two controls (HA-control and negative control) during a test run, both were included in statistical analysis in ToxRat[®].

6.4 Results

6.4.1 Modulation of PTD toxicity by humic acids

Following addition of humic acid to PTD, pH values ranged between 7.5 and 7.8. All tests were valid: in the positive control, mortality at the end of each test (96 hpf) was > 80%; in the negative control, mortality was 0% and in the humic acid control, mortality was 0 - 5%.

The prepared stock and test solutions were clear, with a slight hint of brown. Humic acid itself is a brown powder, but dissolved in dilution water, this coloration was negligible. No aging of the stock solutions was performed, however, the test solutions of the higher treatment groups turned brown during the 24 hours inside the wells.

Over the course of testing period, mortality of zebrafish embryos exposed to 1h old PTD solely or with the addition of 2 or 8 mg/L humic acid (HA) did not change after 24 hpf. All introduced embryos exposed to the two highest test concentrations of 2 and 4 mg/L PTD coagulated within 24 h, no matter if solutions were amended by HA. Embryos exposed to 1 mg/L PTD showed different reactions depending on the addition of humic acid and the HA concentration. In the test without any amendment, 13 of the introduced embryos exposed to 1 mg/L PTD were coagulated within the first 24 hours and one embryo showed a non-detachment of the tail, but recovered after 48 hours. Hence, 13 embryos (65%) were lethally affected at

96 hpf. At the same PTD concentration, but with the addition of 2 mg/L HA, 15 of the introduced embryos (75%) were coagulated throughout the whole test. The addition of 8 mg/L humic acid led to only 1 coagulated embryo (5%) at 1 mg/L PTD. Throughout the testing period, no increase in toxicity was found.

LC₅₀ values for PTD with 2 mg/L and 8 mg/L humic acids could be determined at 0.711 and 1.12 mg/L PTD, respectively, while the LC₅₀ without any amendment was found to be 0.85 mg/L PTD (see Table 16).

Only few surviving embryos showed sublethal effects, mainly a reduction of pigmentation of the eyes and the whole body was found. Additionally, a dose-dependent brownish accumulation between the yolk sac and the swim bladder as observed and documented in standard FETs with PTD (Chapter V) was found throughout the test runs.

EC₅₀ values were determined at 0.59 and 0.98 mg/L PTD with 2 and 8 mg/L humic acids respectively and differed slightly from the EC₅₀ value obtained without humic acids (0.74 mg/L).

Table 16: Overview of LC₅₀ and EC₅₀ values determined in zebrafish embryos at 96 hpf exposed to PTD with the amendment of humic acid. All listed LC₅₀ and EC₅₀ values determined *via* ToxRat[®] probit analysis

		LC ₅₀ (mg/L)	EC ₅₀ (mg/L)
	0 mg/L humic acid	0.85	0.74
1 h old PTD plus	2 mg/L humic acid	0.71	0.59
	8 mg/L humic acid	1.12	0.98

6.4.2 Sampling conditions and river water characterization

To test the influence of native river water on the toxicity, two sampling days at an interval of 10 days were chosen. During sampling for the normal river water (Wednesday, 22.05.2013, 10:00 o'clock), water temperature of the Neckar River was 14.5 °C, oxygen content was 9.4 mg/L, the pH ranged at 8.0 and conductivity was about 790 µS/cm. These data regarding the Neckar River were measured at the watergate in Neckargemünd, approximately 10 km upstream Heidelberg (49°24'38.49"N / 8°46'39.97"E) and were obtained from the Ministry for the Environment, Measurements and Nature Protection, Baden-Württemberg, Germany (LUBW, 2013a).

During the second sampling (Saturday, 01.06.2013, 14:00 o'clock), a flood has reached the sampling point at Heidelberg and the water temperature of the Neckar River was 11.5 °C, oxygen content was determined at 9.5 mg/L, pH was estimated at 7.5 and conductivity was

about 275 $\mu\text{S}/\text{cm}$. Again, these data were obtained from the LUBW (2013a), measured at the watergate in Neckargemünd. Comparing these parameters to the ones obtained for the normal river water taken 10 days before, the conductivity values differed enormously due to the extreme rainfalls before sampling. The day before sampling the flood river water, heavy rains lead to a daily total of 54 mm rainfall and on sampling day the rainfall in the morning was only light but increased in the afternoon with a daily total of 13 mm. As sampling took place during a flood, the water level of the Neckar as well as the discharge were obtained by the flood forecasting program by the LUBW (2013b). The values were measured about 3.5 km upstream the sampling site at the watergate “Karlstor” in Heidelberg ($49^{\circ}24'52.90''\text{N}$ / $8^{\circ}43'04.88''\text{E}$). On Saturday, the Neckar water level kept rising up to 480 cm. However, during sampling time, the water level was around 450 cm. The water level on the days before sampling ranged between 230 and 260 cm and started to rise continuously above 400 cm in the night before sampling. The discharge of the Neckar on sampling day was around 1600 m^3/s .

The sampled water was analyzed for several parameters to identify the organic freight and especially the carbon content. Normal river water was quite clear, with a slightly brownish-green touch and few very small particles in the water column. The river water taken during the event of a flood showed a different appearance: it was quite turbid with small particles, which seemed to be sand and mud, and medium sized particles, mainly small organic particles of woods and leaves, in the water column. A special focus was set on the total organic carbon (TOC), the dissolved organic carbon (DOC) and the SAC_{254} for the indication of the total freight of dissolved aromatic moieties. All of these parameters were significantly higher in the testing water sampled during the flood event. Also, the biological oxygen demand (BOD) was elevated in the flood water carrying more organic freight than the water sampled under normal conditions. The increased SAC_{254} and BOD levels had no impact on embryonic survival during the test, negative control mortality was always 0%.

The standard water parameters required for a valid FET were found to be in the range as required by the OECD TG 236 (OECD, 2013a). In defrosted river water warmed up to 26 $^{\circ}\text{C}$, the dissolved oxygen ranged between 7.2 and 8.7 mg/L and conductivity ranged between 726 and 823 $\mu\text{S}/\text{cm}$ during normal conditions and 344 and 430 $\mu\text{S}/\text{cm}$ in the case of flood Neckar River water. The defrosted river water had to be adjusted to a pH of 7.7 ± 0.1 , and the 100 mg/L PTD stock solutions in adjusted river water remained within this range. During the subsequent test procedure, pH values ranged between 7.4 and 8.2.

Relevant parameters, including ammonium, nitrite and nitrate levels of the river waters are listed in the following table (Table 17).

Table 17: Characterization of the Neckar River water used for the assessment of PTD toxicity under environmentally relevant conditions

	Normal Neckar River water	Flood Neckar River water
Water appearance (color, turbidity)	Clear, slightly brown-greenish, small particles	Turbid, brown-greenish, plenty of small (mainly inorganic) and medium-sized (mainly organic) particles with approximately 1 h sedimentation time
Nitrate	10 mg/L NO ₃ ⁻	n.d.
Nitrite	0.25 mg/L NO ₂ ⁻	0.1 mg/L NO ₂ ⁻
Ammonium	0 mg/L NH ₄ ⁺	0.5 mg/L NH ₄ ⁺
Total Hardness	20 °dH = 3.566 mmol/L	1 °dH = 0.178 mmol/L
Chloride	50 mg/L Cl ⁻	25 mg/L Cl ⁻
Phosphate	1 mg/L P ₂ O ₅ = 1.34 mg/L PO ₄ ⁻	1 mg/L P ₂ O ₅ = 1.34 mg/L PO ₄ ⁻
Total organic carbon (TOC)	3.580 mg/L	22.12 mg/L ¹⁾
Total carbon (TC)	3.663 mg/L	22.52 mg/L ¹⁾
Inorganic carbon (IC)	0.0882 mg/L	0.0395 mg/L ¹⁾
Dissolved organic carbon (DOC) ²⁾	3.010 mg/L	7.096 mg/L
Total carbon (TC)	3.121 mg/L	7.116 mg/L
Inorganic carbon (IC)	0.112 mg/L	0.020 mg/L
Chemical oxygen demand (COD)	14.3 mg/L (supernatant) 13.9 mg/L (homogenate)	14.6 mg/L (supernatant) 36.8 mg/L (homogenate)
Chemical oxygen demand (COD) after acidification	17.3 mg/L (supernatant) 17.2 mg/L (homogenate)	10.2 mg/L (supernatant) 26.5 mg/L (homogenate)
Biological oxygen demand (BOD) after 5 days	1.47 mg/L	6.95 mg/L
Spectral absorption coefficient 254 nm (SAC ₂₅₄)	0.286	1.234

¹⁾Due to turbidity, a 1:10 dilution was analyzed and values were re-calculated; ²⁾after 0.45 µm filtration

6.4.3 Toxicity of *p*-toluenediamine sulfate (PTD) in Neckar River water

Neckar River water sampled under normal water level conditions appeared clear, with only small green-brownish particles. In contrast, Neckar River water sampled during the flood event was highly turbid, with a load of particulate matters in the water column, which, upon settling, made detailed observations of the embryos quite difficult (see examples in Figure 46). Thus, for observations at 24 hpf, a pipette was used to “clean” the well bottom to allow the view on the embryos. In fact, most precipitations were siphoned by the aid of the pipette during the first water exchange.

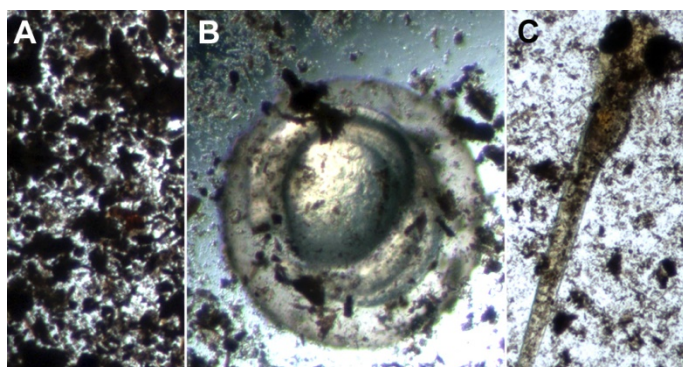


Figure 46: Particulate matters of the river water during a flood event settles from the water column onto the well bottoms. Without siphoning most of the precipitations were found at the bottoms of the wells (A), at 24 hpf when the precipitations were pushed aside using a pipette tip for a better identification of effects in embryos (B) and at 96 hpf, when the hatched larva was observed at different places within the well (C).

For subsequent procedure, all stock solutions were prepared in the turbid water with all its particles in the water column. However, for preparation of test concentration for the renewal in the wells, an excessive precipitation was avoided by allowing sedimentation of particles for approximately 3 minutes before refill with the resulting supernatant. To be absolutely clear about toxicity at the end of the test at 96 hpf, embryos which were difficult to evaluate due to remaining particles at the bottom of the wells were transferred into clear solution for the evaluation.

All tests conducted with river water were valid: No mortality was found in control treatments, while mortality in positive control was between 80 - 100% at the end of the tests.

During the test period of 96 hours, no time-dependent increase in toxicity of PTD was found: The mortality noted after 24 hours of exposure did not change during the course of the test. In Neckar River water, the PTD stock solutions aged for 4 and 8 h showed very similar dose-response relationships no matter if tested with river water during a flood or at normal water levels. Thus, the resulting LC_{50} values were determined in a similar range.

In 4 hours old PTD stock solution, only one embryo exposed to 0.5 mg/L and 1 mg/L was coagulated after 24 hours, while all embryos exposed to 2 and 4 mg/L were coagulated within

24 hours. The PTD stock solution tested in flood water proved most toxic after 4 h of aging, with an LC_{50} of 1.18 mg/L (Table 18).

The PTD stock solution aged for 8 hours was tested with both, normal Neckar River water and Neckar River flood water. The responses in zebrafish embryos were almost identical, with LC_{50} values of 1.47 and 1.39 mg/L for normal and flood Neckar River waters respectively (see Table 18). No embryo in the lower concentration (0.25 – 1 mg/L) showed any lethal effects, while all embryos exposed to 2 and 4 mg/L were coagulated within the first 24 hours.

No acute mortality could be observed for 16 h old stock solution of PTD during the test. Only one embryo was coagulated at 0.25 mg/L because the embryo was squeezed with the pipette tip while renewal of the test concentration at 24 hpf. No LC_{50} value could be determined ($LC_{50} > 4$ mg/L).

The most dominant sublethal effect seen in zebrafish embryos exposed to PTD stock solutions in Neckar River water was the accumulation of yellow-brownish materials in the tissues between the intestinal tract and the swim bladder (see asterisks in Figure 47). This effect was dose-dependent and could be observed in all tested PTD solutions aged for 4, 8 or 16 hours.

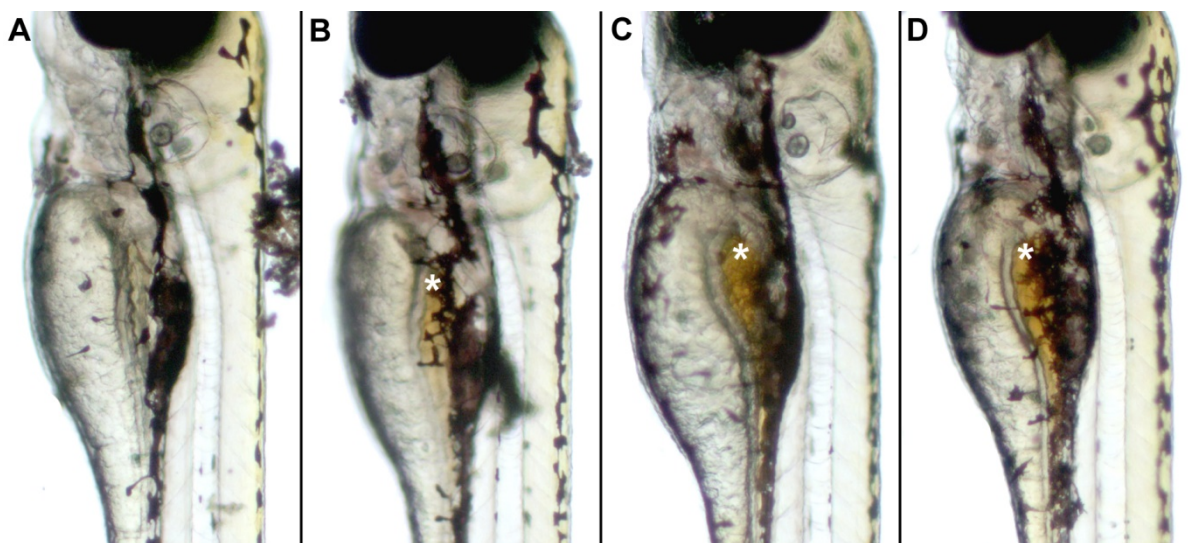


Figure 47: Zebrafish embryos exposed for 96 hours to PTD stock solutions in Neckar River flood water: Whereas no effects were seen in embryos exposed to Neckar River flood water alone (A, negative control), embryos exposed to 1 mg/L PTD aged for 8 hours (B), 2 mg/L (C) and 4 mg/L (D) PTD aged for 16 hours showed a yellow-brownish, dose-dependent accumulation in tissue between the swim bladder and the intestine tract (see asterisks). For the pictures, embryos were anesthetized in MS-222 and the precipitations were washed away as much as possible.

As held true for LC₅₀ data, EC₅₀ values were very similar and ranged between 0.57 mg/L for the PTD solution in Neckar River flood water aged for 4 h, 0.74 mg/L for PTD in normal Neckar River water and 0.53 mg/L with flood water aged for 8 h. Although no toxicity was evident with PTD stock solutions aged for 16 h, sublethal effects could be recorded and an EC₅₀ value was determined at 0.41 mg/L PTD in Neckar River flood water.

All LC₅₀ and EC₅₀ values determined at 96 hpf in river water are summarized in the following table.

Table 18: Overview of LC₅₀ and EC₅₀ values determined in FET with zebrafish embryos at 96 hpf exposed to PTD in Neckar River water. All listed LC₅₀ and EC₅₀ values were determined *via* ToxRat[®] probit analysis.

Age of PTD stock solutions in river water	LC ₅₀ (mg/L)	EC ₅₀ (mg/L)
4 hours	1.18 (flood)	0.57 (flood)
8 hours	1.47 (normal)	0.74 (normal)
	1.39 (flood)	0.53 (flood)
16 hours	> 4.00 (flood)	0.41 (flood)

6.5 Discussion

To mimic environmentally more realistic exposure scenarios in the FET, two different approaches were evolved under laboratory conditions. First, the amendment with humic acid as an artificial source of dissolved organic carbon and second, the performance of the FET in native river water sampled from a typical, anthropogenic influenced river in Germany.

The humic acid (HA) amendment was tested in 1 hour old stock solution of PTD and the concentration was set to 2 mg/L HA or 8 mg/l HA, concentrations similar to the ones found in literature. Within 24 hours of exposure, the color of the test concentrations turned from clear with a slight hint of brown to brown inside the wells, no matter if the test concentrations were HA supplemented. This clearly indicates the reactivity of PTD in the FET medium with and without the addition of HA and the formation of various products by auto-oxidation and self-coupling processes (Meyer and Fischer, 2015) as found for the standard tests with differently aged PTD solutions (Chapter V). Although the chosen HA concentrations were in the range of naturally occurring values, no strong reduction of PTD-induced toxicity in zebrafish embryos could be found. Similar results in effective dose and toxicity levels were found with and without the amendment of humic acid. No significant difference to the cumulative mortalities of zebrafish embryos in media without humic acids (Chapter V or the control run), however, the LC₅₀ value found in the standard FET (0.58 mg/L; see Chapter V) was slightly lower than the

ones determined during this experimental set-up. Nevertheless, this variation might be due to biological variances between fish egg batches.

In natural waters, the combination of fulvic and humic acids is thought to contribute mainly to the covalent binding of substances, especially organic compounds (Bollag and Myers, 1992; De Paolis and Kukkonen, 1997; Fent and Looser, 1995; Haitzer et al., 1998; Parris, 1980; Thorn et al., 1996; Weber et al., 1996). As an aromatic amine, PTD is supposed to react with humic acids in aqueous medium. Parris (1980) studied the reaction of aromatic amines with organic matter derived from soil and proposed two chemical reactions for ring-substituted anilines to humates: a fast reaction of the amino groups with the carbonyl groups of the humates and a second, slower reaction, attributed to the irreversible covalent binding. This mechanism can be applied to humates found in waters. Weber et al. (1996) and Thorn et al. (1996) investigated the reactivity for the covalent binding of aniline with Suwannee River water, unfractionated DOM samples and humic and fluvic acids isolated from Suwannee River. They found humic acid to be more reactive, however since HA contributes to a much smaller account to the DOC in Suwannee River, fluvic acids was the main component to bind aniline in the samples. Additionally, the herein used humic acids sample from the Suwannee River was shown to contain a lower estimates of carboxyl contents than the fluvic acids from the Suwannee River (Ritchie and Perdue, 2003). The applied humic acids concentrations were not able to bind the PTD molecules and the emerging self-coupling products, although it has been postulated, that humic acids or other natural organic matters may serve as a free radical scavenger (Fabrega et al., 2009; Goldstone and Voelker, 2000; Wang et al., 2001). The potential to serve as a scavenger is marginal compared to the modulation of toxicity found with the amendment of ascorbic acid.

Whereas the amendment with low (2 mg/L) and high (8 mg/L) content of Suwannee River humic acids did not significantly influence the toxicity of PTD, the performance of the FET in native river water lowered the toxicity of PTD in zebrafish embryos. It is necessary to consider the complexity of natural river water. The native water sampled during a flood, showed much higher contents of visible material in the water column and thus a much higher total organic carbon level (TOC approx. 6 times elevated). Also the dissolved organic carbon level was about twice as found in river water of a normal stream gauge (3.0 mg/L to 7.1 mg/L DOC). However, no striking difference in toxicity of the 8 hours aged PTD solution was found when comparing the LC₅₀ (96 hpf) value determined in normal river water (1.47 mg/L) to the one determined in flood river water (1.39 mg/L).

A time-dependent reduction of toxicity becomes obvious when comparing the determined LC_{50} values with the ones from the standard FETs. The LC_{50} values (96 hpf) were lowered approximately 2 times for the 4 hours aged PTD solution, 3 times for the 8 hours aged PTD solution and 5 times for the 16 hours aged PTD solutions. This clearly indicates that the molecules within the native river water needed some time to react with the PTD molecules as well as with possibly emerging products. It can be assumed, that the first 4 hours of aging (before start of exposure), the binding of the molecules to the various component of the river water, which are actually able to bind aromatic amines, was still reversible. After approximately 4 hours, the concentration of covalently and thus irreversibly bound PTD molecules to component of the river water might have increased and hence the bioavailability might have decreased correspondingly. Consequently, only the freely dissolved PTD concentration might have contributed to the toxic effects in zebrafish embryos. Several authors found a similar relationship between the bioconcentration of organic chemicals and the presence of dissolved organic matter, hypothesizing the molecule structure after binding is responsible for the reduced uptake into the aquatic organisms (e.g. Fent and Looser, 1995; Haitzer et al., 1998; Landrum et al., 1987; Leverssee et al., 1983; McCarthy and Jimenez, 1985; McCarthy, 1989; Meinelt et al., 2006; Steinberg et al., 2007; Yang et al., 2013). Landrum et al. (1987) suggested the reduced bioavailability to rise from the insufficient time for the chemical compound to dissipate from the “organic matter – chemical compound” complex. Additionally the size of the complex might influence bioavailability: The whole complex might be either too large or too polar for passing biological membranes, hence only the dissolved chemical compound is taken up (Black and McCarthy, 1988; McCarthy, 1989). This might lead to the increasing reduction of toxicity of PTD with a prolonged aging period in the river water (1 h < 4 h < <16 h).

6.6 Conclusions

In river water, the toxicity of PTD has shown to be reduced compared to the FET performed under standardized conditions according to TG 236 (OECD, 2013a), whereas the addition of humic acids of 2 and 8 mg/L did not result in a significantly reduced toxicity. Humic acids might be a good indicator for the behavior of substances in natural environment; however the complexity of aggregation, disaggregation and the formation of complexes with natural occurring organic matters cannot be construed solely from experimental data with humic acids. The laboratory tests with water collected from a typical German river with anthropogenic influences might provide an opportunity to study the behavior of aromatic substances in the aquat-

ic environment under controlled conditions. The toxicity of PTD in the river water was not completely reduced and thus not all PTD and formed reactive products have been eliminated for bioavailability by binding to dissolved organic carbon. However, results showed that approximately 4 hours of aging is needed until more complex structures with DOC might be formed.

6.7 Acknowledgements

The performed tests were conducted in collaboration with the Procter & Gamble Company, Cincinnati OH, USA. The analysis of TOC and DOC were performed at the Department of Hygiene, University of Heidelberg. The measurement of COD was done by members of staff of the sewage wastewater plant, Heidelberg, during their routine measurements.

7. Final Conclusions

The development and approval of alternative methods for the replacement of traditional animal studies became mandatory when the EU Regulation of Chemicals and their safe use - REACH (Registration, Evaluation, Authorization and Restriction of Chemical substances (EC, 2007)) came into force. The accepted suggestion for the replacement or at least refinement of the acute toxicity test with fish is the fish embryo toxicity test (FET). The increase use of embryonic stages within the chorion for the testing of chemicals and new molecular structures, such as nanomaterials, the concerns of false-negative results in the FET due to poor bioavailability of particles have risen. Additionally, some substances need special refinements and a more sophisticated exposure design to fully cover the potential toxicity. Therefore this thesis covered two different aspects. First, the question whether the chorion act as a barrier for bulky or nano-sized substances. Second, whether small modifications of the test design allow the detection of toxicity of several formed products and the appraisal of the behavior in natural waters.

The central issue of the present thesis was the clarification of a critical molecular size to cross the chorion of zebrafish embryos. As the FET is suggested to be performed not only with the zebrafish embryos, but also with the fathead minnow embryo, the basic of the uptake studies was transferred to the slightly prolonged developmental time of the fathead minnow and the structural differences of the chorion. With the application of high solutes of differently sized polyethylene glycols, the critical size for polymers to cross the chorion or embryos of younger than 24 hpf were ascertain to 4,000 Da for the fathead minnow, whereas the size of a chemical to cross the chorion of zebrafish embryos could be narrowed down to 3,000 Da. Contrarily, Creton (2004) found 3,000 Da sized dextran molecules not able to cross the chorion. However, the critical sizes found with PEGs at 24 hpf might only apply to inert, non-branched polymers and a 3-dimensional bulky molecule such as dextran might show a different uptake pattern. In both species, the severity and rate of chorion deformations decreased, representing the increasing permeability of the chorion during proceeding embryonic development. Laser scanning confocal microscopy was used to track nano-sized fluorescent spheres when applied to zebrafish and fathead minnow embryos within their chorion. Carboxylate-modified microspheres were completely blocked by the chorion of zebrafish and fathead minnows, although from the plain physical size they should have been able to be cross the chorion pores. For the uptake across the chorion and, as a second barrier, the embryonic membrane also chemical

properties of the nanoparticles are of major importance. When zebrafish embryos were exposed to plain microspheres of approximately the same size as the carboxylate-modified ones, a signal was detected within the embryos of zebrafish. Interestingly, a strong affinity to lipophilic structures was found. The main fluorescent signal was found at the chorion surface and for the microspheres able to cross the chorion also within the yolk sac. This clearly shows the uptake across the yolk syncytial layer (YSL) into the yolk and hence the overcome of the second barrier after the chorion. An exceptionally strong interaction of the carboxylate-modified microspheres with the chorion was also found for the adherends of the fathead minnow eggs, a plain, smooth area with fringed contour. The FET covers the hatched stage of embryonic fish (the eleuthero embryo approximately from 52 hpf onwards) and thus the chances of detecting a potential (embryo)toxic chemical is very high. However, interaction with structures of the chorion cannot be excluded and thus, for the testing of very bulky and highly charged substances, it might be more suitable to test with dechorionated embryos or expand the testing period, as has been suggested by the OECD (2013a). Differences in toxicity between adult fish and embryos were hitherto stated for Luviquat at 400'000 Da (Henn and Braunbeck, 2011) and other quaternary ammoniums (Léonard et al., 2005).

Since the FET is already used for the assessment of chemical safety and should be applied to a wider range of applications, the possibility of variations in the test design to address possible self-forming products in solution has been ascertained. To place a special emphasis on auto-oxidation and the formation of self-coupling product, oxidative hair dye precursors, primary intermediates, were allowed to age in solution for a certain time period before test exposure started. With this small but effective deviation from the standard protocol, the transformation of the precursors to various products, such as reactive oxygen species and reactive self-coupling products could be assessed in the FET for three hair dye precursors. Moreover, the amendment of ascorbic acid at 0.04% has been found to inhibit successfully the formation of these reactive products, resulting in a strongly reduced toxicity. Since some residues of hair dyes might be introduced un-oxidized into the environment due to misuse or accidents, a more realistic environmental aspect was transferred into the laboratory. The amendment of humic acids as a possible source of carbon did not result in a reduced toxicity. The complexity of aggregation, disaggregation and the formation of complexes with natural occurring organic matters cannot be construed solely from experimental data with humic acids. On the contrary, the performance of the FET in native river water reduced the toxicity. However, results showed that a certain time span is needed until the bioavailability of compounds might be

reduced notably depending on the kinetics of complex-formation, binding and disaggregation. When testing in more complex waters, this time should be given.

Overall, the FET standard test design can be easily modified in the laboratory to learn more about the mode of action of a reactive substance, the modifications by other substances and the toxicity. More information is still needed for possible interactions of chemicals and especially nanoparticles with the chorion. The application of electron microscopy as well as the possibility of more precise imagery with newly developed laser scanning microscopy might be promising approaches. For the quantification of substances inside the egg and embryo, research should focus on the development of methods to the extent of which they become applicable and economically reasonable. Profound knowledge of the test species and the test performance, analytically measured concentrations, a strict documentation of parameters as required by TG 236 and the evaluation of not only lethality but also of all alterations from normal development might enforce the FET as a suitable method.

References

- Adams, S.L., Zhang, T., Rawson, D.M., 2005. The effect of external medium composition on membrane water permeability of zebrafish (*Danio rerio*) embryos. *Theriogenology* 64, 1591-1602.
- Adler, S., Basketter, D., Creton, S., Pelkonen, O., van Benthem, J., Zuang, V., Andersen, K.E., Angers-Loustau, A., Aptula, A., Bal-Price, A., Benfenati, E., Bernauer, U., Bessems, J., Bois, F.Y., Boobis, A., Brandon, E., Bremer, S., Broschard, T., Casati, S., Coecke, S., Corvi, R., Cronin, M., Daston, G., Dekant, W., Felter, S., Grignard, E., Gundert-Remy, U., Heinonen, T., Kimber, I., Kleinjans, J., Komulainen, H., Kreiling, R., Kreysa, J., Leite, S.B., Loizou, G., Maxwell, G., Mazzatorta, P., Munn, S., Pfuhler, S., Phrakonkham, P., Piersma, A., Poth, A., Prieto, P., Repetto, G., Rogiers, V., Schoeters, G., Schwarz, M., Serafimova, R., Tahti, H., Testai, E., van Delft, J., van Loveren, H., Vinken, M., Worth, A., Zaldivar, J.M., 2011. Alternative (non-animal) methods for cosmetics testing: current status and future prospects-2010. *Archives of toxicology* 85, 367-485.
- Aeby, P., Sieber, T., Beck, H., Frank Gerberick, G., Goebel, C., 2009. Skin Sensitization to p-Phenylenediamine: The Diverging Roles of Oxidation and N-Acetylation for Dendritic Cell Activation and the Immune Response. *Journal of Investigative Dermatology* 129, 99-109.
- Agrawal, N.K., Juneja, C.J., Mahajan, C.L., 1978. Protective role of ascorbic acid in fishes exposed to organochlorine pollution. *Toxicology* 11, 369-375.
- Aleksic, M., Thain, E., Roger, D., Saib, O., Davies, M., Li, J., Aptula, A., Zazzeroni, R., 2009. Reactivity profiling: covalent modification of single nucleophile peptides for skin sensitization risk assessment. *Toxicol Sci* 108, 401-411.
- Aleström, P., Holter, J.L., Nourizadeh-Lillabadi, R., 2006. Zebrafish in functional genomics and aquatic biomedicine. *Trends in Biotechnology* 24, 15-21.
- Altman, M., Rieger, M.M., 1968. The function of Bandrowski's base in hair dyeing. *J. Soc. Cosmetic Chemists* 19, 141-148.
- Anguissola, S., Garry, D., Salvati, A., O'Brien, P.J., Dawson, K.A., 2014. High Content Analysis Provides Mechanistic Insights on the Pathways of Toxicity Induced by Amine-Modified Polystyrene Nanoparticles. *PLoS ONE* 9, e108025.
- Ankley, G.T., Villeneuve, D.L., 2006. The fathead minnow in aquatic toxicology: past, present and future. *Aquat Toxicol* 78, 91-102.
- Arenzana, F.J., Carvan, M.J., 3rd, Aijon, J., Sanchez-Gonzalez, R., Arevalo, R., Porteros, A., 2006. Teratogenic effects of ethanol exposure on zebrafish visual system development. *Neurotoxicol Teratol* 28, 342-348.
- Arrigoni, O., De Tullio, M.C., 2002. Ascorbic acid: much more than just an antioxidant. *Biochimica et Biophysica Acta (BBA) - General Subjects* 1569, 1-9.
- Arukwe, A., Goksoyr, A., 2003. Eggshell and egg yolk proteins in fish: hepatic proteins for the next generation: oogenetic, population, and evolutionary implications of endocrine disruption. *Comp Hepatol* 2, 4.
- Asharani, P.V., Yi Lian, W., Zhiyuan, G., Suresh, V., 2008. Toxicity of silver nanoparticles in zebrafish models. *Nanotechnology* 19, 255102.

- Augustine-Rauch, K., Zhang, C.X., Panzica-Kelly, J.M., 2010. In vitro developmental toxicology assays: A review of the state of the science of rodent and zebrafish whole embryo culture and embryonic stem cell assays. *Birth Defects Res C Embryo Today* 90, 87-98.
- Bachmann, J., 2002. Entwicklung und Erprobung eines Teratogenitäts-Screening Testes mit Embryonen des Zebrafisch *Danio rerio*,
- Bai, W., Zhang, Z., Tian, W., He, X., Ma, Y., Zhao, Y., Chai, Z., 2009. Toxicity of zinc oxide nanoparticles to zebrafish embryo: a physicochemical study of toxicity mechanism. *Journal of Nanoparticle Research* 12, 1645-1654.
- Balaguer, A., Chisvert, A., Salvador, A., 2008. Environmentally friendly LC for the simultaneous determination of ascorbic acid and its derivatives in skin-whitening cosmetics. *J Sep Sci* 31, 229-236.
- Basketter, D.A., Clewell, H., Kimber, I., Rossi, A., Blaauboer, B., Burrier, R., Daneshian, M., Eskes, C., Goldberg, A., Hasiwa, N., Hoffmann, S., Jaworska, J., Knudsen, T.B., Landsiedel, R., Leist, M., Locke, P., Maxwell, G., McKim, J., McVey, E.A., Ouedraogo, G., Patlewicz, G., Pelkonen, O., Roggen, E., Rovida, C., Ruhdel, I., Schwarz, M., Schepky, A., Schoeters, G., Skinner, N., Trentz, K., Turner, M., Vanparys, P., Yager, J., Zurlo, J., Hartung, T., 2012. A roadmap for the development of alternative (non-animal) methods for systemic toxicity testing - t4 report. *Altex* 29, 3-91.
- Baumann, L., Ros, A., Rehberger, K., Neuhauss, S.C., Segner, H., 2016. Thyroid disruption in zebrafish (*Danio rerio*) larvae: Different molecular response patterns lead to impaired eye development and visual functions. *Aquat Toxicol* 172, 44-55.
- Baun, A., Hartmann, N.B., Grieger, K., Kusk, K.O., 2008. Ecotoxicity of engineered nanoparticles to aquatic invertebrates: a brief review and recommendations for future toxicity testing. *Ecotoxicology* 17, 387-395.
- Beattie, J.H., Pascoe, D., 1978. Cadmium uptake by rainbow trout, *Salmo gairdneri* eggs and alevins. *Journal of Fish Biology* 13, 631-637.
- Beekhuijzen, M., de Koning, C., Flores-Guillén, M.-E., de Vries-Buitenweg, S., Tobor-Kaplon, M., van de Waart, B., Emmen, H., 2015. From cutting edge to guideline: A first step in harmonization of the zebrafish embryotoxicity test (ZET) by describing the most optimal test conditions and morphology scoring system. *Reproductive Toxicology* 56, 64-76.
- Belanger, S.E., Balon, E.K., Rawlings, J.M., 2010. Saltatory ontogeny of fishes and sensitive early life stages for ecotoxicology tests. *Aquatic Toxicology* 97, 88-95.
- Belanger, S.E., Rawlings, J.M., Carr, G.J., 2013. Use of fish embryo toxicity tests for the prediction of acute fish toxicity to chemicals. *Environ Toxicol Chem* 32, 1768-1783.
- Bendich, A., Machlin, L.J., Scandurra, O., Burton, G.W., Wayner, D.D.M., 1986. The antioxidant role of vitamin C. *Advances in Free Radical Biology & Medicine* 2, 419-444.
- Bendich, A., 1990. Antioxidant Micronutrients and Immune Responses. *Annals of the New York Academy of Sciences* 587, 168-180.
- Bexiga, M.G., Kelly, C., Dawson, K.A., Simpson, J.C., 2014. RNAi-mediated inhibition of apoptosis fails to prevent cationic nanoparticle-induced cell death in cultured cells. *Nanomedicine (Lond)* 9, 1651-1664.

- Bharali, M.K., Dutta, K., 2009. Hepatic histopathological abnormalities in rats treated topically with Para-Phenylene Diamine (PPD). *Journal of Pharmacology and Toxicology* 4, 221-228.
- Bindhumol, V., Chitra, K.C., Mathur, P.P., 2003. Bisphenol A induces reactive oxygen species generation in the liver of male rats. *Toxicology* 188, 117-124.
- Black, M.C., McCarthy, J.F., 1988. Dissolved organic macromolecules reduce the uptake of hydrophobic organic contaminants by the gills of rainbow trout (*Salmo gairdneri*). *Environmental Toxicology and Chemistry* 7, 593-600.
- Blader, P., Strahle, U., 1998. Ethanol impairs migration of the prechordal plate in the zebrafish embryo. *Developmental biology* 201, 185-201.
- Blömeke, B., Pot, L.M., Coenraads, P.J., Hennen, J., Kock, M., Goebel, C., 2015. Cross-elicitation responses to 2-methoxymethyl-p-phenylenediamine under hair dye use conditions in p-phenylenediamine-allergic individuals. *The British journal of dermatology* 172, 976-980.
- Bodannes, R.S., Chan, P.C., 1979. Ascorbic acid as a scavenger of singlet oxygen. *FEBS Letters* 105, 195-196.
- Bodewein, L., Schmelter, F., Di Fiore, S., Hollert, H., Fischer, R., Fenske, M., 2016. Differences in toxicity of anionic and cationic PAMAM and PPI dendrimers in zebrafish embryos and cancer cell lines. *Toxicology and Applied Pharmacology* 305, 83-92.
- Böhler, S., 2012. The fathead minnow embryo as a model for the development of alternative testing methods in ecotoxicology, Diploma thesis, Fakultät für Biowissenschaften, Heidelberg.
- Böhme, S., Stark, H.-J., Reemtsma, T., Kuhnel, D., 2015a. Effect propagation after silver nanoparticle exposure in zebrafish (*Danio rerio*) embryos: a correlation to internal concentration and distribution patterns. *Environmental Science: Nano*.
- Böhme, S., Stark, H.J., Kuhnel, D., Reemtsma, T., 2015b. Exploring LA-ICP-MS as a quantitative imaging technique to study nanoparticle uptake in *Daphnia magna* and zebrafish (*Danio rerio*) embryos. *Analytical and bioanalytical chemistry* 407, 5477-5485.
- Bollag, J.-M., Myers, C., 1992. Detoxification of aquatic and terrestrial sites through binding of pollutants to humic substances. *Science of the Total Environment* 117, 357-366.
- Bonsignorio, D., Perego, L., Del Giacco, L., Cotelli, F., 1996. Structure and macromolecular composition of the zebrafish egg chorion. *Zygote* 4, 101-108.
- Bour, A., Mouchet, F., Silvestre, J., Gauthier, L., Pinelli, E., 2015. Environmentally relevant approaches to assess nanoparticles ecotoxicity: A review. *Journal of hazardous materials* 283, 764-777.
- Brannen, K.C., Panzica-Kelly, J.M., Danberry, T.L., Augustine-Rauch, K.A., 2010. Development of a zebrafish embryo teratogenicity assay and quantitative prediction model. *Birth Defects Res B Dev Reprod Toxicol* 89, 66-77.
- Braunbeck, T., Boettcher, M., Hollert, H., Kosmehl, T., Lammer, E., Leist, E., Rudolf, M., Seitz, N., 2005. Towards an alternative for the acute fish LC(50) test in chemical assessment: the fish embryo toxicity test goes multi-species - an update. *Altex* 22, 87-102.

- Braunbeck, T., Kais, B., Lammer, E., Otte, J., Schneider, K., Stengel, D., Strecker, R., 2014. The fish embryo test (FET): origin, applications, and future. *Environ Sci Pollut Res*, 1-15.
- Brion, F., Tyler, C.R., Palazzi, X., Laillet, B., Porcher, J.M., Garric, J., Flammarion, P., 2004. Impacts of 17beta-estradiol, including environmentally relevant concentrations, on reproduction after exposure during embryo-larval-, juvenile- and adult-life stages in zebrafish (*Danio rerio*). *Aquat Toxicol* 68, 193-217.
- Brion, F., Le Page, Y., Piccini, B., Cardoso, O., Tong, S.K., Chung, B.C., Kah, O., 2012. Screening estrogenic activities of chemicals or mixtures in vivo using transgenic (cyp19a1b-GFP) zebrafish embryos. *PLoS One* 7, e36069.
- Brox, S., Ritter, A.P., Kuster, E., Reemtsma, T., 2014. Influence of the perivitelline space on the quantification of internal concentrations of chemicals in eggs of zebrafish embryos (*Danio rerio*). *Aquat Toxicol* 157, 134-140.
- Brun, N.R., Lenz, M., Wehrli, B., Fent, K., 2014. Comparative effects of zinc oxide nanoparticles and dissolved zinc on zebrafish embryos and eleuthero-embryos: Importance of zinc ions. *Science of The Total Environment* 476-477, 657-666.
- Burden, N., Maynard, S.K., Weltje, L., Wheeler, J.R., 2016. The utility of QSARs in predicting acute fish toxicity of pesticide metabolites: A retrospective validation approach. *Regulatory Toxicology and Pharmacology* 80, 241-246.
- Busquet, F., Strecker, R., Rawlings, J.M., Belanger, S.E., Braunbeck, T., Carr, G.J., Cenijn, P., Fochtman, P., Gourmelon, A., Hübler, N., Kleensang, A., Knöbel, M., Kussatz, C., Legler, J., Lillcrap, A., Martínez-Jerónimo, F., Polleichtner, C., Rzodeczko, H., Salinas, E., Schneider, K.E., Scholz, S., van den Brandhof, E.-J., van der Ven, L.T.M., Walter-Rohde, S., Weigt, S., Witters, H., Halder, M., 2014. OECD validation study to assess intra- and inter-laboratory reproducibility of the zebrafish embryo toxicity test for acute aquatic toxicity testing. *Regulatory Toxicology and Pharmacology* 69, 496-511.
- Carpita, N., Sabularse, D., Montezinos, D., Delmer, D.P., 1979. Determination of the pore size of cell walls of living plant cells. *Science* 205, 1144-1147.
- Chakraborty, C., Hsu, C.H., Wen, Z.H., Lin, C.S., Agoramoorthy, G., 2009. Zebrafish: a complete animal model for in vivo drug discovery and development. *Curr Drug Metab* 10, 116-124.
- Chen, J., Sun, H., Ruan, S., Wang, Y., Shen, S., Xu, W., He, Q., Gao, H., 2015a. *In vitro* and *in vivo* toxicology of bare and PEGylated fluorescent carbonaceous nanodots in mice and zebrafish: the potential relationship with autophagy. *RSC Advances* 5, 38547-38557.
- Chen, Y., Hu, X., Sun, J., Zhou, Q., 2015b. Specific nanotoxicity of graphene oxide during zebrafish embryogenesis. *Nanotoxicology*, 1-11.
- Chiu, L.L., Cunningham, L.L., Raible, D.W., Rubel, E.W., Ou, H.C., 2008. Using the zebrafish lateral line to screen for ototoxicity. *J Assoc Res Otolaryngol* 9, 178-190.
- Chung, K.-T., Murdock, C.A., Stevens Jr, S.E., Li, Y.-S., Wei, C.-I., Huang, T.-S., Chou, M.W., 1995. Mutagenicity and toxicity studies of p-phenylenediamine and its derivatives. *Toxicology Letters* 81, 23-32.

- Clemente, Z., Castro, V.L.S.S., Moura, M.A.M., Jonsson, C.M., Fraceto, L.F., 2014. Toxicity assessment of TiO₂ nanoparticles in zebrafish embryos under different exposure conditions. *Aquatic Toxicology* 147, 129-139.
- Coenraads, P.J., Vogel, T.A., Blomeke, B., Goebel, C., Roggeband, R., Schuttelaar, M.A., 2016. The role of the antioxidant ascorbic acid in the elicitation of contact allergic reactions to p-phenylenediamine. *Contact Dermatitis*.
- Cohen, A., Shmoish, M., Levi, L., Cheruti, U., Levavi-Sivan, B., Lubzens, E., 2008. Alterations in micro-ribonucleic acid expression profiles reveal a novel pathway for estrogen regulation. *Endocrinology* 149, 1687-1696.
- Cohen, S.P., LaChappelle, A.R., Walker, B.S., Lassiter, C.S., 2014. Modulation of estrogen causes disruption of craniofacial chondrogenesis in *Danio rerio*. *Aquat Toxicol* 152, 113-120.
- Cooper, W.J., Zika, R.G., 1983. Photochemical formation of hydrogen peroxide in surface and ground waters exposed to sunlight. *Science(Washington)* 220, 711-712.
- Corbett, J., 1972. Autoxidation of p-phenylenediamine. *J. Sot. Cosmet. Chem* 23, 683-693.
- Corbett, J.F., 1973. Hair Colouring. *Review of Progress in Coloration and Related Topics* 4, 3-7.
- Corbett, J.F., 1976. The chemistry of hair-care products. *Journal of the Society of Dyers and Colourists* 92, 285-303.
- Corbett, J.F., 1999. An historical review of the use of dye precursors in the formulation of commercial oxidation hair dyes. *Dyes and Pigments* 41, 127-136.
- Creton, R., 2004. The calcium pump of the endoplasmic reticulum plays a role in midline signaling during early zebrafish development. *Brain Res Dev Brain Res* 151, 33-41.
- Cunningham, S., Brennan-Fournet, M.E., Ledwith, D., Byrnes, L., Joshi, L., 2013. Effect of nanoparticle stabilization and physicochemical properties on exposure outcome: Acute toxicity of silver nanoparticle preparations in zebrafish (*Danio rerio*). *Environmental Science & Technology* 47, 3883-3892.
- da França, S.A., Dario, M.F., Esteves, V.B., Baby, A.R., Velasco, M.V.R., 2015. Types of hair dye and their mechanisms of action. *Cosmetics* 2, 110-126.
- Dale, A.L., Casman, E.A., Lowry, G.V., Lead, J.R., Viparelli, E., Baalousha, M., 2015. Modeling nanomaterial environmental fate in aquatic systems. *Environmental Science & Technology* 49, 2587-2593.
- Datta, M., Kaviraj, A., 2003. Ascorbic acid supplementation of diet for reduction of deltamethrin induced stress in freshwater catfish *Clarias gariepinus*. *Chemosphere* 53, 883-888.
- de Esch, C., Sliker, R., Wolterbeek, A., Woutersen, R., de Groot, D., 2012. Zebrafish as potential model for developmental neurotoxicity testing: a mini review. *Neurotoxicol Teratol* 34, 545-553.
- De Paolis, F., Kukkonen, J., 1997. Binding of organic pollutants to humic and fulvic acids: influence of pH and the structure of humic material. *Chemosphere* 34, 1693-1704.
- Del Giacco, L., Diani, S., Cotelli, F., 2000. Identification and spatial distribution of the mRNA encoding an egg envelope component of the Cyprinid zebrafish, *Danio rerio*, homologous to the mammalian ZP3 (ZPC). *Dev Genes Evol* 210, 41-46.

- Della Torre, C., Bergami, E., Salvati, A., Faleri, C., Cirino, P., Dawson, K.A., Corsi, I., 2014. Accumulation and embryotoxicity of polystyrene nanoparticles at early stage of development of sea urchin embryos *Paracentrotus lividus*. *Environmental Science & Technology* 48, 12302-12311.
- Dennerly, P.A., 2007. Effects of oxidative stress on embryonic development. *Birth Defects Research Part C: Embryo Today: Reviews* 81, 155-162.
- Denny, J.S., 1987. Guidelines for the culture of fathead minnows '*Pimephales Promelas*' for use in toxicity tests. EPA - Environmental research laboratory, Duluth, MN.
- Devlin, E., Brammer, J., Puyear, R., McKim, J., 1996. Prehatching development of the fathead minnow *Pimephales promelas* Rafinesque, in: *Development*, O.o.R.a. (Ed.). U.S. Environmental Protection Agency, Washington, DC.
- Devlin, E.W., 2006. Acute toxicity, uptake and histopathology of aqueous methyl mercury to fathead minnow embryos. *Ecotoxicology* 15, 97-110.
- Diepgen, T.L., Naldi, L., Bruze, M., Cazzaniga, S., Schuttelaar, M.L., Elsner, P., Goncalo, M., Ofenloch, R., Svensson, A., 2016. Prevalence of contact allergy to p-Phenylenediamine in the European general population. *J Invest Dermatol* 136, 409-415.
- DIN, 1980, German Standard Methods for Examination of Water, Waste Water and Sludge; Summary Action and Material Characteristic Parameters (Group H); Determination of the Chemical Oxygen Demand (COD) in the Range over 15 mg/l (H41), DIN 38409-41:1980-12
- DIN, 1997, Guidelines for the Determination of total organic carbon (TOC) and dissolved organic carbon (DOC); German version EN 1484-1997, DIN EN 1484-1997.
- DIN, 2001. German standard methods for the examination of water, waste water and sludge – Subanimal testing (group T) – Part 6: Toxicity to fish. Determination of the non-acute-poisonous effect of waste water to fish eggs by dilution limits (T 6). DIN 38415-6; German Standardization Organization.
- Documentation, M.V., 2012. Polyethylene glycol in: [MAK Value Documentation (Ed.), The MAK-Collection for Occupational Health and Safety. Wiley-VCH Verlag GmbH & Co. KGaA, pp. 248–270.
- Dolinsky, M., Wilson, C., 1968. p-Phenylenediamine in hair dyes. *J. Soc. Cosmetic Chemists* 19, 411-422.
- Dooley, K., Zon, L.I., 2000. Zebrafish: a model system for the study of human disease. *Curr Opin Genet Dev* 10, 252-256.
- Draelos, Z., 2005. *Hair Care - An Illustrated Dermatologic Handbook*, UK, Taylor & Francis.
- Ducharme, N.A., Reif, D.M., Gustafsson, J.-A., Bondesson, M., 2015. Comparison of toxicity values across zebrafish early life stages and mammalian studies: Implications for chemical testing. *Reproductive Toxicology* 55, 3-10.
- Eaton, J.G., McKim, J.M., Holcombe, G.W., 1978. Metal toxicity to embryos and larvae of seven freshwater fish species - I. cadmium. *Bulletin of Environmental Contamination and Toxicology* 19, 95-103.
- Eaton, R.C., Farley, R.D., 1974. Spawning cycle and egg production of zebrafish, *Brachydanio rerio*, in the laboratory. *Copeia*, 195-204.

- EC, 2007. Regulation(EC) No 1907/2006 of the European Parliament and of the Council of 18 December 2006 concerning the Registration, Evaluation, Authorisation and Restriction of Chemicals (REACH), establishing a European Chemicals Agency, amending Directive 1999/45/EC and repealing Council Regulation (EEC) No 793/93 and Commission Regulation (EC) No 1488/94 as well as Council Directive 76/769/EEC and Commission Directives 91/155/EEC, 93/67/EEC, 93/105/EC and 2000/21/EC, (EC) No 1907/200,
- EC, 2009. Regulation (EC) No 1107/2009 of the European Parliament and of the Council of 21 October 2009 concerning the placing of plant protection products on the market and repealing Council Directives 79/117/EEC and 91/414/EEC, (EC) No 1107/2009,
- ECVAM, E., 2014. EURL ECVAM recommendation on the zebrafish embryo acute toxicity test method (zfet) for acute aquatic toxicity testing. European Union Reference Laboratory for Alternatives to Animal Testing.
- ECVAM, E., 2015. EURL ECVAM status report on the development, validation and regulatory acceptance of alternative methods and approaches. European Union Reference Laboratory for Alternatives to Animal Testing.
- EFSA, 2006. Opinion of the Scientific Panel on Food Additives, Flavourings, Processing Aids and Materials in Contact with Food on a request from the Commission related to an application on the use of polyethylene glycol (PEG) as a film coating agent for use in food supplement products. the EFSA Journal 414, 1-22.
- El-Gendy, K.S., Aly, N.M., Mahmoud, F.H., Kenawy, A., El-Sebae, A.K.H., 2010. The role of vitamin C as antioxidant in protection of oxidative stress induced by imidacloprid. Food and Chemical Toxicology 48, 215-221.
- Elsalini, O.A., Rohr, K.B., 2003. Phenylthiourea disrupts thyroid function in developing zebrafish. Dev Genes Evol 212, 593-598.
- EPA, U.S., <http://cfpub.epa.gov/ecotox/>. U.S. EPA.
- EU, 1976. Council directive of 27 July 1976 on the approximation of the laws of the Member States relating to cosmetic products (76/768/EEC), 76/768/EEC, Official Journal of the European Communities,
- EU, 2009. Regulation (EC) No. 1223/2009 of the European parliament and of the council of 30 November 2009 on cosmetic products, 1223/2009, Official Journal of the European Union,
- EU, 2010. Directive 2010/63/EU of the European parliament and of the council of 22 September 2010 on the protection of animals used for scientific purposes., 2010/63/EU, Amtsblatt der Europäischen Union.
- Fabrega, J., Fawcett, S.R., Renshaw, J.C., Lead, J.R., 2009. Silver nanoparticle impact on bacterial growth: effect of pH, concentration, and organic matter. Environ Sci Technol 43, 7285-7290.
- Fako, V.E., Furgeson, D.Y., 2009. Zebrafish as a correlative and predictive model for assessing biomaterial nanotoxicity. Advanced drug delivery reviews 61, 478-486.
- Fede, A., Grannas, A.M., 2015. Photochemical Production of Singlet Oxygen from Dissolved Organic Matter in Ice. Environ Sci Technol 49, 12808-12815.

- Felix, L.C., Ortega, V.A., Ede, J.D., Goss, G.G., 2013. Physicochemical characteristics of polymer-coated metal-oxide nanoparticles and their toxicological effects on zebrafish (*Danio rerio*) development. *Environmental Science & Technology* 47, 6589-6596.
- Fent, K., Looser, P.W., 1995. Bioaccumulation and bioavailability of tributyltin chloride: Influence of pH and humic acids. *Water Research* 29, 1631-1637.
- Fent, K., 2001. Fish cell lines as versatile tools in ecotoxicology: assessment of cytotoxicity, cytochrome P4501A induction potential and estrogenic activity of chemicals and environmental samples. *Toxicology in Vitro* 15, 477-488.
- Fent, K., Weisbrod, C.J., Wirth-Heller, A., Pielers, U., 2010. Assessment of uptake and toxicity of fluorescent silica nanoparticles in zebrafish (*Danio rerio*) early life stages. *Aquat Toxicol* 100, 218-228.
- Foged, C., Brodin, B., Frokjaer, S., Sundblad, A., 2005. Particle size and surface charge affect particle uptake by human dendritic cells in an in vitro model. *International Journal of Pharmaceutics* 298, 315-322.
- Frankel, E.N., 1996. The Second International Food Data Base Conference: Food Composition Research - The Broader Context. Antioxidants in lipid foods and their impact on food quality. *Food Chemistry* 57, 51-55.
- Froehlicher, M., Liedtke, A., Groh, K.J., Neuhauss, S.C., Segner, H., Eggen, R.I., 2009. Zebrafish (*Danio rerio*) neuromast: promising biological endpoint linking developmental and toxicological studies. *Aquat Toxicol* 95, 307-319.
- Fröhlich, E., 2012. The role of surface charge in cellular uptake and cytotoxicity of medical nanoparticles. *Int J Nanomedicine* 7, 5577-5591.
- Gale, W.F., Buynak, G.L., 1982. Fecundity and Spawning Frequency of the Fathead Minnow—A Fractional Spawner. *Transactions of the American Fisheries Society* 111, 35-40.
- Gao, J., Powers, K., Wang, Y., Zhou, H., Roberts, S.M., Moudgil, B.M., Koopman, B., Barber, D.S., 2012. Influence of Suwannee River humic acid on particle properties and toxicity of silver nanoparticles. *Chemosphere* 89, 96-101.
- Garcia-Käufer, M., Gartiser, S., Hafner, C., Schiwy, S., Keiter, S., Grundemann, C., Hollert, H., 2015. Genotoxic and teratogenic effect of freshwater sediment samples from the Rhine and Elbe River (Germany) in zebrafish embryo using a multi-endpoint testing strategy. *Environmental science and pollution research international* 22, 16341-16357.
- Gauron, C., Rampon, C., Bouzaffour, M., Ipendey, E., Teillon, J., Volovitch, M., Vríz, S., 2013. Sustained production of ROS triggers compensatory proliferation and is required for regeneration to proceed. *Scientific Reports* 3, 2084.
- Gellert, G., Heinrichsdorff, J., 2001. Effect of age on the susceptibility of zebrafish eggs to industrial wastewater. *Water Res* 35, 3754-3757.
- George, S., Lin, S., Ji, Z., Thomas, C.R., Li, L., Mecklenburg, M., Meng, H., Wang, X., Zhang, H., Xia, T., Hohman, J.N., Lin, S., Zink, J.I., Weiss, P.S., Nel, A.E., 2012. Surface Defects on Plate-Shaped Silver Nanoparticles Contribute to Its Hazard Potential in a Fish Gill Cell Line and Zebrafish Embryos. *ACS Nano* 6, 3745-3759.
- Goebel, C., Troutman, J., Hennen, J., Rothe, H., Schlatter, H., Gerberick, G.F., Blomeke, B., 2014. Introduction of a methoxymethyl side chain into p-phenylenediamine attenuates

- its sensitizing potency and reduces the risk of allergy induction. *Toxicol Appl Pharmacol* 274, 480-487.
- Goldstone, J.V., Voelker, B.M., 2000. Chemistry of Superoxide Radical in Seawater: CDOM Associated Sink of Superoxide in Coastal Waters. *Environmental Science & Technology* 34, 1043-1048.
- Goux, A., Pratt, D., Dunsch, L., 2007. The Reaction Mechanism of p-Toluenediamine Anodic Oxidation: An In Situ ESR-UV/Vis/NIR Spectroelectrochemical Study. *ChemPhysChem* 8, 2101-2106.
- Grillo, R., Rosa, A.H., Fraceto, L.F., 2015. Engineered nanoparticles and organic matter: a review of the state-of-the-art. *Chemosphere* 119, 608-619.
- Guha, B., Khuda-Bukhsh, A.R., 2002. Efficacy of vitamin-C (l-ascorbic acid) in reducing genotoxicity in fish (*Oreochromis mossambicus*) induced by ethyl methane sulphonate. *Chemosphere* 47, 49-56.
- Guraya, S.S., 1986. The cell and molecular biology of fish oogenesis, 1986/01/01 ed.
- Gustafson, A.L., Stedman, D.B., Ball, J., Hillegass, J.M., Flood, A., Zhang, C.X., Panzica-Kelly, J., Cao, J., Coburn, A., Enright, B.P., Tornesi, M.B., Hetheridge, M., Augustine-Rauch, K.A., 2012. Inter-laboratory assessment of a harmonized zebrafish developmental toxicology assay - progress report on phase I. *Reprod Toxicol* 33, 155-164.
- Häfeli, N., Schwartz, P., Burkhardt-Holm, P., 2011. Embryotoxic and genotoxic potential of sewage system biofilm and river sediment in the catchment area of a sewage treatment plant in Switzerland. *Ecotoxicol Environ Saf* 74, 1271-1279.
- Hahn, M.E., McArthur, A.G., Karchner, S.I., Franks, D.G., Jenny, M.J., Timme-Laragy, A.R., Stegeman, J.J., Woodin, B.R., Cipriano, M.J., Linney, E., 2014. The Transcriptional Response to Oxidative Stress during Vertebrate Development: Effects of *tert*-Butylhydroquinone and 2,3,7,8-Tetrachlorodibenzo-*p*-Dioxin. *PLoS ONE* 9, e113158.
- Haitzer, M., Höss, S., Traunspurger, W., Steinberg, C., 1998. Effects of dissolved organic matter (DOM) on the bioconcentration of organic chemicals in aquatic organisms—a review—. *Chemosphere* 37, 1335-1362.
- Halder, M., Busquet, F., Strecker, R., Rawlings, J.M., Belanger, S.E., T., B., Carr, G.J., Gourmelon, A., Lillicrap, A.D., Walter-Rhode, S., Cenijn, P., Fochtman, P., Hübler, N., Kussatz, C., Legler, J., Martinez-Jerónimo, F., Polleichtner, C., Rzodeczko, H., Salinas, E., Schneider, K.E., Scholz, S., Weigt, S., Van den Brandhof, E.-J., van der Ven, L.T.M., Witters, H.E., 2012. Final results of the OECD validation study on the transferability, intra- and inter-laboratory reproducibility of the zebrafish embryo toxicity test, in: Halder, M. (Ed.), SETAC World, Berlin.
- Hamilton-Buchanan, F., 1822. An account of the fishes found in the river Ganges and its branches. With a volume of plates in royal quarto. Printed for A. Constable and company; [etc., etc.], Edinburgh.
- Harper, B., Thomas, D., Chikkagoudar, S., Baker, N., Tang, K., Heredia-Langner, A., Lins, R., Harper, S., 2015. Comparative hazard analysis and toxicological modeling of diverse nanomaterials using the embryonic zebrafish (EZ) metric of toxicity. *Journal of Nanoparticle Research* 17, 1-12.
- Hart, N.H., Donovan, M., 1983. Fine structure of the chorion and site of sperm entry in the egg of *Brachydanio*. *Journal of Experimental Zoology* 227, 277-296.

- Heilingötter, R., 1968. Die Funktion der Bandrowski'schen Base bei der Haarfärbung. J. Soc. Cosmetic Chemists 19, 823-825.
- Henn, K., 2011. Limits of the fish embryo toxicity test with *Danio rerio* as an alternative to the acute fish toxicity test., Dissertation, Combined Faculties for the Natural Sciences and for Mathematics, Heidelberg.
- Henn, K., Braunbeck, T., 2011. Dechoriation as a tool to improve the fish embryo toxicity test (FET) with the zebrafish (*Danio rerio*). Comp Biochem Physiol C Toxicol Pharmacol 153, 91-98.
- Hill, A.J., Teraoka, H., Heideman, W., Peterson, R.E., 2005. Zebrafish as a Model Vertebrate for Investigating Chemical Toxicity. Toxicol. Sci. 86, 6-19.
- Hisaoka, K.K., 1958. Microscopic studies of the teleost chorion. Transactions of the American Microbiological Society 77, 3.
- Hisaoka, K.K., Battle, H.I., 1958. The normal developmental stages of the zebrafish, *brachydanio rerio* (Hamilton-Buchanan). Journal of Morphology 102, 311-327.
- Hofmann, A.W., 1863. Jahr. Chem. 42.
- Hohl, M., Schopfer, P., 1991. Water Relations of Growing Maize Coleoptiles : Comparison between Mannitol and Polyethylene Glycol 6000 as External Osmotica for Adjusting Turgor Pressure. Plant Physiology 95, 716-722.
- Hua, J., Vijver, M.G., Ahmad, F., Richardson, M.K., Peijnenburg, W.J.G.M., 2014. Toxicity of different-sized copper nano- and submicron particles and their shed copper ions to zebrafish embryos. Environmental Toxicology and Chemistry 33, 1774-1782.
- Huang, G.-m., Tian, X.-f., Fang, X.-d., Ji, F.-j., 2016. Waterborne exposure to bisphenol F causes thyroid endocrine disruption in zebrafish larvae. Chemosphere 147, 188-194.
- Hutchinson, T.H., Wheeler, J.R., Gourmelon, A., Burden, N., 2016. Promoting the 3Rs to enhance the OECD fish toxicity testing framework. Regulatory Toxicology and Pharmacology 76, 231-233.
- IHSS, I.H.S.S., IHSS - Natural Organic Matter Research, June 2016
- Invitrogen, 2004. MP 05001 - Working with FluoSpheres® Fluorescent Microspheres, Molecular Probes™ - Invitrogen detection technologies.
- Invitrogen, 2005. MP 05000 - FluoSpheres® Fluorescent Microspheres, Molecular Probes™ - Invitrogen detection technologies.
- ISO, 2007, Water quality -- Determination of the acute toxicity of waste water to zebrafish eggs (*Danio rerio*), ISO 15088:2007
- ISO, 2012, Water quality - Determination of the chemical oxygen demand 6060:1989.
- ISO, I.S., 1998, Water quality -- Determination of biochemical oxygen demand after 5 days (BOD 5) -- Dilution and seeding method, ISO 5815:1989.
- Ito, T., Ando, H., Suzuki, T., Ogura, T., Hotta, K., Imamura, Y., Yamaguchi, Y., Handa, H., 2010. Identification of a primary target of thalidomide teratogenicity. Science 327, 1345-1350.
- Jenkinson, C., Jenkins, R.E., Maggs, J.L., Kitteringham, N.R., Aleksic, M., Park, B.K., Naisbitt, D.J., 2009. A Mechanistic Investigation into the Irreversible Protein Binding

- and Antigenicity of p-Phenylenediamine. *Chemical Research in Toxicology* 22, 1172-1180.
- Jensen, K.M., Korte, J.J., Kahl, M.D., Pasha, M.S., Ankley, G.T., 2001. Aspects of basic reproductive biology and endocrinology in the fathead minnow (*Pimephales promelas*). *Comparative Biochemistry and Physiology Part C: Toxicology & Pharmacology* 128, 127-141.
- Kahru, A., Dubourguier, H.-C., 2010. From ecotoxicology to nanoecotoxicology. *Toxicology* 269, 105-119.
- Kais, B., Schneider, K.E., Keiter, S., Henn, K., Ackermann, C., Braunbeck, T., 2013. DMSO modifies the permeability of the zebrafish (*Danio rerio*) chorion-Implications for the fish embryo test (FET). *Aquatic Toxicology* 140–141, 229-238.
- Kashiwada, S., 2006. Distribution of nanoparticles in the see-through medaka (*Oryzias latipes*). *Environ Health Perspect* 114, 1697-1702.
- Kawakubo, Y., Merk, H.F., Al Masaoudi, T., Sieben, S., Blömeke, B., 2000. N-Acetylation of paraphenylenediamine in human skin and keratinocytes. *Journal of Pharmacology and Experimental Therapeutics* 292, 150-155.
- Keth, A., 2012. Die Permeabilität des Chorions des Zebraäbrblings (*Danio rerio*) gegenüber Anilinen und Phenolen, Bachelor thesis, Fakultät für Biowissenschaften, Heidelberg.
- Kettler, K., Veltman, K., van de Meent, D., van Wezel, A., Hendriks, A.J., 2014. Cellular uptake of nanoparticles as determined by particle properties, experimental conditions, and cell type. *Environmental Toxicology and Chemistry* 33, 481-492.
- Kim, D.H., Sun, Y., Yun, S., Kim, B., Hwang, C.N., Nelson, B., Lee, S.H., 2004. Mechanical property characterization of the zebrafish embryo chorion. *Conf Proc IEEE Eng Med Biol Soc* 7, 5061-5064.
- Kim, K.-T., Tanguay, R.L., 2014. The role of chorion on toxicity of silver nanoparticles in the embryonic zebrafish assay. *Environmental Health and Toxicology* 29, e2014021.
- Kim, M.S., Louis, K.M., Pedersen, J.A., Hamers, R.J., Peterson, R.E., Heideman, W., 2014. Using citrate-functionalized TiO₂ nanoparticles to study the effect of particle size on zebrafish embryo toxicity. *Analyst* 139, 964-972.
- Kimmel, C.B., Ballard, W.W., Kimmel, S.R., Ullmann, B., Schilling, T.F., 1995. Stages of embryonic development of the zebrafish. *Dev Dyn* 203, 253-310.
- King-Heiden, T.C., Dengler, E., Kao, W.J., Heideman, W., Peterson, R.E., 2007. Developmental toxicity of low generation PAMAM dendrimers in zebrafish. *Toxicol Appl Pharmacol* 225, 70-79.
- Klüver, N., König, M., Ortmann, J., Massei, R., Paschke, A., Kühne, R., Scholz, S., 2015. Fish embryo toxicity test: identification of compounds with weak toxicity and analysis of behavioral effects to improve prediction of acute toxicity for neurotoxic compounds. *Environ Sci Technol* 49, 7002-7011.
- Knobel, M., Busser, F.J., Rico-Rico, A., Kramer, N.I., Hermens, J.L., Hafner, C., Tanneberger, K., Schirmer, K., Scholz, S., 2012. Predicting adult fish acute lethality with the zebrafish embryo: relevance of test duration, endpoints, compound properties, and exposure concentration analysis. *Environ Sci Technol* 46, 9690-9700.

- Koelmans, A., Besseling, E., Shim, W., 2015. Nanoplastics in the Aquatic Environment. Critical Review, in: Bergmann, M., Gutow, L., Klages, M. (Eds.), Marine Anthropogenic Litter. Springer International Publishing, pp. 325-340.
- Kosmehl, T., Hallare, A.V., Reifferscheid, G., Manz, W., Braunbeck, T., Hollert, H., 2006. A novel contact assay for testing genotoxicity of chemicals and whole sediments in zebrafish embryos. *Environmental Toxicology and Chemistry* 25, 2097-2106.
- Kovřížných Jevgenij, A., Sotníková, R., Zeljenková, D., Rollerová, E., Szabová, E., Wimmerová, S., 2013. Acute toxicity of 31 different nanoparticles to zebrafish (*Danio rerio*) tested in adulthood and in early life stages – comparative study, *Interdisciplinary Toxicology*, p. 67.
- Küster, E., 2005. Cholin- and carboxylesterase activities in developing zebrafish embryos (*Danio rerio*) and their potential use for insecticide hazard assessment. *Aquatic Toxicology* 75, 76-85.
- Laale, H.W., 1977. Biology and use of zebrafish *Brachydanio rerio* in fisheries research. A literature review. *Journal of Fish Biology* 10, 121-173.
- Laban, G., Nies, L.F., Turco, R.F., Bickham, J.W., Sepúlveda, M.S., 2010. The effects of silver nanoparticles on fathead minnow (*Pimephales promelas*) embryos. *Ecotoxicology* 19, 185-195.
- Lammer, E., Carr, G.J., Wendler, K., Rawlings, J.M., Belanger, S.E., Braunbeck, T., 2009. Is the fish embryo toxicity test (FET) with the zebrafish (*Danio rerio*) a potential alternative for the fish acute toxicity test? *Comparative Biochemistry and Physiology Part C: Toxicology & Pharmacology* 149, 196-209.
- Landrum, P.F., Nihart, S.R., Eadie, B.J., Herche, L.R., 1987. Reduction in bioavailability of organic contaminants to the amphipod *pontoporeia hoyi* by dissolved organic matter of sediment interstitial waters. *Environmental Toxicology and Chemistry* 6, 11-20.
- Lange, M., Gebauer, W., Markl, J., Nagel, R., 1995. Comparison of testing acute toxicity on embryo of zebrafish, *Brachydanio rerio* and RTG-2 cytotoxicity as possible alternatives to the acute fish test. *Chemosphere* 30, 2087-2102.
- Lee, K.J., Nallathamby, P.D., Browning, L.M., Osgood, C.J., Xu, X.H., 2007. *In vivo* imaging of transport and biocompatibility of single silver nanoparticles in early development of zebrafish embryos. *ACS Nano* 1, 133-143.
- Lee, K.J., Browning, L.M., Nallathamby, P.D., Desai, T., Cherukuri, P.K., Xu, X.H., 2012. *In vivo* quantitative study of sized-dependent transport and toxicity of single silver nanoparticles using zebrafish embryos. *Chem Res Toxicol* 25, 1029-1046.
- Legradi, J., el Abdellaoui, N., van Pomeran, M., Legler, J., 2015. Comparability of behavioural assays using zebrafish larvae to assess neurotoxicity. *Environmental science and pollution research international* 22, 16277-16289.
- Leino, R.L., Jensen, K.M., Ankley, G.T., 2005. Gonadal histology and characteristic histopathology associated with endocrine disruption in the adult fathead minnow (*Pimephales promelas*). *Environ Toxicol Pharmacol* 19, 85-98.
- Lele, Z., Krone, P.H., 1996. The zebrafish as a model system in developmental, toxicological and transgenic research. *Biotechnology Advances* 14, 57-72.

- Léonard, M., Vanpoucke, M., Petit-Poulsen, V., Porcher, J.M., 2005. Evaluation of the Fish Embryo Test as a Potential Alternative to the Standard Acute Fish Toxicity Test OECD 203, International Symposium on Toxicology Assessment, Skathios, Greece.
- Leversee, G.J., Landrum, P.F., Giesy, J.P., Fannin, T., 1983. Humic Acids Reduce Bioaccumulation of Some Polycyclic Aromatic Hydrocarbons. *Canadian Journal of Fisheries and Aquatic Sciences* 40, s63-s69.
- Lilienblum, W., Dekant, W., Foth, H., Gebel, T., Hengstler, J.G., Kahl, R., Kramer, P.J., Schweinfurth, H., Wollin, K.M., 2008. Alternative methods to safety studies in experimental animals: role in the risk assessment of chemicals under the new European Chemicals Legislation (REACH). *Archives of toxicology* 82, 211-236.
- Lillicrap, A.D., 2010. The use of zebrafish embryos as an alternative approach for ecotoxicity testing, Master Thesis, Exeter.
- Lin, S., Zhao, Y., Nel, A.E., Lin, S., 2013. Zebrafish: An *in vivo* model for nano EHS studies. *Small* 9, 1608-1618.
- Lindstrom-Seppa, P., Korytko, P.J., Hahn, M.E., Stegeman, J.J., 1994. Uptake of waterborne 3,3',4,4'-tetrachlorobiphenyl and organ and cell-specific induction of cytochrome P4501A in adult and larval fathead minnow *Pimephales promelas*. *Aquatic Toxicology* 28, 147-167.
- Linney, E., Upchurch, L., Donerly, S., 2004. Zebrafish as a neurotoxicological model. *Neurotoxicology and Teratology* 26, 709-718.
- Liu, Y., Li, W., Lao, F., Liu, Y., Wang, L., Bai, R., Zhao, Y., Chen, C., 2011. Intracellular dynamics of cationic and anionic polystyrene nanoparticles without direct interaction with mitotic spindle and chromosomes. *Biomaterials* 32, 8291-8303.
- Loucks, E.J., Schwend, T., Ahlgren, S.C., 2007. Molecular changes associated with teratogen-induced cyclopia. *Birth defects research. Part A, Clinical and molecular teratology* 79, 642-651.
- LUBW, L.f.U., Messungen und Naturschutz Baden-Württemberg, 2007. Der Neckar. Das Land und sein Fluss, in: LUBW (Ed.), 1 ed. Verlag regionalkultur, Heidelberg, Karlsruhe.
- LUBW, L.f.U., Messungen und Naturschutz Baden-Württemberg, Fließgewässerbeschaffenheit - Aktuelle Messdaten- Neckar, <http://www.lubw.baden-wuerttemberg.de/servlet/is/78686/>, 23.05.2013
- LUBW, L.f.U., Messungen und Naturschutz Baden-Württemberg., Hochwasservorhersagezentrale Baden-Württemberg, <http://www.hvz.lubw.baden-wuerttemberg.de/>, 03.06.2013
- Lundqvist, M., Stigler, J., Elia, G., Lynch, I., Cedervall, T., Dawson, K.A., 2008. Nanoparticle size and surface properties determine the protein corona with possible implications for biological impacts. *Proc Natl Acad Sci U S A* 105, 14265-14270.
- Maes, J., Verlooy, L., Buenafe, O.E., de Witte, P.A.M., Esguerra, C.V., Crawford, A.D., 2012. Evaluation of 14 Organic Solvents and Carriers for Screening Applications in Zebrafish Embryos and Larvae. *PLoS ONE* 7, e43850.
- Manabe, M., Tatarazako, N., Kinoshita, M., 2011. Uptake, excretion and toxicity of nano-sized latex particles on medaka (*Oryzias latipes*) embryos and larvae. *Aquat Toxicol* 105, 576-581.

- Manner, H.W., Dewese, C.M., 1974. Early embryology of the fathead minnow *Pimephales promelas rafinesque*. *The Anatomical Record* 180, 99-109.
- Manner, H.W., Muehleman, C., 1976. LAS inhibition of diffusion and uptake of tritiated uridine during teleost embryogenesis. *Environmental Biology of Fishes* 1, 81-84.
- Manner, H.W., Vancura, M., Muehleman, C., 1977. The Ultrastructure of the Chorion of the Fathead Minnow, *Pimephales promelas*. *Transactions of the American Fisheries Society* 106, 110 - 114.
- Mattsson, K., Hansson, L.A., Cedervall, T., 2015. Nano-plastics in the aquatic environment. *Environmental Science: Processes & Impacts* 17, 1712-1721.
- McCarthy, J.F., Jimenez, B.D., 1985. Effect of humic substances on the bioaccumulation of organic contaminants by aquatic organisms. *Organic Geochemistry* 8, 141.
- McCarthy, J.F., 1989. Bioavailability and toxicity of metals and hydrophobic organic contaminants. *Aquatic Humic Substances: Influence on Fate and Treatment of Pollutants*. American Chemical Society, Washington DC. 1989. p 263-277, 3 fig, 56 ref.
- McDonald, S., Bishop, A.G., Prenzler, P.D., Robards, K., 2004. Analytical chemistry of freshwater humic substances. *Analytica Chimica Acta* 527, 105-124.
- McGrath, P., Li, C.Q., 2008. Zebrafish: a predictive model for assessing drug-induced toxicity. *Drug Discov Today* 13, 394-401.
- McKim, J.M., 1977. Evaluation of Tests with Early Life Stages of Fish for Predicting Long-Term Toxicity. *Journal of the Fisheries Research Board of Canada* 34, 1148-1154.
- Meinelt, T., Burnison, B.K., Playle, R., Pietrock, M., Wienke, A., Steinberg, C.E.W., 2006. Dissolved organic matter (DOM) modulates the cadmium accumulation in zebrafish (*Danio rerio*) embryos, in: V., L.-I.f.G.u.B.I.i.F.B.e. (Ed.), *IGB Annual Report*. Leibniz-Institut für Gewässerökologie und Binnenfischerei (IGB), Berlin, pp. 121-130.
- Meredith, A.N., Harper, B., Harper, S.L., 2016. The influence of size on the toxicity of an encapsulated pesticide: a comparison of micron-and nano-sized capsules. *Environment international* 86, 68-74.
- Meyer, A., Fischer, K., 2015. Oxidative transformation processes and products of parphenylenediamine (PPD) and para-toluenediamine (PTD)—a review. *Environmental Sciences Europe* 27, 11.
- Michel, B.E., Kaufmann, M.R., 1973. The osmotic potential of polyethylene glycol 6000. *Plant Physiol* 51, 914-916.
- Michibata, H., 1981. Uptake and distribution of cadmium in the egg of the teleost, *Oryzias latipes*. *Journal of Fish Biology* 19, 691-696.
- Mohd Omar, F., Abdul Aziz, H., Stoll, S., 2014. Aggregation and disaggregation of ZnO nanoparticles: Influence of pH and adsorption of Suwannee River humic acid. *Science of The Total Environment* 468-469, 195-201.
- Mold, D.E., Kim, I.F., Tsai, C.M., Lee, D., Chang, C.Y., Huang, R.C., 2001. Cluster of genes encoding the major egg envelope protein of zebrafish. *Mol Reprod Dev* 58, 4-14.
- Mold, D.E., Dinitz, A.E., Sambandan, D.R., 2009. Regulation of Zebrafish Zona Pellucida Gene Activity in Developing Oocytes. *Biology of Reproduction* 81, 101-110.

- Money, N.P., Webster, J., 1988. Cell wall permeability and its relationship to spore release in *Achlya intricata*. *Experimental Mycology* 12, 169-179.
- Money, N.P., 1989. Osmotic Pressure of Aqueous Polyethylene Glycols: Relationship between Molecular Weight and Vapor Pressure Deficit. *Plant Physiology* 91, 766-769.
- Morel, O.J., Christie, R.M., 2011. Current trends in the chemistry of permanent hair dyeing. *Chem Rev* 111, 2537-2561.
- Mulisch, M., Welsch, U., 2015. *Romeis-Mikroskopische Technik*. Springer-Verlag.
- Murata, K., 2003. Blocks to Polyspermy in Fish: A Brief Review, 32nd Symposium. Cooperative Program in Natural Resources (UJNR), Davis and Santa Barbara, California U.S.A.
- Nagel, R., 2002. DarT: The embryo test with the zebrafish *Danio rerio* - a general model in ecotoxicology and toxicology. *Altex* 19 Suppl 1, 38-48.
- Nel, A., Zhao, Y., Mädler, L., 2013. Environmental health and safety considerations for nanotechnology. *Accounts of Chemical Research* 46, 605-606.
- Nel, A.E., Parak, W.J., Chan, W.C.W., Xia, T., Hersam, M.C., Brinker, C.J., Zink, J.I., Pinkerton, K.E., Baer, D.R., Weiss, P.S., 2015. Where are we heading in nanotechnology environmental health and safety and materials characterization? *ACS Nano* 9, 5627-5630.
- Nishimura, Y., Murakami, S., Ashikawa, Y., Sasagawa, S., Umemoto, N., Shimada, Y., Tanaka, T., 2015. Zebrafish as a systems toxicology model for developmental neurotoxicity testing. *Congenital Anomalies* 55, 1-16.
- Nishimura, Y., Inoue, A., Sasagawa, S., Koiwa, J., Kawaguchi, K., Kawase, R., Maruyama, T., Kim, S., Tanaka, T., 2016. Using zebrafish in systems toxicology for developmental toxicity testing. *Congenital Anomalies* 56, 18-27.
- Nohynek, G.J., Fautz, R., Benech-Kieffer, F., Toutain, H., 2004. Toxicity and human health risk of hair dyes. *Food and Chemical Toxicology* 42, 517-543.
- Nohynek, G.J., Duche, D., Garrigues, A., Meunier, P.-A., Toutain, H., Leclaire, J., 2005. Under the skin: Biotransformation of para-aminophenol and para-phenylenediamine in reconstructed human epidermis and human hepatocytes. *Toxicology Letters* 158, 196-212.
- Nohynek, G.J., Antignac, E., Re, T., Toutain, H., 2010. Safety assessment of personal care products/cosmetics and their ingredients. *Toxicology and Applied Pharmacology* 243, 239-259.
- O'Brien, P.J., 1985. Free-radical-mediated DNA binding. *Environ Health Perspect* 64, 219-232.
- OECD, 1992. OECD Guideline for the Testing of Chemicals. Section 2. Effects on Biotic Systems; Test No. 203: Acute Toxicity for Fish, 203, Organization for Economic Cooperation and Development, Paris, France.
- OECD, 2006. OECD Guideline for the testing of chemicals: " Draft proposal for a new guideline Fish Embryo Toxicity (FET) Test" (1st version), Organization for Economic Cooperation and Development, Paris, France.
- OECD, 2012. *Fish Toxicity Testing Framework*. OECD Publishing.

- OECD, 2013a. OECD Guideline for the Testing of Chemicals. Section 2. Effects on Biotic Systems; Test No. 236: Fish Embryo Acute Toxicity (FET) Test, 236, Organization for Economic Cooperation and Development, Paris, France.
- OECD, 2013b. OECD Guideline for the Testing of Chemicals. Section 2. Effects on Biotic Systems; Test No. 210: Fish, Early-life Stage Toxicity Test. Organization for Economic Cooperation and Development, Paris, France.
- Osborne, O.J., Johnston, B.D., Moger, J., Balousha, M., Lead, J.R., Kudoh, T., Tyler, C.R., 2013. Effects of particle size and coating on nanoscale Ag and TiO₂ exposure in zebrafish (*Danio rerio*) embryos. *Nanotoxicology* 7, 1315-1324.
- Osterauer, R., Faßbender, C., Braunbeck, T., Köhler, H.-R., 2011. Genotoxicity of platinum in embryos of zebrafish (*Danio rerio*) and ramshorn snail (*Marisa cornuarietis*). *Science of The Total Environment* 409, 2114-2119.
- Otte, J.C., Schmidt, A.D., Hollert, H., Braunbeck, T., 2010. Spatio-temporal development of CYP1 activity in early life-stages of zebrafish (*Danio rerio*). *Aquat Toxicol* 100, 38-50.
- Ozoh, P.T.E., 1980. Effects of reversible incubations of zebrafish eggs in copper and lead ions with or without shell membranes. *Bulletin of Environmental Contamination and Toxicology* 24, 270-275.
- P&G, 2015. Hair Color - Research Update, in: Kenneally, D., Cunningham, H. (Eds.). P&G Beauty Science.
- Padilla, S., Hunter, D.L., Padnos, B., Frady, S., MacPhail, R.C., 2011. Assessing locomotor activity in larval zebrafish: Influence of extrinsic and intrinsic variables. *Neurotoxicol Teratol* 33, 624-630.
- Panzica-Kelly, J.M., Zhang, C.X., Danberry, T.L., Flood, A., DeLan, J.W., Brannen, K.C., Augustine-Rauch, K.A., 2010. Morphological score assignment guidelines for the dechorionated zebrafish teratogenicity assay. *Birth Defects Research Part B: Developmental and Reproductive Toxicology* 89, 382-395.
- Parng, C., Seng, W.L., Semino, C., McGrath, P., 2002. Zebrafish: a preclinical model for drug screening. *Assay Drug Dev Technol* 1, 41-48.
- Parng, C., Roy, N.M., Ton, C., Lin, Y., McGrath, P., 2007. Neurotoxicity assessment using zebrafish. *Journal of Pharmacological and Toxicological Methods* 55, 103-112.
- Parris, G.E., 1980. Covalent binding of aromatic amines to humates. 1. Reactions with carbonyls and quinones. *Environmental Science & Technology* 14, 1099-1106.
- Paskova, V., Hilscherova, K., Blaha, L., 2011. Teratogenicity and embryotoxicity in aquatic organisms after pesticide exposure and the role of oxidative stress. *Rev Environ Contam Toxicol* 211, 25-61.
- Pelka, K.E., Henn, K., Keck, A., Sapel, B., Braunbeck, T., Size does matter – determination of the critical molecular size for the uptake of chemicals across the chorion of zebrafish (*Danio rerio*) embryos. *Aquatic Toxicology*.
- Peterson, R.T., Nass, R., Boyd, W.A., Freedman, J.H., Dong, K., Narahashi, T., 2008. Use of non-mammalian alternative models for neurotoxicological study. *Neurotoxicology* 29, 546-555.
- Peterson, R.T., MacRae, C.A., 2012. Systematic approaches to toxicology in the zebrafish. *Annu Rev Pharmacol Toxicol* 52, 433-453.

- Picardo, M., Zompetta, C., Marchese, C., De Luca, C., Faggioni, A., Schmidt, R.J., Santucci, B., 1992. Paraphenylenediamine, a contact allergen, induces oxidative stress and ICAM-1 expression in human keratinocytes. *The British journal of dermatology* 126, 450-455.
- Pickering, Q.H., Lazorchak, J.M., Winks, K.L., 1996. Subchronic sensitivity of one-, four-, and seven-day-old fathead minnow (*Pimephales promelas*) larvae to five toxicants. *Environmental Toxicology and Chemistry* 15, 353-359.
- Pot, L.M., Scheitza, S.M., Coenraads, P.-J., Blömeke, B., 2013. Penetration and haptentation of p-phenylenediamine. *Contact Dermatitis* 68, 193-207.
- Power, D.M., Llewellyn, L., Faustino, M., Nowell, M.A., Björnsson, B.T., Einarsdottir, I.E., Canario, A.V.M., Sweeney, G.E., 2001. Thyroid hormones in growth and development of fish. *Comparative Biochemistry and Physiology Part C: Toxicology & Pharmacology* 130, 447-459.
- Praetorius, A., Tufenkji, N., Goss, K.-U., Scheringer, M., von der Kammer, F., Elimelech, M., 2014. The road to nowhere: equilibrium partition coefficients for nanoparticles. *Environmental Science: Nano* 1, 317-323.
- Pullela, P.K., Chiku, T., Carvan, M.J., 3rd, Sem, D.S., 2006. Fluorescence-based detection of thiols *in vitro* and *in vivo* using dithiol probes. *Anal Biochem* 352, 265-273.
- Randebrook, R., 1964. Neue erkenntnisse über den morphologischen aufbau des menschlichen haares. *Journal of the Society of Cosmetic Chemists* 15, 691-706.
- Rasband, W.S., 1997-2014. ImageJ. U. S. National Institutes of Health, Bethesda, Maryland, USA, <http://imagej.nih.gov/ij/>.
- Raschke, T., Koop, U., Dusing, H.J., Filbry, A., Sauermann, K., Jaspers, S., Wenck, H., Wittern, K.P., 2004. Topical activity of ascorbic acid: from *in vitro* optimization to *in vivo* efficacy. *Skin pharmacology and physiology* 17, 200-206.
- Ratte, H.T., Hammers-Wirtz, M., 2003a. Evaluation of the Existing Data Base from the Fish Embryo Test. Umweltbundesamt FKZ: 363 01 062.
- Ratte, T., Hammers-Wirtz, M., 2003b. Evaluation of the Existing Data Base from the Fish Embryo Test, in: Agency), U.G.E. (Ed.). UBA, Dessau.
- Rawson, D.M., Zhang, T., Kalicharan, D., Jongebloed, W.L., 2000. Field emission scanning electron microscopy and transmission electron microscopy studies of the chorion, plasma membrane and syncytial layers of the gastrula-stage embryo of the zebrafish *Brachydanio rerio*: a consideration of the structural and functional relationships with respect to cryoprotectant penetration. *Aquaculture Research* 31, 325-336.
- Reimers, M.J., La Du, J.K., Periera, C.B., Giovanini, J., Tanguay, R.L., 2006. Ethanol-dependent toxicity in zebrafish is partially attenuated by antioxidants. *Neurotoxicology and Teratology* 28, 497-508.
- Ritchie, J.D., Perdue, E.M., 2003. Proton-binding study of standard and reference fulvic acids, humic acids, and natural organic matter. *Geochimica et Cosmochimica Acta* 67, 85-96.
- Robbins, C.R., 2012. Chemical Composition of Different Hair Types, Chemical and Physical Behavior of Human Hair. Springer Berlin Heidelberg, Berlin, Heidelberg, pp. 105-176.

- Roex, E.W.M., de Vries, E., van Gestel, C.A.M., 2002. Sensitivity of the zebrafish (*Danio rerio*) early life stage test for compounds with different modes of action. *Environmental Pollution* 120, 355-362.
- Rowe, V., Wolf, M., 1982. Polyethylene glycols, in: GD, C. (Ed.), *Industrial Hygiene and Toxicology*. Wiley & Sons, New York, pp. 3844-3852, 3902, 3904-3905.
- Rubinstein, A.L., 2006. Zebrafish assays for drug toxicity screening. *Expert Opin Drug Metab Toxicol* 2, 231-240.
- Ruenraroengsak, P., Tetley, T.D., 2015. Differential bioreactivity of neutral, cationic and anionic polystyrene nanoparticles with cells from the human alveolar compartment: robust response of alveolar type 1 epithelial cells. *Particle and Fibre Toxicology* 12, 19.
- Russel, W.M.S., Burch, R.L., 1959. *The Principles of Humane Experimental Techniques*. Methuen, London, UK.
- Sachse, A., Henrion, R., Gelbrecht, J., Steinberg, C.E.W., 2005. Classification of dissolved organic carbon (DOC) in river systems: Influence of catchment characteristics and autochthonous processes. *Organic Geochemistry* 36, 923-935.
- Sano, K., Inohaya, K., Kawaguchi, M., Yoshizaki, N., Iuchi, I., Yasumasu, S., 2008. Purification and characterization of zebrafish hatching enzyme – an evolutionary aspect of the mechanism of egg envelope digestion. *FEBS Journal* 275, 5934-5946.
- Savolainen, K., Alenius, H., Norppa, H., Pyökkänen, L., Tuomi, T., Kasper, G., 2010. Risk assessment of engineered nanomaterials and nanotechnologies—A review. *Toxicology* 269, 92-104.
- SCCP, S.C.o.C.P., 2006. Opinion on p-Phenylenediamine, SCCP, Scientific Committee on Consumer Products,
- SCCP, S.C.o.C.P., 2007. Opinion of the SCCP on toluene-2,5-diamine, SCCP, Scientific Committee on Consumer Products,
- SCCS, S.C.o.C.S., 2013. Opinion on 2-methoxy-methyl-p-phenylenediamine, SCCS, Scientific Committee on Consumer Safety,
- SCCS, S.C.o.C.S., 2016. Notes of Guidance for Testing of Cosmetic Ingredients and Their Safety Evaluation by the SCCS - 9th revision, 1564/15, SCCS, Scientific Committee on Consumer Safety,
- Schiller, V., Wichmann, A., Kriehuber, R., Muth-Kohne, E., Giesy, J.P., Hecker, M., Fenske, M., 2013. Studying the effects of genistein on gene expression of fish embryos as an alternative testing approach for endocrine disruption. *Comp Biochem Physiol C Toxicol Pharmacol* 157, 41-53.
- Schirmer, K., Tanneberger, K., Kramer, N.I., Volker, D., Scholz, S., Hafner, C., Lee, L.E., Bols, N.C., Hermens, J.L., 2008. Developing a list of reference chemicals for testing alternatives to whole fish toxicity tests. *Aquat Toxicol* 90, 128-137.
- Schmitt, E.A., Dowling, J.E., 1994. Early eye morphogenesis in the zebrafish, *Brachydanio rerio*. *The Journal of comparative neurology* 344, 532-542.
- Scholz, S., Fischer, S., Gundel, U., Kuster, E., Luckenbach, T., Voelker, D., 2008. The zebrafish embryo model in environmental risk assessment--applications beyond acute toxicity testing. *Environmental science and pollution research international* 15, 394-404.

- Scholz, S., Sela, E., Blaha, L., Braunbeck, T., Galay-Burgos, M., García-Franco, M., Guinea, J., Klüver, N., Schirmer, K., Tanneberger, K., Tobor-Kaplon, M., Witters, H., Belanger, S., Benfenati, E., Creton, S., Cronin, M.T.D., Eggen, R.I.L., Embry, M., Ekman, D., Gourmelon, A., Halder, M., Hardy, B., Hartung, T., Hubesch, B., Jungmann, D., Lampi, M.A., Lee, L., Léonard, M., Küster, E., Lillicrap, A., Luckenbach, T., Murk, A.J., Navas, J.M., Peijnenburg, W., Repetto, G., Salinas, E., Schüürmann, G., Spielmann, H., Tollefsen, K.E., Walter-Rohde, S., Whale, G., Wheeler, J.R., Winter, M.J., 2013. A European perspective on alternatives to animal testing for environmental hazard identification and risk assessment. *Regulatory Toxicology and Pharmacology* 67, 506-530.
- Schulte, C., Nagel, R., 1994. Testing acute toxicity in the embryo of zebrafish, *Brachydanio rerio*, as an alternative to the acute fish test - preliminary results. *ATLA* 22, 12-19.
- Schulte, C., 1997. Entwicklung und Validierung einer Methode zur Ermittlung der Toxizität von Chemikalien gegenüber Embryonen von *Brachydanio rerio*, *Biology*,
- Segner, H., 1998. Fish cell lines as a tool in aquatic toxicology. *EXS* 86, 1-38.
- Segner, H., 2004. Cytotoxicity assays with fish cells as an alternative to the acute lethality test with fish. *Altern Lab Anim* 32, 375-382.
- Selderslaghs, I.W., Van Rompay, A.R., De Coen, W., Witters, H.E., 2009. Development of a screening assay to identify teratogenic and embryotoxic chemicals using the zebrafish embryo. *Reprod Toxicol* 28, 308-320.
- Sessa, A.K., White, R., Houvras, Y., Burke, C., Pugach, E., Baker, B., Gilbert, R., Thomas Look, A., Zon, L.I., 2008. The effect of a depth gradient on the mating behavior, oviposition site preference, and embryo production in the zebrafish, *Danio rerio*. *Zebrafish* 5, 335-339.
- Shaw, B.J., Handy, R.D., 2011. Physiological effects of nanoparticles on fish: A comparison of nanometals versus metal ions. *Environment International* 37, 1083-1097.
- Sheftel, V.O., 2000. *Indirect Food Additives and Polymers: Migration and Toxicology* American Chemical Society.
- Sipes, N.S., Padilla, S., Knudsen, T.B., 2011. Zebrafish—As an integrative model for twenty-first century toxicity testing. *Birth Defects Research Part C: Embryo Today: Reviews* 93, 256-267.
- Sneddon, L.U., 2009. Pain perception in fish: indicators and endpoints. *ILAR J* 50, 338-342.
- Spence, R., Gerlach, G., Lawrence, C., Smith, C., 2008. The behaviour and ecology of the zebrafish, *Danio rerio*. *Biological Reviews* 83, 13-34.
- Spengler, J., Bracher, M., 1990. Toxicological tests and health risk assessment of oxidative hair dye mixtures. *Cosmetics & Toiletries* 105, 67-76.
- Spitsbergen, J.M., Kent, M.L., 2003. The State of the Art of the Zebrafish Model for Toxicology and Toxicologic Pathology Research--Advantages and Current Limitations. *Toxicol Pathol* 31, 62-87.
- Steinberg, C.E.W., Höss, S., Kloas, W., Lutz, I., Meinelt, T., Pflugmacher, S., Wiegand, C., 2004. Hormonelike effects of humic substances on fish, amphibians, and invertebrates. *Environmental Toxicology* 19, 409-411.
- Steinberg, C.E.W., Meinelt, T., Timofeyev, M.A., Bittner, M., Menzel, R., 2007. Humic substances - Part 2: Interactions with organisms. *Environ Sci Pollut Res* 15, 128-135.

- Steuter, A.A., Mozafar, A., Goodin, J.R., 1981. Water Potential of Aqueous Polyethylene Glycol. *Plant Physiology* 67, 64-67.
- Storm, G., Belliot, S.O., Daemen, T., Lasic, D.D., 1995. Surface modification of nanoparticles to oppose uptake by the mononuclear phagocyte system. *Advanced drug delivery reviews* 17, 31-48.
- Stouthart, X.J.H.X., Haans, J.L.M., Lock, R.A.C., Bonga, S.E.W., 1996. Effects of water pH on copper toxicity to early life stages of the common carp (*Cyprinus carpio*). *Environmental Toxicology and Chemistry* 15, 376-383.
- Strähle, U., Scholz, S., Geisler, R., Greiner, P., Hollert, H., Rastegar, S., Schumacher, A., Selderslaghs, I., Weiss, C., Witters, H., Braunbeck, T., 2012. Zebrafish embryos as an alternative to animal experiments--a commentary on the definition of the onset of protected life stages in animal welfare regulations. *Reprod Toxicol* 33, 128-132.
- Syberg, K., Hansen, S.F., 2016. Environmental risk assessment of chemicals and nanomaterials - The best foundation for regulatory decision-making? *Science of The Total Environment* 541, 784-794.
- Thienpont, B., Tingaud-Sequeira, A., Prats, E., Barata, C., Babin, P.J., Raldúa, D., 2011. Zebrafish Eleutheroembryos Provide a Suitable Vertebrate Model for Screening Chemicals that Impair Thyroid Hormone Synthesis. *Environmental Science & Technology* 45, 7525-7532.
- Thomas, J.D., 1997. The role of dissolved organic matter, particularly free amino acids and humic substances, in freshwater ecosystems. *Freshwater Biology* 38, 1-36.
- Thomas, T., Thomas, K., Sadrieh, N., Savage, N., Adair, P., Bronaugh, R., 2006. Research strategies for safety evaluation of nanomaterials, part VII: Evaluating consumer exposure to nanoscale materials. *Toxicol Sci* 91, 14-19.
- Thorn, K.A., Pettigrew, P.J., Goldenberg, W.S., Weber, E.J., 1996. Covalent Binding of Aniline to Humic Substances. 2. ¹⁵N NMR Studies of Nucleophilic Addition Reactions. *Environmental Science & Technology* 30, 2764-2775.
- Tierney, K.B., 2011. Behavioural assessments of neurotoxic effects and neurodegeneration in zebrafish. *Biochim Biophys Acta* 1812, 381-389.
- Ton, C., Parng, C., 2005. The use of zebrafish for assessing ototoxic and otoprotective agents. *Hearing Research* 208, 79-88.
- Ton, C., Lin, Y., Willett, C., 2006. Zebrafish as a model for developmental neurotoxicity testing. *Birth defects research. Part A, Clinical and molecular teratology* 76, 553-567.
- Treuel, L., Jiang, X., Nienhaus, G.U., 2013. New views on cellular uptake and trafficking of manufactured nanoparticles. *Journal of The Royal Society Interface* 10.
- US EPA, U.S.E.P.A., 2006. Histopathology guidelines for the fathead minnow, *Pimephales promelas*, 21-day reproduction assay.,
- Van Leeuwen, C.J., Griffioen, P.S., Vergouw, W.H.A., Maas-Diepeveen, J.L., 1985. Differences in susceptibility of early life stages of rainbow trout (*Salmo gairdneri*) to environmental pollutants. *Aquatic Toxicology* 7, 59-78.
- Vaughan, P.P., Blough, N.V., 1998. Photochemical Formation of Hydroxyl Radical by Constituents of Natural Waters. *Environmental Science & Technology* 32, 2947-2953.

- Volz, D.C., Hipszer, R.A., Leet, J.K., Raftery, T.D., 2015. Leveraging Embryonic Zebrafish To Prioritize ToxCast Testing. *Environmental Science & Technology Letters* 2, 171-176.
- Wagner, M., Scherer, C., Alvarez-Muñoz, D., Brennholt, N., Bourrain, X., Buchinger, S., Fries, E., Grosbois, C., Klasmeier, J., Marti, T., 2014. Microplastics in freshwater ecosystems: what we know and what we need to know. *Environ Sci Eur*.
- Wang, F., Bexiga, M.G., Anguissola, S., Boya, P., Simpson, J.C., Salvati, A., Dawson, K.A., 2013. Time resolved study of cell death mechanisms induced by amine-modified polystyrene nanoparticles. *Nanoscale* 5, 10868-10876.
- Wang, G.S., Liao, C.H., Wu, F.J., 2001. Photodegradation of humic acids in the presence of hydrogen peroxide. *Chemosphere* 42, 379-387.
- Wang, H., Gong, Z., 1999. Characterization of two zebrafish cDNA clones encoding egg envelope proteins ZP2 and ZP3. *Biochimica et Biophysica Acta (BBA) - Gene Structure and Expression* 1446, 156-160.
- Wang, T., Bai, J., Jiang, X., Nienhaus, G.U., 2012. Cellular Uptake of Nanoparticles by Membrane Penetration: A Study Combining Confocal Microscopy with FTIR Spectroelectrochemistry. *ACS Nano* 6, 1251-1259.
- Weber, E.J., Spidle, D.L., Thorn, K.A., 1996. Covalent Binding of Aniline to Humic Substances. 1. Kinetic Studies. *Environmental Science & Technology* 30, 2755-2763.
- Weigt, S., Huebler, N., Strecker, R., Braunbeck, T., Broschard, T.H., 2011. Zebrafish (*Danio rerio*) embryos as a model for testing proteratogens. *Toxicology* 281, 25-36.
- Weigt, S., Huebler, N., Strecker, R., Braunbeck, T., Broschard, T.H., 2012. Developmental effects of coumarin and the anticoagulant coumarin derivative warfarin on zebrafish (*Danio rerio*) embryos. *Reproductive Toxicology* 33, 133-141.
- Weil, M., Meißner, T., Busch, W., Springer, A., Kühnel, D., Schulz, R., Duis, K., 2015. The oxidized state of the nanocomposite Carbo-Iron[®] causes no adverse effects on growth, survival and differential gene expression in zebrafish. *Science of The Total Environment* 530, 198-208.
- Westerfield, M., 2000. The zebrafish book. A guide for the laboratory use of zebrafish (*Danio rerio*). 4th ed. Univ. of Oregon Press, Eugene.
- White, J.M., Kullavanijaya, P., Duangdeeden, I., Zazzeroni, R., Gilmour, N.J., Basketter, D.A., McFadden, J.P., 2006. p-Phenylenediamine allergy: the role of Bandrowski's base. *Clin Exp Allergy* 36, 1289-1293.
- Wolf, R., Andersen, T., Hessen, D.O., Hylland, K., 2016. The influence of DOC and UVR on the genomic integrity of *Daphnia magna*. *Functional Ecology*, n/a-n/a.
- www.Fahrrad-Tour.de, Neckarradweg, http://www.fahrrad-tour.de/Neckar/Karte/Bilder/UebersichtNeckar_01.gif, 24.05.2013
- Yang, L., Ho, N.Y., Alshut, R., Legradi, J., Weiss, C., Reischl, M., Mikut, R., Liebel, U., Müller, F., Strähle, U., 2009. Zebrafish embryos as models for embryotoxic and teratological effects of chemicals. *Reproductive Toxicology* 28, 245-253.
- Yang, S.P., Bar-Ilan, O., Peterson, R.E., Heideman, W., Hamers, R.J., Pedersen, J.A., 2013. Influence of Humic Acid on Titanium Dioxide Nanoparticle Toxicity to Developing Zebrafish. *Environmental Science & Technology* 47, 4718-4725.

References

- Young, E., Zimerson, E., Bruze, M., Svedman, C., 2016. Two sensitizing oxidation products of p-phenylenediamine patch tested in patients allergic to p-phenylenediamine. *Contact Dermatitis* 74, 76-82.
- Zanoni, T.B., Hudari, F., Munnia, A., Peluso, M., Godschalk, R.W., Zanoni, M.V., den Hartog, G.J., Bast, A., Barros, S.B., Maria-Engler, S.S., Hageman, G.J., de Oliveira, D.P., 2015. The oxidation of p-phenylenediamine, an ingredient used for permanent hair dyeing purposes, leads to the formation of hydroxyl radicals: Oxidative stress and DNA damage in human immortalized keratinocytes. *Toxicol Lett* 239, 194-204.
- Zauner, W., Farrow, N.A., Haines, A.M., 2001. In vitro uptake of polystyrene microspheres: effect of particle size, cell line and cell density. *Journal of controlled release : official journal of the Controlled Release Society* 71, 39-51.

Annex

- (1) Table of detailed compilation of affected, coagulated and hatched embryos exposed from 0 hpf onwards to differently sized PEGs
- (2) Table of detailed compilation of affected, coagulated and hatched embryos exposed from 24 hpf onwards to differently sized PEGs
- (3) Table of detailed compilation of affected, coagulated and hatched embryos exposed from 48 hpf onwards to differently sized PEGs

Annex

Annex I: Detailed compilation of affected, coagulated and hatched embryos exposed from 0 hpf onwards to the differently sized PEGs obtained in 3 independent runs. Percentage of effects (E) and coagulated embryos (K) are noted in the first column; hatched embryos (G) are shown in second column for each run. The percentage and severity of chorion deformations of the unhatched and not coagulated embryos are also shown. Introduced embryos per run = 10. Data produced jointly with A. Keck

	Exposure from 0 hpf onwards																										
	Run 1						Run 2						Run 3														
	E (K)	Scale of deformation/Percentages of deformation						E (K)	Scale of deformation/Percentages of deformation						E (K)	Scale of deformation/Percentages of deformation											
		G	0	0.5	1	1.5	2		2.5	3	G	0	0.5	1		1.5	2	2.5	3	G	0	0.5	1	1.5	2	2.5	3
NK	24 hpf	0	0	100	0	0	0	0	0	0	0	0	0	0	0	0	0	0	100	0	0	0	0	0	0	24 hpf	
	48 hpf	0	0	100	0	0	0	0	16.66	0	100	0	0	0	0	0	0	0	0	100	0	0	0	0	0	0	48 hpf
	72 hpf	0	0	100	0	0	0	0	0	0	100	0	0	0	0	0	0	0	0	100	0	0	0	0	0	0	72 hpf
	96 hpf	0	0	100	0	0	0	0	0	0	100	0	0	0	0	0	0	0	2.5	75	0	0	0	0	0	0	96 hpf
PEG 2000	120 hpf	8.33	75	2.5	0	0	0	0	8.33	58.33	41.66	0	0	0	0	0	0	0	100	0	0	0	0	0	0	120 hpf	
	24 hpf	0	0	100	0	0	0	0	0	0	100	0	0	0	0	0	0	0	0	100	0	0	0	0	0	0	24 hpf
	48 hpf	0	0	100	0	0	0	0	0	0	100	0	0	0	0	0	0	0	0	100	0	0	0	0	0	0	48 hpf
	72 hpf	0	0	100	0	0	0	0	0	0	100	0	0	0	0	0	0	0	0	100	0	0	0	0	0	0	72 hpf
PEG 3000	96 hpf	0	0	100	0	0	0	0	10	30	70	0	0	0	0	0	0	20	80	0	0	0	0	0	0	96 hpf	
	120 hpf	10	70	30	0	0	0	0	20	80	20	0	0	0	0	0	0	100	0	0	0	0	0	0	0	120 hpf	
	24 hpf	0	0	90	10	0	0	0	0	0	90	10	0	0	0	0	0	0	100	0	0	0	0	0	0	0	24 hpf
	48 hpf	0	0	100	0	0	0	0	0	0	100	0	0	0	0	0	0	0	100	0	0	0	0	0	0	0	48 hpf
PEG 4000	72 hpf	0	0	100	0	0	0	0	0	0	100	0	0	0	0	0	0	0	100	0	0	0	0	0	0	0	72 hpf
	96 hpf	0	10	90	0	0	0	0	10	40	60	0	0	0	0	0	0	40	60	0	0	0	0	0	0	0	96 hpf
	120 hpf	10	80	20	0	0	0	0	40	100	0	0	0	0	0	0	0	100	0	0	0	0	0	0	0	0	120 hpf
	24 hpf	0	0	100	0	0	0	0	0	0	80	0	10	0	0	0	0	0	90	0	0	10	0	0	0	0	24 hpf
PEG 6000	48 hpf	0	0	100	0	0	0	0	0	0	90	10	0	0	0	0	0	0	100	0	0	0	0	0	0	0	48 hpf
	72 hpf	0	0	100	0	0	0	0	0	0	90	10	0	0	0	0	0	0	100	0	0	0	0	0	0	0	72 hpf
	96 hpf	0	0	100	0	0	0	0	10	10	90	0	0	0	0	0	0	40	60	0	0	0	0	0	0	0	96 hpf
	120 hpf	20	70	30	0	0	0	0	20	70	30	0	0	0	0	0	0	90	10	0	0	0	0	0	0	0	120 hpf
PEG 8000	24 hpf	0	0	0	0	0	0	0	40	0	0	0	0	0	30	40	30	0	0	0	0	0	0	0	0	0	24 hpf
	48 hpf	10	0	30	10	20	30	10	40	0	10	0	0	10	40	40	0	0	50	0	10	20	10	10	10	0	48 hpf
	72 hpf	0	0	90	10	0	0	0	40	0	50	0	0	0	20	30	0	0	90	10	0	0	0	0	0	0	72 hpf
	96 hpf	0	10	90	0	0	0	0	50	50	10	0	0	0	10	30	0	20	30	60	10	0	0	0	0	0	96 hpf
PEG 12000	120 hpf	60	70	0	0	0	0	0	80	30	30	0	0	0	10	30	0	50	70	0	0	20	10	0	0	0	120 hpf
	24 hpf	0	0	0	0	0	0	0	70	0	0	0	0	0	0	0	100	0	0	0	0	0	0	0	0	0	24 hpf
	48 hpf	40	0	0	0	0	0	0	90	10	0	0	0	0	10	80	0	70	0	0	0	0	0	0	0	100	48 hpf
	72 hpf	40	0	0	0	0	0	0	90	10	0	0	0	0	10	80	0	90	10	0	0	0	0	0	0	50	72 hpf
PEG 12000	96 hpf	80	50	0	0	0	0	0	100	50	10	0	0	0	10	40	100	80	60	0	0	0	0	0	0	40	96 hpf
	120 hpf	90	60	0	0	10	0	0	100	80	10	0	0	0	0	0	20	80	10	90	0	0	0	0	10	10	120 hpf

Annex III: Detailed compilation of affected, coagulated and hatched embryos exposed from 48 hpf onwards to the differently sized PEGs obtained in 3 independent runs. Percentage of effects (E) and coagulated embryos (K) are noted in the first column; hatched embryos (G) are shown in second column for each run. The percentage and severity of chorion deformations of the unhatched and not coagulated embryos are also shown. Introduced embryos per run = 10. Data produced jointly with A. Keck

	Exposure from 48 hpf onwards																
	Run 1				Run 2				Run 3								
	E (K)	Scale of deformation/Percentages of deformation			E (K)	Scale of deformation/Percentages of deformation			E (K)	Scale of deformation/Percentages of deformation							
	G	0	0.5	1	1.5	2	2.5	3		G	0	0.5	1	1.5	2	2.5	3
NK	8.33	0	100	0	0	0	0	0	0	0	100	0	0	0	0	0	0
72 hpf	8.33	8.33	91.66	0	0	0	0	0	0	8.33	91.66	0	0	0	0	0	0
96 hpf	8.33	83.33	16.66	0	0	0	0	0	0	16.66	83.33	0	0	0	0	0	0
120 hpf	10	0	100	0	0	0	0	0	0	0	100	0	0	0	0	0	0
PEG 2000	0	40	60	0	0	0	0	0	0	0	100	0	0	0	0	0	0
96 hpf	50	80	20	0	0	0	0	0	10	20	80	0	0	0	0	0	0
120 hpf	20 (10 K)	11.11	88.88	0	0	0	0	0	0	0	100	0	0	0	0	0	0
PEG 3000	10 (10 K)	22.22	77.77	0	0	0	0	0	0	0	100	0	0	0	0	0	0
96 hpf	30 (10 K)	66.66	33.33	0	0	0	0	0	20	80	0	0	0	0	0	0	0
120 hpf	0	0	100	0	0	0	0	0	0	0	100	0	0	0	0	0	0
PEG 4000	0	30	70	0	0	0	0	0	0	10	90	0	0	0	0	0	0
96 hpf	10	70	30	0	0	0	0	0	10	40	60	0	0	0	0	0	0
120 hpf	0	0	80	0	0	0	0	0	0	0	50	0	10	10	30	0	0
PEG 6000	0	80	20	0	0	0	0	0	0	10	90	0	0	0	0	0	0
96 hpf	20	100	0	0	0	0	0	0	0	70	30	0	0	0	0	0	0
120 hpf	10	0	0	0	0	0	0	0	0	0	0	0	0	0	0	0	0
PEG 8000	30	40	0	0	0	0	0	0	0	20	40	10	0	10	20	0	0
96 hpf	40	80	0	0	0	0	0	0	10	40	50	0	0	10	0	0	0
120 hpf	50	0	0	0	0	0	0	0	30	0	0	0	0	0	0	0	0
PEG 12000	30	70	0	0	0	0	0	0	50	30	0	0	0	0	0	0	0
96 hpf	50	80	0	0	0	0	0	0	40	40	0	0	0	0	0	0	0
120 hpf																	